STUDIES ON SIGNALS MEDIATING OR PREVENTING THE INTRACRINE INDUCTION OF CHROMATIN COMPACTION AND CELL DEATH BY HIGH MOLECULAR WEIGHT FIBROBLAST GROWTH FACTOR 2

BY

XIN MA

A Thesis
Submitted to the Faculty of Graduate Studies
In Partial Fulfillment of the Requirements
For the Degree of

Doctor of Philosophy

Department of Human Anatomy and Cell Sciences

University of Manitoba
Winnipeg, Manitoba
March, 2011

THE UNIVERSITY OF MANITOBA

FACULTY OF GRADUATE STUDIES

*****

COPYRIGHT PERMISSION

STUDIES ON SIGNALS MEDIATING OR PREVENTING THE INTRACRINE INDUCTION OF CHROMATIN COMPACTION AND CELL DEATH BY HIGH MOLECULAR WEIGHT FIBROBLAST GROWTH FACTOR 2

BY

XIN MA

A Thesis/Practicum Submitted to the Faculty of Graduate Studies of the University of Manitoba In Partial Fulfillment of the Requirements of the Degree of Doctor of Philosophy

an abstract of this thesis/practicum.

TABLE OF CONTENTS

For

Ma Ying Lin

Zhao Fang

and

Zhao Qing Yan

Acknowledgements

First and foremost I'd like to thank my supervisor Dr. Elissavet Kardami. It has been an honor to be her Ph.D. student. She has taught me, both consciously and unconsciously, how good experimental biomedicine is done. I appreciate all her contributions of time, ideas, and funding to make my Ph.D. experience productive and stimulating. The joy and enthusiasm she has for her research was contagious and motivational for me, even during tough times in the Ph.D. pursuit. The members of the Vetta's group have contributed immensely to my personal and professional time at University of Manitoba. The group has been a source of friendships as well as good advice and collaboration. Dr. Xitong Dang has guided me, at the very beginning of the program, through a number of basic experimental procedures such as cell cultures, transfection and always as an unlimited resource of knowledge on molecular biology. Dr. Barb Nickel is really a Protein Master and my co-advisor with whom I discuss my findings, ideas and experimental designs every week in the last two years of my program. The weekly conversation with her is really inspirational and illuminating. I will never forget her lovely and enjoyable stories about how protein experiments were done before Western Blotting was developed. Moreover, I would like to acknowledge the skillful technical assistance of Robert Fandrich. Without his help, I cannot even orient myself in the laboratory, no need to mention billions and billions of cardiomyocytes he has cultured to coordinate my project. Appreciation also goes to other student fellows, Sarah Jimenez, Maya Jeyaraman, Jon-Jon Santiago, Wattamon Srisakuldee. Thanks for making the lab such a great place for fun and research. I will never forget all the funny stories shared with you about how silly mistakes we experienced in the experiments (like running gel in PBS). These images will

be in my mind forever. Special thanks to fellow student, Jon-Jon Santiago for collaboration with my project by helping me culture human atria-derived fibroblasts and immunohistochemical experiments.

Besides my supervisor and lab members, I would like to thank my advisory committee. Dr. Judy Anderson is, at any time, trying to help me with her imponderable insight opinions in sciences and encourage me when every tiny advance has been made. All her questions are delicately designed to guide me into bigger pictures and point to a promising research direction. Every year in the committee members meeting, she always "protects" me from other committee members' questions by saying "let us not challenge Xin Ma with such tough question", and then asks me an even "tougher" question herself. I am so grateful for the all the valuable suggestions from her and I think the serious and rigorous attitude I have learned from her is my life-long treasures. Dr. James Davie is a master of gene transcription and chromatin remodeling. It is Dr. Davie that taught me how histone proteins are modified so that chromatin is remodeled correspondingly and how to address and resolve the questions in my project. The ease with which he has shown to me how to master complicated scientific questions also showed me what top scientists look like. Dr. Jiming Kong is the only Chinese professor in my graduate committee, but indispensible. I cannot count how many times I knocked his door and came out of his office with lots of very good advice and a bunch of notes, how many antibodies I have "borrowed" from him and how much coffee I have had in his lab. Dr. Nasrin Mesaeli, who served in my committee for several years, deserves my heartfelt appreciation and respect as well. Whenever, in low spirits, I brought to her some troublesome results or questions unsolvable by me, she was there, full of enthusiasm,

making things more comprehensible and always encouraging me. Many thanks also go to Dr. Thomas Klonisch (Department head of Human Anatomy and Cell Sciences), Dr. Sabine Hombach-Klonisch, Dr. Hugo Bergen(Graduate Committee Chair in Human Anatomy) , Xie Xueping, Dr. Zhao Ruozhi, Dr. Zhang Tong, Dr. Cheng Keding, Guo Jun, Dr. Xu Yanjun for your immeasurable help to me to get through my PhD program.

I'd like to take the chance to appreciate all the funding bodies, Canadian Institutes of Health Research (CIHR), Manitoba Health Research Council (MHRC), University of Manitoba Graduate Fellowship (UMGF) and Manitoba Graduate Scholarships (MGS), Institute of Cardiovascular Sciences for financially supporting me through the program.

I also like to thank all the peoples sharing friendships with me in Winnipeg through the process of my program. The members from UM Badminton club (Dr. Wang Xikui, Ricky, Lois, Rogers, Iran), Vietnam Badminton club (Sylvania, Jason, Patt) and YMCA (Bao Ge, Sun liwei, David, Micheal, Jerry, Rowan, Wei). The tennis club members: Sim, Lou, and the Rock'n Roll band members: Dang Weimin, Tang Rui, Zhang Shengli, He Qiangwei, Ge Heng. I enjoy every minute I have with you and your friendships warm my heart in Winnipeg, especially in winter at minus 50 ^{o}C. I also want to say thanks to the following peoples outside Winnipeg keeping in touch with me all the time: Gao Yuanyuan, Lin Liqin, Li Lei and Li Rong, Yang Zitong, Mo Zhenping. Thank you all.

Last but not least, I thank all my family members for their support on me all along the PhD program. Ma Ying Lin (my father), Zhao Fang (my mother), Zhao Qing Yan (my sister), Zhao Rong and Zhao Pei Lun (my aunts), Wen Yan Fei (Wendy, my fiancée).

Without your continuous unconditional love, encouragement and guidance, it would not have been possible for me to overcome all the tough times and complete my PhD degree.

Abstract

Fibroblast growth factor 2 (FGF2) is a multifunctional protein translated as CUG-initiated, high molecular weight (hi FGF2) or AUG-initiated, low molecular weight (lo FGF2) isoforms with potentially distinct functions. Previous work showed that overexpression of hi- but not lo FGF2 elicited chromatin compaction resulting in cell death, by an intracrine route. A series of studies were undertaken aimed at extending our understanding of the intracrine action of Hi FGF2. Major findings are as follows:

a. Hi FGF2 overexpression induces apoptotic cell death, as indicated by increased TUNEL staining, and mitochondrial participation (cytochrome c release to cytosol, rescue of the hi FGF2 phenotype by the anti-apoptotic protein Bcl-2
b. Increased expression of pro-survival signals/proteins that are known to upregulate Bcl-2, such as nuclear Akt; the PIM-1 kinase; and the heat shock protein hsp70, also rescued the hi FGF2-induced phenotype.
c. The hi-FGF2 effect was associated with sustained, intracrine, activation of ERK, and was blocked by ERK inhibitors
d. FGF2 isoform specific affinity chromatography followed by mass spectroscopy identified several proteins as potentially interacting with hi FGF2; of these, the p68 RNA helicase and the hsp70 were further confirmed as interacting partners, by co-immunoprecipitation.
e. Increased nuclear co-localization, and possibly interaction, between hi FGF2 and overexpressed hsp70 correlated with rescue from hi FGF2 induced cell death.

f. Factors associated with cardiac pathology (isoproterenol, angiotensin II, endothelin I) also upregulated endogenous hi FGF2 in cardiac cells in culture. Adriamycin-induced cardiotoxicity in the rat, known to be linked to increased incidence of apoptosis, was also associated with increased endogenous hi FGF2.

g. Hi FGF2 is expressed in the human heart (atria) and localizes in both cytosol and nuclei, suggesting a participation in human heart physiology and pathophysiology.

Work presented here is consistent with the notion that endogenous hi FGF2 up-regulation may play a role in promoting cell death during prolonged tissue stress and dysfunction. It follows that processes related to hi FGF2 upregulation, hi FGF2-nuclear protein interactions and mechanisms of hi FGF2 induced cell death, represent potential therapeutic targets for modulating cell death.

LIST OF FIGURES

LIST OF TABLES

LIST OF ABBREVIATIONS

Ad ..... adenovirus

AIF……..…….. apoptosis inducing factor

anti-P-H3 ..... anti-phospho histone 3

AP-1……..…activator protein 1

AUG ..... methionine

BAEC …….……bovine arterial endothelial cells

BCA ..... bicinchonic acid

BH domain…….....…….……..Bcl-2 homology domain

Bcl-2…….....……cell lymphoma

bFGF ..... basic fibroblast growth factor

BSA ..... bovine serum albumin

°C ..... degrees centigrade

Ca2+ ..... calcium

CAD…….. caspase-activated DNase

cDNA. .....complimentary deoxyribonucleic acid

ChiP .....chromatin immunoprecipitation

CK2…….....…….casein kinase 2

CM…….....……. conditioned media

CO_2 ..... carbon dioxide

CUG ..... leucine

DISC…….....……..…….. death-inducing signaling complex

DMEM ..... Dulbecco's modified Eagle's medium

dn ..... dominant negative

DNA. ..... deoxyribonucleic acid

DNase..... deoxyribonuclease

DUSP…….....…….. dual-specificity phosphatase

E2…….....……17 beta-estradiol

ECL…….....…….. chemiluminescence

EDTA..... ethylenediaminetetraacetic acid

Egr-1 ..... early growth response-1 protein

eIF…….....…….. eukaryotic translation initiation factor

Endo G…….....…….…….... endonuclease G

ER…….....…….…….endoplasmic reticulum

ERK ..... extracellular-signal-regulated protein kinase

FADD.....……Fas-associated death domain

FBS .....fetal bovine serum

FGF2……..... fibroblast growth factor 2

FGFR1 ..... fibroblast growth factor receptor 1

FIF…….....FGF2-interacting-factor

g ..... grams

GTP .....guanosine 5' -triphosphate

h ..... hour

HDAC5…….....…….histone deacetylase 5

hi ..... high molecular weight

hnRNP A1…….....…….heterogeneous nuclear ribonucleoprotein A1

HUVEC…….....….human umbilical vein endothelial cells

IGF-1…….....insulin-like growth factor-1

HEK293….....……Human Embryonic Kidney 293 cell line

hnRNP K…….....… heterogeneous nuclear riboprotein K

HRP…….....… horseradish peroxidase

HSPG…….....……heparin sulphate proteoglycans

hsp70….....…heat shock protein 70

IgG ……..... immunoglobulin G

IMAC…….....… immobilized metal ion affinity chromatography

I/R..... ischemia-reperfusion

IRES ..... internal ribosomal entry site

JNK1.....c-Jun N-terminal Kinase

kDa ..... kilodalton

L .....liter

Lo ..... low molecular weight

M ..... molar

MAPK ..... mitogen activated protein kinase

MEK ..... MAP kinase kinase

g ..... microgram

µ..... microliter

M..... micromole

MAPK..... mitogen activated protein kinase

MEK1⁄2.....mitogen protein kinase kinase 1 and 2

ml ..... milliliter

mM.....millimole

m.o.i. ..... multiplicity of infection

MPT .....mitochondrial permeability transition

mRNA..... messenger ribonucleic acid

MW.....molecular weight

NaCl..... sodium chloride

NCI..... Nuclear compaction index

NLS …….. nuclear localization signal / sequence

N.S. ..... not significant

ORF..... open reading frame

PBS..... phosphate buffered saline

phospho p42/44 ..... phosphorylated MAPK

pI.....isoelectric point

PIC.....protease inhibitor cocktail

PI3K.....phosphoinositide 3- kinase

PIP2.....phosphotidylinositol 4, 5-bisphosphate

PIP3.....phosphatidylinositol (3, 4, 5)-trisphosphate

PKA..... protein kinase A

PKC ..... protein kinase C

PRMT5.....arginine methyltransferase 5

PVDF..... polyvinylidene difluoride

RNA..... ribonucleic acid

RNase.....ribonuclease

ROS..... reactive oxidative species

RPM ..... rotations per minute

rRNA..... ribosomal RNA

scrambled shRNA……..…non-specific shRNA skim milk powder (SMP)

SDS ..... sodium dodecyl sulfate

SDS-PAGE.....sodium dodecyl sulphate polyacrylamide gel electrophoresis

SEM.....standard error of the mean

shRNA(p68).....p68-specific shRNAs

SMN ..... survival of motor neurons protein

SP-1.....stimulating protein 1

TBST……..... Tris buffered saline with TWEEN

TRAIL ……..... TNF-related apoptosis-inducing ligand

Tris-HCl .....tris (hydroxymethyl) aminomethane - hydrochloric acid

TBST…….....Tris-buffered saline containing 0.1% Tween-20

TSI.....TUNEL staining index

U .....units

UTR.....untranslated region

UV..... ultraviolet

LIST OF COPYRIGHT MATERIAL FOR WHICH PERMISSION WAS OBTAINED

Some of the work presented in this thesis (and accompanying comments) has been published previously and is reproduced here by permission. Publications include:

1) **Fibroblast growth factor-2 and cardioprotection.** Kardami E, Detillieux K, Ma X, Jiang Z, Santiago JJ, Jimenez SK, Cattini PA. Heart Fail Rev. 2007 Dec;12(3-4):267-77. Review

   Contribution: Comments on hi FGF2 induced apoptotic chromatin compaction in HEK 293 cells

2) **Chromatin compaction and cell death by high molecular weight FGF-2 depend on its nuclear localization, intracrine ERK activation, and engagement of mitochondria.** Ma X, Dang X, Claus P, Hirst C, Fandrich RR, Jin Y, Grothe C, Kirshenbaum LA, Cattini PA, Kardami E. J Cell Physiol. 2007 Dec;213(3):690-8.

   Contribution: I did all the experiments, drafted the manuscript, and revised as required.

3) **Preferential accumulation and export of high molecular weight FGF-2 by rat cardiac non-myocytes.** Santiago JJ, Ma X, McNaughton LJ, Nickel BE, Bestvater BP, Yu L, Fandrich RR, Netticadan T, Kardami E. Cardiovasc Res. 2010 Sep

   Contribution: I contributed experimental work for Figure 4, which is similar to Figure 27 in this thesis.

Copies of letters of permission are included as the end of this thesis as an Appendix

CHAPTER 1

REVIEW OF THE LITERATURE

1.1 Fibroblast Growth Factor 2

1.1.1 A brief history

The initial report on fibroblast growth factor 2 (FGF2) can be traced back to the discovery as early as in 1938 that brain extracts were particularly rich in mitogenicity for fibroblasts [1]. Follow-up studies showed that extracts from bovine pituitary glands were also capable of stimulating BALB/c 3T3 fibroblasts to proliferate. However, the original purification, using various standardized protein chromatographic technologies, resulted in large proteolytic fragments that were mitogenically inactive. The binding affinities of the effective mitogens in pituitary gland extracts to highly sulphated oligosaccharide heparin were soon recognized, therefore leading to high-efficiency purification protocol afforded by heparin-sepharose chromatography. Isoelectric focusing of heparin-binding mitogens separated into two peaks: one with acidic isoelectric point (pI) (~5) and molecular weight 15,000 to 18,000, the other with basic pI (8~10) and molecular weight 16,000 to 18,000. These established the two closely related fibroblast growth factors, designated as acidic FGF (FGF1) and basic FGF (FGF2) [1]. The very high heparin-binding capacity of acidic and basic FGF has provided a powerful tool to isolate purified polypeptides, and thus study these molecules further both structurally and functionally.

To date, five human and three rat FGF2 isoforms have been identified and all of

them are translated from a single mRNA using different start codons [2]. Translation from the AUG start codon generates the 18 kDa low molecular mass (lo) FGF2, while translation from CUG start codons generates high molecular mass (hi) FGF2, at 21-23 kDa in rat, and 21-34 kDa in human [3]. Although closely related, the hi and lo FGF2 isoforms exhibit different biological characteristics shown by extensive research over the last 20 years. This review will summarize information regarding FGF2 expression, intracellular location and biological activities, concentrating on the difference between hi and lo FGF2 in various aspects as documented so far.

1.1.2 FGF2 gene and protein expression

The FGF2 gene has been assigned to chromosome 4q26 in human, and chromosome 2q25 in the rat [4]. The gene is responsible for producing both hi and lo FGF2 isoforms. The organization of the human FGF2 gene includes two introns, each 1.6 kbp long and three exons constituting a transcribed 3.6 kbp region [5]. The upstream promoter region of human FGF2 gene was identified and found to include five GC boxes representing stimulating protein 1 (Sp-1) binding sites and one potential activator protein 1 (AP-1) site as well as two negative regulatory elements, one in the non-transcribed 5'-promoter region and the other within transcribed (but non-translated) sequences 3' of the upstream promoter region [5]. In the case of the rat FGF2 promoter, multiple GC-rich start sites (P_0, P_1, and P_2), instead of a TATA box region, have been identified as responsible for initiating transcription in neuronal and glial cells and the P_0 site (5'-GCGGGGGCG-3') is recognized as putative

constituent region for early growth response 1 (Egr-1) binding [6]. The involvement of the Egr-1 transcription factor in regulating FGF2 gene promoter activities, and two interacting cis-DNA elements were established in subsequent studies [7]. Sp-1 and two corresponding regulatory sites located at positions −3, +14 (assuming transcription starts from position 0) were identified as regulating FGF2 transcription in rat neonatal cardiomyocytes [8]. As to human FGF2, histone deacetylase 5 (HDAC5) has been shown to bind to the FGF2 promoter *in vivo* in human umbilical vein endothelial cells (HUVECs) [9]. The cis- and trans-elements interaction appears to inhibit gene promoter since siRNA silencing of HDAC5 induced significant increase of FGF2 mRNA level.

Several stimuli have been reported to stimulate FGF2 gene transcription. These include certain mitogens such as phorbol ester and serum [6] and interestingly, FGF2 itself acts to stimulate its own synthesis at the transcriptional level [10].

Post-transcriptionally, FGF2 gene is regulated by an endogenous complementary (antisense) RNA, designated FGF antisense (FGF-AS) RNA. The FGF-AS transcript was first identified in *Xenopus laevis* and has since been discovered in a variety of other vertebrate species including chicken, rat and human [11]. The FGF-AS transcripts are transcribed from opposite DNA strand to FGF2 coding strands and three FGF-AS mRNA species are produced due to alternative RNA splicing [12]. Murphy and his colleagues showed all three species suppressed cellular FGF2 protein levels by interfering with the translational process and further studies show two regions of complementarity, 583 and 56 bp in length, in the 3'-untranslated

region of the FGF2 mRNA as targeting sites for FGF2 antisense RNA [13]. Interestingly, the FGF-AS transcripts do encode an evolutionarily conserved nudix motif protein, designated as GFG proteins [12]. However, the function of GFG remains unclear to date.

Mature FGF2 mRNAs seem to possess certain distinct features remarkably different from common descriptions for regular mRNA molecules. Multiple FGF2 transcripts have been identified. Five FGF2 mRNA species have been isolated from different types of human cells, measuring 1033, 3341, 4024, 5397, and 6774 nucleotides [3, 14]. Alignment of all transcripts revealed a shared sequence in the 5' untranslated region (UTR), measuring 485 nt and the AUG-initiated open reading frame (ORF), positioned 485 nt to 951nt from the 5'-end, but significant difference in the length of their 3' UTR, measuring 83, 2390, 3073, 4446, and 5823 nt, respectively [3]. A polyadenylation tail is found at 3' end of all mRNA species, with the shortest mRNA species including only one poly A site while the longest transcripts include up to 8 poly A sites.

The question of the function of 3' UTR of FGF2 mRNA and its multiple polyadenylation sites in mRNA metabolism and in the translation process was extensively addressed by Prats and colleagues. They focused on the 3'-UTR (5823 nt) of the longest FGF2 mRNA species which harbors eight potential polyadenylation sites (A1 to A8), with A8 located at the 3' end of the mRNA [15]. A 122-nt long destabilizing element has been recognized to localize between the A1 and A2 sites and deletion mutagenesis showed that this element functions to regulate mRNA

stability [15]. A translational enhancer (TE), located immediately upstream from the eighth poly (A) site was identified to play a role in regulating translational events [16]. The TE element seems to be potential mechanism to selectively initiate translation of hi FGF2 isoforms since its presence favors the use of the CUG start codons. The TE segment measures 1370-nucleotides, composed of two functional domains cooperating in an additive manner. Examination of FGF2 mRNA species in primary skin fibroblasts showed 95.5% long mRNAs cleaved at A8, which corresponds to their predominant hi FGF2 protein products. The evidence has suggested a novel potential mechanism for cells to regulate translational processes via modifying mRNA length. However, COS-7 and HeLa cells (two kinds of transformed cells also producing predominantly hi FGF2) exhibit 100% and 92% short mRNAs cleaved at A1, respectively, suggesting there might be other mechanisms regulating use of the CUG codon over the AUG codon [16].

In addition to the polymorphic 3' UTR, the 5' UTR, shared by all FGF2 transcripts, is also unusually lengthy and exhibits certain uncommon features [3]. Four CUG initiation codons (positions 86, 320, 347 and 362 nt) have been identified in human FGF2 mRNA 5' UTR, located 5' upstream to the AUG-initiated open reading frame (located from 485 to 951 nt). The CUG start codons give rise to four additional high molecular mass FGF2 isoforms (22, 22.5, 24, 34 kDa FGF2s).

The typical translational process in both prokaryotes and eukaryotes is initiated by a series of major events including: recruitment of the 40S ribosomal subunit to the 5' end cap structure of the mRNA; linear scanning of the mRNA in a 3' direction until

encountering an initiation codon; binding of the 60S ribosomal subunits to the small subunits to start translation (Molecular Biology of The Cell, 4th edition, 2002). This so-called cap-dependent translation is exclusively applied to the production of the 34 kDa FGF2 isoform [17]. Translation of the other isoforms is independent of such cap-recognition mechanism due to the presence of a stable secondary hair-pin structure, composed of GC nucleotide-rich regions, in the 5' UTR downstream to CUG codon generating 34kDa FGF2 species [3]. Such hair-pin structure is linearized with difficulty by the eIF4A RNA helicase, thus creating obstacles for ribosomal subunit to scan through. Today, it is widely accepted that an alternative mechanism, termed internal ribosome entry (IRES), accounts for translational initiation of all the other FGF2 isoforms. The internal ribosome entry site was identified in the region between the first and second CUG start codons of the 5' UTR of FGF2 RNA [18]. Further studies defined a 176-nt sequence, spatially organized into two stem-loop regions and a G quartet motif in this region necessary and sufficient for IRES function [19]. Regulation of the IRES activities has been shown to relate to translational initiation from both CUG and AUG start codons of 5' downstream positions.

One of the trans-acting elements has been identified as heterogeneous nuclear ribonucleoprotein A1 (hnRNP A1) and the direct interaction between IRES and hnRNP A1 is indicated in UV cross-linking and electrophoretic mobility shift assays [20]. The protein appears to positively regulate IRES activities because recombinant hnRNP A1 stimulates IRES-dependent initiation in *in vitro* translation assays, and siRNA-mediated knock down of hnRNP A1 specifically inhibits translation at the

four IRES-dependent initiation codons.

Certain stimuli act to upregulate 18-24 kDa FGF2 gene expression via stimulating IRES activities. These include a high dose of glucose applied to aortal wall cells, testosterone applied to adult sperm cells and differentiation and maturation in neural cells[3]. However, this IRES-dependent mechanism does not explain how the cells selectively start translation from AUG codons (to synthesize lo FGF2) or from CUG codons (to generate hi FGF2 products) since translation initiated via IRES-dependent mechanisms generates both hi and lo FGF2 isoforms. Failure in further search for a second IRES between the AUG codon and an immediately upstream CUG codon also rule out the possibilities that an IRES-dependent mechanism exists to serve such purpose [19]. As yet, the factors regulating selective translation of hi FGF2 or lo FGF2 still remain unidentified.

To summarize, translation of the 18, 22, 22.5, and 24 kDa FGF2 isoforms is initiated in a cap-independent and IRES-dependent manner, while expression of the 34kDa FGF2 is exclusively dependent on cap recognition.

Post-translational modifications and/or processing can play a critical role in regulating intracellular distribution and function of proteins. Here I will summarize the major findings regarding to hi FGF2 post-translational modifications and processing.

Methylation is the first documented modification resulting in 1- to 2-kDa increase in molecular mass, which is inhibited by methionine starvation and by the methyltransferase inhibitors 5'-deoxy-5'-methylthioadenosine (MTA) and

3-deaza-adenosine. Methylation is important for nuclear translocation of hi FGF2 since its inhibition results in a significant decrease in nuclear FGF2 [21]. The inhibition of methylation leads to cytoplasmic enrichment of hi FGF2 in HEK293T cells [22]. Furthermore, arginine methyltransferase 5 (PRMT5) was identified to be responsible for hi FGF2 methylation. Interestingly, not only intracellular distribution but also intranuclear distribution was altered via inhibition of arginine methylation [22]. This will be discussed in detail in FGF2 localization section.

Limited proteolysis. Hi FGF2 can be converted to a lo FGF2-like form during the inflammatory response *in vivo* [23]. Hi FGF2 is anti-angiogenic, while lo FGF2 is angiogenic, promoting migration of endothelial cells [24]. Conversion of hi FGF2 to a lo FGF2-like protein by thrombin proteolysis, resulted in lo FGF2 biological activities [23]. The cleavage of the amino terminal extension of hi FGF2 was found to be mediated by thrombin, a key coagulation factor and inflammatory mediator. Therefore, conversion of hi to lo FGF2 by limited proteolysis is adding another level of regulation of hi FGF2, providing a potential therapeutic target to antagonize its detrimental effects.

FGF2 phosphorylation. FGF2 phosphorylation and resultant effects have been studied mainly by Baird and colleagues. Within cells, FGF2 has been shown to be phosphorylated by cAMP-dependent protein kinase A (PKA) on Thr-112 and by protein kinase C (PKC) on Ser-64 (assuming AUG-coded methionine at position 1), respectively [25]. Effects of phosphorylation on receptor-binding capacity, heparin-binding capacity, and the biological activity were examined in the same study.

The PKA- (but not PKC-) - phosphorylated FGF2 showed significantly increased binding affinity (3-8 times) to FGF2 high affinity receptors on the plasma membrane, compared to non-phosphorylated FGF2. As yet, experimental results did not reveal other significant differences on either binding affinities to immobilized heparin/cell-associated glycosaminoglycans or mitogenic activities between PKA- (or PKC-)- phosphorylated and non-phosphorylated FGF2. Another kinase phosphorylating FGF2, distinct from PKA and PKC, has been reported to localize within nuclei of SK-Hep-1 cells, even though the identity of the kinase has not been determined yet [26]. Interestingly, FGF2 is phosphorylated by a protein kinase associated with the outer surface of a target cell, adding another mechanism of post-translational modification for exported FGF2. It appears that the event is dependent on cAMP formation within cells and association of basic FGF with its low and/or high affinity binding sites [27].

1.1.3 Hi and lo FGF2 localization

The intracellular distribution of proteins relates to their biological effects and different subcellular localization may serve as a mechanism to stimulate different signal transductions pathways, accounting for the variation in responses of the expressing cells. Here I will summarize information regarding human and rat FGF2 intracellular localization and corresponding mechanisms, discovered to date. Regardless of species, however, it is established that lo FGF2 can be released from cells through an ATP-dependent exocytotic mechanism lacking involvement of the

endoplasmic reticulum (ER)-Golgi system, to act in a paracrine or autocrine manner, or can remain intracellular in both cytosolic and nuclear fractions. Hi FGF2 is mostly intracellular and nuclear, exerting effects via an intracrine mode of action. It should be noted, however, that even hi FGF2 has been reported as being released by cells [28].

1.1.3.1 Subcellular distribution of human FGF2 isoforms

The subcellular distribution of human hi and lo FGF2 has been described as early as 1991 by Rifkin and colleagues [29]. These authors reported that the 18 kDa FGF2 occurs predominantly in the cytosol whereas hi FGF2 localizes to the nucleus. In search of nuclear localization signals (NLS) responsible for nuclear distribution of hi FGF2, the NH2-terminal extension of the 24kDa FGF2 was fused to beta-galactosidase, a cytosolic protein, to construct a chimeric protein and allowed to be overexpressed in cultured cells via gene transfer. The chimeric protein accumulated in the nuclei of transfected cells, establishing that N-terminal extension is sufficient to serve as NLS for hi FGF2 [29]. Multiple GR repeats occur in a scattered pattern within the N-terminal extension of hi FGF2 [30], including one of particular interest reported by Dono et al [31]. This GR-enriched sequence is highly conserved between species and located, in human FGF2, between the methionine encoded by the AUG start codon and leucine encoded by the immediately 5' CUG codon, i.e. existing in all hi FGF2 isoforms. A chimeric protein containing lo FGF2 plus the GR-motif exhibits similar nuclear accumulation as hi FGF isoforms [31]. To date, it is widely accepted

that the N-terminal extension serves as an NLS for hi FGF2, within which the conserved GR motif is probably responsible for nuclear localization.

It should be noted that the localization pattern of lo FGF2 might be affected by its expression level and the cell type involved. For example, lo FGF2 concentrated in the nucleus in transfected baby hamster kidney (BHK-21) cells, whereas it was both cytoplasmic and nuclear in untransfected BHK-21 cells [32]. Lo FGF2 accumulated in the nucleus when overexpressed in mouse fibroblast NIH 3T3 and HEK 293 cells [33], while other reports suggested that lo FGF2 was predominantly cytoplasmic [34]. Despite the difference in relative levels compared to hi FGF2, lo FGF2 is also detected in the nucleus of all types of cell examined. Given the fact that a standard NLS or GR-repeats or motif present in the N-terminal extension of hi FGF2 does not exist in lo FGF2, the signals controlling the nuclear distribution of lo FGF2 have been studied. A 17-amino acid sequence, located at the carboxyl terminal of lo FGF2 was found to be sufficient and necessary to guide fusion proteins containing GFP or a GFP dimer into the nucleus, whereas the fluorescent proteins alone localized to both cytosol and nucleus [35]. Detailed studies revealed the sequence is composed of two groups of basic amino acid residues separated by eight amino acid residues, in which Lys119 and Arg129 are the key amino acid residues in regulating both nuclear and nucleolar localization, whereas Lys128 is required only for nucleolar localization. These findings agree with those for rat lo FGF2 in which C-terminals sequence is responsible for its nuclear distribution [36].

1.1.3.2 Subcellular distribution of rat FGF2 isoforms

Rat hi and lo FGF2 exhibit a similar localization pattern to their human counterparts, described above. Sub-nuclear distribution patterns for hi and lo rat FGF2 have been studied in some detail by Claus and colleagues [36]. Several sub-nuclear structures exist within nuclei including chromatin, nucleoplasm, nucleolus and Cajal bodies. Cajal bodies are spherical sub-organelles found in the nucleus of proliferative cells like embryonic cells and tumor cells, or metabolically active cells like neurons [37]. They largely consist of proteins and RNA and can be visualized by immunofluorescence against marker protein p80/Coilin. Functionally, Cajal bodies are involved in important RNA-related metabolic processes such as snRNP biogenesis, maturation and recycling, histone mRNA processing and telomere maintenance [38]. The nucleolus is another non-membrane bound structure within the nucleus and it is widely established that ribosomal RNA (rRNA) is transcribed and assembled within the structures (Molecular Biology of The Cell, 4th edition, 2002). Claus and colleagues documented that in lo / hi FGF2-overexpressing Schwann cells, lo FGF2 localized in Cajal bodies and nucleoli, whereas hi FGF2 was distributed in a punctate pattern in the nucleoplasm, periphery of nucleoli, and co-localized with mitotic chromosomes or DNA of quiescent cells [36]. The functional consequences of such differences in localization are still unknown.

The role of the N-terminal extension as a NLS in guiding the nuclear distribution was also established for rat hi FGF2, and the conserved GR-motif and multiple shorter GR repeats within ATE was found to be determinant for NLS function [22]. Arginine

methylation is required for nuclear shuttling after synthesis, as for human hi FGF2 protein, even though the position of the targeted arginine is undefined yet. Claus and colleagues reported that the protein arginine methyltransferase 5 (PRMT5) catalyzes the methyl-group transfer reaction specifically using as substrates both hi FGF2 and its specific binding partner survival motor neuron proteins. Co-immunoprecipitation showed the three proteins exist in a common complex and PRMT5 is capable of catalysis in *in vitro* methylation assays [22].

As mentioned, human lo FGF2 includes a 17-amino acid sequence at the carboxyl terminal, serving as a non-canonical NLS responsible for nuclear localization [35]. It is presumed that this sequence serves the same function in rat lo FGF2 because the lo FGF2 sequence is highly conserved between human and rat species (one amino acid difference). Even though systemic deletion mutation has not been performed yet, two amino acids (arginine at 149 and 151 position, assuming methionine as position 0 at the start of the lo FGF2 protein) were discovered to be key regulators required for nuclear localization [36]. The lo FGF2 mutant R149G/ R151G failed to localize to the nuclei of overexpressing cells. Interestingly, hi FGF2, when carrying such a mutation, was also incapable of shuttling into nuclei, suggesting its necessary role in directing nuclear localization, compared to the NLS located on N-terminal extensions.

1.1.4 FGF2 Export

FGF2 is released from viable cells in an ongoing manner as well as from dying cells during tissue injury [24]. Most studies using cultured cells have reported or assumed that only lo FGF2 is released by the cells whereas hi FGF2 remains intracellular [3]. A small number of studies, however, have shown the presence of hi FGF2 in the extracellular space [39]. *In vivo*, FGF2 is detected at the basal lamina and the extracellular matrix, presumably in association with heparin sulphate proteoglycans (HSPGs). It is also detected in serum and other body fluids [40]. In the heart, it is documented that cardiomyocytes release FGF2 on a beat-to-beat basis, under normal conditions [10]. Cardiac fibroblasts, a rich source of released FGF2 [28] and a major cardiac population that exists in close proximity with myocytes, would be stretched passively by myocyte contraction, and thus also release FGF2 to the extracellular matrix. Increased contractility and/or increased endogenous FGF2 expression result in increased levels of heart-released FGF2 [10]. Pathologically, a number of acute or chronic diseases are associated with increased FGF2 levels in the blood or urine [24], even though its role in pathogenesis of these diseases is still an enigma. It is important to note, all *in vivo* studies on FGF2 present in extracellular fluid or matrix did not differentiate between the FGF2 isoforms being released because these studies rely almost exclusively on ELISA-based FGF2 detection with antibodies that are not isoform-specific.

The mechanism of FGF2 release from viable cells is not well understood. Analysis of the FGF2 amino acid sequence does not reveal a classic export signal sequence. It occurs via an ATP-dependent, endoplasmic reticulum/Golgi-independent

transportation pathway [41]. Pharmacological inhibitors of the Na^+/K^+ ATPase pump can prevent FGF2 export from a number of cell lines, implicating the Na^+/K^+ ATPase in this process [42]. Furthermore, it is documented that FGF2 can also be released through plasma membrane vesicle shedding and non-lethal transient membrane disruptions [24]. Research done in Dr. Kardami's laboratory indicated that hi FGF2 is released from cardiac non-myocytes, by a mechanism requiring caspase-1 activity[28]. The released FGF2 is free to interact with cell-surface receptors of cells in close proximity, thus exerting effects in a paracrine or autocrine mode of action.

1.1.5 FGF2 signal transduction

The biological effects of extracellular FGF2 are mediated by binding to high-affinity FGF receptors (FGFR1-4) of the tyrosine kinase family[43]. FGFR1 is the most abundant FGFR in embryonic, neonatal, and adult cardiomyocytes [24]. HSPGs, which function partly to sequester FGF2 in the extracellular matrix until signaling is triggered, are also present at the plasma membrane and act as lower affinity 'receptors' to facilitate interaction of the ligand with FGFR [24] . Plasma membrane HSPGs may in fact carry their own signaling capacity in response to FGF2 binding[44]. Activated FGFRs recruit and phosphorylate other signaling molecules culminating in the activation of major signal transduction pathways such as all three branches of the mitogen activated protein kinase (MAPK pathway), the phospholipase C-protein kinase C (PKC)- and Src- associated pathways [45].

An additional, concurrent pathway for extracellular FGF2-triggered signaling is initiated by binding and activating FGFR1 at the plasma membrane, followed by

FGF2-FGFR1 internalization and nuclear translocation. Activated nuclear FGFR1 may then activate a number of genes directly [46-47]. Thus the end-effects of extracellular FGF2 are brought about by signals activated downstream of the plasma membrane FGFR as well as by those triggered by internalized FGF2 and FGF2/FGFR complexes that translocate to the nucleus and affect gene expression directly [48]. Internalization followed by nuclear translocation is reported to be essential for the mitogenic response to lo FGF2. It occurs during the G1 stage of the cell cycle and is mediated by lo FGF2 binding to translokin, a ubiquitous cytosolic protein [49]. Activation of casein kinase 2 (CK2) through the interaction of its beta-subunit with lo FGF2 in the nucleus is also essential for the induction of the mitogenic response [24]. FGF2-dependent CK2 activation leads to the phosphorylation of the nucleolar protein nucleolin, and the activation of rRNA transcription [48]. It is important to note that stimulation of rRNA transcription, leading to ribosome biogenesis, is not only required for cell duplication in anticipation of mitotic division, but also for the maintenance of cardiac hypertrophy [50]. Hi FGF2 does not interact with the translokin system [49], it is however transported to the nucleus by its N-terminal extension [51].

1.1.6 The biological activities of FGF2 isoforms

1.1.6.1 General introduction

The biological activities of lo and hi FGF2 isoforms have been extensively studied. In cultures, intracellular overexpression via gene transfer or exogenous

addition of recombinant FGF2 isoforms were applied to examine cellular responses regarding basic cell culture characteristics such as proliferation, differentiation, migration, and viability. These *in vivo* models involved the studies of the FGF2 expression pattern in animals, the physiological role in expressing cells, as well as the effect of locally applied FGF2, or genetic knock-in and knock-down of FGF2 expression. To date, increasing evidence indicates that lo and hi FGF2 exert different effects on various cellular processes, summarized in the following section.

1.1.6.2 Different effects of hi versus lo FGF2 isoforms overexpression on cultured cells *in vitro*.

Ectopic protein expression by gene transfer with the assistance of chemical or viral technologies has been widely applied to allow the protein of interest to be overexpressed within cells and study the cellular response as a result. In NIH 3T3 cells (standard fibroblast cell line), overexpression of lo FGF2 significantly increases cell migration, while hi FGF2 has no effect on migration, compared to control-transfected parental cells[52]. Hi FGF2 overexpression in stable cell lines allowed cell survival in low serum (1% FBS) culturing media, suggesting a pro-survival role under starvation circumstances [3]. Hi FGF2 expression conferred to skin fibroblasts resistance to UV radiation [53] and to N-(phosphonacetyl)-l-aspartate (PALA), a drug inhibitor of de novo pyrimidine biosynthesis [54]. These findings have suggested that lo FGF2 serves to increase cell migration while hi FGF2 maintains cell survival under stress in fibroblastic cells. The enhanced cellular

resistance to ionizing radiation was reproducibly observed in HeLa cells expressing 24-kDa but not the 18 kDa molecular weight form of FGF2 [55].

Even though most previous studies reported pro-proliferation activities by hi and lo isoforms, a study by Lemiere and colleagues reported that tetracycline- -regulated overexpression of hi FGF2 in C6 rat glioma cells elicited mitotic arrest, which was not observed by lo FGF2 overexpression [56]. The inhibitory effect was mediated by preventing 4E-BP1 phosphorylation. These findings are similar to studies from Dr. Kardami's laboratory on cardiomyocytes [57] and HEK 293 cells [58], as will be discussed in section **1.1.8**.

There are very few data comparing effects of hi versus lo FGF2 overexpression on cell differentiation. In PC12 cells, lo FGF2 promoted differentiation towards a neuronal phenotype while hi FGF2 stabilized an endocrine phenotype, corroborating the idea of FGF2 isoform-specific effects on cell differentiation [59].

The profiles of gene transcription in response to hi versus lo FGF2 overexpression in stable cell lines have been studied by Quarto and her colleagues [60]. In NIH 3T3 fibroblasts stably expressing different FGF2 forms, cDNA microarray-based study has indicated hi but not lo FGF2 stimulates transcription of genes associated with growth inhibition and tumor suppression activities. Levels of proteins expressed by genes whose mRNA level has been modified by hi FGF2 overexpression has not been examined so far.

1.1.6.3 Different effects of added hi or lo FGF2 on cultured cells

Very few studies have been published comparing the effects of added pure hi versus lo FGF2 on cells in culture. The assumption has been that because both hi and lo FGF2 bind to the same FGF receptors and HSPG low-affinities receptors, their downstream effects would be similar. This assumption was seriously challenged by Levin and colleagues [61]. They reported that lo and hi FGF2 have completely opposite effects on cell migration of bovine arterial endothelial cells (BAEC) [61]. Hi FGF2 also inhibited migration of mammary carcinoma cells (MCF-7) induced by insulin-like growth factor-1 (IGF-1) which served as the chemoattractant [61].

The FGFR1–mediated estrogen receptor (ER) activation is required for the inhibitory effect of hi FGF2 on migration, as demonstrated in subsequent studies [62]. Interestingly, lo FGF2, despite activating FGFR1, fails to activate ER. Finally, a truncated mutant of hi FGF2 consisting of the 55 amino acids of the amino-terminal end and the first 31 amino acids of the core sequence, retained ability to inhibit migration and was equally effective as wild-type hi FGF2 [63]. Some of the heparin-binding ability of lo FGF2 is attributed to the region within these 31 amino-acids, and thus it is possible that heparin-binding is required for the hi FGF2 specific effect on migration.

The effect of lo and hi FGF2 on cell growth was also studied using BAEC and MCF-7 by the same group. Even though both lo and hi FGF2 were equally effective in promoting proliferation of MCF-7 cells, lo FGF2 promoted BAEC proliferation in a dose-dependent manner whereas hi FGF2 had no effect at any concentration [61]. However, the related signaling transduction leading to such different effect by hi and

lo FGF2 remains undefined.

1.1.6.4 Different biological activities of FGF2 isoforms *in vivo*

The *in vivo* expression pattern of FGF2 has been examined by measuring FGF2 transcript level, IRES activities and protein levels. FGF2 transcripts exist in most developing and adult human organs including brain, heart, lung, pancreas, and IRES activities were detected in adult brain and testis by analyzing transgenic mice expressing a bicistronic luciferase vector with a FGF2 IRES segment [3]. However, the most direct evidence regarding hi and lo FGF2 protein distribution is provided by Western blotting analysis following tissue protein extraction and SDS-PAGE.

Lo FGF2 is considered to be ubiquitously expressed while hi FGF2 is detected in a number of tissues including heart, testis, brain, adrenal gland, eye, aorta, lung, peripheral nerves [3]. It should be noted when considering tissues composed by heterogeneous cell populations, that different types of constituting cells may have different FGF2 isoform expression patterns. For example, Chlebova et al. reported that human epiphyseal growth plate cartilage is responsible for bone growth and is composed of proliferating chondrocytes making both hi and lo FGF2 as well as non-proliferating cells expressing only lo FGF2 [3]. These findings might require re-examination for confirmation.

The physiological and pathophysiological roles of FGF2 have been investigated via genetic experiments using knock-out and knock-in transgenic mice. Studies on FGF2 knockout (KO) mice, in which all isoforms of FGF2 are absent ($FGF2^{-/-}$ [64] &

FGF2 $^{\text{exon 3-ko/exon 3-ko}}$[65]) has indicated that FGF2 functions to regulate vascular tone, bone remodelling，and cortical neurogenesis[66]. To differentiate between FGF2 isoform-specific functions, two transgenic mouse strains, in which lo FGF2 or hi FGF2 was ablated (FGF2$^{\text{lmw-ko/lmw-ko}}$ [67]or FGF2$^{\text{hmw-ko/hmw-ko}}$ [66]）, respectively, were generated. The hi FGF2 knockout mice show normal fertility and life span, normal myocardial architecture, blood vessel and cardiac capillary density, as their lo FGF2 knockout counterpart [66]. A significant decrease in the recovery of post-ischemic contractile function in lo FGF2-deficient heart, compared to wildtype hearts was discovered, indicating a cardioprotective effect for lo FGF2 in ischemia-reperfusion (I/R) injury [68]. In contrast, hi FGF2-deficient hearts exhibited significant improvement in post-ischemic recovery of cardiac function [69], indicating that hi FGF2 contributes to the development of post-ischemic myocardial dysfunction [69]. Another strain of transgenic mice engineered to overexpress the human hi FGF2 (24 kDa) isoform was also analyzed in the I/R models in the same studies and consistently, a significant decrease in the recovery of cardiac function from I/R injuries was observed [69]. FGF2 was implicated in 17 beta-estradiol (E2)-induced angiogenesis and endothelial cell migration and proliferation *in vivo* [67]. Studies on lo FGF2 knockout mice subject to E2 treatment suggested a physiological role for the intracellular hi FGF2 in mediating the effect of estradiol on endothelial cell growth and migration, even though direct evidence is missing due to the absence of Fgf2 hmw-/- mice in these experiments [67].

Another strategy to study hi and lo FGF2 *in vivo* is to overexpress hi or lo FGF2

in cultured cells via transient transfection, followed by implantation of overexpressing cells into recipient animals. NBT-II cells, a type of rat bladder carcinoma cells, were transfected with hi or lo FGF2 or vehicle, followed by subcutaneous implantation into immunodeficient nude mice [70]. Spontaneous lung metastases were only seen in mice implanted with cells overexpressing hi but not lo FGF2 or vehicle vector. These findings suggested that endogenous hi FGF2 may play a role in activating a metastatic property of carcinoma cells.

The effect of hi and lo FGF2 overexpression on neuronal regeneration was examined by Grothe and colleagues. Schwann cells have been tested as artificial nerve grafts to reconstruct massive defects in the peripheral nerves, and with overexpression of different isoforms of FGF2, the Schwann cells exhibit significantly different regeneration-promoting effects. Lo FGF2 had an inhibitory effect on myelination of regenerating axons, whereas hi FGF2 mediated early recovery of sensory functions and stimulation of long-distance myelination of regenerating axons [71]. These findings might serve to develop new therapeutic strategies in peripheral nerve repair by engrafting hi FGF2-overexpressing Schwann cells to assist in axonal regeneration.

1.1.7 Hi FGF2 interacting proteins

1.1.7.1 FGF2-interacting-factor

FGF2-interacting-factor (FIF), also known as anti-apoptotic protein 5 (Api5) or AAC11, is a nuclear protein and exists as either full-length (55 kDa) or

N-terminally truncated (25 kDa) variants [72]. This protein is ubiquitously expressed in embryonic and adult tissues, and in various human tumor cell lines, and functions as a potent anti-apoptotic factor [72]. Overexpression of FIF in BALB/c3T3 fibroblasts allow cultures to survive in serum-free medium for up to 12 weeks, compared to 10 days for wild-type cells [73]. In cervical carcinoma cells, FIF overexpression allows transfected cells to survive in serum-free medium for up to 2 weeks, compared to 1 week for vector alone or wild-type cells, and the invasion of carcinoma cells was significantly enhanced in response [74].

The interaction between FGF2 and FIF was identified through the screening of GAL4-based yeast two-hybrid expression libraries, using 24kDa or 18kDa FGF2 isoforms as bait [72]. FIF seems to interact equally well with both isoforms of FGF2 in the test tube, indicating that the FIF-binding motif is located within the C-terminal 155 amino acids. Interestingly, co-immunoprecipitation experiments showed that only hi FGF2 bound to FIF within cells. The structural basis of this difference is still unknown. In terms of functional significance, it seems that hi FGF2 requires FIF to mediate estradiol induced angiogenesis *in vivo* and endothelial cell migration and proliferation *in vitro* [67].

1.1.7.2 Survival of motor neurons protein (SMN), arginine methyltransferase 5 (PRMT5) and splicing factor 3a (SF3a66)

SMN is a 38 kDa protein found in the cytoplasm and nucleus of all types of cells [36]. As a key component of small nuclear ribonucleoproteins (snRNPs), SMN

regulates the assembly of the RNA-protein complex responsible for pre-mRNA splicing. Loss or mutation of the survival motor neuron 1 gene (SMN1) leads to reduced protein level or dysfunction of SMN. This is clinically associated with spinal muscular atrophies (SMAs), a common form of neurogenetic disorder characterized by the loss of lower motor neurons and atrophy of muscle [75]. It appears that SMA plays an essential role in cellular survival exclusively in lower motor neurons, because SMA, caused by reduction of the ubiquitously expressed protein, affects only this portion of the body [36]. The interaction of hi but not lo FGF2 with SMN in Schwann cells has been shown in co-immunoprecipitation experiments and immunofluorescence microscopy revealed that hi FGF2 and SMN co-localize in the nucleoplasm and nuclear gems [36]. Another SMN-binding protein is PRMT5 that methylates SMN for its function in snRNP assembly; it also interacts with hi but not lo FGF2 [22]. PRMT5, SMN and hi FGF2 proteins exist in a common complex in Schwann cells.

Another protein involved in mRNA modification was also found to interact with FGF2. Through a yeast two-hybrid screen with lo and hi FGF2 as bait and pull-down assays, the 66-kDa subunit,SF3a66, was discovered [76]. The splicing factor binds to both lo and hi FGF2 isoforms, suggesting the portion responsible for the interaction is located on the common core sequence of the two FGF2 isoforms.

The two interacting proteins, SMN and SF3a66 are involved in similar pathways, suggesting that FGF2 might play a novel intra-nuclear role in the modulation of splicing processes within cells, even though supportive evidence is

missing.

1.1.8 Findings in Dr. Kardami's laboratory

1.1.8.1 FGF2 isoforms and acute cardioprotection

FGF2 and its role in the adult heart have been studied in Dr. Kardami's laboratory over many years. In earlier studies, work by Padua and others [77-78] demonstrated that administration of lo FGF2 to the isolated perfused adult rat heart prior to ischemia elicited significantly better functional recovery, and reduced muscle damage after ischemia and reperfusion. Those protective effects were dependent on protein kinase C activity. Later studies [79-80] showed that intra-cardial injection of lo FGF2 during coronary occlusion in an *in vivo* model of 'heart attack' elicited significantly smaller infarcts and better functional recovery, both acutely and in a sustained fashion, detectable 6-8 weeks post-infarction. The beneficial effects of lo FGF2 were evident even if it was administered after ischemia and during reperfusion [79]. In terms of the signal transduction mechanism mediating beneficial effects, it was found that a lo FGF2 mutant carrying a serine to alanine (S105A) mutation, characterized by diminished affinity to FGFR1, was no longer cardioprotective. This showed that binding to FGFR1 mediates lo FGF2 cardioprotection [80]. Another lo FGF2 mutant, carrying a mutation (S117A) rendering it incapable of activating casein kinase II (CK2), and stimulating DNA synthesis was still capable of acute cardioprotection, indicating that CK2 was not required for this acute effect [79]. In summary, the acute cardioprotective effects of lo FGF2 are mediated by FGFR1-PKC,

but not CK2.

Administration of recombinant hi FGF2 to the perfused heart (ex vivo) or during myocardial infarction *in vivo* was as effective as lo FGF2 in eliciting acute cardioprotection [81-82]. When administered during reperfusion, hi FGF2 was as effective as lo FGF2 in protecting from ischemia-reperfusion injury; both hi and lo were effective in activating cardiac PKC α, ε, ζ as well as the Akt pathway; however hi FGF2 appeared more potent compared to lo FGF2 in promoting translocation of PKC ζ to membrane compartments, and in activating S6 kinase [81].

1.1.8.2 Chronic effects of FGF2 isoforms.

Although both hi and lo FGF2 were, when administered directly to the heart, equally protective from ischemic injury in the short term, differences emerged when the long term effects were studied. Thus, while lo FGF2-induced protection was sustained, resulting in non-hypertrophic hearts and increased angiogenesis at 6-8 weeks post-treatment, hi FGF2 administration *in vivo* resulted in development of substantial myocardial hypertrophy, detectable at 2-8 weeks post treatment, no angiogenesis, and functional deterioration at later time points [82]. A direct hypertrophic effect of hi but not lo FGF2 was further confirmed in *in vitro* studies, using neonatal cardiomyocytes [82]. Thus it would appear that hi and lo FGF2 elicit isoform-specific long-term effects in the heart, detrimental and beneficial, respectively. The mechanism mediating these differences requires further investigation.

1.1.8.3 Expression of FGF2 isoforms during cardiac injury

Early studies [83] showed that isoproterenol-induced cardiac injury was associated with an early (24 h) transient elevation in cardiac hi FGF2, coinciding with cardiomyocyte damage as well as cellular infiltration. Later studies [84] showed significant upregulation of cardiac hi FGF2 in a mouse model of exaggerated cardiac hypertrophy and fibrosis. Taken together, these data suggested that hi FGF2 may be actively involved in cardiomyocyte damage and overall cardiac pathology. This question was addressed by gene transfer-mediated expression of hi and lo FGF2.

1.1.8.4 Effects of ectopically expressed FGF2 isoforms in cardiac myocytes and HEK 293 cells

Specifically engineered rat cDNAs expressing only lo or only hi FGF2 were introduced in neonatal cardiomyocytes [85]. These studies showed a predominantly nuclear localization for hi FGF2, while lo FGF2 was detected in both cytoplasmic and nuclear compartments. Unexpectedly, hi FGF2 overexpression was associated with nuclei containing variable numbers of condensed chromatin "clumps"; this effect was absent in lo FGF2 overexpression. These differences between rat hi and lo FGF2 regarding effects on nuclear phenotype were found to also hold true for human hi and lo FGF2 expressed in rat cardiomyocytes [86].

These studies were limited by relatively low transfection efficiency afforded by the conventional, calcium-phosphate-mediated, gene-transfer techniques in primary cells. This limitation was overcome by the construction of adenoviral vectors

expressing lo or predominantly hi human FGF2, and generously provided to our lab by Dr. Meenard Herlyn (Wistar Institute, Philadelphia) [87]. These adenoviral vectors achieve a nearly 100% transfection efficiency in cardiomyocytes, nearly 50% of which displayed the condensed chromatin phenotype [57]. Using these reagents it was determined that chromatin compaction induced by hi but not lo FGF2 was linked to inhibition of mitosis, and promotion of cell death with apoptotic features [57].

In my Master's project, I investigated the effects of ectopically expressed rat as well as human hi versus lo FGF2 using HEK 293 cells. In these studies I established that the ability of hi FGF2 to elicit a compacted nuclear phenotype was neither species nor cell-type specific. My studies also showed activation of caspase 3 in hi FGF2 transfected cultures, indicating that the observed DNA condensation was linked to apoptosis. I also showed that ERK½ activity was required for the effect of hi FGF2; finally, I found that shuttling of hi FGF2 to the nucleus was necessary for induction of DNA condensation since a cytoplasmic hi FGF2 mutant, carrying R149G and R151G mutations, failed to elicit DNA condensation at all [58]. Overall, my Master's studies established a reliable cell line model to investigate the mechanism of hi FGF2-induced chromatin compaction and cell death, and furthermore, identified ERK½ and mitochondrial engagement in mediating the nuclear events.

1.2 Apoptosis

1.2.1 General introduction

The term apoptosis was first used by Kerr, Wyllie and Currie in 1972 to

describe a morphologically distinctive form of cell death [88]. It was found to occur during various physiological processes including, amongst others, normal cell turnover, adaptive immunity activation (both cell-mediated and humoral immunity) and hormone-dependent atrophy [89]. Apoptosis plays a pivotal role in embryogenesis in both invertebrate and vertebrate organisms. One of the remarkable early (1999) studies concentrated on the development of an invertebrate, the nematode *Caenorhabditis elegans* [90]. In this organism, 131 out of the 1090 somatic cells that form the adult undergo apoptosis at particular developmental stages and this is invariant between worms of same species. This led to the notion that apoptosis, in this scenario, was genetically determined as an eliminating event. Apoptosis was therefore accepted as a unique form of "programmed" cell death, until other forms of programmed cell death were discovered [91-93]. Apoptotic events were documented in human embryonic growth as well, in neuronal and nephric development as well (Langman's Medical Embryology, Sadler, T. W. 2006). More than 50% of neurons are lost by apoptosis during development as a result of limited neurotrophic support from the target tissue they are destined to innervate [94]. In the adult, apoptosis is responsible for normal cell turnover and therefore maintaining homeostasis in multicellular organisms. Inappropriate apoptosis (too much or too little) may be a primary etiological factor contributing to many human diseases, such as neurodegenerative diseases, autoimmune disease and carcinogenesis. Furthermore, apoptosis has also been implicated in contributing to cardiovascular diseases including ischemia- and ischemia-reperfusion- induced damage, and drug-induced

cytotoxicity [89].

1.2.2 Morphological features of apoptosis

Dynamic morphological changes occur during apoptosis [88]. The dying cell displays nuclear pyknosis, cell shrinkage, denser cytoplasm and more tightly packed organelles. Histological examination using hematoxylin and eosin staining reveals the apoptotic cell as a round or oval shape with dark eosinophilic cytoplasm and dense purple nuclear DNA fragments. Subsequent events include extensive plasma membrane blebbing, followed by chromatin fragmentation (karyorrhexis), and finally, formation of apoptotic bodies via a process termed “budding”. The apoptotic bodies represent plasma-membrane-bound cytoplasm surrounding pockets of densely packed organelles with or without nuclear fragments. The budding bodies are phagocytosed by macrophages and degraded by digestive enzymes after fusion of phagosomes and lysosomes. Apoptosis is not associated with an inflammatory response and this serves as one of the distinguishing criteria between apoptosis and necrosis [89]. The absence of inflammation may be attributed to an intact plasma membrane enclosing the organelles within apoptotic bodies preventing the release of detrimental, pro-inflammatory molecules into the interstitial environment; in addition, phagocytosis by surrounding cells does not release pro-inflammatory cytokines such as tumor necrosis factors and reactive oxygen species [89].

1.2.3 Biochemical features of apoptosis

Caspases, a group of proteolytic proteins expressed in most types of cells, play a critical role in apoptotic events. These enzymes exist as inactive pro-enzyme forms (pro-caspases). The pro-enzyme, once activated, can subsequently cleave (at an aspartic acid site) and activate other pro-caspases, therefore initiating a protease cascade. [95]. At present, ten major caspases have been identified and different pathways leading to apoptotic events may involve different caspases. [89]. The involvement of Ca^{2+}-and Mg^{2+}-dependent endonucleases is another significant biochemical feature accounting for chromatin fragmentation (karyorrhexis) in apoptosis [89]. A diagnostic marker of karyorrhexis is the characteristic "DNA ladder" seen in agarose gel electrophoresis. Another biochemical feature is movement of phosphatidyl-serine that is normally found in the inner leaflet of the lipid bilayer to the outer layer of the plasma membrane [96]. This exposed phosphatidyl-serine serves as recognition signal for phagocytic cells to surround and engulf the apoptotic cells, minimizing the damage to adjacent normal tissues. Certain proteins including annexin I [97], annexin V [98] and calreticulin [99] also translocate to the cell surface and serve as recognition ligands as well. All these signals are believed to work cooperatively to allow quick identification and ensuing clearance of apoptotic cells [89]

1.2.4 Mechanisms of apoptosis

To date, two major pathways are widely accepted: the extrinsic or death receptor pathway and the intrinsic or mitochondrial pathway [100]. There is cross-talk between

the two pathways [101]. Studies of the extrinsic pathway dominated the field in the 1990s until mitochondrial engagement was discovered by Xiaodang Wang's group in 1996 [102]. The extrinsic pathway is initiated by interaction of transmembrane death receptors with their corresponding ligands. The best-characterized ligands and corresponding death receptors include FasL/FasR, TNF-α/TNFR1, Apo3L/DR3, Apo2L/DR4 and Apo2L/DR5 [89]. The sequences of events that define the extrinsic phase of apoptosis are best documented for FasL/FasR and TNF-α /TNFR1. In this model, upon binding of ligand to receptor, the adaptor Fas-associated death domain (FADD) and procaspase-8 are recruited locally to form a death-inducing signaling complex (DISC) [103]. The DISC formation leads to cleavage of the associated procaspase-8 into the active caspase-8, marking the initiation of the execution phase of apoptosis [104]. Caspase-8 can directly cleave and activate caspase-3 and as a consequence, trigger effector molecules, such as endonucleases, to exert their pro-apoptotic effect. The execution pathway will be discussed at the end of this review.

The intrinsic pathway leading to apoptosis is initiated by a great variety of stimuli that do not act via membrane-bound receptors but are instead generating intracellular signals. Such signals may include, but are not limited to, suppression of anti-apoptotic factors or upregulation of pro-apoptotic factors within the cells. Mitochondria play a crucial role in these intrinsic pathways. The first evidence of mitochondrial engagement was suggested by the discovery that Bcl-2 lacking the C-terminal transmembrane domain failed to anchor in the outer mitochondrial

membrane and was unable to prevent apoptosis [105]. Soon after, mitochondrial permeability transition (MPT), a non-specific channel (pore) formation and opening at the inner mitochondrial membrane, resulting in release of mitochondrial contents including cytochrome C into the cytosol, was reported. More significantly, the released cytochrome C was essential for caspase-3 activation [102] while the protective effect of Bcl-2 was achieved by preventing release of cytochrome C from mitochondria [106]. Formation of the mitochondrial permeability transition pore elicits disturbances in mitochondrial transmembrane potential and two major groups of pro-apoptotic factors normally sequestered in mitochondria are released [107]. The first group, including cytochrome C, Smac/DIABLO and the serine protease HtrA2/Omi, is released into the cytosol and activates the caspase-dependent pathway. The second group, including apoptosis inducing factor (AIF) and endonuclease G (Endo G), translocates from mitochondria to the nucleus and stimulates apoptosis in a caspase-independent fashion. Nuclear apoptosis inducing factor elicits chromatin condensation and activates nucleases to fragment DNA into 50–300 kb pieces. Endonuclease G also serves as an execution effector, cleaving the chromatin to produce DNA fragments. AIF and endonuclease G are not thought of as initiators of apoptosis because their translocation occurs after the cells are already committed to die.

The execution phase, the final pathway of apoptosis, is the convergence of both extrinsic and intrinsic pathways. The initiation of this phase of apoptosis is marked by activation of the execution caspases including caspase-3, caspase-6, and

caspase-7[108]. These execution caspases will subsequently activate cytoplasmic endonucleases for degrading nuclear material, and proteases for degrading nuclear and cytoskeletal proteins. Caspase-3, the most important of the executioner caspases, is activated by caspase-8, caspase-9, or caspase-10 [109]. Under healthy conditions, the endonuclease, caspase-activated DNase (CAD) is complexed with its inhibitor, ICAD. However, in apoptotic cells, ICAD is cleaved by caspase-3, releasing CAD which cleaves chromosomal DNA within the nuclei and causes chromatin condensation [110]. Caspase-3 also elicits cytoskeletal disintegration and reorganization of the cell into apoptotic bodies by acting on an actin-binding protein, gelsolin, recognized as one of the key substrates of caspase-3 [111]. Gelsolin, following cleavage by caspase-3, will cleave its complexing actin filaments resulting in disruption of the cytoskeleton and reorganization of cellular morphology.

1.2.5 Role of cytochrome C in apoptosis

Cytochrome C is a small heme protein found in the electron transport chain in the inner membrane of the mitochondrion. It undergoes oxidation and reduction reactions, transferring electrons between complex III (Cytochrome b-c1 complex) and complex IV (Cytochrome C oxidase complex). The first hint about the role cytochrome C in apoptosis stems from the discovery by Xiaodong Wang's group that cytochrome C was present in the cytosol and responsible for caspase activation in a cell-free system [102]. Subsequent studies further confirmed its association with apoptosis biochemically and genetically. First, recombinant cytochrome C was

purified and its competence to activate caspase in total extracts from non-apoptotic cells was established [102]. Second, a protein complex termed apoptosome, composed of cytochrome C, Apaf-1, procaspase-9 and dATP was identified in the cytosol. Cytochrome C, upon release into cytosol, interacts with the cytosolic protein Apaf-1 and subsequently the third component, dATP, and the fourth one, procaspase 9, are recruited sequentially. The formation of the complete complex, termed apoptosome, results in cleavage and activation of procaspase-9 into its active form, triggering a caspase cascade of events leading to apoptosis [105]. Genetically, cytochrome C-deficient mice fail to survive due to the obligatory role of cytochrome C in cellular respiration. This makes it impractical to study its requirement for apoptosis in animals via this transgenic methodology. However, a cytochrome C mutation of lysine 72 to alanine (K72A) was soon established, which retains the protein function for normal electron transfer but fails to recruit Apaf-1. This finding was applied to generate 'knock-in' mice and comprehensive analysis including the cellular response to pro-apoptotic stimuli, was performed. It was found that the mutation significantly reduces the interaction of cytochrome C with Apaf-1, reduces caspase-3 activation by ten-fold *in vitro*, and enhances cellular resistance to apoptotic stimuli, whereas the normal cytochrome C release and its respiratory function were not affected [112].

1.2.6 The role of Bcl-2 family proteins in mitochondria-mediated apoptosis

Crucial evidence linking apoptosis and mitochondria emerged when Bcl-2 (B-cell lymphoma 2) was found to inhibit cell death [113]. The protein is encoded by

Bcl-2 gene found in the immunoglobulin locus on chromosome 18q and initially was discovered during the cloning of one of the most frequent translocations in follicular lymphomas [114]. Subsequent studies revealed the genes encoding 20 Bcl-2 relatives in mammals, all of which shared at least one conserved Bcl-2 homology (BH) domain and possess apoptosis-regulating activities [115]. Functional analysis reveals that the Bcl-2 family includes five anti-apoptotic / prosurvival proteins (Bcl-2, Bcl-xL, Bcl-w, A1 and Mcl-1) and seven pro-apoptotic proteins. The anti-apoptotic proteins consist of four Bcl-2 homologous (BH) domains (BH1, BH2, BH3, and BH4), whereas the pro-apoptotic Bcl-2 group is divided into two groups of proteins depending on the number of BH domains: Bax, Bak and Box contain three BH domains (BH1, BH2, BH3) (collectively termed Bax death family in some literature) and the BH3-only family (Bad, Bik, Bim and Bid) contains only one BH3 domain (hence their names) [115]. The anti-apoptotic members secure mitochondrial integrity, prevent cytochrome C release and rescue cells from apoptotic death, while the proapoptotic Bcl-2 proteins possess the opposite effect. It should be noted both groups of pro-apoptotic members of Bcl-2 family proteins (Bax death family and BH3-only family) are required to initiate apoptosis[105].

Two important findings have been reported illustrating the central role of Bax/Bak in apoptosis: first, *bax−/−bak−/−* double knock-out cells exhibit extreme resistance to a great array of apoptotic stimuli [116]; second, neither activation of BH3-only proteins nor suppression of pro-survival Bcl-2 proteins is adequate to induce apoptotic events in the absence of both Bax and Bak [117]. These findings

suggest other Bcl-2 proteins work as positive and negative regulators targeting the Bax and Bak proteins.

Detailed studies have been conducted on the behavior of Bax proteins in apoptosis. Under healthy conditions, Bax exists as a monomer (26kDa) in the cytosol and when the cell is subjected to a pro-apoptotic stimulus, it translocates to mitochondria, oligomerizes to form foci on mitochondria and induces cytochrome C release [115]. The next question would be how other Bcl-2 proteins regulate this process, thus exerting anti- or pro-apoptotic effects. Two hypothetical models have been proposed regarding these questions, although no final conclusions have been reached. The direct activation model [118] states that BH3-only proteins (Bim/Bid/Puma) interact with antiapoptotic Bcl-2 proteins under healthy state, and apoptotic stimuli would dissemble the complex and release BH3-only proteins. Consequently, the freed BH3-only proteins activate Bax, resulting in the downstream cell death event. In the indirect model [119] Bcl-2 anti-apoptotic proteins interact with Bax under normal conditions, thus guarding the mitochondria from Bax invasion. Upon induction of apoptosis, the BH3-only proteins replace Bax to complex with the anti-apoptotic proteins, therefore releasing Bax to trigger its downstream effect on mitochondria. Solid evidence does exist for both models and the contradictions between two models have not been explained in a satisfactory way to date. However, there is no doubt that interaction between three groups of proteins (Bcl-2 prosurvival proteins, BH3-only proteins, Bax) is a key event in activating Bax-mediated mitochondrial disintegration and cytochrome C release.

Another important and unsolved issue is how Bax induces cytochrome C release after translocation into and oligomerization on mitochondria. Crystallization studies have revealed that three-dimensional structures of the Bax proteins resemble certain bacterial exotoxins capable of punching holes in the membranes to kill cells [120]. Also in cell-free systems, Bax complexes with Bid and lipids to form openings in the outer mitochondrial membrane, allowing passage of up to 2000-kDa molecules [121]. This might represent part of the mechanism mediating Bax-induced cytochrome C release.

1.2.7 The role of Akt in apoptosis

Akt, also known as protein kinase B, is a cytoplasmic serine/threonine kinase that phosphorylates substrates which collectively contribute to the control of cellular metabolism and the programmed cell death machinery. It is therefore referred to as survival kinase by some [122]. Its protective role in apoptosis was first indicated in experiments by Wendel and colleagues, during a screen for suppressors of myc protein-induced apoptosis [123]. To date, the pro-survival effect of an Akt-mediated pathway has been confirmed in various apoptotic models. For instance, activated Akt prevents cardiomyocyte apoptosis induced by multiple pathological insults including ischaemia and reperfusion, pressure overload, hypoxia, hypoglycaemia and cardiotoxic drugs[124]. Genetic studies have shown that mammalian cells possess three closely related Akt genes that generate Akt1, Akt2, and Akt3 presenting functional differences. The classical activation pathway of Akt upon interaction of

extracellular ligands with the plasma membrane receptors has been well documented [124] . Briefly, Akt is associated with the plasma membrane in an inactive state and upon stimulation of tyrosine kinase/cytokine receptors or G-protein coupled receptors, phosphoinositide 3-kinase (PI3K) catalyses the phosphorylation of phosphotidyl-inositol 4, 5-bisphosphate (PIP2) into phosphatidylinositol (3, 4, 5)-trisphosphate (PIP3). Increased PIP3 levels recruit phosphoinositide-dependent protein kinase 1 (PDK1) to the membrane, resulting in its activation, followed by cytoplasmic Akt recruitment and phosphorylation on Thr308 residue by PDK1. The partially activated Akt dissociates from the plasma membrane, accumulates in the cytoplasm and translocates to the nucleus. Before exerting its multifunctional effects, a second phosphorylation at Ser473 has to occur, mediated by the mammalian target of rapamycin complex 2 (mTORC2). Dually phosphorylated Akt is then able to phosphorylate a great array of downstream targets in the cytosol and nucleus, regulating various cellular processes. These include glucose transport, glycolysis, glycogen synthesis, suppression of gluconeogenesis, protein synthesis, cell size enlargement, cell cycle progression, repression of apoptosis, and preservation of mitochondrial integrity. Certain important apoptotic regulators or mediators have been identified as downstream substrates phosphorylated by Akt molecules, which may account for its repressing effects on apoptotic events. The mechanisms through which Akt prevents apoptosis include, but are not limited to, the following: Akt directly phosphorylates and inactivates the proapoptotic Bcl-2 protein Bad [125]; Akt and serine/threonine-protein kinase 1 (SGK1) act synergistically to phosphorylate and

inactivate Forkhead homolog 1 (rhabdomyosarcoma)-like protein 1 (FKHRL1), a transcription factor that up-regulates pro-apoptotic Bcl-2 proteins such as Bim and death receptor components such as death receptor 5 [126]; Akt regulates the IκB/NF-κB transcription factor complex by phosphorylating the serine/threonine kinase Cot[127], resulting in the proteasomal degradation of IκB, the activation of NF-κB, and the transcription of an array of antiapoptotic genes; Akt phosphorylates and activates MDM2, a protein that binds p53 and facilitates its degradation, thus preventing p53-mediated apoptosis [128]; Akt phosphorylates and thus inactivates caspase-9 [129] and Bad, and phosphorylates and thus stabilizes the anti-apoptotic protein XIAP [130], inhibiting mitochondrial-dependent apoptosis. In cardiomyocytes, the cellular targets of Akt mediating anti-apoptotic effects reside within the nuclear compartment. Sussman and colleagues have shown that Akt targeted to the nucleus (Akt-nuc) exerts significant cardioprotective, proliferative, and inotropic effects in cardiomyocytes [124], corroborating the notion that the Akt translocating to nuclei after activation accounts for its pro-survival effects. The same group reported that the anti-apoptotic effect attributable to Akt is mediated by a downstream kinase, PIM-1 [131]. PIM-1 belongs to a three-member family of serine/threonine kinases, which shares homology and largely overlapping functions with other two family members, Pim-2 and Pim-3, although the latter two are expressed not as highly as PIM-1 in the heart [124]. PIM-1 is constitutively active and thus its level of activity is regulated by its intracellular accumulation [132]. Akt has been shown to mediate upregulation of PIM-1 by variety of hormones, cytokines, and mitogens, many of which are

associated with cardioprotective signaling [124]. Overexpression of nuclear Akt also increases PIM-1 levels within cells [133]. The downstream signals phosphorylated by PIM-1 include proteins mediating transcription, cell growth, proliferation, and survival [124]. The anti-apoptotic effects of PIM-1 may be partially accounted for by its cytosolic actions. PIM-1 inactivates the pro-apoptotic Bad protein via phosphorylation and enhances Bcl-2 activity [124]. Furthermore, PIM-1 enhances mitochondrial resistance to calcium-induced swelling and inhibits cytochrome C release in response to apoptotic stimuli [134]. The cytoprotective effects of increased nuclear Akt are believed to be mediated, at least in part, by PIM-1 upregulation.

1.2.8 Apoptosis and Heart Diseases

Apoptosis has been detected in the developing, normal as well as diseased heart. In the developing heart, programmed cell death is essential to form cardiac valves and outflow tracts including the aorta and pulmonary arteries [135]. Apoptosis is reported to be a very rare event in normal human adult hearts, with prevalence of one TUNEL positive cardiomyocyte in 10,000 [136] and its physiological role remains under investigation. The rate of cardiac myocyte apoptosis can increase several hundred fold under pathological circumstances, including dilated and ischemic cardiomyopathies, hypertrophic heart disease and arrhythmogenic right ventricular dysplasia [137]. For instance, quantitative estimates of apoptosis in the hearts of patients with end-stage cardiomyopathy shows up to 6,500 apoptotic nuclei per million myocytes counted in the failing hearts, a 230-fold increase in apoptosis compared with non diseased hearts

[138]. Even so, the absolute prevalence is typically < 1%, raising the question whether such low levels of apoptosis can produce heart failure. It should be noted that a small amount of cell loss over time in an organ like the heart with very limited capacity for regeneration can create a significant reduction in cardiac muscle mass leading to heart failure, as has been corroborated in animal models [139]

Signal transduction leading to apoptotic events in cardiomyocytes involves cytosolic release of cytochrome C and activation of caspase-3 [139]. As described in the reviews on apoptotic mechanisms, cytochrome C release and caspase-3 activation are the hallmarks of apoptotic processes, which normally conclude in fragmentation of nuclei and cell death. However, there are some interesting variations in the progression of apoptosis in failing hearts. The histological examination of failing hearts reveals a large number of cardiomyocytes displaying cytochrome C release and caspase-3 activation but possessing apparently normal nuclei, thus remaining unaffected by the apoptotic process [137]. This finding points to a possible cessation of the apoptotic process before it is completed. This phenomenon lacking terminal morphological features of apoptosis despite the activation of the apoptotic pathway have been widely documented and defined as “apoptosis interruptus” , while cardiac myocytes that exhibit these features have been labeled as “zombie myocytes” [140]. The mechanisms halting dying cells from completing the apoptotic process, and the significance of such incomplete death, remain to be elucidated.

1.3 ERK and cell death: mechanisms of ERK-induced apoptosis

1.3.1 General introduction

ERK1⁄ERK2 (also known as p42 ⁄ p44 MAPK) are two isoforms of the extracellular signal-regulated kinase (ERK) belonging to the family of mitogen-activated protein kinases (MAPKs) [141]. These enzymes are activated through a sequential phosphorylation cascade initiated upon binding of extracellular ligands to membrane-bound receptors, and mediate signal transduction to the nucleus [142]. In brief, ligand-induced receptor activation on the plasma membrane is followed by recruitment of one of the Raf kinases, A-Raf, B-Raf and C-Raf (or Raf1) to membrane-bound GTP-loaded Ras. The complexing of Ras and Raf results in Raf activation and the active form subsequently phosphorylates two serine residues on the kinase mitogen protein kinase kinase 1 and 2 (MEK1⁄ 2), which in turn activate ERK½ by phosphorylating threonine and tyrosine residues on the dual-specificity motif (T-E-Y). Upon activation, ERK½ is capable of phosphorylating a number of cytoplasmic and nuclear targets, thus performing important biological functions. The ERK ½ activation is involved in regulating various cellular processes including proliferation, differentiation and migration [143]. There is substantial evidence that ERK ½ promotes cell proliferation as well as survival [144]. However, there is also evidence that ERK ½ activation can have the opposite effect and result in apoptotic cell death. This section will describe situations in which ERK½ activation mediates cell death, and discuss the role of ERK ½ subcellular localization and duration of activation on its effects.

1.3.2 Ras/RAF/ERK½ pathway-mediated apoptosis

An early report documenting the involvement of Ras/Raf/ERK½ in apoptosis can be traced back to 1996: MCF-7 cells were rescued from taxol (an antitumor compound) -induced apoptosis, by lessening Raf via the benzoquinone ansamycin, geldanamycin [145]. Soon after, Watabe and colleagues reported that depletion of MEK by antisense cDNA expression prevented bufalin-induced apoptosis in U937 leukemic cells [146]. To date, studies using MEK inhibitors or expression of the dominant negative form of Ras/Raf/ERK½ pathways in apoptotic cellular models have confirmed the involvement of the Ras /Raf /ERK pathway in cell death events.

A great number of well-established pro-apoptotic stimuli of the intrinsic pathway have been shown to involve Ras/Raf/ERK½ pathways. This statement is best exemplified by apoptosis induced by DNA-damaging agents including cisplatin, doxorubicin, etoposide, ultraviolet light, gamma irradiation and antitumor compounds, such as taxol resveratrol, quercetin, phenethyl isothiocyanate, betulinic acid, apigenin, oridonin, miltefosine, shikonin [141]. The implication of ERK½ in extrinsic pathways was also well documented. The pro-apoptotic stimuli reported so far include, but are not limited to, TNF-related apoptosis-inducing ligand (TRAIL), TNFα, Fas or CD40 ligand [141].

The mechanism by which Ras/Raf/ERK activation mediates intrinsic and extrinsic cell death pathways depends on the cell type and the nature of the injury. The extrinsic pathway involves signal transduction leading to caspase-8 activation that in turn cleaves caspase-3 to initiate the execution phase of apoptosis. ERK½ can

potentiate caspase-8 activation by one of following mechanisms [141]. Either the Ras / Raf /ERK pathway promotes activation of membrane-bound death receptors by extracellular signals through increasing the protein level of death receptors such as Fas, DR4 or DR5 or ERK activation upregulates the expression of Fas-Associated protein with Death Domain (FADD), the adaptor molecule bridging the Fas-receptor to caspase-8, therefore enhancing caspase-8 recruitment and activation. Interestingly, caspase-8 can be activated by ERK½ activities in a death-receptor independent mode suggesting ERK½ can stimulate the extrinsic death pathway free of extracellular pro-apoptotic stimuli [147]

ERK activity is associated with regulation of the expression of the Bcl-2 family of proteins, i.e. upregulation of proapoptotic members Bax, PUMA and Bak while downregulating antiapoptotic members such as Bcl-2 and Bcl-Xl [141]. In addition, ERK has been shown to directly suppress mitochondrial respiration [148] and disturb mitochondrial membrane potential [149]. As a consequence, the mitochondrial membrane is disrupted and cytochrome C is released to trigger the downstream portion of the intrinsic pathway [141].

The p53 protein is a tumor suppressor gene that is upregulated in response to DNA damage [150]. As a transcription factor, p53 regulates a great array of genes, such as Bcl-2 family proteins, to initiate apoptotic events [64]. Degradation of p53 requires an interacting protein Mdm2 that behaves as a ubiquitin ligase toward p53 upon phosphorylation on serine 166 [151]. It should be noted the expression level and transcription factor activities of p53 are key regulating mechanisms by which cells

determine survival or death. DNA-damaging agents have been found to induce p53 upregulation and modulate Bcl-2 protein in an MEK-dependent manner [141] and it is proposed that ERK½ activation may participate in regulation of p53 accumulation or its transcription factor activity within cells in several ways. First, active ERK½ has been shown to directly interact with p53 and the interaction results in p53 phosphorylation on serine 15 by the kinase [152] which functions to stabilize the protein and prevent intracellular degradation by inhibiting p53 interaction with Mdm2 [153]. Secondly, sustained ERK activation results in inhibition of Mdm2 phosphorylation on serine 166, therefore downregulating ubiquitination of p53 for degradation in proteosomes [151]. Thirdly, ERK activity is involved in p53 phosphorylation on threonine 55, which promotes its DNA-binding activity as a transcription factor, resulting in downregulation of Bcl-2 gene expression [154]. To summarize, these findings suggest that upregulation of p53 expression and transcriptional activities, as well as downregulation of p53 degradation, serve as important mechanisms for Ras／Raf／ERK-mediated apoptosis.

1.3.3 ERK-mediated cellular behavior: cell death or survival?

Since activation of Ras/Raf/ERK½ results in cell death or survival, a reasonable explanation for differential response may lie in the duration of ERK½ activation and subcellular localization of active ERK½.

The time-course studies on the majority of apoptotic cell death models mediated by Ras/Raf/ERK½ revealed an activation mode for ERK½, characterized by unusual

duration, in which ERK is maintained phosphorylated for up to 72 h [155]. The prolonged ERK½ activation appears to be required for induction of cell death since even delayed treatment with U0126, a MEK inhibitor, at late stage of ERK½ activation is still able to reverse the induction of apoptotic cell death [147]. After realizing the importance of the sustained mode of ERK ½ activation, the crucial question was how the sustained ERK½ activation is maintained. It appears that reactive oxidative species (ROS) induced by pro-apoptotic stimuli are playing an important role. DNA-damaging agents such as doxorubicin, cisplatin or etoposide catalyze the formation of ROS [156]. In addition, ERK activity has been linked to upregulation of NO synthase expression, accounting for another ROS source [157]. The ROS generated in apoptotic cells sustains ERK½ activation in two ways. First, ROS is capable of activating ERK½, thus potentiating the stimulatory effect of pro-apoptotic stimuli on Ras/Raf/ERK½ [158]. ERK½ activity upregulates NO synthase production, therefore, a positive feedback mechanism may exist between ERK½ activation and ROS production. The signal transduction mediating ROS-induced activation of the Ras/Raf/ERK½ pathway was also examined. ROS can directly oxidize Ras on residue C118, which potentiates its recruitment and activation of Raf at the plasma membrane [141]. In addition, direct oxidation of the cysteine-rich domain of Raf is also documented, resulting in its autoactivation [159]. Secondly, prolonged ERK activity could be attributed to ROS-induced inhibition of tyrosine phosphatases and dual-specificity phosphatase (DUSP). DUSP and tyrosine phosphatases contain a cysteine residue required for their catalytic activity that

dephosphorylates active ERK½ [160-161]. ROS have been shown to oxidize DUSP1 and DUSP6, ERK-directed phosphatases, on catalytic cysteine residues C258 and C293, respectively. ROS alone acts on ERK tyrosine phosphatases PP1/2A on residue C62, abolishing their effect to dephosphorylate active ERK½ [141]. To conclude, these findings suggest ROS is playing an important role in sustained ERK½ activation by different mechanisms. In addition to sustained ERK activity, whether or not the ERK-mediated signaling pathway leads to cell death also depends on its aberrant subcellular localization. Indeed, apoptosis induced by estradiol, tamoxifen, zinc, cephaloridine, doxorubicin, resveratrol or a dominant negative mutant of Rac or Cdc42 are all associated with sustained ERK activity that accumulates within nucleus [141]. In MDA-MB-231 human breast cancer cells, for example, taxol-induced apoptosis correlates to sustained nuclear ERK½ activation and ROS production which could promote such accumulation of active ERK by inhibiting DUSP [162]. In the same studies, overexpression of nuclear DUSP results in the deactivation of nuclear ERK½ and abrogates induction of apoptosis, clearly indicating that nuclear sequestration of ERK½ activity is required for induction of apoptosis. To conclude, active ERK½ aberrantly localizing in the nuclear compartment in a prolonged manner could play a role in mediating apoptotic cell death.

1.4 P68 RNA helicase

The p68 protein, also referred to as DDX5, is one of the first proteins identified as a member of the DEAD box family of proteins [163], that exhibit RNA helicase

activity *in vitro* [164]. The p68 helicase participates in RNA processing and the expression of p68 correlates with organ maturation /differentiation. The significance of this, however, remains elusive [165].

The p68 protein interacts with and serves as a transcriptional coregulator for the nuclear receptor estrogen receptor alpha (ERα) [166]. ERα is a steroid hormone receptor predominantly present in nuclei and is known as a ligand-activated transcription factor. That is, when bound to estrogen diffusing across plasma and nuclear membranes, it undergoes conformational change, dimerizes and binds to a cis-elements known as an estrogen response element sequence. When bound to DNA, the steroid hormone receptors can positively or negatively regulate gene transcription. The p68 protein mimics estrogen hormone in that it interacts with and stimulates the transcriptional activity of ERα, serving as a transcriptional coactivator for ERα -responsive genes [166]. The p68 protein also co-purifies with steroid receptor co-activator, SRC1, and the RNA co-activator, SRA, which are two component proteins found in the trans-element complex of ERα [167]. These findings put forward the hypothesis that p68 may act as a bridge between transcription factors and their coactivators [168].

Recent reports show that p68 acts as a potent co-activator for the tumor suppressor gene p53 [169]. The p53 protein is a transcription factor induced by stress, such as DNA damage, and induces p53-responsive gene expression leading to cell cycle arrest and apoptosis [170]. At least five important pieces of evidence support a role for p68 in the regulatory effect of p53 on gene transcription [169]. P68 was

co-immunoprecipitated with p53 at the p53-responsive promoter region in response to DNA damage. P68 silencing significantly inhibited the expression of p53 target genes in response to DNA damage. Coexpression of p68 up-regulated p53-responsive promoter activities, suggesting that p68 functions as a transcriptional co-activator for p53. Recently, the interaction of p68 with p53 was shown to facilitate the p53-mediated processing of primary micro-RNAs to precursor micro-RNA in HCT116 cells and human diploid fibroblasts. As documented, p53 promotes the post-transcriptional maturation of several microRNAs that suppress translation of proteins involved in cell growth, and this may contribute to mitotic arrest by p53 [171].

In addition, p68 has been shown to interact with, and behave as a transcriptional co-repressor of HDAC1 [172]. The transcription co-activating or co-repressing activities of p68 are independent of its RNA helicase activity. A helicase inactive mutant of p68 stimulates p53 transcriptional activity as efficiently as the wild-type protein and was also reported to activate or repress target genes of ERα and HDAC respectively. These findings indicate the activity of p68 in transcriptional regulation is separate from RNA processing, establishing p68 as a multifunctional protein in multiple cellular processes.

A few words will be dedicated to another DEAD-box helicase protein, p72, due to its close relation to p68 both structurally and functionally. The p72 helicase shares 90% amino-acid sequence homology over the conserved core of p68 while exhibiting significant divergence at the N- and C-termini [167]. This protein also possesses

helicase activities *in vitro*, and referred to as Ddx17. The p68 and p72 helicases can exist as heterodimers [173], leading to the idea that the function of p68 might also be shared by p72. This point has been supported by findings that p72 shows an equally essential role in splicing the *c-H-RAS* and *CD44* genes as p68 [173], and the transcriptional co-regulation activity of p68 for ERα or HDAC are also shared by p72 [165]. However, the co-activating effect of p68 for p53 transcriptional activity is not shared by p72, since silencing p72 (unlike p68) had no effect [169].

1.5 Heat shock protein 70

1.5.1 General introduction

Heat shock protein 70 (hsp70) is a molecular chaperone that is upregulated during the cellular response to various stress conditions and is considered to be protective [174]. In this role, hsp70 functions by binding to its protein substrates to stabilize the native conformation and prevent denaturation or aggregation until conditions improve [175]. However, a mounting body of evidence has suggested that hsp70 plays a role during normal cellular processes [174]. It directs the folding of newly synthesized proteins and facilitates the intracellular transport of proteins or vesicles, the assembly and disassembly of protein complexes, and the degradation of unwanted proteins. This protein therefore is broadly participating in protein homeostasis under both normal and stress circumstances.

Consistent with the versatile behavior of hsp70 discovered at the molecular and cellular level, clinical studies have revealed its crucial role in a wide range of diseases

including neurodegeneration, cancer, allograft rejection and infection[174]. This review will briefly summarize hsp70 structure, function and involvement in pathophysiology (particularly apoptosis).

1.5.2 Family members of hsp70 and domain architecture

Eukaryotes usually express multiple hsp70 family members and the intracellular localization of these proteins has been characterized [174]: mt hsp70 (Grp75 / mortalin / hspA9) is in mitochondria, BiP (Grp78 / hspA5) is in the endoplasmic reticulum, and hsp72 (hspA1A) and heat shock cognate 70 (hsc70/ hspA8) are in the cytosol and nucleus. The functions of individual protein members in specific locations have been investigated extensively. For the purpose of this review hsp70 will be used as a generic term for all identified family-member proteins, to discuss the common, shared properties.

The hsp70 family of chaperones shares a highly conserved architecture consisting of an amino-terminal ~40 kDa adenine nucleotide-binding domain (NBD or ATPase) and a 27 kDa carboxy-terminal substrate/peptide-binding domain (SBD or PBD), joined by a short linker region [176]. Further structural analysis reveals that two domains (I and II) constitute the NBD region, part of which (Ia and IIa subdomains) spatially form a nucleotide-binding cassette area responsible for ATP interaction [177]. The SBD consists of a 10 kDa α-helix subdomain and a 15 kDa sandwich structure of β-sheets connected by extended loops. It is the extended motif of the β-sandwich loops that is responsible for binding to the substrate peptides and the

α-helix subdomain for determining availability of chaperone for the substrate peptides [178].

1.5.3 Mechanisms of chaperone function

Chaperone action of hsp70 on substrate proteins is achieved by a series of cycling events. Equally important is the fact that the function of this group of proteins is, to a large extent, dependent on co-chaperone proteins, serving as activators for ATPase in ensuing events [179]. This paragraph will summarize the information relevant to both prokaryotic and eukaryotic hsp70s.

The structural and functional features of hsp70 are best understood for the bacterial homolog DnaK [180]. As mentioned, the crystallization studies of hsp70 structure revealed ATP-binding domains in the nucleotide-binding domain, shown as a cleft by Ia and IIa subdomains, a substrate-binding domain consisting of a “lid” (alpha helix), “base” (beta- sandwich), and looping conformation extended from the beta sheet as the binding site for substrate peptides. Upon binding to ATP molecules, the α-helical lid remains open and rapid peptide binding by hsp70 occurs via hydrogen bonding [178]. This state is believed to be a transient intermediate, which can proceed to either release the bound polypeptide or bind it more strongly if the polypeptide needs to be corrected. Determining whether or not the chaperone needs to act on the bound proteins requires participation of co-chaperones. The co-chaperones function to activate hsp70 ATPase [180]. ATP hydrolysis drives the modification of the nucleotide-binding domain conformation that is transmitted to substrate binding

domain, resulting in closing of the lid and stable holding of the bound peptide [180]. In *E. coli*, the protein responsible for activating hsp70 ATPase is DnaJ while in mammalian cells, an extensive family of proteins has been identified, including Hdj1/hsp40 and Hdj2 as best known co-chaperones of hsp70. The ADP product from ATP hydrolysis will be eventually replaced by ATP again, resulting in the dissociation of a substrate peptide to finish the chaperone cycle. Over 50 proteins have been identified in the co-chaperone family for hsp70; eukaryotic co-chaperones inhabit various cell compartments and assist in the function of hsp70 [180].

Results from DnaK and eukaryotic hsp70 chaperones indicate hsp70 works on two different kinds of target proteins, i.e. newly synthesized polypeptides and those damaged by stress. In *E. coli*, it is proposed that all nascent peptides from the ribosomal translational machinery are subject to the action of the DnaK–DnaJ–GrpE system [181]. In eukaryotic cells, hsp70 chaperones are also responsible for directing the folding of 15–20% of all newly synthesized polypeptides [182]. However, there is not much known about the function of this chaperone mechanism in stress conditions, even though there is a report documenting that hsp70 interacts with small polypeptides under certain stress conditions, presumably protecting the proteins from intramolecular misfolding and subsequent formation of aggregates [180]. The released polypeptide may assume a correct conformation, transferred to an alternative chaperone system for further modification and /or digested by the proteasomal or lysosomal systems [180].

1.5.4 The role of hsp70 in apoptosis

Hsp70 has been documented as a quintessential inhibitor of apoptosis. Cells from *hsp70.1-/-* and *hsp70.3 -/-* knock-out mice (the two genes coding for inducible hsp70 chaperones in response to apoptotic stimuli) have shown significant sensitivities to great array of lethal stimuli [183]. Ablation of hsp70 results in spontaneous apoptosis in testicular germ cells and carcinoma cells [184]. Overexpression of hsp70 prevents apoptotic events triggered by hyperthermia, oxidative stress, staurosporine, ligation of the Fas/Apo‑1/CD95 death receptor or anticancer drugs [184]. The mechanisms of how these effects are exerted have been studied extensively and the major apoptotic pathways affected by hsp70 are summarized in the text.

The extrinsic apoptotic pathways involve ligation of the cell-death receptor and subsequent signal transduction leading to the caspase cascade. One of the mediators in the pathway identified is c-Jun N-terminal Kinase (JNK1). In the apoptotic milieu induced by hyper-osmolarity, hsp70 binds to and blocks JNK1 activity while depletion of hsp70 significantly potentiates JNK and caspase-3 activation and apoptosis [185-186]. In the case of the intrinsic death pathway, hsp70 has been shown to inhibit Bax translocation and insertion into the outer mitochondrial membrane [187]. At the post-mitochondrial level, hsp70 interacts with and disrupts the downstream pathways mediated by AIF and endo-G [184].

An important feature of hsp70 as a pro-survival factor compared to other rescuing effectors is that overexpression of the protein can reverse cell death at a very late stage, marked by CAD (caspase-activated DNase) activation [188]. It is reported

that hsp70 regulates the enzymatic activity and proper folding of CAD, and via interaction-mediated conformational change, deactivates the effects of CAD on chromatin DNA [189].

Hsp70 has also been shown to protect from cell death via alternative mechanisms, such as by interacting and stabilizing protein kinase C (PKC) and Akt, maintaining their protective roles to rescue cell from dying [190]. In cardiomyocytes, hsp70-induced protection from oxidative stress-induced apoptosis is reported to be mediated by nucleolin/C23, by an as-yet-unknown mechanism [191].

In vivo studies have shown that high hsp70 expression in certain types of cancers, including breast, endometrial, oral, colorectal and prostate cancer and certain leukemias is linked to poor prognosis [174]. It is possible hsp70 expression, by enhancing resistance to either anti-cancer drugs or attack from the immune system, provides a survival advantage to carcinoma cells.

It should also be noted that there are reports of 'unexpected' effects of hsp70 on cells in culture and *in vivo*. Expression of hsp70 is upregulated in hearts subjected to pro-hypertrophic stimuli including aortic banding, isoproterenol-infusion or angiotensin II treatment, and even by swimming [192]. Overexpression of hsp70 in cardiomyocytes was shown to promote a hyperthophic response to such stimuli [192]. Furthermore, in human breast cancer cells 'treatment' with hsp70 has been reported to induce mitotic arrest through an unknown mechanism [193].

1.6 Objectives and Rationale

The intracrine mechanism of action of hi FGF2 is still incompletely understood. There is furthermore a nearly complete lack of information regarding a potential relationship between endogenous hi FGF2 expression and cardiac pathology. A series of studies were undertaken to investigate these questions. Three major objectives were pursued:

Objective 1: **to study aspects of the mechanism by which hi FGF2 upregulation causes DNA condensation and cell death.**

Rationale: In my master's project I observed that chromatin compaction by hi FGF2 was prevented by ERK inhibition and Bax-translocation inhibitors, indicating that the ERK½ signaling pathway and mitochondria are involved in hi FGF2-induced apoptosis. However, these studies did not address the effect of overexpressed hi FGF2 on ERK½ activation, and did not discriminate between intracrine and autocrine pathways of activation. Additional studies are also required to confirm mitochondrial involvement in the effects of hi FGF2. Finally, it is not known if 'pro-survival' kinases such as Akt and its downstream nuclear target kinase PIM-1 can counteract the pro-death effects of hi FGF2. Thus, I investigated the hypotheses that: (i) hi FGF2 overexpression causes sustained ERK½ activation by an intracrine pathway; (ii) hi FGF2 overexpression causes cytochrome C release from mitochondria; (iii) overexpression of Bcl-2 will prevent the effects of hi FGF2 on nuclei; and that (iv) overexpression of Akt (and its downstream kinase PIM-1) will rescue cells from hi FGF2-induced chromatin compaction and cell death.

Objective 2: To identify proteins interacting with hi FGF2 but not lo FGF2; and use knockdown approaches to determine if they are required to mediate its effects on chromatin.

Rationale. Several proteins have been identified that appear to interact specifically with hi FGF2. It is likely that the different FGF2 isoforms recruit different complexing partners to stimulate different signaling pathways resulting in different cellular effects. Here, I examined the hypotheses that: (i) by using immunoaffinity columns conjugated to recombinant hi FGF2 or lo FGF2, followed by mass spectroscopy analysis, I will be able to isolate isoform-specific binding partners (from nuclear extracts); (ii), complementary approaches such as co-immunoprecipitation will confirm hi FGF2 interaction with its candidate binding partners; and (iii) knockdown of selected binding partners will prevent the effects of hi FGF2 on chromatin.

Objective 3. To assess presence of hi FGF2 in human cardiac tissue; and study endogenous hi FGF2 accumulation in models of cardiac pathology and in response to stress-associated stimuli.

Rationale. Studies from Dr. Kardami's laboratory, as well as other groups, have shown that intracellular accumulation of hi FGF2 via overexpression results in cardiac cell death. The physiological relevance of these findings has not been examined. As a first step in addressing this issue, I have initiated a series of studies to: (i) determine if hi FGF2 is present in the nuclei of human heart tissue; (ii) to examine endogenous hi

FGF2 accumulation by cells in culture, in response to ‘stress’ stimuli linked to cardiovascular disease and cell death (endothelin I, angiotensin II, isoproterenol, high glucose); and (iii) to examine cardiac hi FGF2 accumulation *in vivo*, in models of cardiomyopathy (mdx mouse, adriamycin-induced cardiotoxicity). My overall hypothesis related to objective 3 is that endogenous hi FGF2 levels will be upregulated in response to stress stimuli and in cardiomyopathies.

CHAPTER 2

MATERIALS AND METHODS

2.1 Cell cultures

2.1.1 Human Embryonic Kidney 293 cell line (HEK293)

HEK293 cells were obtained from Stratagene and maintained (passages 2–10) in Dulbecco's Modified Eagle's Medium (DMEM) supplemented with 10% (v/v) fetal bovine serum (FBS) and 100 U penicillin and streptomycin per ml at 37° C in humidified air with 5% CO_2.

2.1.2 Primary cultures of rat neonatal cardiac myocytes and fibroblasts

Procedures have been described [57]. Sprague-Dawley rat pups (one or two day old) were sacrificed by decapitation and the hearts were excised and placed on Petri dish with cold phosphate buffered saline (PBS) supplemented with glucose (3.5g/L). The hearts were minced into 1 mm^3 pieces and digested with collagenase (740 U /digest), trypsin (370 U/digest) and DNase l (2880 U/digest). The digestive enzyme was inactivated by Hy-Clone FBS (GIBCO) and the resultant cells suspensions were filtered through a nytex membrane and centrifuged at 2000g for 5 min. The supernatant was discarded and the pellet containing heterogeneous cardiac cells were resuspended in ADS buffer (6.8 g NaCl, 4.76 g HEPES, 0.14 g $NaH_2PO_4 \bullet H_2O$, 1.0 g glucose, 0.4 g KCl, 0.2 g $MgSO_4 \bullet 7H_2O$, pH7.35 in 1L distilled H_2O).

With another filtration through a nytex membrane, the cells suspension was centrifuged at 3500 g for 30 min on a discontinuous Percoll gradient (Amersham

Biosciences). The top layers of cells were transferred to cell culture dishes and maintained in Ham's Mixture Nutrient F-10 medium supplemented with 10% FBS and 1% penicillin /streptomycin, labeled as P0 rat neonatal cardiac fibroblasts. The bottom layers of cells (cardiomyocytes) were plated on collagen-coated tissue culture dishes or coverslips at a density of 0.4 x 10^6 cells / 35 mm culture dish in DMEM supplemented with 10% FBS, 10% horse serum and 400 U penicillin / streptomycin. Cells were maintained overnight and the next day the cell debris was removed by rinsing with calcium- and magnesium-free (CMF) PBS solution and fresh culture medium was applied. As established previously [57], the myocytes purified in this manner contained less than 5% non-myocytes.

2.1.3 Primary cultures of rat adult cardiomyocytes

Hearts were obtained from male Sprague-Dawley rats weighing 300 to 350 g. The rats were intravenously injected with heparin (1000 U/100 g b.wt.) and anesthetized with xylazine (10mg/kg) and ketamine (60 mg/kg). The heart was excised and perfused for 5 min in a Langendorff apparatus using Ca^{2+} -free buffer containing 90 mM NaCl, 10 mM KCl, 1.2 mM KH_2PO_4, 5 mM $MgSO_4$, 15mM $NaHCO_3$, 30 mM taurine, 20mM glucose pH 7.4 gassed with 95% O_2 and 5% CO_2 mixture. Another perfusion was performed for 30 min using the same medium supplemented with 0.04% collagenase and 50 mM $CaCl_2$. The atrium was removed and the ventricle was minced into approximately 1 mm^3 small pieces, subjected to digestion in a fresh collagenase solution containing 2% bovine serum albumin (BSA) at 37°C for 30 min. Ventricular

fragments were further triturated and cell suspensions were collected and subjected to successive incubation in buffers with calcium concentration gradient (350 mM, 700 mM, 1400 mM, 1800 mM) for 15min per incubation at room temperature. Finally the cardiomyocytes were obtained via centrifugation and cultured in media enriched with 5 mM creatine, 2 mM L-carnitine, 5 mM taurine, 0.1 mM insulin, 10 mM cytosine arabinoside, 100 IU/ml, penicillin /streptomycin and 10% fetal calf serum on 6-well plates coated with 10μg/ml laminin. After 3 hours, the medium was replaced with the same culture medium but without serum. The procedure generated rod-shaped myocytes accounting for 80% of the final cell population, as monitored by phase contrast microscopy.

2.1.4 Human embryonic cardiac fibroblasts and human patient-derived atrial fibroblasts

Primary culture stocks for human embryonic cardiac fibroblasts were purchased from Cell Applications Inc., and human patient-derived atrial fibroblasts were provided by Jon-Jon Santiago (PhD student in Dr. Kardami's laboratory), as part of a collaboration between our laboratory and that of a clinician scientist, Dr. Rakesh Arora (St. Boniface Research Centre). Both kinds of fibroblasts were maintained in Basal Medium (Invitrogen), supplemented with 10% Growth Supplements (Cell Applications Inc.) and 400 U penicillin / streptomycin before being subjected to various treatments.

2.2 Cell culture treatments

Rat neonatal cardiac myocytes and fibroblasts, rat adult cardiac myocytes or human patient-derived fibroblasts were placed in a medium containing 2% FBS, 10 μg /ml/each insulin, transferin, selenium, 20 μg/ml ascorbic acid and 0.2% BSA in Ham's Mixture Nutrient F-10 media. After overnight incubation, cells were treated with angiotensin II (Ang II), endothelin I (ET-1), isoproterenol or glucose at different concentrations. After 2-5 days, cells were rinsed with ice-cold PBS, frozen in liquid nitrogen and stored in -80 ˚C until biochemical analysis. Alternatively, cells grown on coverslips were fixed with 4% paraformaldehyde for immunofluorescence studies.

2.3 Plasmids

The human hi FGF2 cDNA (pcDNA3-363) encoding three isoforms of CUG-initiated human hi FGF2hi FGF2 (migrating at 22.5, 23.1, and 24 kDa) but not AUG-initiated (18 kDa) FGF2, has been described in a previous publication from Dr. Kardami's laboratory [86]. Construction and characterization of cDNAs generating DsRed- labeled rat hi FGF2 was described previously [194]. The cDNA for wild-type human Bcl-2 cDNA has been described previously [58].

The p68 short-hairpin RNAs subcloned to pGIPZ vector were from Open Biosystems. The pGIPZ lentiviral plasmid vector that expresses green fluorescent protein (GFP) and small interfering RNA (siRNA) vector construct were from Open Biosystems.

2.4 Adenoviral vectors

Adenoviral vectors expressing CUG-and / or AUG-initiated species of human FGF2 were described previously [195]; although the adenoviral vector used to overexpress human 22-24 kDa hi FGF2 is also expressing lo FGF2, the overriding effect is that of hi FGF2 [57]. The adenoviral vector carrying a dominant-negative version of the upstream activating kinase for ERK½ (MKK1) has been described [196]. Adenoviral vectors for wild type AKT, nuclear AKT, and PIM-1 kinase were generous gift from Dr. M. Sussman (University of California, San Diego) and have been described in [124]. The hsp70 adenovirus was purchased from Vector Biolabs (Catalog No. 1047),

2.5 Reagents

Inhibitor PD 98059 (Cell Signaling Technology, Inc., Danvers, MA); mitochondrial-pathway apoptosis inhibitor, Bax inhibiting peptide (Bip V5), and its inert control peptide Bip–NC (Calbiochem/EMD Biosciences, La Jolla, CA); immunoglobulin (Ig) from non-immune mouse serum (Sigma–Aldrich, St. Louis, MO); kit for fluorescein (FITC)-based detection of apoptosis (programmed cell death) at the single-cell level, based on labeling of DNA strand breaks (TUNEL technology) (Roche Applied Science, Indianapolis, IN) were from sources listed in brackets.

2.6 Transient gene transfer

Plasmid cDNAs were introduced into HEK 293 cells using TransIT® -293

Transfection Reagent (Mirus Bio Corp., Madison, WI), according to the manufacturer's instructions. Briefly, HEK 293 cells were brought to 60~70 % confluency before transfection procedures were initiated; 3 μl of TransIT® -293 Transfection Reagent was diluted with 200 μl of serum-free DMEM and incubated at room temperature for 10~15 min. The plasmid cDNAs (1 μg / 35 mm plate or 2 μg / 100mm plate) was added to the diluent and incubated at room temperature for another 15 min. Finally, the above mixture was added drop-wise to cells. For co-transfection procedures, plasmid cDNAs of different kinds were mixed with diluted TransIT® -293 Transfection Reagent individually, as described above and added to the cells simultaneously for maximizing co-transfection efficiency. This method resulted consistently in high single- (60~70%) and co- (30~35%) transfection efficiency, evaluated by immunostaining and microscopy.

2.7 Protein Extraction

2.7.1 Protein extraction from cell cultures

2.7.1.1 Total cell lysate extraction

Cells grown to 60~90 % confluency on 35 mm well/ 100 mm plates were rinsed with ice-cold PBS twice and homogenized in 100-200 μl of lysis buffer (1% SDS, 50 mM Tris pH 8.0, 1 mM EDTA, 1 mM EGTA, 20 mM β-glycerophosphate, 10 mM NaF, 2 mM sodium orhovanadate, supplemented with the following inhibitors (at 1:100 dilution): Protease Inhibitor Cocktail (PIC; Sigma # P8340), Phosphatase Inhibitor Cocktail Set II (EMD Cat No. 524625) and IV (EMD Cat No. 524628).

These protease and phosphatase inhibitor cocktails were used in all our preparative procedures. Cell homogenates were transferred into 1.5 ml centrifuge tubes, boiled, sonicated and clarified by centrifugation at 14,000 rmp at 4° C for 15min. Samples were prepared for SDS/PAGE analysis by mixing with concentrated "sample buffer" to a final concentration of: 62.5 mmol/L Tris-HCl pH 6.8, 1% SDS, 10% glycerol, 0.005% bromophenol blue, and 5% ß-mercaptoethanol).

2.7.1.2 Subcellular fractionation

Nuclear and cytosolic cellular fractions were obtained using the Nuclei EZ Prep Nuclei Isolation Kit, (Sigma Aldrich Inc). Briefly, cells grown on 100 mm plates were rinsed twice with ice-cold PBS and scraped with 200 µl of Nuclei EZ lysis buffer into 1.5 ml centrifuge tubes. After incubation on ice for 15 minutes, nuclei were pelleted by centrifugation at 500 x g for 5 minutes at 4° C and supernatant containing cytoplasmic components was saved for SDS-PAGE. After extensive washing with EZ lysis buffer, pellets containing intact nuclei were lysed by 1xSDS lysis buffer, boiled, sonicated and centrifugated at 14,000 rpm 15 min at 4 ° C, and the resulting supernatant containing all SDS-soluble nuclear proteins was collected for SDS-PAGE analysis.

2.7.1.3 Subcellular fractionation for hi and lo FGF2 affinity chromatography

All steps were performed on ice unless otherwise indicated. 12x100 mm plates of HEK293 cells were scraped using 100 µl/ plate buffer A (10 mM HEPES/KOH pH

7.9, 10 mM KCl, 0.1 mM EDTA, 1 mM DTT, 60 mM β-glycerophosphate, 10 mM sodium fluoride, 1.5 mM $MgCl_2$) supplemented with protease and phosphatase inhibitors. Lysates were transferred to 1.5 ml centrifuge tubes and incubated on ice for 15 min. After addition of 10% NP-40 to a final concentration of 0.25% NP-40, lysates were briefly mixed and nuclei pelleted by centrifugation at 4000g at 4°C for 4 minutes. The resultant supernatant (cytosolic fraction) was stored on ice. The nuclear pellet was resuspended in ½ volume cold buffer B (20 mM HEPES/ KOH pH 7.9, 0.4 M NaCl, 1 mM EDTA, 1 mM DTT, 1.5 mM MgCl2) and left on ice for 15 minutes with occasional mixing. The soluble nuclear fraction was collected by centrifugation at 20,000g at 4°C for 5 minutes. Aliquots (100 µg/each) of nuclear and cytosolic lysate were subjected to hi and lo FGF2 affinity chromatography.

2.7.2 Cardiac tissue extraction

Heart tissues from mdx mice (6 weeks) or adriamycin-treated rats, along with control animals, were generously provided by Drs. Judith Anderson (Department of Human Anatomy and Cell Sciences, University of Manitoba) and Pawan Singal (Department of Physiology, University of Manitoba). Hearts were frozen in liquid nitrogen and stored at -80°C. Tissue (approx 30 mg) was powdered using a mortar and pestle with liquid nitrogen and transferred to a 15 ml tube on ice. Approximately 10 volumes "TMN" buffer/ weight (300 µl) was added to the tissue. TMN buffer was made as follows: 10 mM Tris-HCl pH 7.4, 100 mM NaCl, 300 mM sucrose, 2 mM $MgCl_2$, 1% (v/v) thiodiglycol, 60 mM β-glycerophosphate, 10mM NaF, 0.25% (v/v)

NP-40 containing the following inhibitors at a 1:100 dilution: protease inhibitor cocktail (PIC;Sigma # P8340), phosphatase inhibitor cocktail Set II (EMD Cat No. 524625) and IV (EMD Cat No. 524628). Following homogenization using a glass and Teflon homogenizer, samples were transferred to 1.5 ml microcentrifuge tubes and an equal volume of 2x SDS buffer (20% (v/v) glycerol, 100 mM Tris-HCl pH 6.8, 2% (w/v) SDS, 60 mM β-glycerophosphate, 5mM EDTA, 5mM EGTA, 2mM sodium orthovanadate, 1mM sodium fluoride) with inhibitors was added. The samples were boiled for 5 minutes, sonicated at 40 Hz for 3x5 seconds and centrifuged at 21000 g for 15 min at 4°C, to remove insoluble material.

2.8 Determination of protein concentration

Protein concentrations were determined using the bicinchoninic acid (BCA) assay (Sigma Aldrich Inc), according to manufacturer's instruction. Briefly, a standard curve was prepared using serial dilutions of BSA in double distilled water ranging from 2 μg/ml to 20 μg/ml. Standards and appropriately diluted samples were pipetted in triplicate into 5 ml glass tubes. The reaction solutions [solution A and solution B (50:1 v/v)] were added and the tubes were incubated at 60°C for 30 minutes. The tubes were then allowed to cool down to room temperature and the standard & sample proteins were analyzed by taking optical density, OD562 nm, readings. Finally the sample protein concentrations were evaluated from the BSA standard curve.

2.9 SDS-PAGE

Protein samples were analyzed by sodium dodecyl sulphate polyacrylamide gel electrophoresis (SDS-PAGE). In all cases, a 4 % stacking gel was combined with a resolving gel composed of 10 %, 12% or 15% acrylamide, dependent on the size of proteins to be evaluated. Protein samples were mixed with concentrated SDS sample buffer (final concentration : 62.5 mmol/L Tris-HCl pH 6.8, 1% SDS, 10% glycerol, 0.005% bromophenol blue, and 5% ß-mercaptoethanol), and boiled for 5 min prior to loading. A standard molecular weight (MW) marker (Biorad, Cat No 161-0317, 6.5-200 kDa) and Kaleidoscope Protein Standard marker (Biorad, Cat No 161-0375, 10-250 kDa) were always included. Gels were electrophoresed at constant 100 voltage till the samples reached the bottom of resolving gel. The composition of resolving gel of various percentages and stacking gel is shown in Table 1.

2.10 Western blotting

Proteins resolved in SDS-polyacrylamide gels were transferred to polyvinylidene difluoride (PVDF) membranes (Roche Diagnostics, IN) and after being stained with 0.1% (w/v) Ponceau S to monitor proper protein transfer and visualize the molecular weight markers the membrane was rinsed and blocked with 10% skim milk powder (SMP) in Tris-buffered saline containing 0.1% Tween-20 (TBST) for 1 hour at room temperature. Membranes were incubated with primary antibodies for one hour at room temperature or overnight at 4˚C; washed extensively (5x in SMP/TBST) and subsequently incubated with secondary antibodies (in 1% SMP in TBST) for one hour at room temperature. Finally the blots were washed with TBST (5x) and the

antigen-antibody complexes were visualized by chemiluminescence (ECL, GE Healthcare/ Bio-Sciences, Inc., Piscataway, NJ) and autoradiography. For multiple probings, the membranes were stripped of bound antibody in buffer containing 62 mM Tris pH 6.8, 2% SDS, and 100 mm β-mercaptoethanol at 60°C for 15 min and subjected to same Western blotting procedures with different primary antibodies, as described above. The antibodies used in Western blotting are shown in Table 2. Antibodies used to detect all FGF2 isoforms by western blotting are a mouse monoclonal anti-FGF2 antibody from UBI, or two types of goat polyclonal anti-FGF2, from Santa Cruz Biotechnology.

2.11 Immunofluorescence

Cells were grown to 60~90 % confluency on glass coverslips in 35 mm dishes. The cells were rinsed 3x with ice-cold PBS, fixed with 4 % (w/v) fresh paraformaldehyde / PBS (4°C for 15 minutes) and permeabilized with 0.1% Triton X-100 / PBS (4 ° C for 15 minutes). For single immunofluorescence studies, samples were incubated with primary antibodies and subsequently secondary antibodies conjugated with FITC or Texas Red. For double-immunofluorescence studies, cells were incubated with a mixture of two primary antibodies raised in different species, and then in a mixture of secondary antibodies conjugated with FITC or Texas-Red. All the steps described above were followed by extensive PBS washes. Finally the coverslips were mounted to slides for microscopic analysis using ProLong® Gold anti-fade reagent with DAPI (Roche). The antibodies used in immunofluorescence are shown in Table 2.

2.12 TUNEL Staining

Cells grown on coverslips were fixed (4% w/v paraformaldehyde / PBS), permeabilized (0.1% v/v Triton / PBS) and incubated in the TUNEL mix (5 µl of terminal deoxyribonucleotidyl transferase + 45 µl of reaction buffer) (Roche kit, 3333566) for 60 min at 37°C in the dark. The cells were rinsed 5x with PBS and subjected to immunostaining before analyzed using epifluorescence microscopy.

2.13 Immunoprecipitation

HEK293 cells, grown to confluency in 100 mm plates, were scraped (300 µl/100 mm plate) into cold 1x RIPA buffer (150 mM NaCl, 1% (v/v) NP-40, 0.25% (w/v) deoxycholate, 0.1% (w/v) SDS, 50 mM, Tris-HCl pH 8.0, 1 mM EGTA, 1 mM EDTA, 1 mM $Na3VO_4$), containing protease and phosphatase inhibitors. Samples were incubated on ice for 15 min, sonicated briefly and centrifuged at 10,000g at 4 °C for 10 minutes. Supernatants were processed for determination of protein concentration. An aliquot (20 µg of total protein) was mixed with concentrated SDS/PAGE sample buffer and stored as "Total Extract". For immunoprecipitation, 900 -1500 µg total protein was pre-absorbed by protein A- or protein G- sepharose (GE Healthcare Bio-Sciences, AB) and then incubated with anti-human hi FGF2 antibodies (1 µg antibodies/100 µg total proteins); anti-p68 RNA helicase, or anti-hsp70 antibodies (1µg antibodies /500 µg total protein); or with an equivalent amount of non-specific immunoglobulin of the same class and subtype as the primary antibody (Sigma-Aldrich), at 4˚C overnight. The immuno-complex was collected with 40 µl protein A-

or protein G- sepharose slurry (1:1 v/v) at 4˚C for 1 hr and pelleted down by centrifugation at 500 g at 4˚C for 2 min. An aliquot from the supernatant (same volume as the one containing total protein) which contained non-immunoprecipitated proteins, was stored in SDS/PAGE sample buffer. The pelleted sepharose beads, containing immunoprecipitated proteins, were washed 5x with RIPA, and mixed with 40 μl 2xSDS sample buffer. All the prepared samples ("Total lysates", "Non-Immunoprecipitated Proteins", "Immunoprecipitated Proteins") were boiled, centrifuged and analyzed by SDS-PAGE and Western blotting. The antibodies used in immunoprecipitation and western blotting are shown in Table 2.

2.14 Immunohistochemistry

Human patient-derived atrial tissue cryosections and cardiac fibroblasts derived from human atrial tissue were provided by Dr. R. Arora and Mr. Jon-Jon Santiago. Paraffin sections were used for immunohistochemistry. The sections were de-paraffinized by incubation with 100% xylene, followed by 100%, 95% and finally 70% ethanol at room temperature for 20 min for each incubation, respectively. After extensive PBS rinse, the slides were then incubated within citrate buffer at 60-90°C for 30 minutes, followed by air-dry cooling in the room temperature for another 20 minutes. To eliminate non-specific background from immunostaining, the sections were successively subjected to: 3% BSA/ PBS (w/v) for 30 minutes; 3% H_2O_2/PBS (v/v) for 10 minutes; Avidin and Biotin blocking Kit (Vector Laboratories Inc.). Incubation with primary antibodies (polyclonal anti-human hi FGF2, or non-specific

immunoglobulin in 1% BSA/ PBS (w/v)) proceeded at room temperature overnight, followed by biotinylated secondary antibody (Jackson Laboratory) (1/400) for 30 minutes at room temperature. Subsequently, the sections were subjected to ABC staining kit (Vector Laboratories Inc. Cat No PL-6100) for 30 minutes at room temperature and Nova-red Kit (Vector Laboratories Inc. Cat No SK-4800) and finally counter-stained with Hematoxylin (Vector Laboratories Inc. Cat#H-3404) or DAPI at room temperature for 3 minutes. Prior to mounting, a 2% solution of sodium bicarbonate (w/v) was applied to sections at room temperature for 1 min, followed by dehydration using 95% and 100% ethanol and xylene for 3 minutes. It should be noted that all the steps were followed by extensive washing with PBS. Images were taken using a Zeiss Axioscope microscope using Axiovision software.

2.15 Protein purification

Rat hi FGF2 (23 kDa) and lo FGF2 (18 kDa) cDNA were ligated into the multiple cloning sites of pET-19b vector (Novagen). The carbenicillin-resistant plasmids were transformed into competent *E. Coli*, BL21(DE3) pLysS strain (Novagen), and the transformants grown on Luria-Bertani (LB) solid medium overnight. A single colony was selected into 3 ml LB medium supplemented with carbenicillin (50 μg/ml) and incubated overnight at 37°C with agitation at 225 rpm. These cultures were used to inoculate 500 ml of medium composed of 24 g/L yeast extract (Fisher Scientific) , 12 g/L tryptone (Fisher Scientific), 12.5 g/L dibasic potassium phosphate, 2.3 g/L monobasic potassium phosphate, 4.0 ml/L glycerol, supplemented with carbenicillin

(100 mg/L) and chloramphenicol (34mg / L). To induce protein expression, isopropyl-b-D thiogalactopyranoside (IPTG, 1mM) was added when the culture was between 0.4–0.6 OD_{600} units and the culture was incubated a further 4 hours. The bacteria were collected by centrifugation at 6,000 x g for 10 min at 4 ° C and the pellets stored at -80°C.The His-tagged recombinant proteins were purified by immobilized metal ion affinity chromatography (IMAC) with Ni-Sepharose (GE Healthcare), following the manufacturer's instruction. Briefly, the bacterial pellet was resuspended in 20 ml binding buffer (5 mM imidazole, 0.5 M sodium chloride, 20 mM Tris-HCL pH 7.9 , glycerol 100ml /L, β-mercaptoethanol 350 µl /L , 0.1% NP-40) and the cells lysed by three alternating freeze-thaw cycles followed by sonication on ice. The homogenate was clarified by centrifugation at 6000 x g at 4 °C and filtration using 1.2 µm disposable filters (Millipore Corp., Bedford, Mass.). The samples were applied to Ni-Sepharose columns to allow binding of His-tagged recombinant protein. The columns were subsequently washed with 10x column volumes of binding buffer, washing buffer (100mM imidazole , 0.5M sodium chloride, 20mM Tris-HCL pH 7.9 , glycerol 100ml / L, beta-mercaptoethanol 350 µl /L) containing 0.1% NP-40 and finally washing buffer without NP-40. The recombinant lo and hi FGF2 were eluted using elution buffer (0.5M imidazole , 1M sodium chloride, 40mM Tris-HCL pH 7.9 , glycerol 100ml / L, beta-mercaptoethanol 350 µl /L). Fractions (1ml) were collected into tubes containing 2 µl of 500 mM EDTA pH 8.0 (final concentration 1mM EDTA) to chelate any nickel leaked from the column. Fractions were analyzed by SDS/PAGE, stained with Coomassie Blue (0.1% w/v Coomassie

Brilliant Blue R-250 in 45% (v/v) methanol 9% (v/v) acetic acid) and de-stained using 10% (v/v) acetic acid and 40% (v/v) methanol. Fractions containing purified lo or hi FGF2 were pooled. The biological activity of the purified proteins was tested by incubating HEK293 cells with lo or hi FGF2 recombinant protein (2 ng / ml) for 15 min. The total cell lysates (20 µg) were analyzed for phospho-ERK ½ by Western blotting.

Human hi FGF2 was produced, purified and tested following similar procedures as those for the rat FGF2 isoforms, after its cDNA (encoding 22.5, 23.1, and 24.2kDa isoforms) was ligated into the multiple cloning sites of pET-19b vector (Novagen).

2.16 Cross-linking of recombinant protein to CNBr-activated sepharose

The purified FGF2 proteins were dialyzed against coupling buffer (0.5M sodium chloride, 0.1 M sodium bicarbonate, pH 8.3) at 4°C overnight with stirring. Proteins were cross-linked to CNBr-activated sepharose (GE Healthcare), following the manufacturer's instructions. Briefly, the proteins were incubated with sepharose overnight at 4°C and excess ligand was removed by washing with coupling buffer. The remaining active groups were blocked with 0.1M Tris HCl pH 8.0, 0.5 M NaCl for two hours at 4°C. Finally the column was subjected to three cycles of alternating basic and acidic pH (0.1 M Tris-HCl pH 8.0, 0.5 M NaCl) and 0.1 M acetic acid pH 4.0, 0.5 M NaCl) and stored in immunoprecipitation buffer (50 mM HEPES pH 7.5, 1% NP-40, 10% glycerol 100 mM NaCl), supplemented with 0.02% sodium azide, at 4°C.

2.17 Isolation of nuclear or cytosolic proteins bound to hi or lo FGF2 affinity columns.

Nuclear and cytosolic protein fractions obtained via methods described in **7.1.3.** were mixed with 1/3 volume of 4x "binding buffer" (20 mM HEPES/KOH pH 7.9, 4% NP-40, 40% glycerol, 400 mM NaCl), and pre-absorbed with control CNBr-sepharose for 1 hour at 4°C with mixing. After removal of sepharose beads by centrifugation, the supernatant was divided into three equal-volume aliquots placed in 1.5 ml tubes, for binding to control-, lo- and hi- FGF2-conjugated CNBr-sepharose (40 µl 1:1 slurry), at 4°C overnight. The sepharose beads were collected by centrifugation, washed extensively, placed in 40 µl 2x SDS/PAGE gel sample buffer, and boiled for 5 min. Thus eluted proteins were resolved in 12 % SDS-PAGE, stained with Coomassie-Blue and destained briefly. Bands representing proteins bound only to hi- but not lo- FGF2 or control- sepharose beads were excised with a clean scalpel on a clean glass plate. The gel bands were minced into approximate 1 mm^3 pieces, proteolytically digested by trypsin, and sent for identification by HPLC-mass spectrometry (www.proteome.ca).

2.18 Purification of antibodies

A 12 amino-acid sequence (GRGRGRAPERVG) uniquely present at the amino terminal extension of human hi FGF2 was synthesized and used (by the company, as per our request) to obtain a rabbit polyclonal antiserum (Sigma Aldrich, Inc.). The resulting antiserum was subjected to human hi FGF2-conjugated

CNBr-sepharose chromatography to obtain affinity purified antibodies. Briefly, 1 ml of antiserum was diluted with 9 ml of binding buffer (40 mM Tris-HCl pH 8.0, 0.2M NaCl) and clarified with 1.2 μm disposable filters (Millipore Corp., Bedford, Mass.). The diluents were incubated with human hi FGF2-sepharose at room temperature for 2-3 hr, and after extensive washing with binding buffer, bound immunoglobulin was eluted with 4M $MgCl_2$. The eluate was dialyzed against 10 % glycerol in binding buffer at 4°C overnight, followed by immunoglobulin quantification by spectroscopy, obtaining optical density readings at 280 nm wavelength (A280). The concentration of antibodies was calculated using the formula: Concentration (mg/ml) = 1.55 x A280. Finally, the antibodies were stored in – 20°C.

2.19 Data collection and statistical analysis.

The Nuclear Compaction Index (NCI) was determined by fluorescence microscopy and scoring of visual fields. NCI represents the fraction of hi FGF2-overexpressing cells displaying a characteristic nuclear morphology (compacted and/or fragmented chromatin) over the total number of hi FGF2 overexpressing cells, per visual field. In cultures subjected to hi FGF2 overexpression by gene transfer, TUNEL staining index (TSI) was determined by fluorescence detection and scoring as the fraction of hi FGF2 overexpressing cells which stained positive for TUNEL over the total hi FGF2 over-expressing cells. In non-overexpressing cultures, TSI reflection the fraction of cells displaying TUNEL staining over total number of cells per field. A total of 24 fields (up to a total ~1,200 cells from three separate coverslips/group)

were scored, using a low magnification (10x) lens. In some experiments findings are presented as ‘relative NCI’ by arbitrarily defining control group values as 1.0.

The student’s T test (GraphPad InStat 3.0 program) was applied when comparing two groups, whereas one way ANOVA was used in experiments including more than two groups for comparison. Differences were considered significant when $P<0.05$.

CHAPTER 3

RESULTS

3.1 Signal transduction pathways leading to hi FGF2-induced apoptotic chromatin compaction

3.1.1 Hi FGF2 expression promotes TUNEL staining. We have previously shown that ectopic expression of human or rat hi (but not lo) FGF2 induced chromatin compaction in HEK 293 cells, detectable at 24-72 hr post transfection [58]. Chromatin compaction was associated with increased levels of the 17 kDa form of caspase-3 (activated form) indicating an apoptotic phenotype. We have now conducted additional studies to interrogate the features of hi FGF2-induced apoptosis.

DsRed-hi FGF2 was expressed in HEK 293 cell cultures by gene transfer, and cells were examined for TUNEL staining (an indicator of programmed cell death; green) 72 hr later. DsRed fluorescence (red) served to identify hi FGF2 expressing cells, and DAPI to visualize nuclei. Figure 1 shows representative images of cells that overexpress hi FGF2, display chromatin compaction, and stain positive for TUNEL; non-over-expressing cells are shown to be TUNEL-negative. Determination of the TUNEL-staining index showed a significant increase in TUNEL-stained cells in hi FGF2 overexpressing cultures (Figure 1B).

3.1.2 Hi FGF2 overexpression decreases markers of cell proliferation. Previous studies showed that overexpression of hi FGF2 inhibited DNA synthesis in myocytes [57]. We examined if a similar response would be present in HEK 293 cells. We

used anti-BrdU labeling as an indicator of DNA synthesis, and anti-Ki-67 staining as a marker of actively proliferating cells. Figure 2 shows that HEK 293 cells overexpressing hi FGF2 had significantly decreased incidence of anti-BrdU labeling as well as anti-Ki-67 labeling compared to non-overexpressing cells.

3.1.3 Hi FGF2 expression promotes cytochrome C release to the cytosol. We used western blotting and densitometry to measure relative levels of cytochrome C in cytosolic and particulate fractions from hi FGF2 overexpressing and control -transfected cultures. As shown in Figure 3, hi FGF2 expression was associated with a statistically significant increase in relative cytosolic cytochrome C levels and a concordant decrease in cytochrome C levels of the particulate fraction which contains mitochondria.

3.1.4 The hi FGF2-induced chromatin compaction is prevented by expression of the anti-apoptotic protein Bcl-2. Mitochondria engagement was also studied by examining whether overexpressing the anti-apoptotic member of the Bcl-2 family, Bcl-2, would rescue the hi FGF2 induced nuclear phenotype. Overexpression of Bcl-2 was achieved by gene transfer and verified by anti-Bcl-2 staining. Under the conditions of our experiment, anti-Bcl-2 cytosolic staining is only detectable in cultures transfected with the Bcl-2 cDNA. Co-overexpression of DsRed hi FGF2 and Bcl-2 was verified by co-immunostaining (Fig.4A). Our data indicated that Bcl-2 overexpression significantly attenuated the incidence of hi FGF2-induced chromatin

compaction (Fig.4A, B). Successful overexpression of both DsRed hi FGF2 and Bcl-2 was further confirmed in Western blotting (Figure 4C).

3.1.5 ERK ½ activation is involved in hi FGF2-induced apoptosis. In my Master's studies I showed that a specific inhibitor (PD 98059; 20 mM) of the upstream activating kinase (MEK1) for ERK ½ prevented hi FGF2-induced chromatin compaction. These results have been reproduced here for comparative purposes (Fig.5). An additional approach was used to further confirm the requirement of the ERK ½ pathway: ERK½ activation was inhibited by overexpression of a dominant-negative upstream activating kinase MKK1 (MKK1 dn). This treatment was effective in decreasing hi FGF2-induced nuclear compaction (Figure 5). Statistical analysis shows that both PD98059 and MKK1 (dn) significantly prevent hi FGF2-induced apoptotic chromatin compaction (Fig.5 B and C). The inhibitory effect of PD 98059 on ERK½ activation was confirmed, as shown in Fig.6A. Furthermore, PD 98059 had no effect on levels of hi FGF2 overexpression (Figure 6B). Thus PD98059 prevented hi FGF2 induced apoptosis by effectively abolishing ERK ½ activation and not by down-regulating hi FGF2 expression.

We examined the effect of hi FGF2 overexpression on the relative levels of total ERK ½ and phospho (active) - ERK ½. Western blotting and densitometry approaches showed that hi FGF2 overexpression resulted in significant upregulation of both total but especially phospho-ERK, at both 24 and 72 hr post-transfection, in total cell lysates. At the later time point in particular, while non-overexpressing cultures had

negligible ERK activity, hi FGF2 overexpression resulted in robust ERK activation. Nuclear ERK levels were also examined. As shown in Fig.7 (e and f), hi FGF2 overexpression resulted in significant increases in total and especially phospho-ERK ½ in nuclear extracts, compared to non-overexpressing cultures.

To distinguish between intra-crine or auto- and para- crine activation of ERK ½ by hi FGF2 overexpression, we used neutralizing FGF2 antibodies capable of blocking the activity of both hi and lo FGF2 when acting on the cells from the outside-in [197]. Neutralizing FGF2 antibodies were added to cultures one hour prior to transfection with hi FGF2. Cultures were also stimulated with added recombinant 18 kDa FGF2 for 30 min. As shown in Figure 8a, the neutralizing antibodies were capable of preventing ERK ½ phosphorylation induced by extracellular-acting FGF2. These antibodies did not reduce ERK ½ phosphorylation associated with hi FGF2 overexpression, supporting an intra-crine pathway of activation.

It is possible that hi FGF2 overexpression stimulated expression and release of bioactive factors that could be responsible for ERK activation. To test for this possibility, conditioned media (CM) from non-overexpressing and hi FGF2 overexpressing cultures were used to 'stimulate' HEK293 cells for 15 min. This was followed by examining phospho-ERK½ levels in total cell lysates. As seen in Figure 8C, the phospho-ERK ½ levels are not significantly different between cells stimulated by CM from non-transfected cultures and the one stimulated by CM from hi FGF2-transfected cell cultures. Thus the observed stimulation of ERK½ is not caused by factors released into conditioned medium upon hi FGF2 overexpression.

Previously, we found that that the Bax-inhibiting peptide Bip V5 abolished the hi FGF2-induced nuclear compaction [58]. We now asked if Bip V5 also prevented the hi FGF2-induced stimulation of ERK½. As shown in Figure 9, hi FGF2-induced ERK ½ activation remained unchanged in the presence of Bip V5, or its inactive control peptide Bip NC.

3.1.6 Nuclear AKT and PIM-1 overexpression reduce hi FGF2- apoptosis in cardiomyocytes. The AKT and its downstream activated kinase in the nucleus, PIM-1, have well documented anti-apoptotic effects in the literature. We addressed the question whether hi FGF2-induced apoptosis in cardiomyocytes could be abolished by overexpression of wild-type / nuclear AKT and PIM-1. To this end, cardiomyocytes were infected with hi FGF2 adenovirus and either wild-type / nuclear AKT or PIM-1 adenovirus. Following transfection, cells were examined for immunofluorescent analysis after 72 hr incubation. As shown in Figure 10 A-E, nuclear (but not wild-type) AKT and PIM-1 overexpression significantly reduce the DNA compaction by hi FGF2, suggesting a protective role of AKT - PIM-1 pathway in the apoptotic model by hi FGF2.

We examined the effect of hi FGF2 or lo FGF2 overexpression on chronic levels of activated endogenous Akt, estimated by its phosphorylation at threonine 308 (p-Akt). Rat neonatal cardiomyocytes were infected with adenoviral vectors for hi or lo FGF2, or vector alone. At 72 hr post-infection total cell lysates were analyzed by western blotting for anti-p-Akt. As shown in Figure 10F, lo FGF2 overexpressing

cultures had significantly increased p-Akt compared to either control or hi FGF2-overexpressing cultures.

3.2 Hi FGF2 interacting proteins

3.2.1 Identification of proteins interacting with hi but not lo FGF2, via affinity chromatography and HPLC-mass spectrometry.

3.2.1.1 Purification of recombinant hi and lo rat FGF2. To create lo- or hi FGF2 affinity columns, recombinant FGF2 isoforms containing an N-terminal His tag were expressed in *E. coli* and isolated using immobilized metal ion affinity chromatography with Ni-Sepharose columns. The preparative procedures, as monitored in SDS/PAGE and Coomassie brilliant blue staining (Fig. 11 A and B), resulted in a single protein band indicative of successful isolation of pure recombinant hi and lo FGF2. This was confirmed by western blotting showing recognition of the purified proteins by anti-FGF2 antibodies; Fig.11C. Biological activity of purified proteins was tested by assessing stimulation of ERK ½ phosphorylation in HEK 293 cells. Vehicle-treated cultures were used as controls. As shown in Fig. 11D, both purified proteins induced significant increase of ERK ½ phosphorylation level compared to control cultures, without affecting total ERK levels.

3.2.1.2 Creation of hi and lo FGF2-sepaharose affinity columns. Purified rat hi and lo FGF2 were coupled to CNBr-activated Sepharose as per manufacturer's instructions and success of the conjugation procedure was monitored via SDS/PAGE.

A total of 4 mg purified proteins were used per 1 ml packed volume of sepharose beads. Typical results are shown in Fig.11E: there was a clear decrease in lo as well as hi FGF2 levels in samples after conjugation, compared to those before conjugation. Thus created hi- and lo FGF2 affinity columns were used for isolation of binding proteins. Non-conjugated sepharose was also used as a control.

3.2.1.3 Affinity Chromatography and MS/MS Peptide Sequencing. We obtained cytosolic and nuclear extracts from HEK293 cells and used them as source material for affinity chromatography. A total of 0.7 mg nuclear protein, or 1 mg cytosolic protein was used as source material. All samples were pre-absorbed by passage through non-conjugated CNBr-activated sepharose, and then mixed with 40 μl of: control, non-protein-conjugated sepharose; lo FGF2-sepharose; hi FGF2-sepharose. Proteins that were tightly bound to the sepharose beads were eluted into SDS/PAGE buffer, resolved by SDS/PAGE in 12% gels; and visualized by Coomassie Brilliant Blue staining. As shown in Fig. 12, 10x main gel bands representing hi but not lo FGF2 interacting partners (indicated by arrows and numbered) were identified, two from the nuclear fraction (number 1 band at approximately 66 kDa; number 2 band at approximately 35 kDa) and eight from the cytosolic fraction (ranging from 21 kDa to 45kDa). Gel bands were excised and sent for HPLC-Mass spectrometry (www.proteome.ca) for identification.

Tables on 3 $_{1\text{-}9}$ list the highest probability results for each gel band as obtained from MS/MS Peptide Sequencing, according to the Proteomics Database from Global

Proteome Machine Organization (http://www.thegpm.org/). Based on results shown in Table 3_1, nuclear proteins with the highest probability for being in gel band #1 (at ~ 66kDa) were p68 RNA helicase, heterogeneous nuclear riboprotein K (hnRNP K), and hsp70. Of these, p68 and hsp70 were selected for further investigation.

Several categories of proteins were picked up as potentially interacting with hi FGF2 (but not lo FGF2). Their size from SDS/PAGE was similar to their size listed in Tables $3_{1\text{-}9}$. These include several proteins involved in multiple aspects of RNA metabolism: Table 3_1, hnRNP K, hnRNAP L; Table 3_2, hnRNP A1; Table 3_3, 40S ribosomal protein S4, U2 snRNP-A'; Table 3_4, 40S ribosomal protein S2, and S3;Table 3_6, hnPNP A2/B1; Table 3_7 , eukaryotic translation initiation factor 3 subunit I (eIF3i); Table 3_8, eIF-3h, eIFm. Proteins associated with regulation of apoptosis and identified in this screen (Table 3_2, Table 3_5) are C1QBP (complement component 1 Q subcomponent binding protein), and the nucleolar phosphoprotein B23 (Table 3_7).

3.2.1.4 Preparatory experiments for verification of the MS/MS Peptide sequencing data. To determine if hi FGF2 (but not lo FGF2) does indeed interact with p68, and/or hsp70, we decided to use co-immunoprecipitation approaches. Firstly, however, we examined if p68 and/or hsp70 were detectable by western blotting using commercially available antibodies, in extracts from various cell types used in our experiments, including HEK293 cells, rat as well as human primary cardiac fibroblasts, and rat neonatal cardiomyocytes. As shown in Fig.13, these proteins were

indeed detected in all of these cells. In addition, we needed to obtain and characterize antibodies capable of specifically recognizing and immunoprecipitating hi FGF2; and validate the immunoprecipitation competence of commercially available anti-p68, and anti-hsp70 antibodies.

3.2.2 Creation and characterization of anti-human hi FGF2-specific antibodies.

Fig. 14 shows human (A) and rat (B) FGF2 cDNA nucleotide- and corresponding amino acid- sequences, according to a gene bank database. The grey highlighted amino acid sequence (GRGRGRAPERVG) which is present in the human but not rat hi FGF2 N-terminal extension represents an antigenic region, used successfully by others to obtain anti-human hi FGF2-specific antibodies[61]. We used a commercial resource (Sigma Genosys) to synthesize this sequence, conjugate it to keyhole limpet hemocyanin, and use it to elicit polyclonal antibodies in rabbits. The resultant anti-hi FGF2 rabbit serum was subjected to affinity chromatography (human hi FGF2-sepharose) to isolate purified anti-hi FGF2 immunoglobulin. To create a human hi FGF2 affinity column, recombinant human hi FGF2 protein (the 24 kDa isoform) with N-terminal His tag was expressed in *E. coli* and isolated using Ni-Sepharose chromatography. The purification, detection, sepharose conjugation, and activity monitoring of human hi FGF2 are shown in Fig.15, and were identical to those shown for rat FGF2 isoforms (Fig.11).

Affinity purified anti-hi FGF2 antibodies were tested for their ability to detect human hi FGF2 by immunofluorescence and immunoprecipitation. HEK 293 cells

overexpressing human hi or lo FGF2 were subjected to dual immunostaining with anti-hi FGF2 (rabbit polyclonal; green), anti-FGF2 (mouse monoclonal; red), recognizing all FGF2 isoforms (Fig.16A). Cells were also counter-stained with DAPI, to identify nuclei (blue). In cultures overexpressing human hi FGF2, both anti-hi FGF2 and anti-FGF2 antibodies detected the same strongly staining nuclei. Detection by the monoclonal antibody confirms overexpression of FGF2, and co-detection with anti-hi FGF2 shows its ability to recognize FGF2 as well. In cultures overexpressing human lo FGF2, the monoclonal antibody detects overexpressing cells (nuclei) shown by the strong red color, confirming overexpression of lo FGF2. In this case, the anti-hi FGF2 antibodies are incapable of detecting overexpressing cells, demonstrating their specificity for only the human hi FGF2 isoform.

Human anti-hi FGF2 antibodies were tested for their ability to immunoprecipitate hi FGF2 from overexpressing HEK293 cultures, using protein A-sepharose to pull down antigen-antibody complexes. Lysates from human hi FGF2 overexpressing cells as well as immunoprecipitated proteins were analyzed by SDS/PAGE and Western blotting and probed with monoclonal anti-FGF2 antibodies. Results are shown in Fig.16B. Strong FGF2 signal at >20 kDa is seen in total lysates, demonstrating overexpression of hi FGF2. No anti-FGF2 signal in the 20-30 kDa range was present in proteins pulled down by protein A-sepharose in the absence of anti-hi FGF2 antibodies. In contrast, two strongly immunoreactive bands at 23-25 kDa were present in proteins pulled down by anti-hi FGF2-protein A sepharose. These proteins are consistent with the size of human hi FGF2. A strong immunoreactivity at ~55kDa

is non-specific, as it is found in controls as well. Taken together, data shown in Fig.16 show that anti-hi FGF2 antibodies are capable of detecting overexpressed human hi FGF2 by immunofluorescence and immunoprecipitation.

We next examined whether anti-hi FGF2 antibodies can detect endogenously expressed hi FGF2, using commercially obtained human embryonic cardiac fibroblasts. These cells were subjected to double immunofluorescence staining with anti-hi FGF2 (green) and anti-FGF2 (red), and counterstained with DAPI (blue, nuclei); Fig.17A. Anti-hi FGF2 stained nuclei as well as cytosol of these cells, although staining was stronger at nuclear sites. Monoclonal anti-FGF2 also showed mainly nuclear anti-FGF2 staining (Fig.17A-b), although at higher exposures cytosolic staining was also evident with these antibodies as well (Fig.17A-e). Non-specific rabbit IgG (used as control) did not elicit any cellular staining, even under over-exposure photography conditions (Fig.17A-d).

Results from immunoprecipitation of embryonic human cardiac fibroblasts with anti-human hi FGF2 antibodies are shown in Fig.17B. Human embryonic cardiac fibroblasts, examined by western blotting, elicited a clear anti-FGF2 signal at 18-25 kDa (lo and hi FGF2). Larger-size immunoreactive bands are also present, possibly representing FGF2 aggregation products. Anti-hi FGF2 immunoprecipitated protein(s) around 23-25 kDa, consistent with human hi FGF2. These antibodies did not immunoprecipitate lo FGF2, as shown by the absence of the 18 kDa band. The 18 kDa FGF2 band, as well as immunoreactive bands >30 kDa (likely aggregation products of lo FGF2) remained in cell lysates after removal of proteins

immunoprecipitated with anti-hi FGF2.

Taken together results from Figs 16 and 17 show that anti-hi FGF2 antibodies can immunoprecipitate endogenous as well as overexpressed human hi FGF2.

3.2.3 Examination of potential p68 (or hsp70)-hi FGF2 (endogenous) interaction via co-immunoprecipitation

3.2.3.1 Immunoprecipitation with anti-hi FGF2 does not co-precipitate p68 or hsp70. We examined if immunoprecipitation with anti-hi FGF2 antibodies will also pull down its potential interacting partners p68, and/or hsp70. Fig.18 summarizes results obtained using extracts from human atrial fibroblast cultures. Cell extracts were subjected to immunoprecipitation with anti-hi FGF2 and immunoprecipitated proteins were analyzed by western blotting using: A, FGF2 antibodies recognizing both lo and hi FGF2 isoforms; B, p68 antibodies; and C, hsp70 antibodies. Probing for FGF2 showed that hi and lo FGF2 isoforms were clearly detected in total lysates before immunoprecipitation (Fig.18A, lane 1). After removal of proteins immunoprecipitated with anti-hi FGF2, relative levels of hi FGF2 were reduced in cell extracts (lane 5). This was not observed after removal of proteins precipitated with control sepharose (lane 6). A strong immunoreactive band centering around 23 kDa was observed in proteins immunoprecipitated with anti-FGF2 (lane 3). This band was not pulled down by control sepharose beads (without immunoglobulin), lane 2, nor by non-specific immunoglobulin (lane 4). Larger size immunoreactive bands were also present in total lysates, possibly representing lo FGF2 aggregation products. A ~55 kDa band was

present in samples pulled down by all types of protein A sepharose beads and likely represents non-specific binding to Protein A sepharose. The anti-hi FGF2 antibodies did not immunoprecipitate lo FGF2, as shown by the absence of the 18 kDa band.

The immunoblot shown in (A) was re-probed for p68, using anti-p68 monoclonal antibodies. As shown in Fig.18B, these antibodies detected the p68 band in unfractionated extracts (lane 1), as well as in extracts depleted from anti-hi FGF2 immunoprecipitated proteins (lane 5); and extracts depleted from non-immune IgG precipitated proteins (lane 6). The p68 band was not detected in proteins immunoprecipitated by anti-hi FGF2 antibodies. A faint band around 55 kDa is non-specific as it is present in all protein A-sepharose precipitates (lanes 2,3,4).

The immunoblot shown in (A) was re-probed for hsp70, using anti-hsp70 monoclonal antibody. As shown in Fig.18C, this antibody detected the hsp70 band in unfractionated extracts (lane 1), as well as in extracts depleted from anti-hi FGF2 immunoprecipitated proteins (lane 5); and extracts depleted from non-immune IgG precipitated proteins (lane 6). The hsp70 band was not detected in proteins immunoprecipitated by anti-hi FGF2 antibodies. A faint band around 55 kDa is non-specific as it is present in all protein A-sepharose precipitates (lanes 2,3,4).

Taken together data shown in Fig.18 indicate that the anti-hi FGF2 antibodies immunoprecipitated hi FGF2 that was not associated with either p68, or hsp70.

3.2.3.2 Immunoprecipitation with anti-p68 as well as anti-hsp70 antibodies co-precipitates hi FGF2. We next examined whether immunoprecipitation with

anti-p68, and/or anti-hsp70 would co-precipitate hi FGF2. Extracts from HEK293 cells were subjected to immunoprecipitation with anti-p68 or anti-hsp70 monoclonal antibodies, and immunoprecipitated proteins analyzed by western blotting and probed for p68 (Fig.19A), hsp70 (Fig.19B), FGF2 (Fig.19C).

Fig.19A shows that p68 was present in the original lysate (lane 1), and that it was not pulled down non-specifically by protein G sepharose (lane 2). Anti-p68 clearly immunoprecipitated its corresponding antigen, p68 (lane 3). Antibodies to hsp70 did not co-precipitate p68 (lane 4). Mouse immunoglobulin heavy and light chains (arrows) are also detected in both anti-p68 and anti-hsp70 immunoprecipitates, as the detecting antibody is from the same species.

Fig.19B shows that hsp70 was present in the original lysate (lane 1). Some hsp70 was pulled down non-specifically by the protein G-sepharose beads (lane 2). There was no hsp70 amongst proteins immunoprecipitated by anti-p68 antibodies (lane 3); anti-hsp70 antibodies clearly immunoprecipitated hsp70, as seen by the strong signal in lane 4. Mouse immunoglobulin heavy chains (lanes 3,4) and light chains (lane 3) were also detected, as expected, since the detecting antibody is from the same species as the immunoprecipitating antibody. Taken together, data from Fig.19A and B suggest that there is no interaction between p68 and hsp70.

Fig.19C shows that anti-FGF2 antibodies (goat) recognizing both lo and hi FGF2 isoforms detect a strong 24 kDa band and a weaker ~28 kDa band pulled down by anti-p68, as well as by anti-hsp70. The 28 kDa band is likely a non-FGF2 reactivity, as it is present, in comparable amounts, even amongst proteins pulled down by protein

G-sepharose alone. A faint ~24 kDa reactivity is also pulled down by protein G-sepharose, and may represent residual hi FGF2 that dues to its 'stickiness' bound to protein G sepharose in a non-specific fashion. The much larger 24 kDa hi FGF2 amount pulled down by anti-p68 or hsp70, however, indicates specific interaction between hi FGF2 and p68, and between hi FGF2 and hsp70Please note that although FGF2 is not detectable in HEK293 extracts (Fig.19, lane 1) under the exposure conditions used for lanes 1-4, both hi and lo FGF2 bands are detected upon longer exposure of the blot (lane 1').

Taken together, data shown in Fig.19 indicate that p68 as well as hsp70 can interact with human hi FGF2, but not lo FGF2. Also, these interactions may be mutually exclusive: hi FGF2 interacting with p68 does not interact (directly or indirectly) with hsp70. If it did, hsp70 should be present in Fig.19B, lane 3. Similarly, hi FGF2 interacting with hsp70 does not interact (directly or indirectly) with p68; if it did, p68 should be detectable in Fig.19A, lane 4. It is possible that both p68 and hsp70 recognize the same domain on the N-terminal extension of human hi FGF2, and thus when one is bound, the other one is excluded from interaction.

3.2.4 Examination of potential p68-(DsRed) hi FGF2 interaction

3.2.4.1 Anti-p68 antibodies do not co-precipitate overexpressed DsRed rat hi FGF2. We examined if anti-p68 antibodies would co-precipitate overexpressed DsRed-labeled rat hi FGF2. HEK 293 cells were transfected with DsRed rat hi FGF2 and extracted 2 days later. Cell lysates were subjected to immunoprecipitation

with monoclonal anti-p68 antibodies and the immunoprecipitated proteins were analyzed by Western blotting for p68, and FGF2 (Fig.20). As expected, anti-p68 detected p68 in cell extracts before removal of immunoprecipitated proteins (lane 1); a very strong p68 band was present in the anti-p68 immunoprecipitate (lane 4). Probing for FGF2 (detecting DsRed hi FGF2 at ~ 50 kDa) showed that this protein was absent in non-transfected but present in transfected cells (Fig.20, lanes 1 and 2, respectively). It would appear, however that DsRed hi FGF2 was pulled down non-specifically only, by all protein G-sepharose columns (lanes 3-5); there was no increase in anti-FGF2 reactivity in the anti-p68 immunoprecipitate. Relative levels of DsRed hi FGF2 were similar in cell extracts after removal of anti-p68 or non-immune IgG-precipitated proteins. We conclude that the anti-p68 antibodies pull down p68 that does not interact with DsRed rat hi FGF2.

3.2.4.2 Effect of p68 knockdown on the hi FGF2-induced chromatin compaction.

We examined if p68 was required for hi FGF2 to exert its effects on chromatin compaction. This was addressed by introducing two different, commercially available, p68-specific shRNAs, shRNA1(p68), shRNA2(p68), in HEK293 cells, aimed at reducing endogenous p68 levels. The sequence of all these shRNAs was shown in Table 4.

We examined if expression of the p68-specific shRNAs or of a control non-specific shRNA (scrambled shRNA) would by themselves affect nuclear morphology of HEK293 cells. Please note that the plasmid vector for p68 shRNA is

engineered in a bicistronic pattern to express EGFP proteins as well, allowing us to identify the transfected cells. As shown in Fig.21 (A), neither scrambled shRNA, nor the two specific shRNAs for p68 had any effect on nuclear compaction index, which remained indistinguishable to that of control cultures.

We also determined if the p68-specific shRNAs are indeed effective in decreasing p68 levels, and if so, if they interfere with the ability of DsRed rat hi FGF2 to promote apoptosis. HEK293 cells were co-transfected with DsRed rat hi FGF2 and EGFP-labeled p68 specific or scrambled shRNAs. Fig.22 (upper panel) shows the p68 content of non-transfected and transfected cells in a representative western blot. The scrambled shRNA had no effect on relative p68 content (compare lane 2 to lane 1). Both p68 specific shRNAs decreased relative p68 content (compare lanes 3, 4 to lane 1). Comparable DsRed rat hi FGF2 expression between the different groups is indicated when the same blot is probed for FGF2 (Fig.22, lower panel).

Decreased p68 content did not seem to change the DsRed rat hi FGF2-induced chromatin compaction/cell death (Fig.23). Representative fluorescence images are shown in Fig.23A, while corresponding quantitative data are presented in Fig.23B. DsRed rat hi FGF2, irrespectively of the co-expression of either scrambled or p68-specific shRNAs (and reduction in p68), retained its ability to promote chromatin compaction (Fig.23, A, B).

3.2.5 Overexpression of hsp70 prevents the hi FGF2-induced nuclear compaction, possibly by translocating to the nucleus. Hsp70 is well established

as an anti-apoptotic molecule in a great variety of apoptotic models, and cell types. We used rat neonatal cardiomyocytes to examine if overexpression of hsp70 (by adenoviral transduction, Ad-hsp70) would rescue the cells from hi FGF2 induced chromatin compaction and ensuing cell death.

Pilot data characterized the effect of various doses (m.o.i.) of hsp70 on nuclear morphology and established that up to 75 m.o.i. had no adverse effect (data not shown). Thus rat neonatal cardiomyocytes were transduced with control vector, Ad-human hi FGF2 (100 m.o.i.), in the absence or presence of co-transduction with 50 or 70 m.o.i. of Ad-hsp70. Two days post-transduction cells were subjected to immunofluorescence with anti-human hi FGF2 and anti-hsp70 antibodies, and counterstained for DAPI. Representative microscopic photographs at lower and higher magnification are shown in Fig.24, A and B, respectively. As expected, in hi FGF2-alone overexpressing cultures, hi FGF2 was found predominantly in the nucleus (Fig.24A-d, Fig.24B-h), and induced a compacted chromatin phenotype (Fig.24A-f, Fig.24Bi). In hsp70 overexpressing cultures hsp70 was found predominantly in cytoplasm (Fig.24A-h, Fig.24B-d), and did not affect nuclear morphology by itself. In hi FGF2 and hsp70 co-overexpressing cultures (Fig.24A-k, Fig.24B-j), hsp70 was localized not only in cytoplasm but also in the nucleus, suggesting translocation. Hi FGF2 localization remained nuclear in the co-transduced cultures (Fig.24A-j, Fig.24B-h).

The DNA compaction by hi FGF2 was significantly prevented by hsp70 overexpression (Fig.24A-l, Fig.24B-l). Quantitative data are shown in Fig.24C. The hi

FGF2-induced nuclear compaction index (NCI) was significantly decreased in cultures overexpressing either 50 or 70 m.o.i. Ad-hsp70. As this effect was accompanied by increased hsp70 localization in the nucleus (translocation), it is logical to suggest that the translocation itself may have been achieved via interaction with hi FGF2, and that nuclear presence of hsp70 was important in preventing the nuclear effects of hi FGF2.

We used a higher resolution and magnification lense (67x) to obtain additional images of co-overexpressing cardiomyocytes, stained for hi FGF2 (green) and hsp70 (red). The merging of these images elicited a yellow color in areas of potential co-localization, and possibly hi FGF2-hsp70 interaction, most strongly in an area within the nuclear periphery (Fig.25). Areas devoid of hsp70 within the nucleus but still staining for hi FGF2 can also be seen within nuclei.

Fig. 26 shows western blot-based detection and quantification of overexpressed hsp70 and hi FGF2. Successful overexpression of hsp70 in Ad-hsp70-alone transduced cultures is shown in Fig.26A, lane 2; successful overexpression of human hi FGF2 (in the presence or absence of hsp70 overexpression) is shown in Fig.26A, lanes 3 and 4, respectively. Interestingly, overexpression of hi FGF2 seemed to promote a small but statistically significant increase in endogenous hsp70. In addition, an extra anti-hsp70 immunoreactive band, migrating slightly faster than the original band and thus a possible degradation product of the overexpressed larger protein, was detected only in hi FGF2 overexpressing cultures (Fig.26A, lane 4).

3.3 Effect of pathophysiological stimuli on endogenous hi FGF2 expression. We initiated a series of studies to examine if various agents associated with the induction of cardiac pathology (hypertrophy, fibrosis, cell death) would affect endogenous hi FGF2 accumulation in cardiac cells such as: primary cultures of rat cardiac fibroblasts and cardiac myocytes; human atria-derived fibroblasts. We also examined expression and localization of hi FGF2 in human atrial tissue, and in diseased animal model hearts, associated with increased incidence of myocytes cell death.

3.3.1 Rat heart cells. Fig.27 shows the effect of (A,B) isoproterenol (a β-adrenergic agonist; 10 μM), and, (C,D), glucose (25 mM) on hi FGF2 acummulation by rat neonatal cardiac fibroblasts. Isoproterenol induced a significant increase in rat neonatal fibroblast-associated hi FGF2, detectable at 48 h post-treatment (Fig.27A); this increase was no longer evident at 96 h post-treatment (Fig.27B). Glucose, on the other hand had no effect on hi FGF2 accumulation at either 48 or 96 hour post-treatment, compared to mannitol-treated fibroblasts. Mannitol treatment (25mM) was used in control cultures.

Similar studies, conducted on neonatal cardiac myocytes, are shown in Fig.28. Neither isoproterenol, nor glucose had any effect on hi FGF2 accumulation at any time point.

In another series of studies we used rat primary adult cardiomyocyte cultures, and stimulated them with isoproterenol (10 μM), angiotensin II (10^{-7} M) or endothelin

I (10^{-7} M). Cells were analyzed at 24 and 48 hr post-stimulation. As shown in Figure 29, none of these agents had an effect on hi FGF2 accumulation, compared to control cultures at any of the time points examined. Taken together, our results from rat heart--derived cells indicate that while cardiac fibroblast-derived hi FGF2 is increased by stimuli such as angiotensin II and isoproterenol, linked to cardiac hypertrophy, fibrosis and cell death, cardiac myocyte-associated hi FGF2 remains unaffected under the same conditions.

3.3.2 Human heart cells. We extended our studies to include human heart (atria) derived primary fibroblasts. These cells were grown out of atrial appendages dissected from human patients during cardiac surgery, by another PhD student in the laboratory (Mr. Jon-Jon Santiago) as part of his PhD research project. These cells (frozen at P1) were used for our experiments at passage P2. As shown in Fig.30, stimulation with isoproterenol induced significant upregulation of hi FGF2 at 48h. This increase was no longer evident at a later time point, 96 h. Angiotensin II stimulation resulted in significant hi FGF2 upregulation by 48 h; this increase was no longer present at 96 h. Chronic endothelin 1 treatment of human atria-derived fibroblasts caused significant hi FGF2 upregulation, assessed at 96 and 144 h (Fig.30C). High glucose, on the other hand, did not affect relative hi FGF2 levels at any of the time points tested (24, 48, 96 h); Fig.30D. Taken together our results indicate that hypertrophy and heart failure-associated stimuli upregulate cardiac fibroblast hi FGF2 expression.

3.3.3 Human heart tissue. We used immunohistochemistry to assess hi FGF2 localization in human atrial tissue. Paraffin sections were stained for hi FGF2, using our own affinity purified anti-hi FGF2 antibodies; antigen-antibody complexes were visualized by horseradish peroxidase (HRP)-catalyzed conversion of 3,3-diaminobenzidine (DAB), creating brown color. Nuclei were counterstained blue, using hematoxylin staining. Fig.31a,b shows representative images: hi FGF2 was detected in the cytosol of atrial cardiac myocytes (light brown), as well as within nuclei; nuclear anti-hi FGF2 staining appeared more intense (very dark brown). In a close-up image (Fig.31b) nuclei are present staining only blue, with no brown; as well as nuclei staining both blue and dark brown, confirming hi FGF2 accumulation to the nucleus. Some myocyte nuclei appear to have condensed chromatin, suggested by their darker blue color and overall compact size (Fig.31b,c). Dark anti-hi FGF2 staining seems to co-stain the condensed nuclei (Fig.31b). Fig.31c, d show images from atrial heart sections subjected only to nuclear staining. Specificity of the anti-hi FGF2 staining is indicated by the absence of any brown staining in sections incubated without primary antibodies; please compare images shown in Fig.31e,f, incubated without and with anti-hi FGF2 antibodies.

3.3.4 Animal Models. In a final series of pilot experiments, shown in Fig.32, we examined relative hi FGF2 levels in diseased, compared to normal, mouse and rat hearts. The mdx muscular dystrophy mouse is characterized by the development of skeletal muscle [198] and cardiac muscle lesions [199]. We obtained several mouse

hearts from both male and female mice of 6 weeks of age (from Dr. Judy Anderson, University of Manitoba), and examined their hi FGF2 content. As shown in Fig.32A, male mdx mouse hearts had significantly reduced hi FGF2 content compared to their normal counterparts; this was not the case for female Mdx mouse hearts (Fig.32B).

Adriamycin is used as an effective anti-cancer treatment, but is associated with development of cardiomyopathic heart [200]. We obtained hearts from rats subjected or not to Adriamycin treatment (from Dr. Pawan Singal, University of Manitoba), as in [201], and analyzed them for their hi FGF2 content: as seen in Fig.32C hearts from Adriamycin-treated rats had significantly increased hi FGF2 content compared to normal hearts.

In conclusion. This series of exploratory studies on endogenous hi FGF2 expression shows that:

a) Cardiac fibroblast hi FGF2 (but not cardiac myocyte hi FGF2) becomes upregulated in response to several agents linked to the promotion of cardiac pathology (angiotensin II, endothelin 1, isoproterenol)

b) High glucose did not affect hi FGF2 accumulation by either fibroblasts or myocytes

c) Human atrium-derived fibroblasts respond to pathological stimuli in a manner similar to their rat counterparts, by upregulating their hi FGF2.

d) Hi FGF2 is detected in human atrial cardiomyocyte cytosol as well as nucleus, in situ

e) Increased nuclear hi FGF2 is detected in human atrial myocyte nuclei with

apparently condensed chromatin, in situ.

f) Hearts from Adriamycin-treated rats have increased hi FGF2 content compared to control hearts.

Figure 1

A

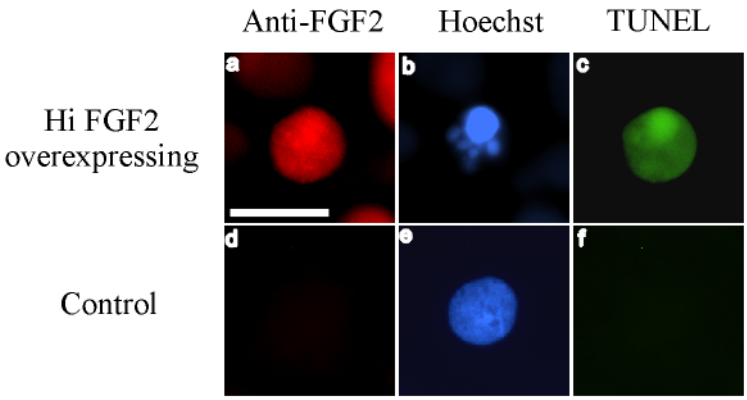
Anti-FGF2
Hoechst
TUNEL
Hi FGF2 overexpressing
Control
a
b
c
d
e
f

B

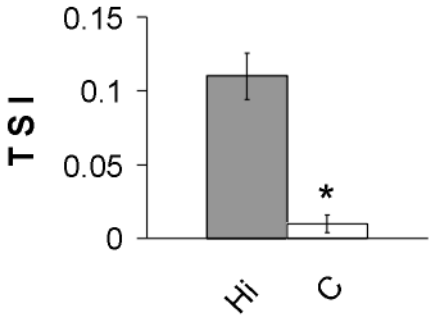
TSI
0.15
0.1
0.05
0
*
Hi
C

Figure 1. Overexpression of hi FGF2 in HEK293 cells increases TUNEL staining

(A) Representative triple-stained images of cells from (a,b,c) human hi FGF2 overexpressing , or (d,e,f) non-overexpressing control cultures, and stained for (a,d) FGF2 (monoclonal anti-FGF2 antibodies), (b,e) Hoechst, and (c,f) TUNEL, at 72 hr post-transfection. Scale bar = 20 μM. Cumulative data are shown in (B), presenting theTUNEL staining index (TSI, fraction of cells that are positive for TUNEL) in hi FGF2 overexpressing (Hi) versus non-overexpressing control cells (C), as indicated. Data are shown as the mean± SD, n=3, *P < 0.0001.

Figure 2

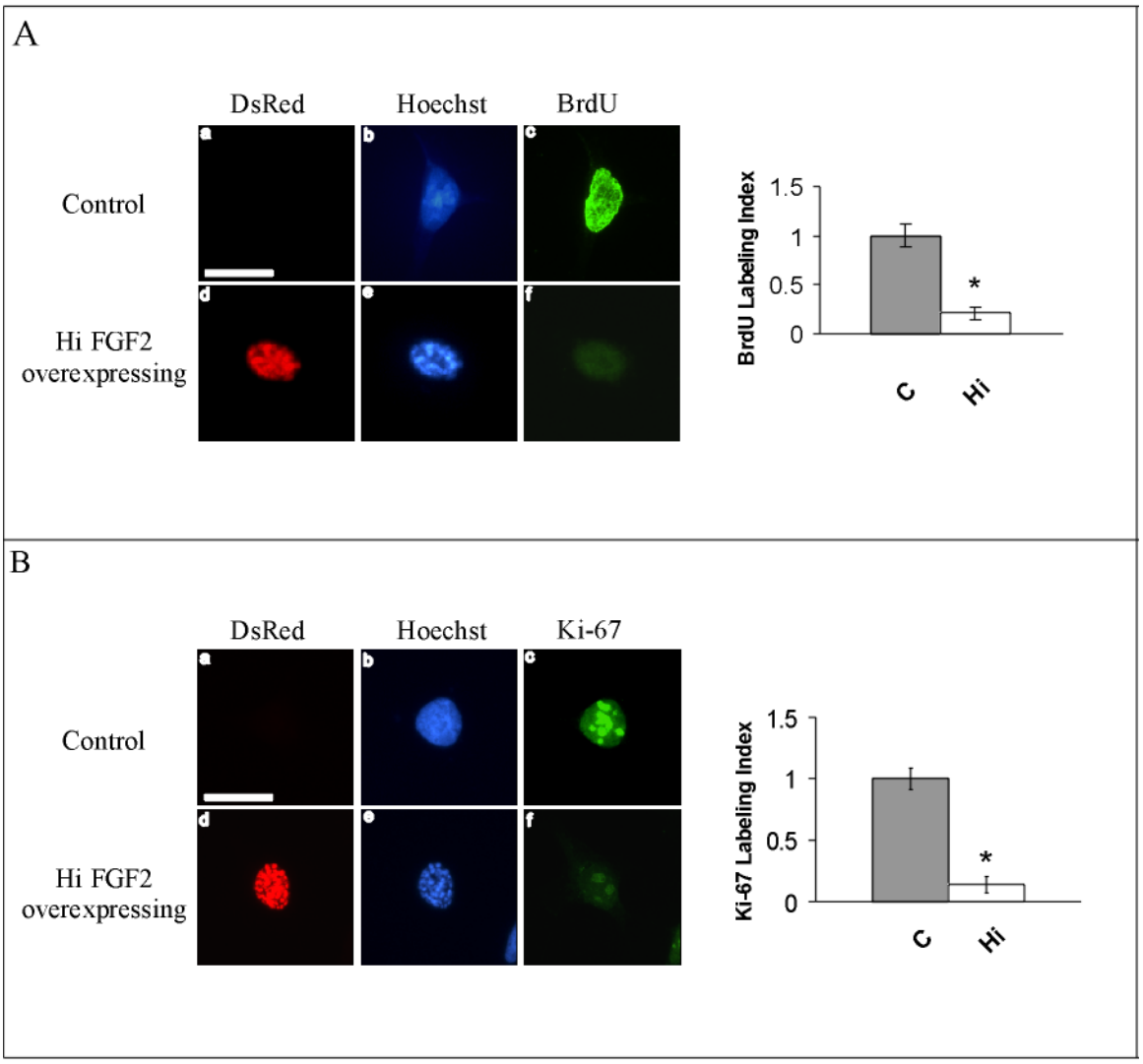
A
DsRed
Hoechst
BrdU
Control
Hi FGF2 overexpressing
BrdU Labeling Index
1.5
1
0.5
0
*
C
Hi
B
DsRed
Hoechst
Ki-67
Control
Hi FGF2 overexpressing
Ki-67 Labeling Index
1.5
1
0.5
0
*
C
Hi

Figure 2. Overexpression of hi FGF2 impacts negatively on expression of cell proliferation markers. HEK 293 cells were transfected with DsRed hi FGF2, and 48 hr later were processed for immunofluorescence staining for (A) BrdU, a marker of DNA synthesizing cells, or (B) Ki-67, a marker of proliferating cells. Cells were also counter-stained for Hoechst, to visualize nuclei. **(A).** Representative triple-fluorescence images of (a,b,c) control cells or (d,e,f) cells overexpressing DsRed hi FGF2. DsRed staining (red) represents hi FGF2 expression and is detected in (d) but not (a). Hoechst staining is shown in (b,e; blue), and anti-BrdU staining (green) is shown in (c,f). Cumulative data show the fraction of BrdU incorporating cells (BrdU Labeling Index) in (C) control and (Hi) hi FGF2 overexpressing cells. **(B).** Representative triple-fluorescence images of (a,b,c) control cells or (d,e,f) cells overexpressing DsRed hi FGF2. DsRed staining (red) represents hi FGF2 expression and is detected in (d) but not (a). Hoechst staining is shown in (b,e; blue), and anti-Ki-67 staining (green) is shown in (c,f). Cumulative data show the fraction of Ki-67-positive cells (Ki-67 Labeling Index) in (C) control and (Hi) hi FGF2 overexpressing cells. Data are shown as the mean ± S.D., n=3, *P<0.001.

Figure 3

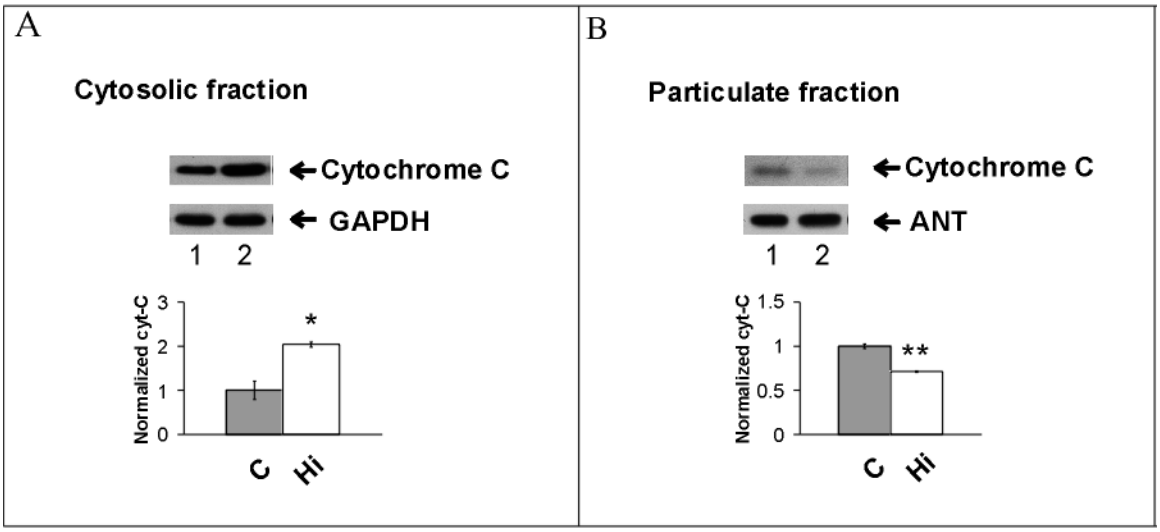
A
Cytosolic fraction
Cytochrome C
GAPDH
1 2
Normalized cyt-C
3
2
1
0
*
C
Hi
B
Particulate fraction
Cytochrome C
ANT
1 2
Normalized cyt-C
1.5
1
0.5
0
**
C
Hi

Figure 3. Overexpression of hi FGF2 stimulates release of cytochrome C to the cytosol. Panels (A) and (B) show representative Western blots for cytochrome C in, respectively, the cytosolic and particulate cellular fractions, as indicated. Staining for GAPDH (a cytosolic protein) and ANT (a mitochondrial inner membrane protein) are used to indicate equivalent protein loading. Corresponding cumulative data for relative cytochrome C levels in fractions from (C) control or (Hi) Hi FGF2 overexpressing cultures are included in each panel. Data are presented as mean ± SD, n=3. *P < 0.05 and **P < 0.0005, compared to control cell cultures.

Figure 4

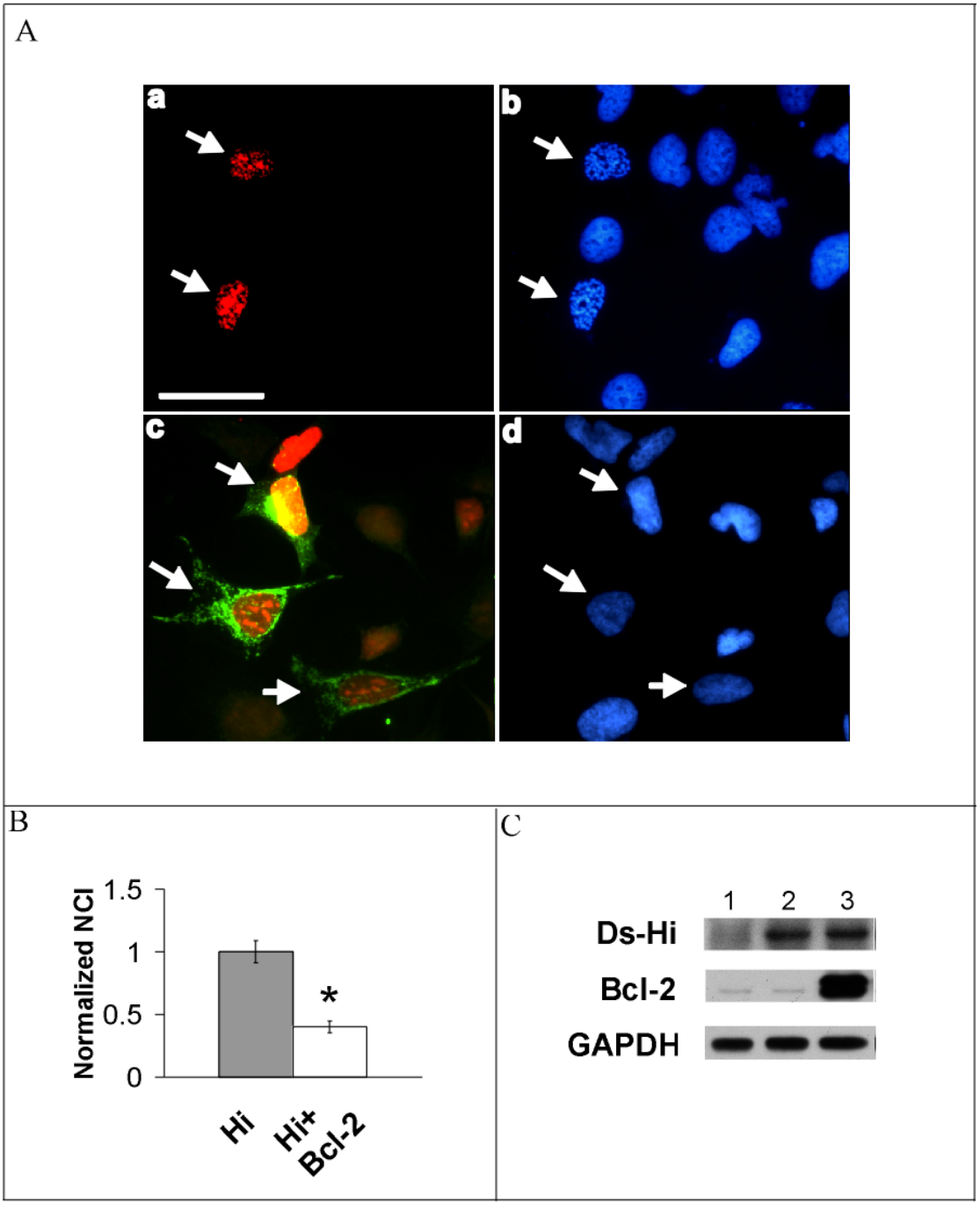
A
a
b
c
d
B
Normalized NCI
1.5
1
0.5
0
*
Hi
Hi+ Bcl-2
C
1
2
3
Ds-Hi
Bcl-2
GAPDH

Figure 4. The Hi FGF2-induced chromatin compaction is prevented by Bcl-2 overexpression. Cells, transfected with DsRed-Hi FGF2 in the absence or presence of co-transfection with Bcl-2, were assessed 24 hours after transfection. (A). All cells were triple-stained for Hi FGF2 (DsRed; red); Bcl-2 (green) and nuclei (blue). Representative images of cells expressing hi FGF2 (a,c) without (a) or with (c) Bcl-2 co-overexpression. Corresponding nuclear images are shown in (b), and (c), respectively. (B) Relative nuclear compaction index (fraction of cells with compacted chromatin) is shown for cultures overexpressing hi FGF2, (Hi) in the absence, and (Hi+Bcl-2) in the presence of Bcl-2 overexpression. Data are shown as the mean ± SD, n=3. *$P < 0.0001$ (C). Representative western blot images of total cell lysates probed for DsRed (Ds-Hi) hi FGF2 (monoclonal anti-FGF2 antibodies); Bcl-2; and GAPDH, used to show equivalent protein loading. Lanes 1, 2 and 3 correspond, respectively, to control, hi FGF2-transfected, and hi FGF2 plus Bcl-2 transfected cultures.

Figure 5

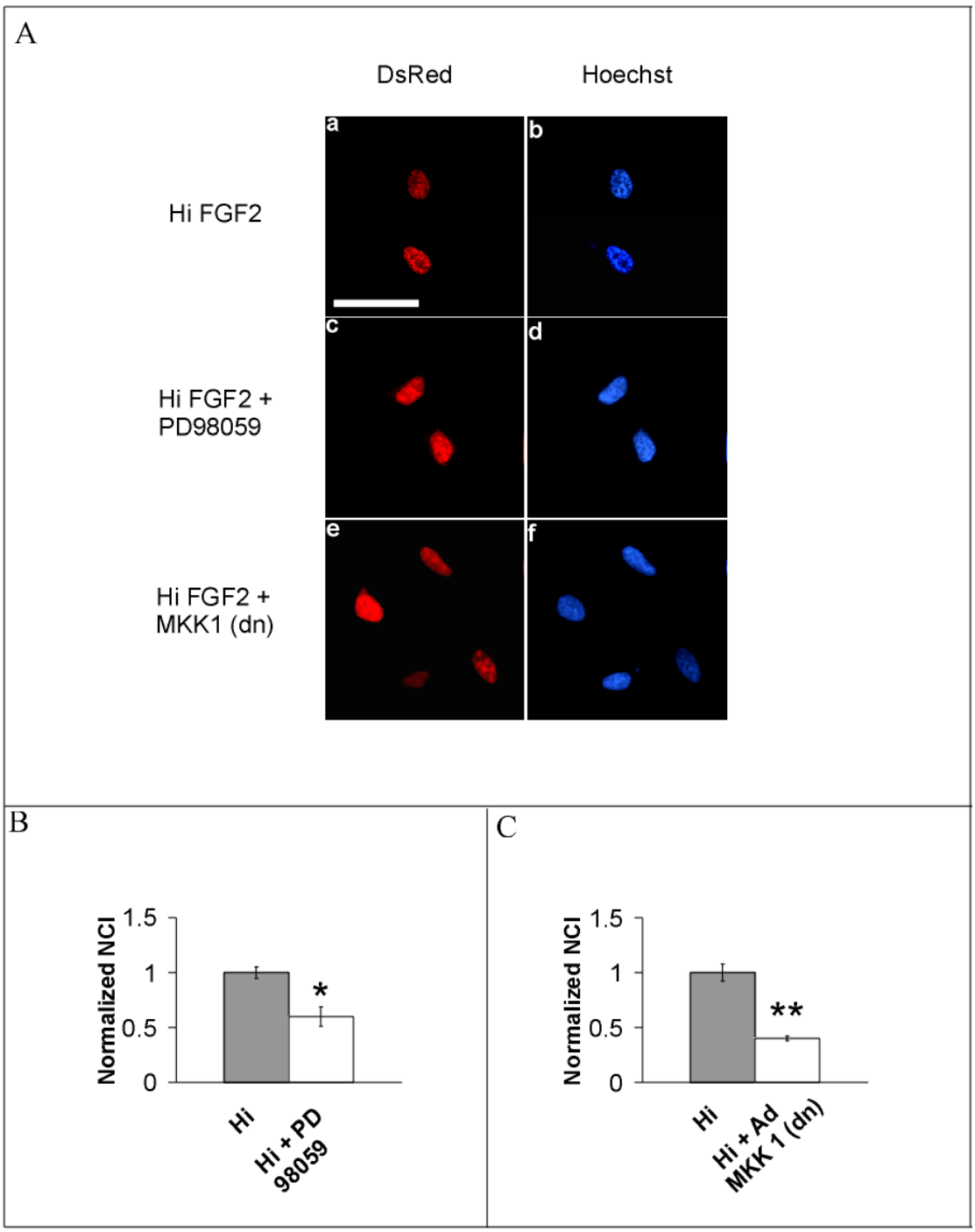
A
DsRed
Hoechst
Hi FGF2
Hi FGF2 + PD98059
Hi FGF2 + MKK1 (dn)
a
b
c
d
e
f
B
Normalized NCI
1.5
1
0.5
0
*
Hi
Hi + PD 98059
C
Normalized NCI
1.5
1
0.5
0
**
Hi
Hi + Ad MKK 1 (dn)

Figure 5. Inhibition of the ERK ½ activation pathway prevents chromatin compaction by hi FGF2. (A) Representative immunofluorescence images of HEK 293 cells double-labeled for DsRed (a, c, e) and DNA (b, d, f), one day after transfection with a cDNA for DsRed hi FGF2, (a,b) in the absence or (c,d) presence of 20 μM PD 98059 , or (e,f) co-expression of dominant-negative (dn) MKK1. Scale bar= 50 μM. Cumulative data for the effect of PD 98059 or MKK1 (dn) on the hi FGF2-induced chromatin compaction are shown in, respectively, (B) and (C). Hi denotes data from cultures overexpressing hi FGF2 in the absence of inhibitors. Hi+PD 98059 and Hi+MKK1 (dn) denote data from cultures overexpressing hi FGF2 in the presence of the corresponding inhibitors, as indicated. Data were normalized by arbitrarily defining values from hi FGF2 overexpressing cultures as 1. NCI is significantly decreased by both PD 98059 and MKK1 (dn). Data are shown as the mean ± SD, n=3. *$P < 0.05$ and **$P < 0.005$.

Figure 6

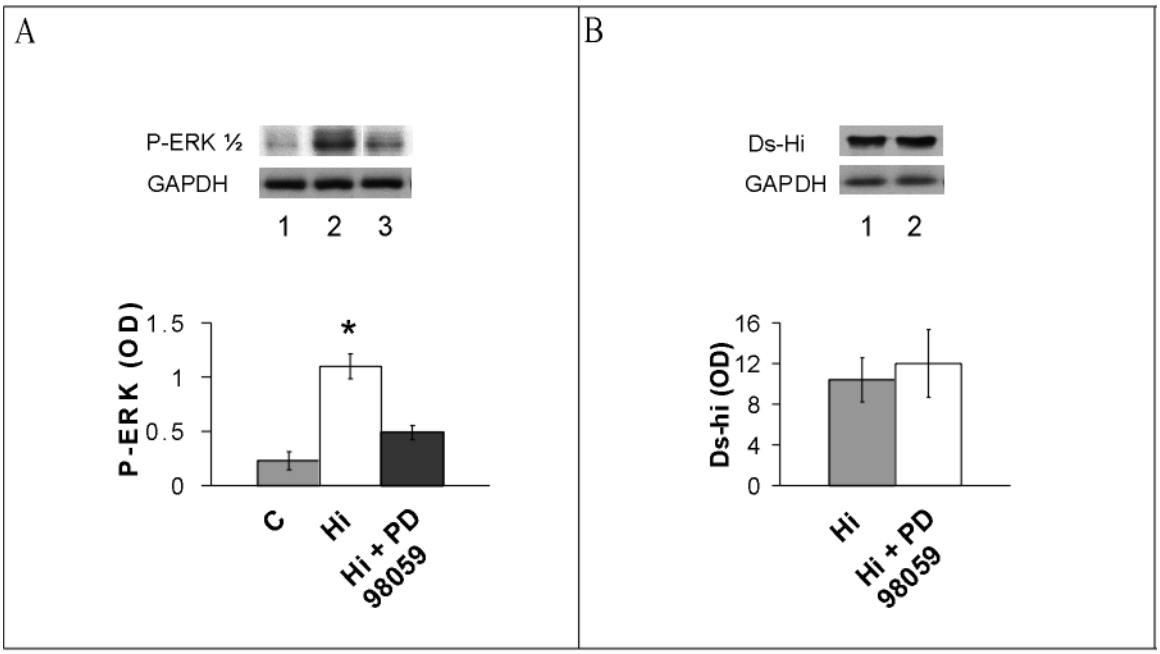
A
P-ERK ½
GAPDH
1 2 3
P-ERK (OD)
1.5
1
0.5
0
*
C
Hi
Hi + PD 98059
B
Ds-Hi
GAPDH
1 2
Ds-hi (OD)
16
12
8
4
0
Hi
Hi + PD 98059

Figure 6. PD 98059 is effective in decreasing hi FGF2-induced ERK ½ activation but does not affect levels of hi FGF2 accumulation. (**A**) Representative Western blots for phosphorylated ERK ½ level (P-ERK ½) in total cell lysate from, lane 1, control cultures, lane 2, DsRed hi FGF2 overexpressing cultures (24hr), lane 3, DsRed hi FGF2 overexpressing cultures (24hr) in the presence of 20 μM PD 98059. GAPDH, serving as a loading control is also included. Densitometry-based quantification of phosphorylated ERK ½ level relative to GAPDH expression and statistical analysis are also included. Data are presented as the mean ± S.D., n=3, *P<0.001. **(B)** Representative Western blots using monoclonal anti-FGF2 antibodies for DsRed hi FGF2 levels in total cell lysates from, lane 1, DsRed hi FGF2 overexpressing cultures, lane 2, DsRed hi FGF2 overexpressing cultures in the presence of 20 μM PD 98059, at one day post-transfection. GAPDH serving as loading controls is also included. Densitometry-based quantification of DsRed hi FGF2 level relative to GAPDH expression and statistical analysis are shown in the lower panel. Data are presented as the mean ± S.D., n=3, * P<0.05.

Figure 7

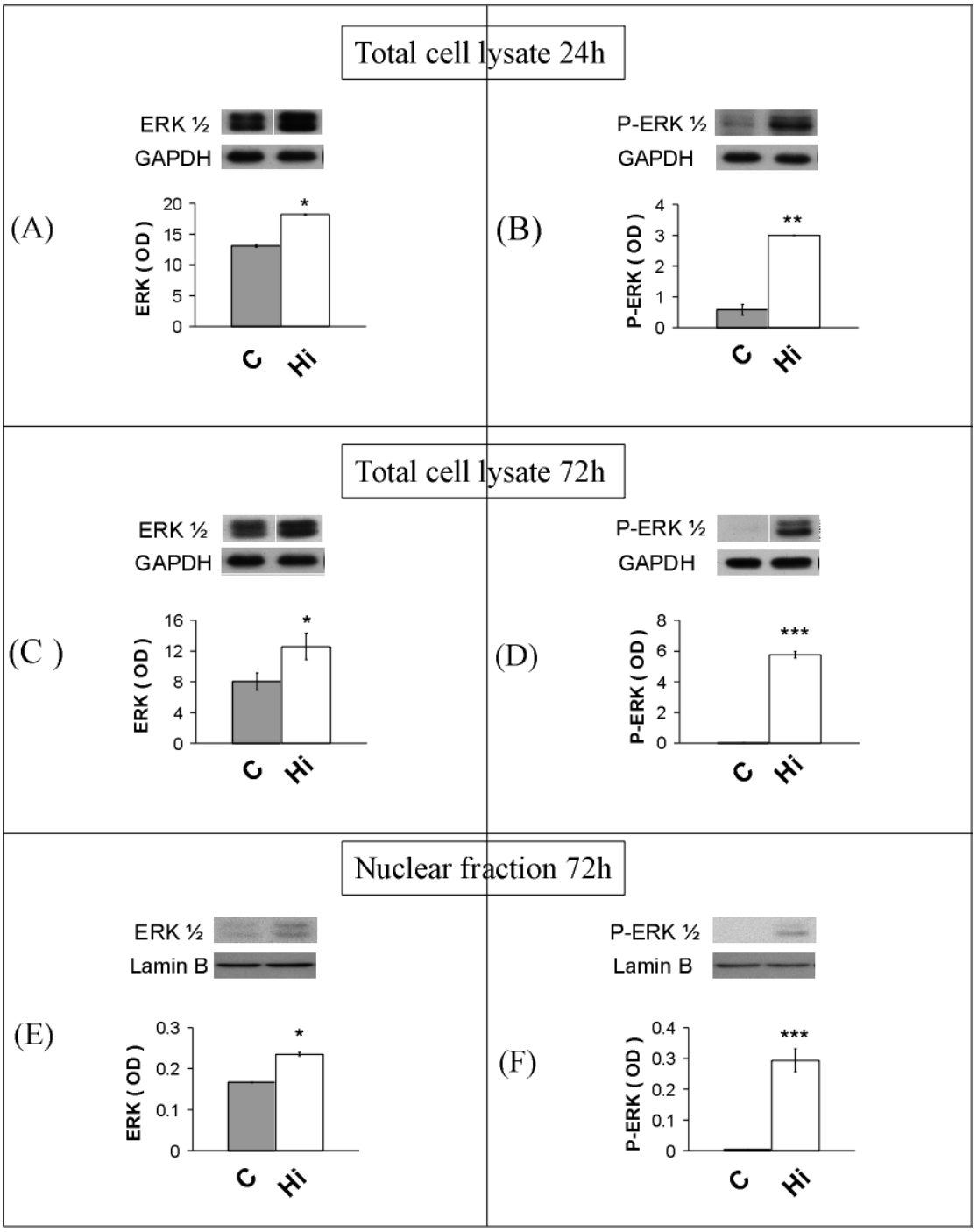
Total cell lysate 24h
ERK ½
GAPDH
(A)
ERK (OD)
20
15
10
5
0
*
C
Hi
P-ERK ½
GAPDH
(B)
P-ERK (OD)
4
3
2
1
0
**
C
Hi
Total cell lysate 72h
ERK ½
GAPDH
(C)
ERK (OD)
16
12
8
4
0
*
C
Hi
P-ERK ½
GAPDH
(D)
P-ERK (OD)
8
6
4
2
0
***
C
Hi
Nuclear fraction 72h
ERK ½
Lamin B
(E)
ERK (OD)
0.3
0.2
0.1
0
*
C
Hi
P-ERK ½
Lamin B
(F)
P-ERK (OD)
0.4
0.3
0.2
0.1
0
***
C
Hi

Figure 7. Hi FGF2 induces sustained activation and nuclear accumulation of ERK½ in HEK 293 cells.

Representative Western blots and corresponding cumulative data showing the effect of (Hi) hi FGF2 overexpression on total ERK ½ (ERK ½) as well as phosphorylated ERK ½ (P-ERK ½) levels, in arbitrary optical density (OD) units, compared to non-overexpressing cells (control, C), detected in total cell lysates and in nuclear fractions, at 24 and 72 hr post-transfection, as indicated. Data from total cell lysates, obtained at 24 and 72 hr post-transfection are shown in (A, B) and (C, D) respectively. Data from nuclear fractions obtained at 72 hr post-transfection are shown in (E,F). Immunoreactivity signals for GAPDH or Lamin B, serving as loading controls are also shown. Data are presented as mean± SEM, n=3.*P<0.05, **P < 0.005, ***P < 0.001.

Figure 8

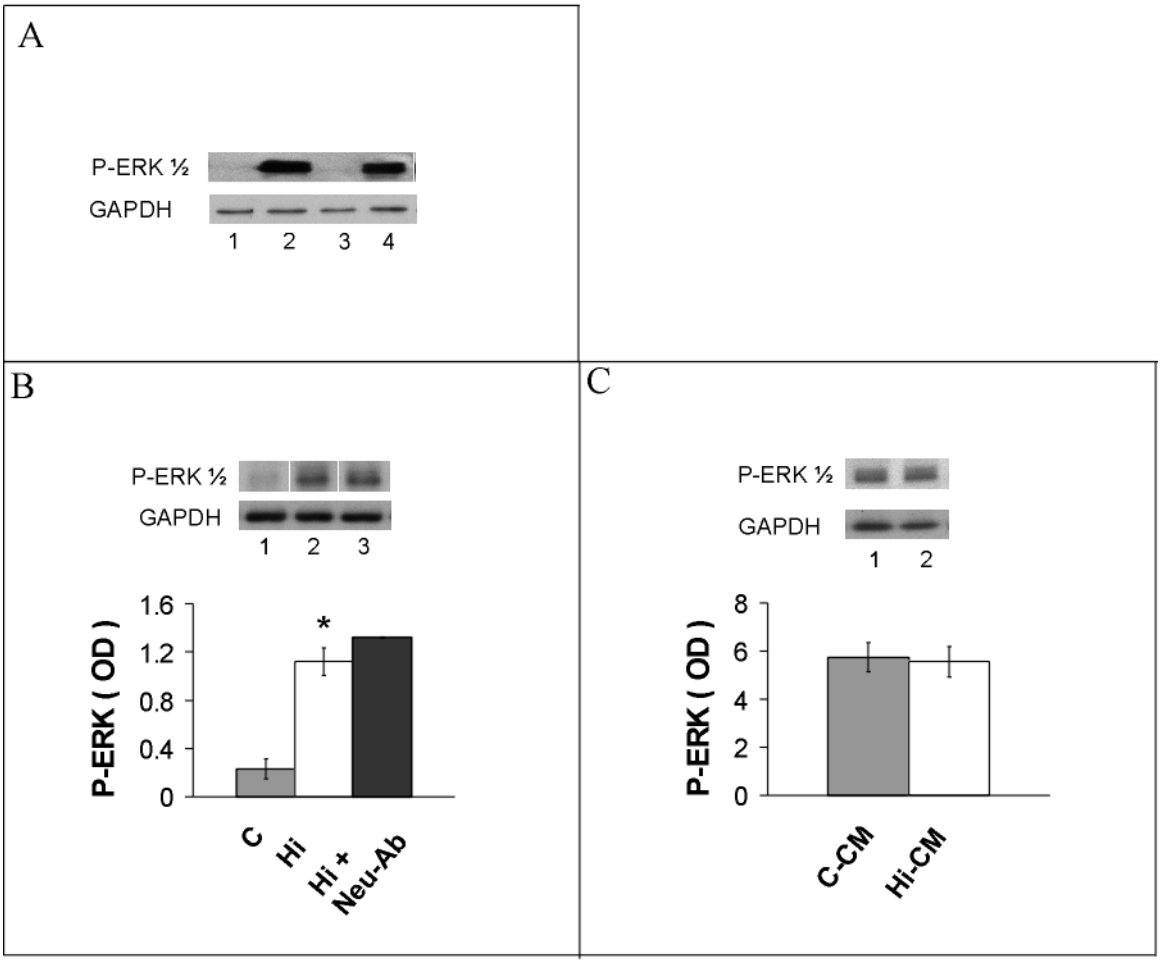
A
P-ERK ½
GAPDH
1 2 3 4
B
P-ERK ½
GAPDH
1 2 3
P-ERK (OD)
1.6
1.2
0.8
0.4
0
*
C
Hi
Hi + Neu-Ab
C
P-ERK ½
GAPDH
1 2
P-ERK (OD)
8
6
4
2
0
C-CM
Hi-CM

Figure 8. Hi FGF2 activates ERK by an intracrine mode of action.

A: Neutralizing FGF2 antibodies prevented ERK ½ activation induced by added FGF2. Representative Western blot for phosphorylated ERK ½ in total cell lysates (20 μg protein/lane), from, lane 1, control cultures, lane 2, cultures treated with added FGF2 (0.5 ng/ml, 30 min), lane 3, cultures treated with FGF2 in the presence of neutralizing FGF2 antibodies (20 μg/ml), lane 4, cultures treated with FGF2 in the presence of non-specific antibodies (20 μg/ml). **B: Neutralizing FGF2 antibodies did not affect ERK activation by overexpressed hi FGF2.** Representative Western blot for phosphorylated ERK ½ in, lane 1, total cell lysates from control cultures, lane 2, cultures transfected with DsRed hi FGF2, lane 3, cultures transfected with DsRed hi FGF2 and kept in the presence of neutralizing FGF2 antibodies **.** Cumulative data are also included showing phospho-ERK (P-ERK) levels in arbitrary optical density (OD) units. C, Hi, Hi+neu-Ab demote values corresponding to control unstimulated cultures, hi FGF2 overexpressing cultures, Hi FGF2 overexpressing cultures supplemented with FGF2 neutralizing antibodies. **(C). Conditioned media from hi FGF2 overexpressing cultures do not show an increased ability to activate ERK ½**. Representative Western blot for phosphorylated ERK ½ in total lysates from, lane 1, cell cultures incubated with conditioned medium from non-overexpressing cultures, lane 2, conditioned medium from hi FGF2 overexpressing cultures. GAPDH, served as loading control, was also included. Data in B, C, are presented as mean± SEM, n=3.*P<0.05.

Figure 9

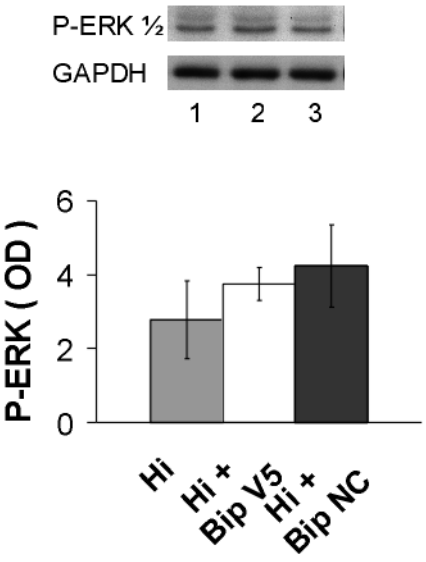

Figure 9. The Bax inhibiting peptide V5 had no effect on the hi FGF2-induced ERK ½ phosphorylation. Representative Western blot for phosphorylated ERK ½ (P-ERK ½) in total cell lysates from cultures transfected with DsRed Hi FGF2 and, lane 1, left untreated, lane 2, treated with the Bip V5 peptide, lane 3, treated with an inert control peptide Bip NC. GAPDH serving as loading controls is also included. Densitometry-based quantification of phosphorylated ERK ½ level relative to GAPDH expression and statistical analysis are shown in the lower panel. Data are presented as the mean ± S.D., n=3, P>0.05.

Figure 10

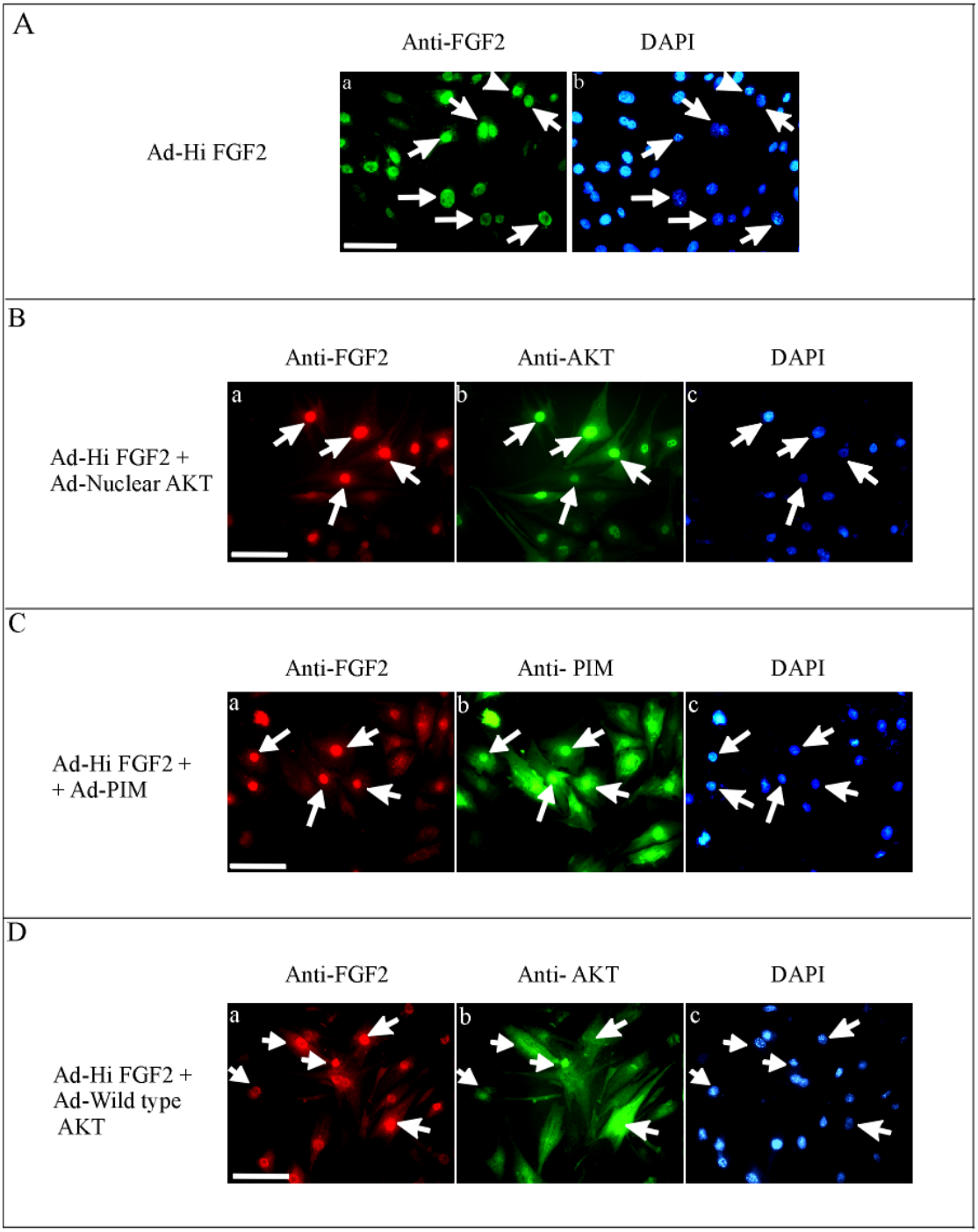
A
Anti-FGF2
DAPI
Ad-Hi FGF2
a
b
B
Anti-FGF2
Anti-AKT
DAPI
Ad-Hi FGF2 +
Ad-Nuclear AKT
a
b
c
C
Anti-FGF2
Anti- PIM
DAPI
Ad-Hi FGF2 +
+ Ad-PIM
a
b
c
D
Anti-FGF2
Anti- AKT
DAPI
Ad-Hi FGF2 +
Ad-Wild type
AKT
a
b
c

Figure 10 (continued)

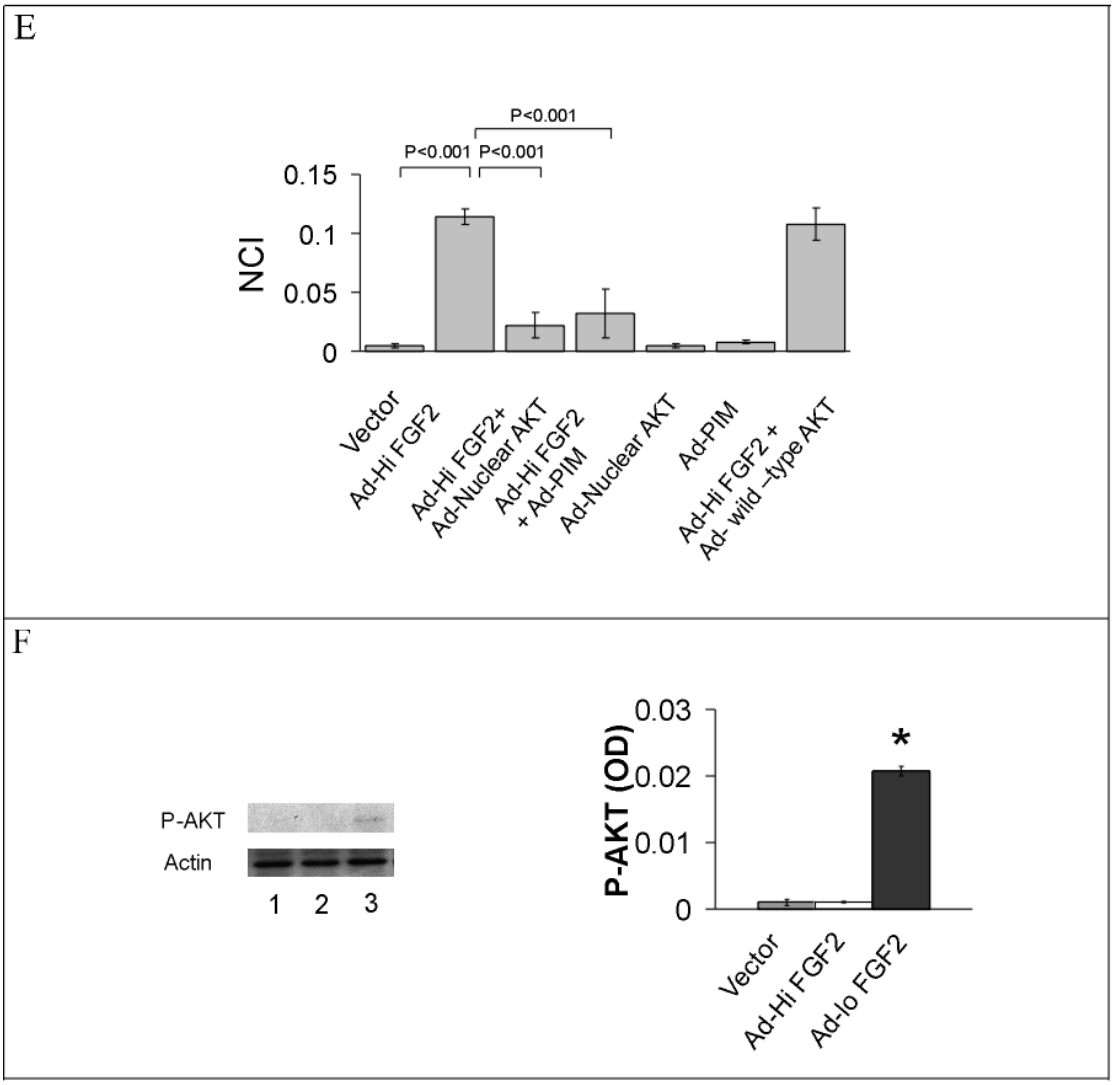

Figure 10. Overexpression of nuclear AKT and its downstream kinase PIM-1 attenuates the hi FGF2-induced chromatin compaction in rat neonatal cardiomyocytes. A. Representative immunofluorescent images of cells labeled for hi FGF2 (green) (anti-human hi FGF2 antibodies) and DNA (blue) at 72 h post-infection with human hi FGF2 adenovirus (100 m.o.i.). The cells expressing human hi FGF2 displayed DNA condensation (arrows). Bar=50 mM. **B-D.** Representative immunofluorescent images of cells labeled for FGF2 (red) (anti-human hi FGF2 antibodies), AKT / PIM-1 (green) and DNA (blue) at 72 h post-infection with human hi FGF2 adenovirus (100 m.o.i.) and nuclear AKT (100 m.o.i.) (**B**) or PIM-1 (100 m.o.i.) (**C**) and wild type AKT (100 m.o.i.) (**D**). Nuclear AKT / PIM-1 but not wild type AKT co-overexpression prevented hi FGF2-induced chromatin compaction (arrows). Bar=50 mM. **E.** The statistical analysis on NCI in hi FGF2/ nuclear AKT / PIM -1 alone infected cultures, and in hi FGF2- and nuclear and wild type AKT / PIM -1-co-infected cultures. There is a significant decrease of NIC in hi FGF2 and nuclear (but not wild type) AKT/ PIM-1 co-infected cultures. Data are shown as the mean ± SD, n=3. **F.** Representative western blot images of total cell lysates probed for AKT phosphorylated at threonine308; and actin, used to show equivalent protein loading. Lanes 1, 2 and 3 correspond, respectively, to adenoviral vector alone-, hi FGF2- and lo FGF2-adenovirus infected rat neonatal cardiomyocytes cultures. Densitometry-based quantification of phosphorylated AKT level relative to actin expression and statistical analysis are shown in the right panel. Data are presented as the mean ± S.D., n=3, * P< 0.001.

Figure 11

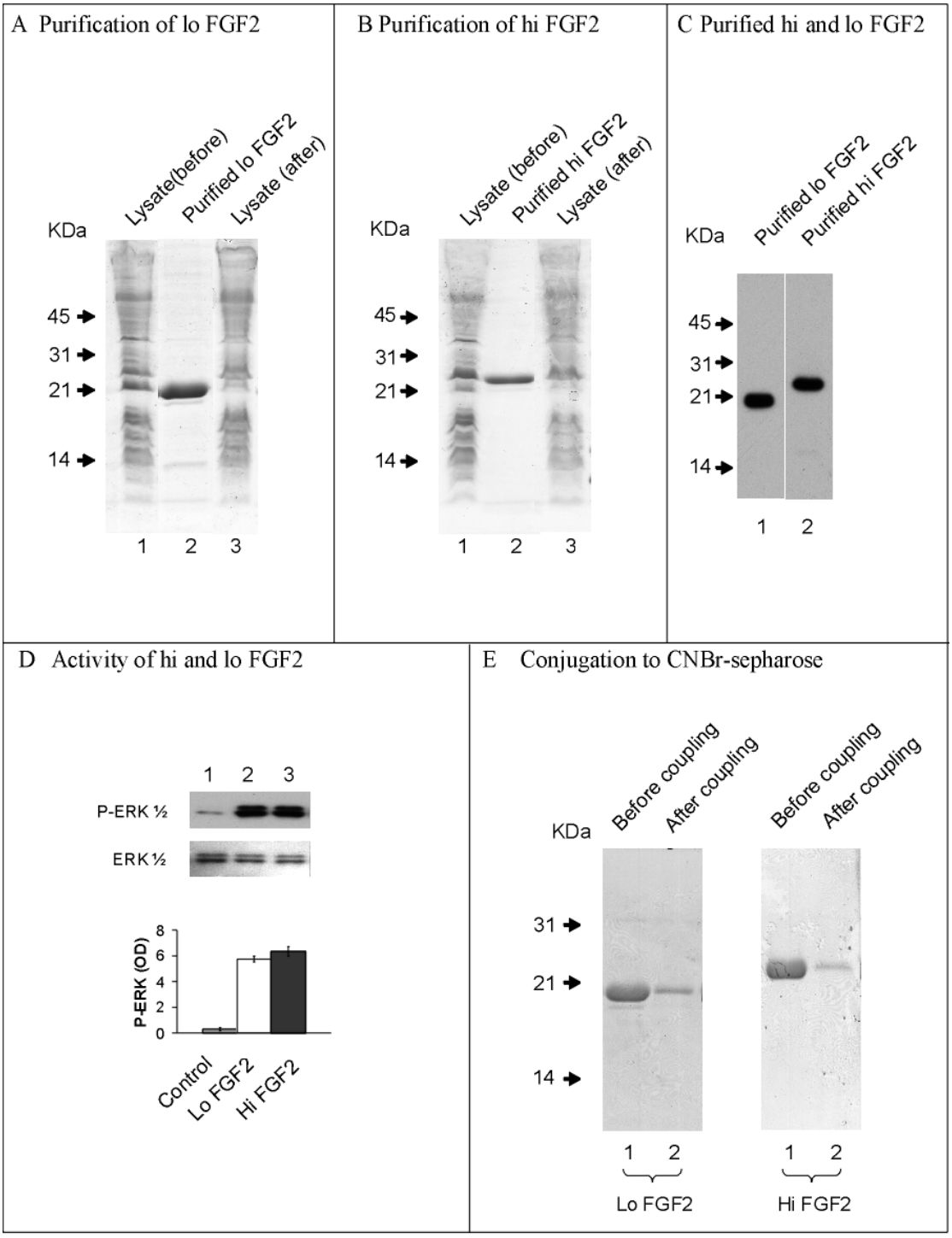
A Purification of lo FGF2
Lysate(before)
Purified lo FGF2
Lysate (after)
KDa
45
31
21
14
1 2 3
B Purification of hi FGF2
Lysate (before)
Purified hi FGF2
Lysate (after)
KDa
45
31
21
14
1 2 3
C Purified hi and lo FGF2
Purified lo FGF2
Purified hi FGF2
KDa
45
31
21
14
1 2
D Activity of hi and lo FGF2
1 2 3
P-ERK ½
ERK ½
P-ERK (OD)
8
6
4
2
0
Control
Lo FGF2
Hi FGF2
E Conjugation to CNBr-sepharose
Before coupling
After coupling
Before coupling
After coupling
KDa
31
21
14
1 2
1 2
Lo FGF2
Hi FGF2

Figure 11. Preparation and characterization of recombinant rat hi and lo FGF2.

A and B. Images of proteins isolated using Ni-Sepharose affinity chromatography from bacterial cultures expressing, respectively, histidine (His)- tagged rat lo or hi FGF2; analyzed by SDS/PAGE and detected by Coomassie Brilliant Blue staining. In both panels, lanes 1 and 3 show the bacterial extract protein pattern before and after Ni-Sepharose chromatography, respectively. Lane 2 shows the Ni-Sepharose bound protein. **C.** Representative western blot of proteins (4ng/lane) obtained by Ni-Sepharose chromatography and probed for FGF2 (monoclonal anti-FGF2 antibodies). **D.** Representative western blot of lysates (20µg/lane) obtained from HEK293 cells stimulated or not with 2 ng/ml of lo or hi FGF2, and probed, for phospho- and total ERK. Lanes 1, 2 and 3: results from, respectively, non-treated, control (con) cells; lo FGF2-treated-; hi FGF2-treated cells, as indicated. **E.** Coomassie Brilliant Blue stained gels, showing SDS/PAGE analysis of the same lo or hi FGF2-containing solution, before (lane 1) and after (lane 2) conjugation to CNBr-Sepharose, as indicated.

Figure 12

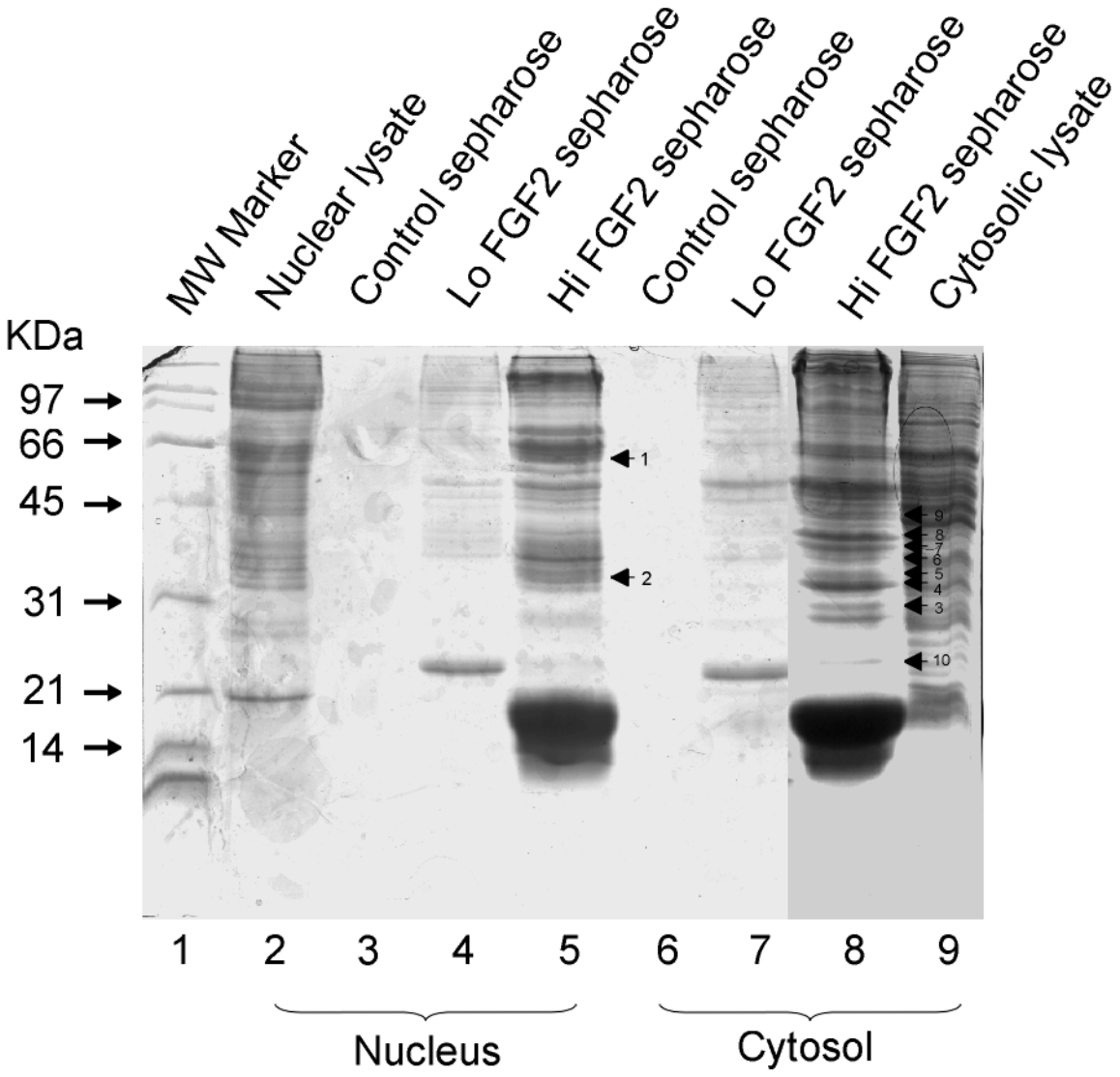
MW Marker
Nuclear lysate
Control sepharose
Lo FGF2 sepharose
Hi FGF2 sepharose
Control sepharose
Lo FGF2 sepharose
Hi FGF2 sepharose
Cytosolic lysate
KDa
97
66
45
31
21
14
1
2
3
4
5
6
7
8
9
10
1 2 3 4 5 6 7 8 9
Nucleus
Cytosol

Figure 12. SDS/PAGE analysis of HEK293 nuclear or cytosolic proteins bound by hi- and lo- FGF2 affinity columns. Coomassie Brilliant Blue stained gel, containing: lane 1, molecular weight markers; lane 2, total nuclear lysate, lanes 3,4 and 5 contain, nuclear proteins bound, respectively, to control-sepharose, lo FGF2-sepharose, and hi FGF2-sepharose; lanes 6,7 and 8 contain cytosolic proteins bound to, respectively, control-sepharose, lo FGF2-sepharose and hi FGF2 sepharose; lane 9, total cytosolic lysate. Arrows point to bands found only in the hi FGF2 sepharose-bound fraction, labeled 1-10. These were excised and sent for identification by HPLC-mass spectrometry.

Figure 13

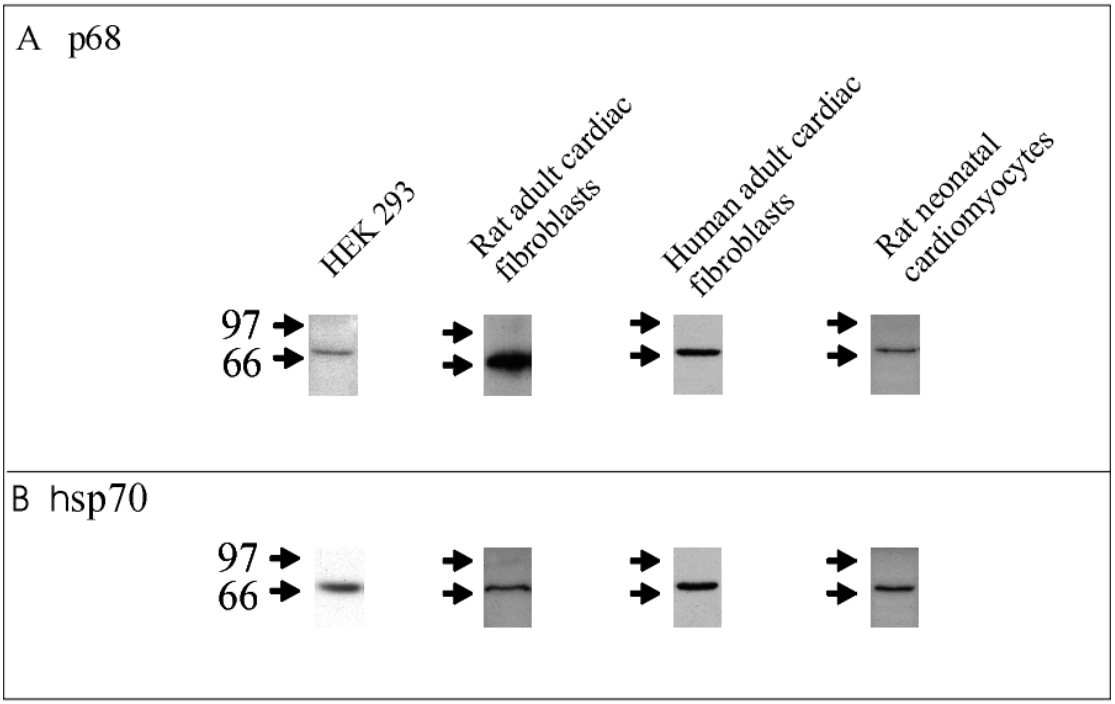
A p68
HEK 293
Rat adult cardiac fibroblasts
Human adult cardiac fibroblasts
Rat neonatal cardiomyocytes
97
66
B hsp70
97
66

Figure 13. Expression of p68 and hsp70 proteins by different cell types.

Panels A and B include representative western blot images of lysates (20 µg/lane) obtained from different cell types, as indicated, and probed for (A), p68, and (B), hsp70. Cell types analyzed included human HEK293 cells, primary rat adult heart fibroblasts, primary rat neonatal cardiomyocytes, and primary human atria-derived fibroblasts.

Figure 14

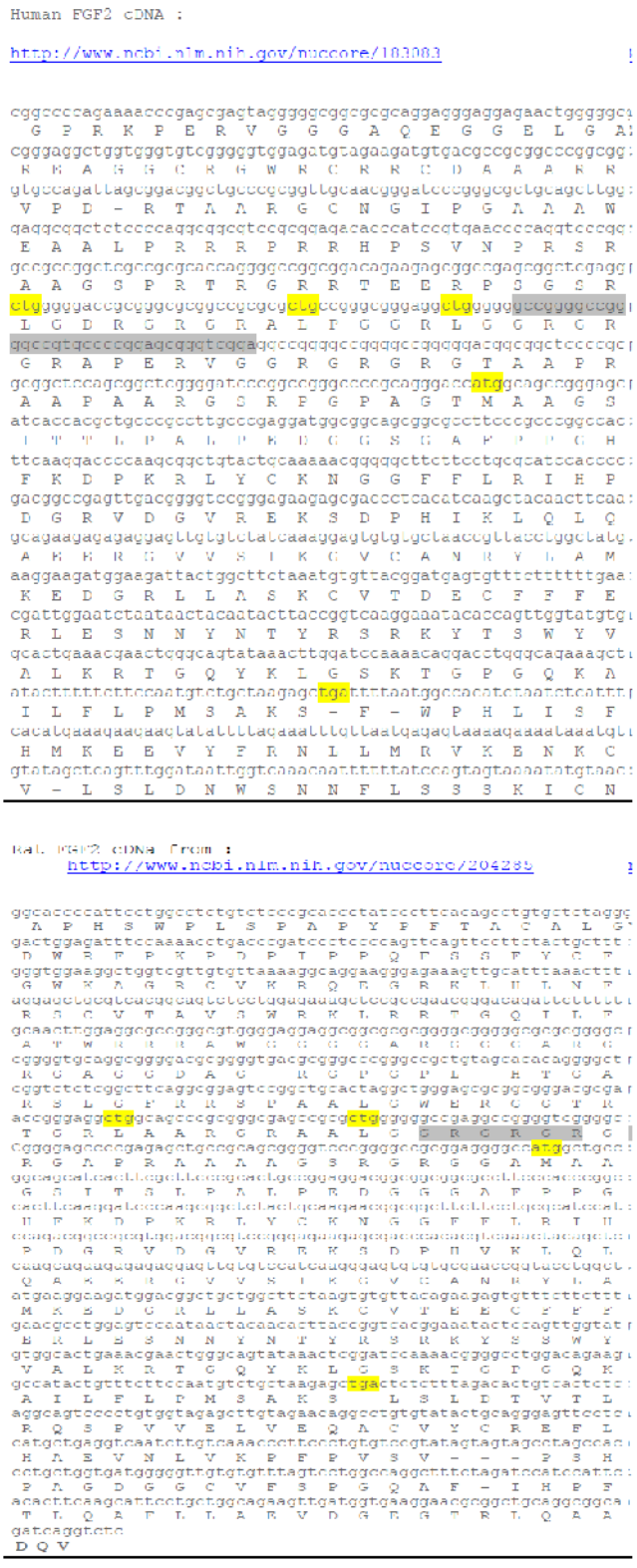
Human FGF2 cDNA :
http://www.ncbi.nlm.nih.gov/nuccore/103003
Rat FGF2 cDNA from :
http://www.ncbi.nlm.nih.gov/nuccore/204285

Figure 14. The nucleotide sequence of human (A) and rat (B) FGF2 cDNA and the corresponding amino acid sequence. A, the AUG codon generating 18 kDa lo FGF2 is 5' flanked by three CUG codons, producing three hi FGF2 isoforms (22.5kDa, 23.1kDa, 24.2kDa). The stop codon (TGA) was also labeled. As highlighted as grey, the peptide consisting of 12 amino acids represents an antigenic region in the amino terminal extension of human hi FGF2, as established by Piotrowicz and colleagues.[61]. The rat lo FGF2 core sequence, synthesized from the AUG codon, shares high homology with its human counterpart; in contrast there is substantial differences between rat and human FGF2 in the amino terminal extension of hi FGF2. Only two CUG codons are present in the 5’ flanked region of the rat FGF2 nucleotide sequence.

Figure 15

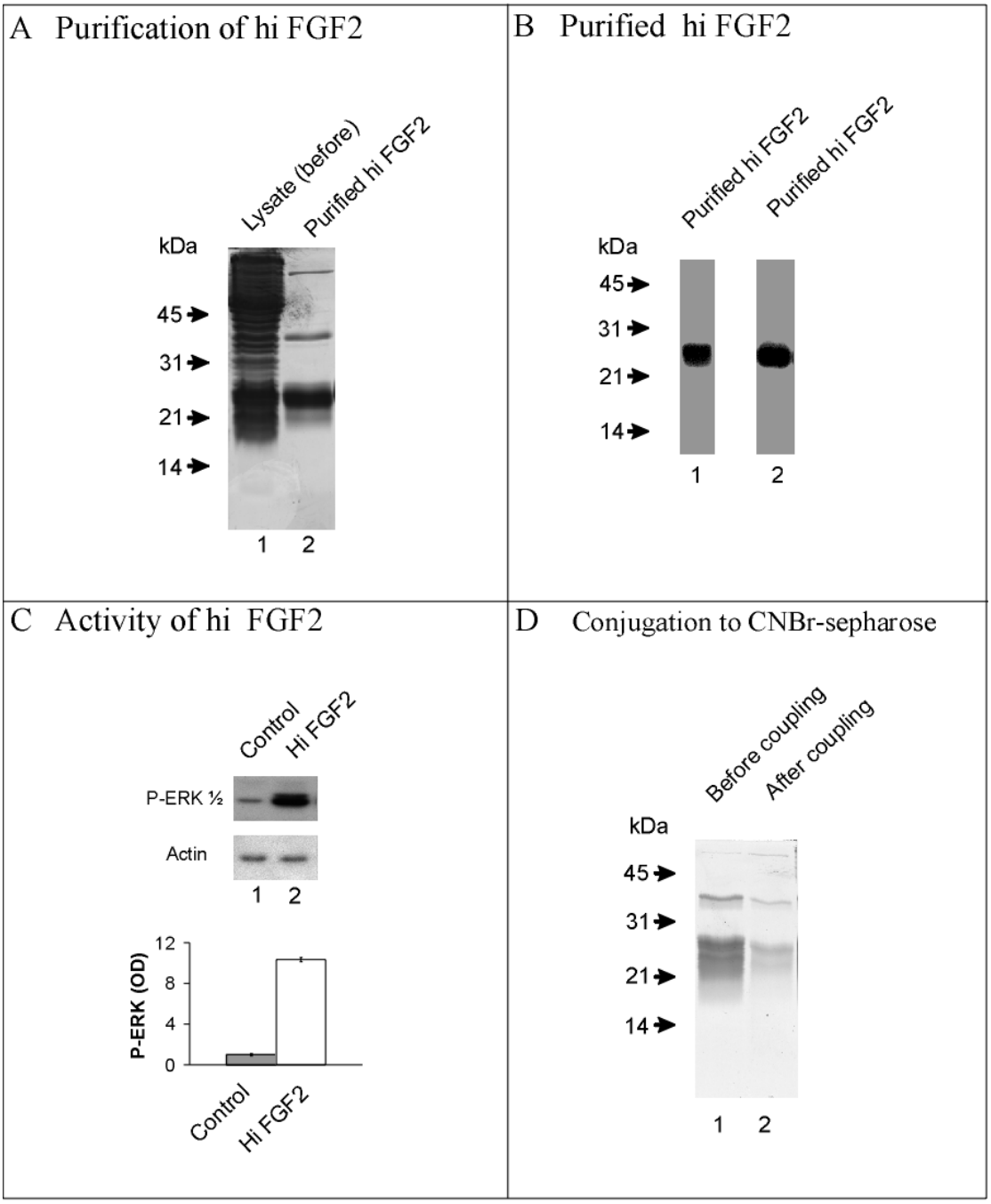
A Purification of hi FGF2
Lysate (before)
Purified hi FGF2
kDa
45
31
21
14
1 2
B Purified hi FGF2
Purified hi FGF2
Purified hi FGF2
kDa
45
31
21
14
1 2
C Activity of hi FGF2
Control
Hi FGF2
P-ERK ½
Actin
1 2
P-ERK (OD)
12
8
4
0
Control
Hi FGF2
D Conjugation to CNBr-sepharose
Before coupling
After coupling
kDa
45
31
21
14
1 2

Figure 15. Preparation and characterization of recombinant human hi FGF2

A. Image of proteins isolated using Ni-Sepharose affinity chromatography from bacterial cultures expressing histidine (His)-tagged human hi FGF2; analyzed by SDS/PAGE and detected by Coomassie Brilliant Blue staining. Lane 1, bacterial extract protein pattern before Ni-Sepharose chromatography; lane 2, Ni-Sepharose bound protein. **B.** Representative western blots of proteins (4 ng/lane) purified by Ni-Sepharose chromatography and probed for (1) FGF2 (monoclonal anti-FGF2 antibodies), and (2) histidine. **C.** Representative western blot of lysates (20µg/lane) obtained from HEK293 cells stimulated or not with 2 ng/ml of human hi FGF2, and probed for phospho- and total ERK. Lanes 1, 2: results from, respectively, non-treated, control (con) cells; hi FGF2-treated cells, as indicated. **D.** Coomassie Brilliant Blue stained gels, showing SDS/PAGE analysis of the same human hi FGF2-containing solution, before (lane 1) and after (lane 2) conjugation to CNBr-Sepharose, as indicated.

Figure 16

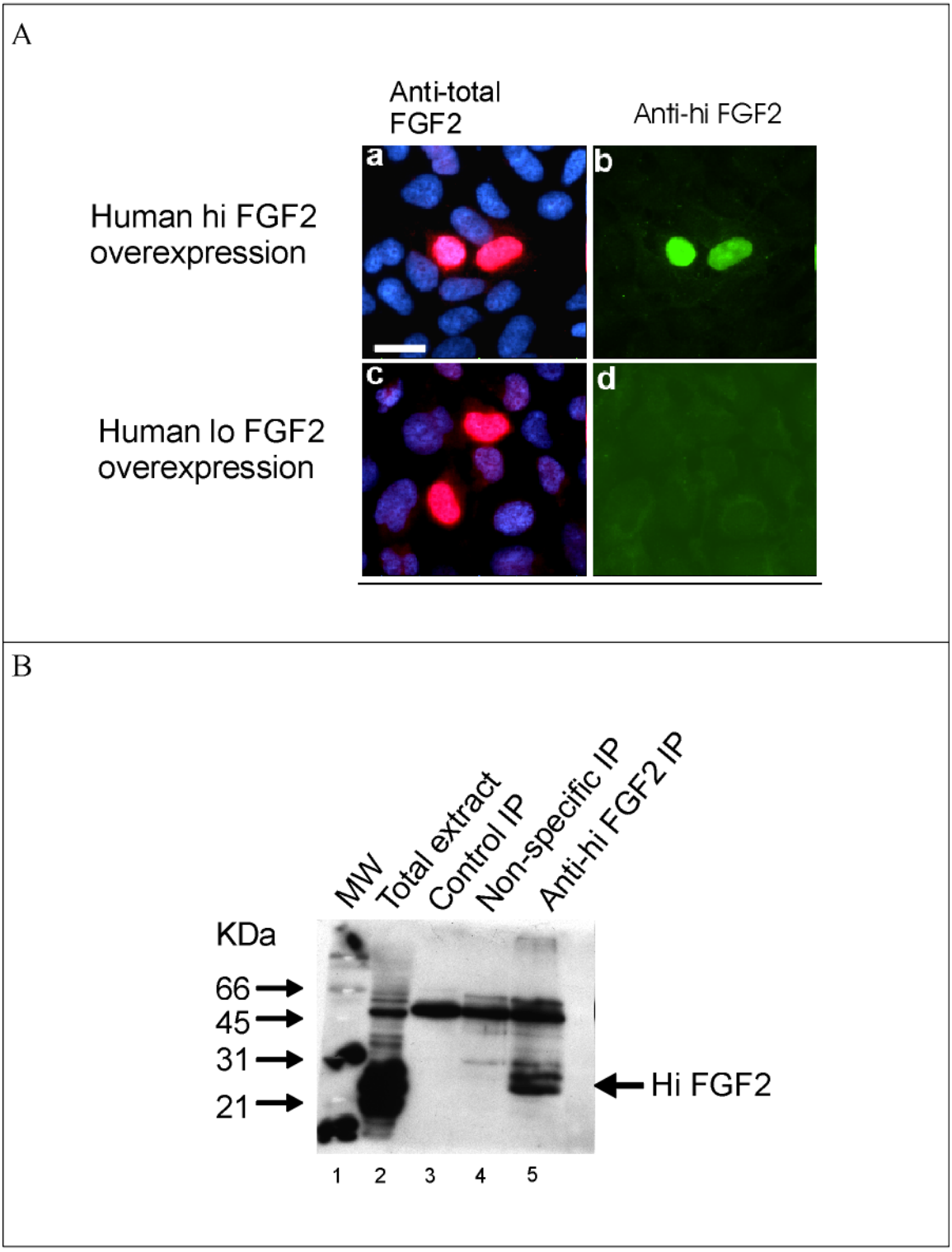
A
Anti-total FGF2
Anti-hi FGF2
Human hi FGF2 overexpression
Human lo FGF2 overexpression
a
b
c
d
B
MW
Total extract
Control IP
Non-specific IP
Anti-hi FGF2 IP
KDa
66
45
31
21
Hi FGF2
1 2 3 4 5

Figure 16. Characterization of human hi FGF2-specific antibodies by immunofluorescence and immunoprecipitation of human hi FGF2 overexpressing cells

A. Anti-human hi FGF2 antibodies recognized overexpressed hi FGF2 but not lo FGF2 by immunofluorescence. HEK293 cells overexpressing human hi FGF2 (panels a and b) or lo FGF2 (panels c and d) through transient gene transfer were incubated with antibodies recognizing all FGF2 isoforms (monoclonal anti-FGF2 antibodies, red; panels a and c) and antibodies raised against a sequence present in the N-extension of human hi FGF2 (anti-human hi FGF2 antibodies) (green; see panel b and d). All samples were counter-stained for DNA with DAPI (blue). Image d has been slightly overexposed. Sizing bar=20μM.

B. Overexpressed human hi FGF2 is immunoprecipitated by anti-human hi FGF2 antibodies. Representative western blot probed for FGF2 (monoclonal anti-FGF2 antibodies). Lane 1, total extract (20μg) derived from HEK293 cells overexpressing human hi FGF2; lanes 2, 3 and 4 contain proteins from (human hi FGF2 overexpressing) HEK293 cells that were precipitated by respectively, control-sepharose (no primary antibody), anti-hi FGF2 antibodies and sepharose, non-specific antibodies and sepharose. Arrow points to bands corresponding to human hi FGF2.

Figure 17

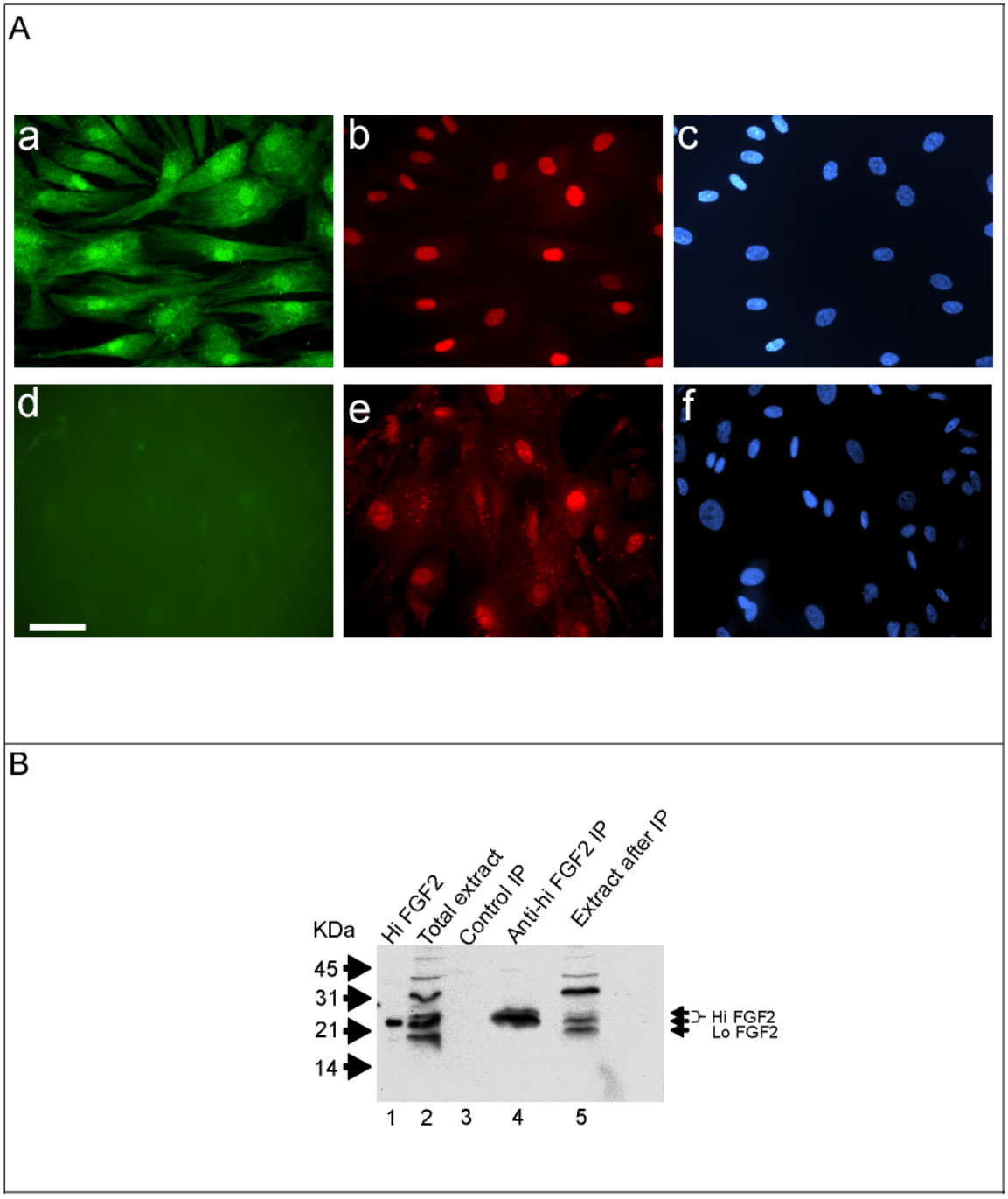
A
a
b
c
d
e
f
B
KDa
Hi FGF2
Total extract
Control IP
Anti-hi FGF2 IP
Extract after IP
45
31
21
14
1
2
3
4
5
Hi FGF2
Lo FGF2

Figure 17. Human anti-hi FGF2 antibodies detect and immunoprecipitate endogenous hi FGF2, in human embryonic cardiac fibroblasts.

Panel A. Images **a,b,c** show the same visual field from human embryonic fibroblast cultures subjected to triple-fluorescence staining with **(a, green)** rabbit anti-human hi FGF2 antibodies, **(b, red)** monoclonal anti-FGF2 antibodies, **(c, blue),** nuclear DAPI staining. Images **d,e,f**, show the same visual field subjected to triple-fluorescent staining after incubation with, **(d, green),** non-specific rabbit immunoglobulin, **(e, red),** monoclonal anti-FGF2 antibodies, **(f, blue),** DAPI staining. Bar in d = 20μM.

Panel B. **Endogenous human hi FGF2 (but not lo FGF2) is precipitated by anti-human hi FGF2 antibodies**. Western blot probed for FGF2 with the monoclonal anti-FGF2 antibodies. **Lane 1**, recombinant hi FGF2 (0.5 ng), used as positive control. **Lane 2**, lysate (20 μg) from human embryonic cardiac fibroblasts. **Lanes 3 and 4,** contain proteins bound to protein A-sepharose beads and derived from 900 μg cell extract protein. Before incubation with protein A sepharose, cell extracts were subjected to, **lane 3**, no treatment, **lane 4**, incubation with anti-human hi FGF2-specific and affinity purified rabbit antibodies. Lane 5 shows cell extract after removal of protein A sepharose bound proteins. Arrows show migration of hi and lo FGF2 isoforms.

Figure 18

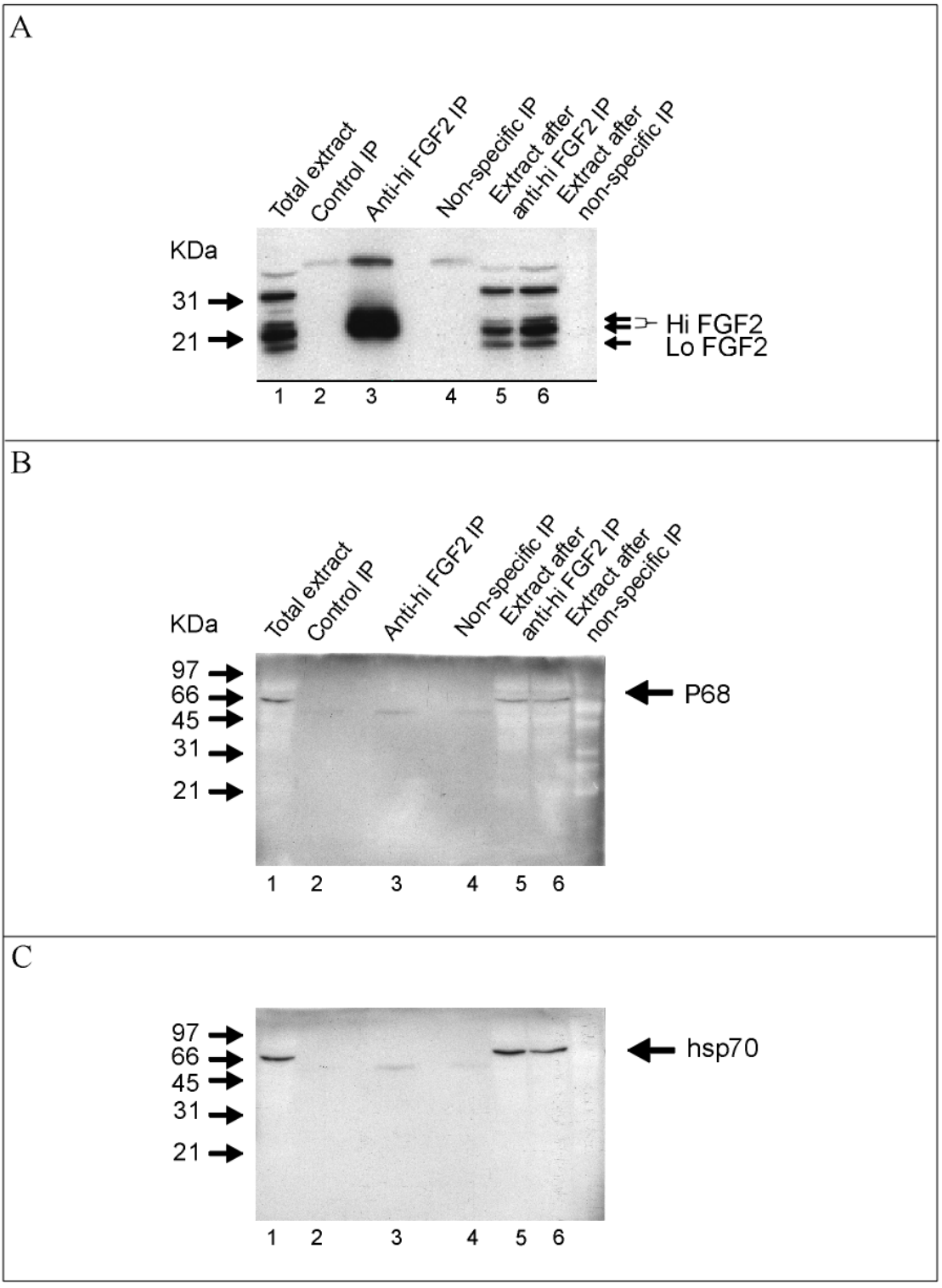
A
Total extract
Control IP
Anti-hi FGF2 IP
Non-specific IP
Extract after anti-hi FGF2 IP
Extract after non-specific IP
KDa
31
21
Hi FGF2
Lo FGF2
1 2 3 4 5 6
B
Total extract
Control IP
Anti-hi FGF2 IP
Non-specific IP
Extract after anti-hi FGF2 IP
Extract after non-specific IP
KDa
97
66
45
31
21
P68
1 2 3 4 5 6
C
97
66
45
31
21
hsp70
1 2 3 4 5 6

Figure 18. Anti-hi FGF2 antibodies immunoprecipitate endogenous hi FGF2 which is not associated with p68 RNA helicase or hsp70 in human embryonic cardiac fibroblasts. Panels A, B, C show the same western blot probed for (a), FGF2 (monoclonal anti-FGF2 antibodies), (B), p68, (C), hsp70. **Lane 1**, extract from human embryonic cardiac fibroblasts. **Lanes 2,3,4** contain proteins bound to protein G-sepharose beads and derived from extracts (900 μg protein) of human embryonic cardiac fibroblasts. Before incubation with protein G sepharose, cell lysates were subjected to, **lane 2**, no treatment, **lane 3**, incubation with anti-hi FGF2 antibodies (40 μg), **lane 4**, incubation with non-specific immunoglobulin (40 μg). Lanes 5 and 6 show cell lysates after immunoprecipitation with anti-hi FGF2, or non-immune immunoglobulin, respectively. Arrows indicate electrophoretic migration of hi and lo FGF2, as indicated.

Figure 19

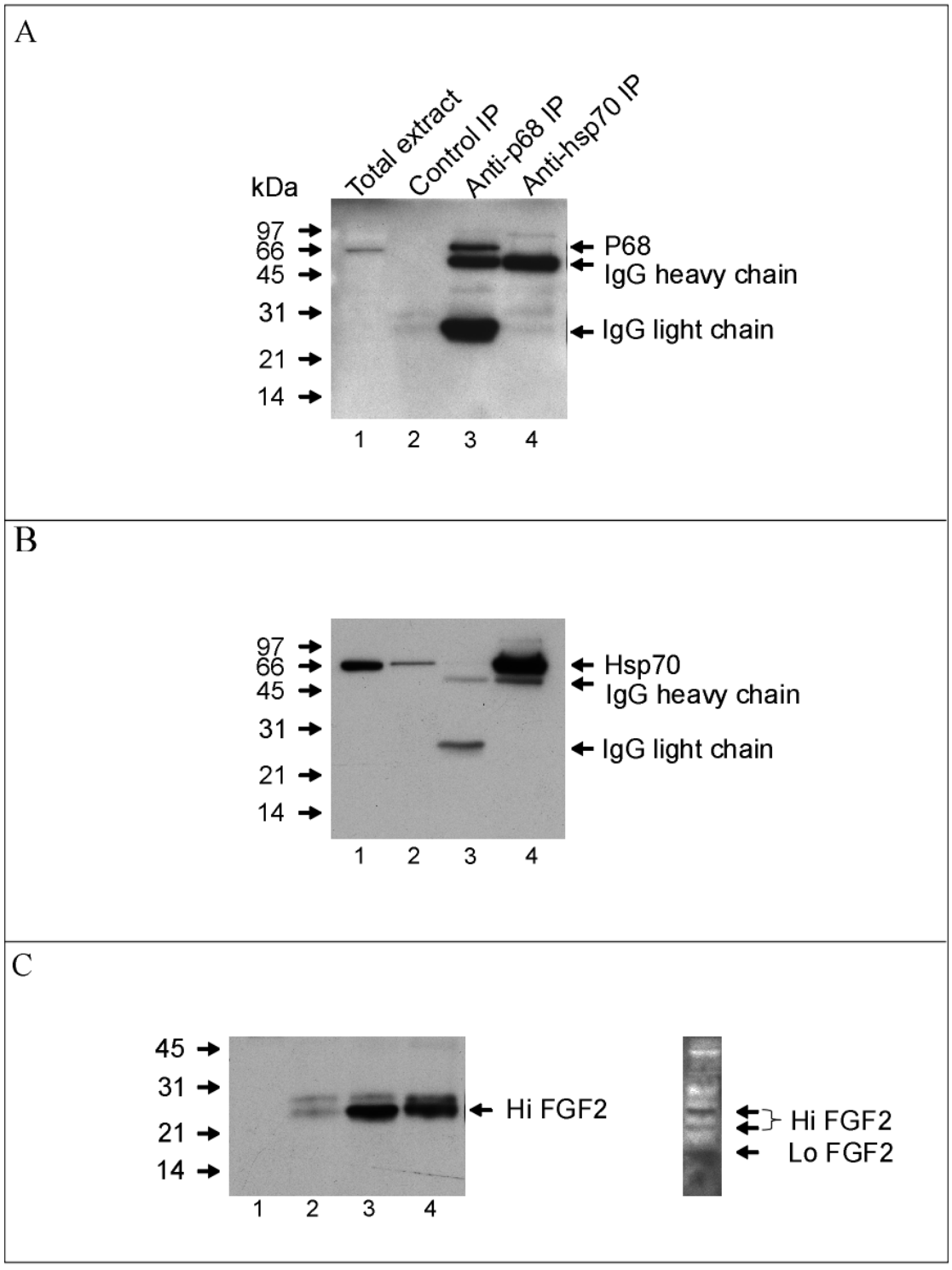
A
Total extract
Control IP
Anti-p68 IP
Anti-hsp70 IP
kDa
97
66
45
31
21
14
P68
IgG heavy chain
IgG light chain
1 2 3 4
B
97
66
45
31
21
14
Hsp70
IgG heavy chain
IgG light chain
1 2 3 4
C
45
31
21
14
Hi FGF2
1 2 3 4
Hi FGF2
Lo FGF2

Figure 19. Anti-p68 or anti-hsp70 antibodies immunoprecipitate p68 or hsp70, respectively, and co-precipitate hi FGF2, from HEK293 cells. Panels A,B and C show western blotting analysis of proteins immunoprecipitated from HEK293 cell extracts with anti-p68, or anti-hsp70 antibodies (as indicated), and probed for (A), p68, (B), hsp70, and (C), FGF2 (goat polyclonal antibodies, Santa Cruz, sc-1390,). In all panels: lane 1, cell extract (20 μg) before immunoprecipitation; lane 2, proteins precipitated by control sepharose; lane 3, proteins immunoprecipitated with anti-p68 antibodies; lane 4, proteins immunoprecipitated with anti-hsp70 antibodies. Immunoglobulin heavy chains (~55 kDa) and light chains (~29 kDa) are indicated by single arrows (panels A and B). Included in panel C (lane 1') is an overexposed version of lane 1 detecting endogenous hi and lo FGF2 that are not detectable under short exposure conditions (lane 1), when probed for FGF2.

Figure 20

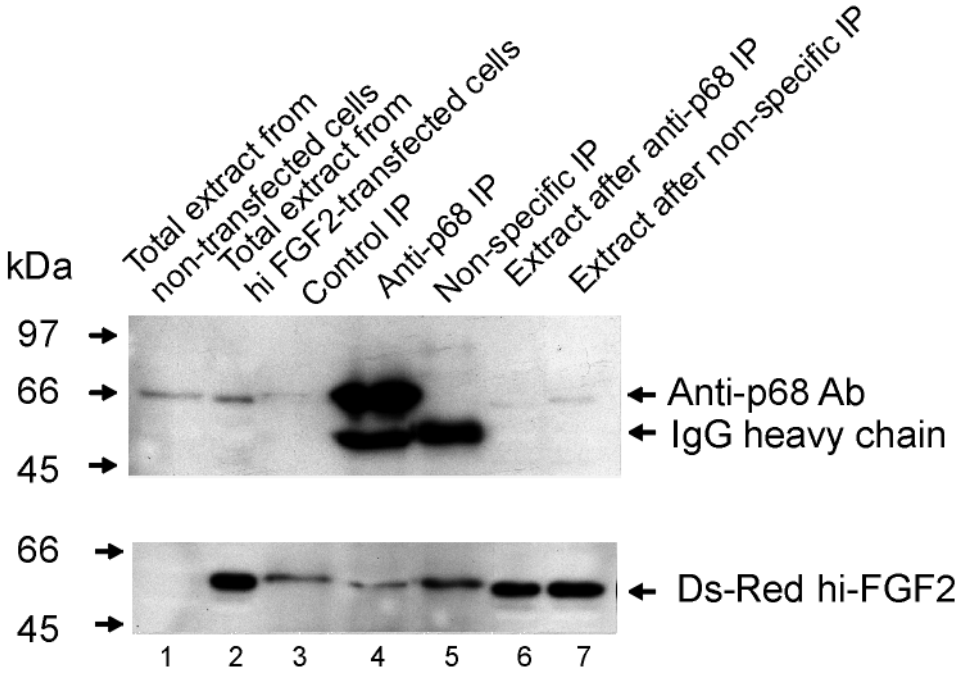
Total extract from non-transfected cells
Total extract from hi FGF2-transfected cells
Control IP
Anti-p68 IP
Non-specific IP
Extract after anti-p68 IP
Extract after non-specific IP
kDa
97
66
45
66
45
Anti-p68 Ab
IgG heavy chain
Ds-Red hi-FGF2
1 2 3 4 5 6 7

Figure 20. Anti-p68 antibodies immunoprecipitate p68 which is not associated with overexpressed DsRed rat hi FGF2. Representative western blot of proteins derived from HEK293 cells overexpressing DsRed hi FGF2, and immunoprecipitated with anti-p68 antibodies, followed by probing for p68, or FGF2 (goat polyclonal antibodies, Santa Cruz, sc-1390), as indicated (double arrows). Lane 1, extract from non-transfected cultures (20μg); lane 2, extract from DsRed hi FGF2 overexpressing cultures (20μg); lanes 3, 4 and 5 contain proteins derived from DsRed hi FGF2 overexpressing cultures and bound to protein G-Sepharose in the presence of, respectively, no primary antibodies (Control-), anti-p68-antibodies (p68-), and non-specific antibodies (NS IgG-). Lanes 6 and lane 7, total cell lysates from overexpressing cultures after removal of proteins immunoprecipitated (Ipp) with anti-p68, or non-specific antibodies, respectively (20μg). Arrow in upper panel shows reactivity with immunoglobulin heavy chain.

Figure 21

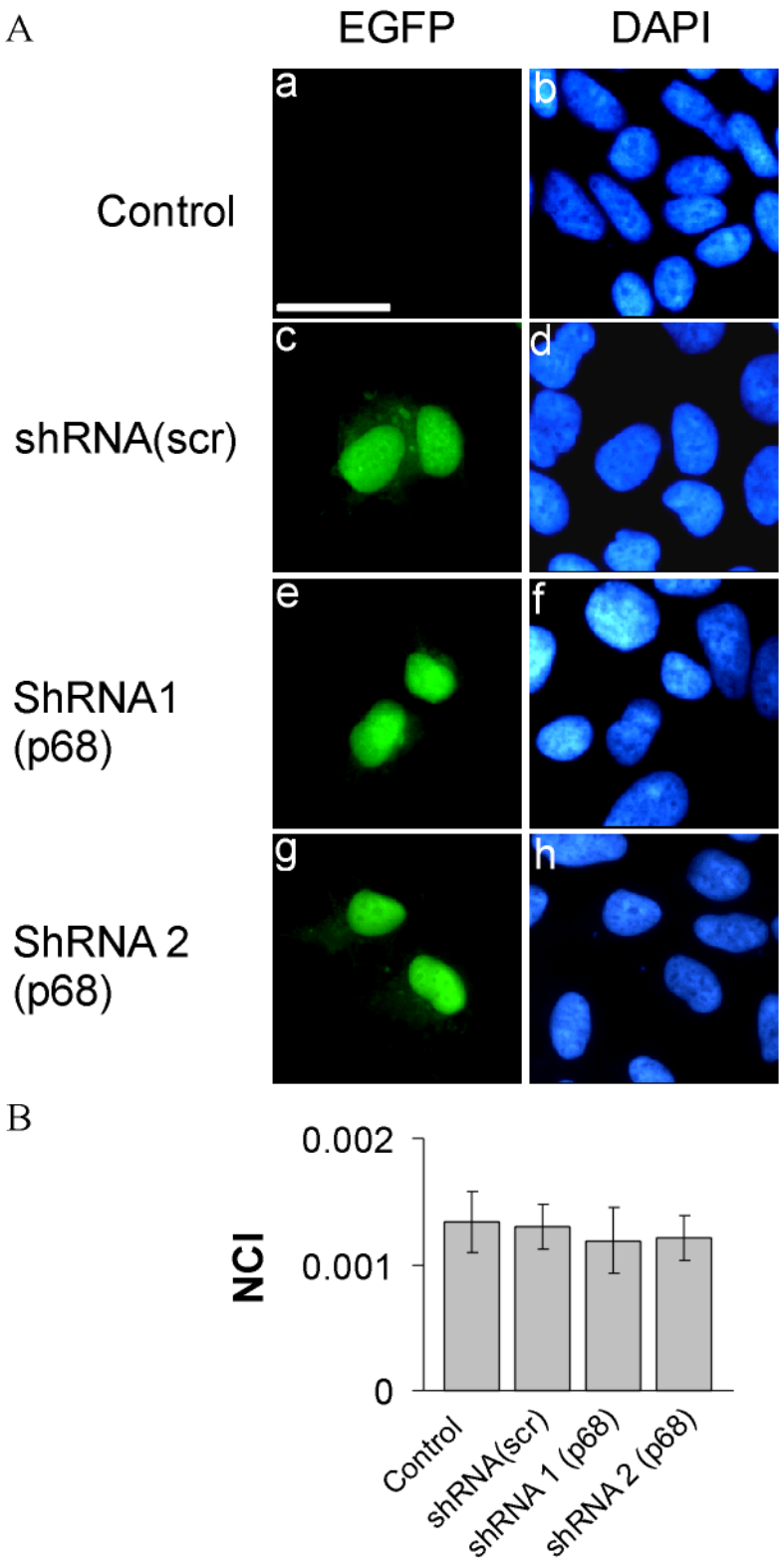
A
EGFP
DAPI
a
b
Control
c
d
shRNA(scr)
e
f
ShRNA1
(p68)
g
h
ShRNA 2
(p68)
B
NCI
0.002
0.001
0
Control
shRNA(scr)
shRNA 1 (p68)
shRNA 2 (p68)

Figure 21. Incubation with shRNA for p68 does not affect the nuclear phenotype of HEK 293 cells. (A) Representative double-labeled images of HEK293 cells subjected, or not, to treatment with various EGFP-labeled shRNAs. Images (a,c,e,g) show EGFP (green) label, while (b,d,f,h) corresponding staining with DAPI (blue). Images (a,b) show non-treated, control, cells; (c,d) are cells treated with scrambled (scr) shRNA; (e,f) cells treated with shRNA1(p68); (g,h) cells treated with shRNA2(p68). Scale bar in a represents 50 μm. (B). Quantitative data presented nuclear compaction index (NCI) corresponding to the groups shown in (A); n=3 and $P>0.05$.

Figure 22

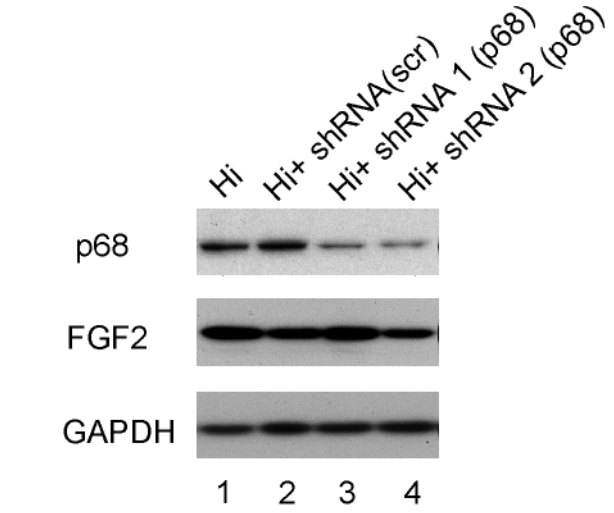
Hi
Hi+ shRNA(scr)
Hi+ shRNA 1 (p68)
Hi+ shRNA 2 (p68)
p68
FGF2
GAPDH
1
2
3
4

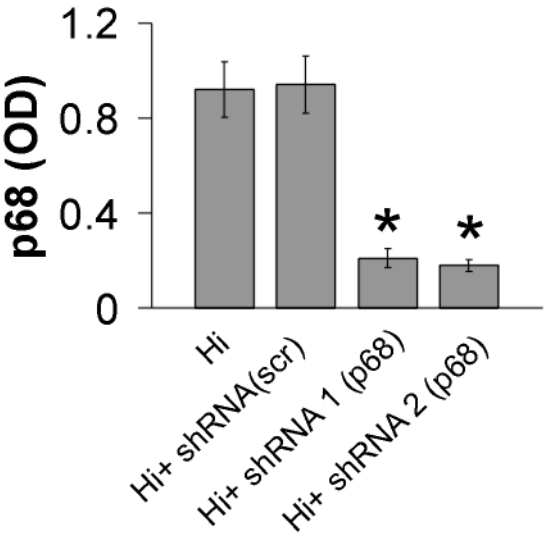
p68 (OD)
1.2
0.8
0.4
0
*
*
Hi
Hi+ shRNA(scr)
Hi+ shRNA 1 (p68)
Hi+ shRNA 2 (p68)

Figure 22. Knocking-down endogenous p68 by shRNA interference. Representative western blot (**upper panel**) showing the knocking-down effect of shRNA1 (p68) and shRNA2 (p68) in total cell lysates from HEK 293 cells co-transfected with DsRed hi FGF2 with or without EGFP-shRNA (scrambled), EGFP-shRNA1(p68). The blot was probed for p68, FGF2 (monoclonal anti-FGF2 antibodies) and GAPDH, as indicated. Quantitative data (**lower panel**) are presented as mean± SEM, n=3.*P<0.001. Lane 1, cultures transfected with DsRed-hi FGF2; lanes 2, 3 and 4, cultures transfected with DsRed-hi FGF2, and co-transfected with, respectively, EGFP-shRNA (scrambled), EGFP-shRNA1(p68), and, EGFP-shRNA2(p68); as indicated.

Figure 23

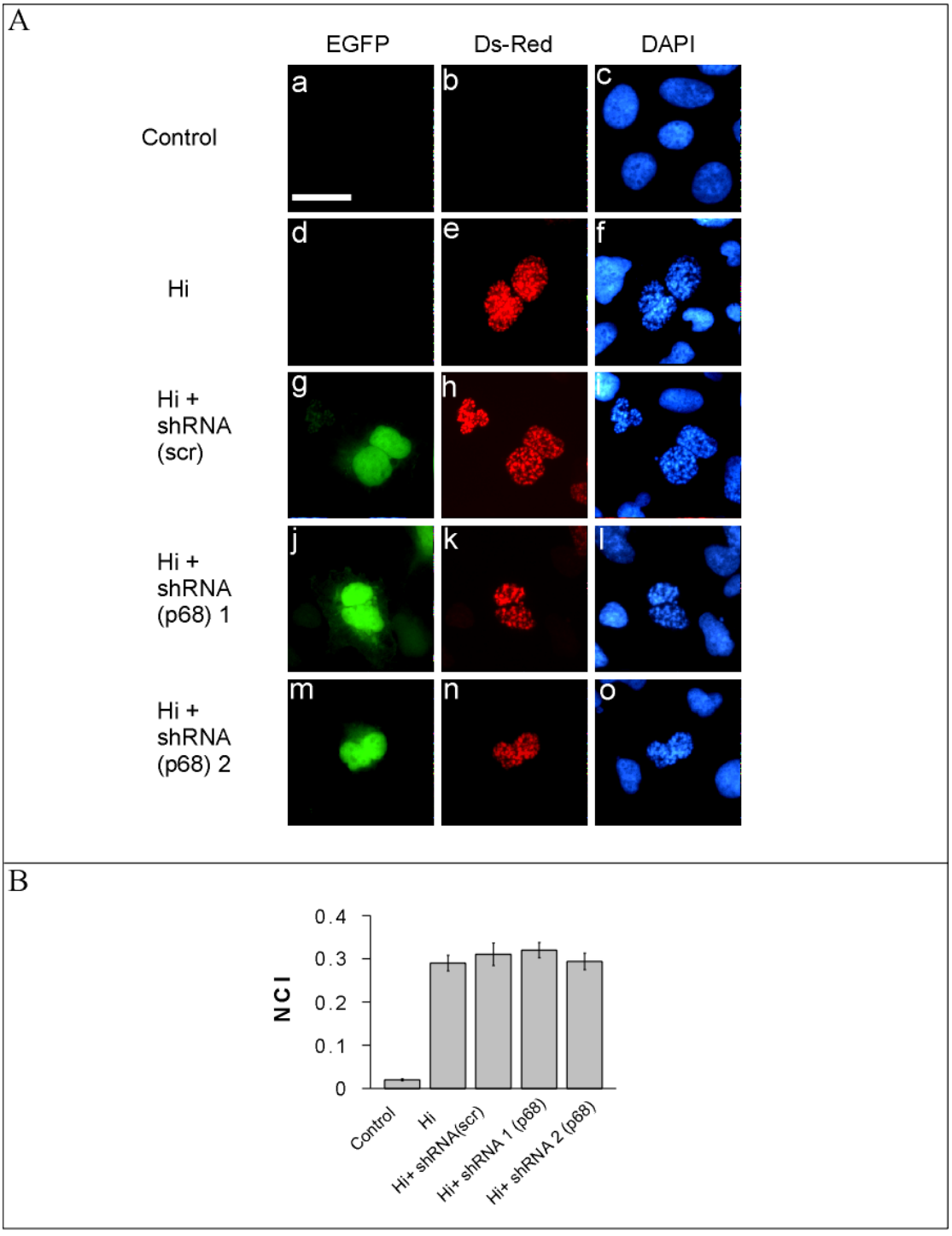
A
EGFP
Ds-Red
DAPI
Control
Hi
Hi + shRNA (scr)
Hi + shRNA (p68) 1
Hi + shRNA (p68) 2
a
b
c
d
e
f
g
h
i
j
k
l
m
n
o
B
NCI
0.4
0.3
0.2
0.1
0
Control
Hi
Hi+ shRNA(scr)
Hi+ shRNA 1 (p68)
Hi+ shRNA 2 (p68)

Figure 23. Decreasing p68 by shRNA knockdown does not affect the DsRed hi FGF2-induced chromatin compaction in HEK 293 cells. (A) Representative triple-fluorescence images, for EGFP (green), DsRed (red), and DAPI (blue) of HEK 293 cells subjected to (a,b,c) no transfection; (d-o) transfection with DsRed-hi FGF2 cDNA. Images (g,h,i) are from cells co-transfected with scrambled EGFP-shRNA; (j,k,i) from cells co-transfected with EGFP-shRNA1(p68); (m,n,o) from cells co-transfected with EGFP-shRNA2(p68). Scale bar represents 50 μm. (B) shows nuclear compaction index (NCI) of the groups included in panel (A); with n=3 and $p>0.05$ between cells overexpressing DsRed.

Figure 24

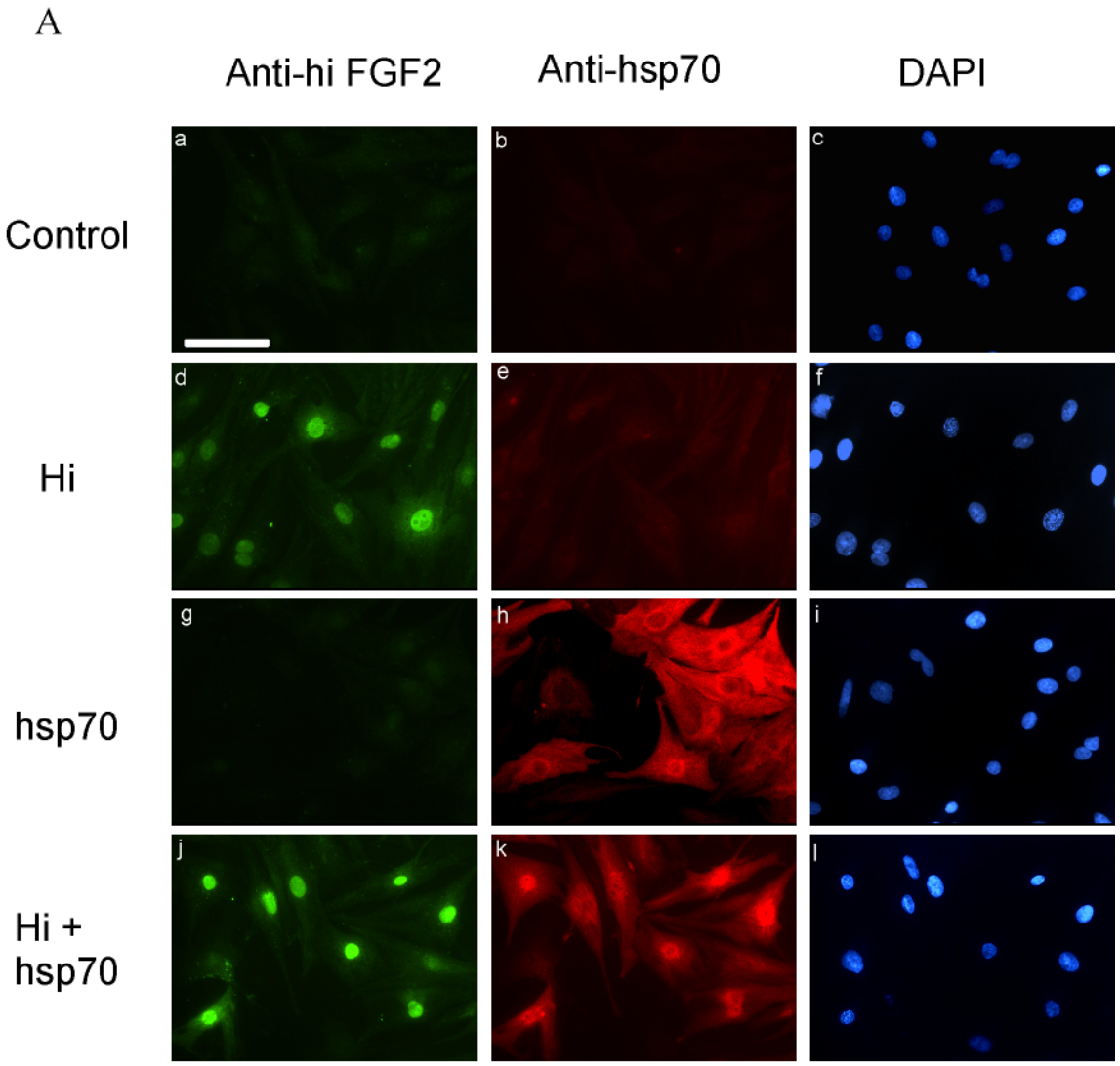
A
Anti-hi FGF2
Anti-hsp70
DAPI
Control
Hi
hsp70
Hi +
hsp70
a
b
c
d
e
f
g
h
i
j
k
l

Figure 24 (continued)

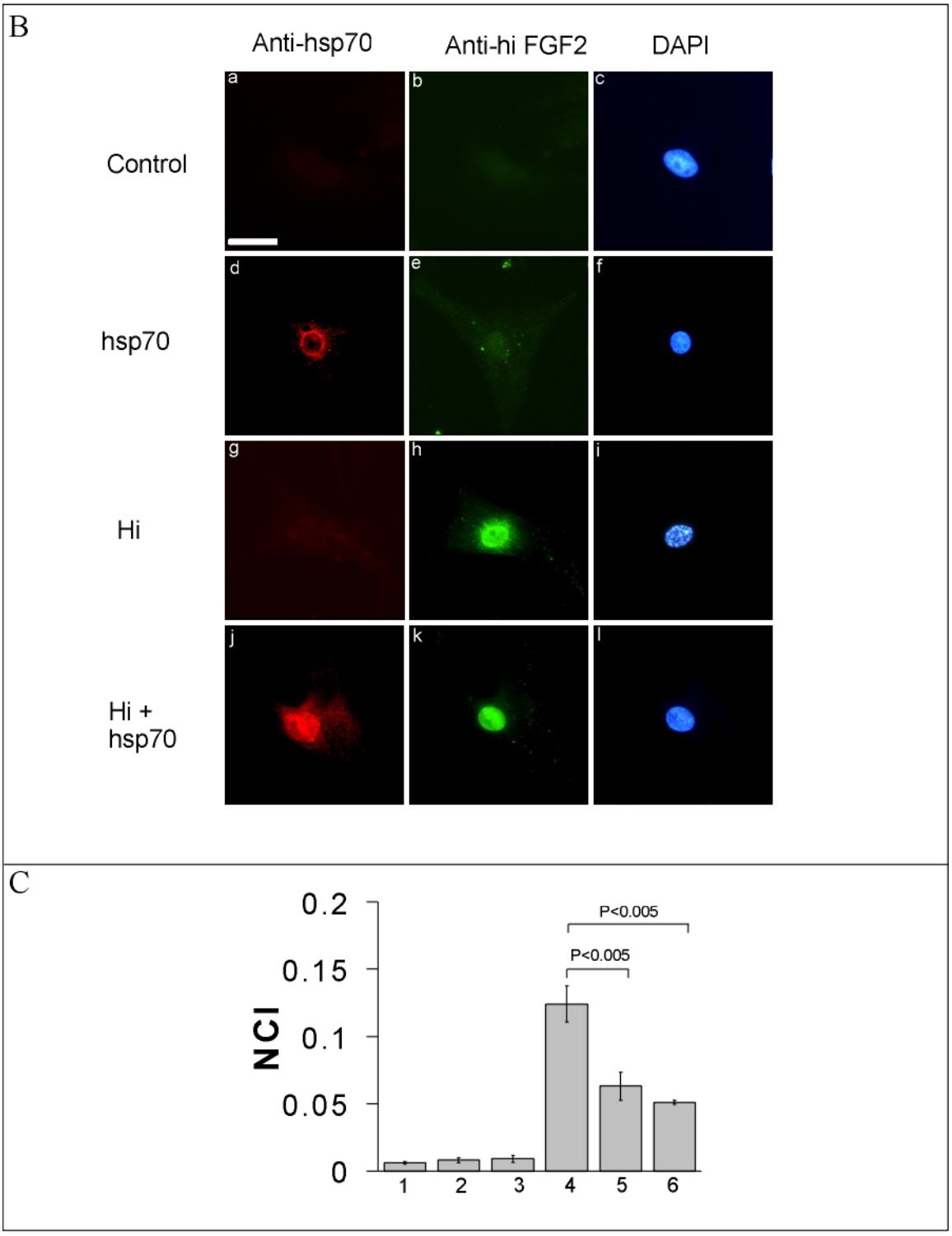

Figure 24. Overexpressed hsp70 prevents the hi FGF2-induced chromatin compaction in cardiomyocytes.

(A,B). Representative images of cardiac myocytes triple-labeled with anti-human hi FGF2 antibodies (green), anti-hsp70 antibodies (red), and DAPI (blue), as indicated. In both panels: images (a,b,c), control myocytes, transduced with empty adenoviral vector; (d,e,f), myocytes transduced with Ad-hi FGF2; (g,h,i) myocytes transduced with Ad-hsp70; (j,k,l), myocytes transduced with both Ad-hi FGF2 and Ad-hsp70. Scale bar=100 μM in (A) and 50 μM in (B). **(C)**. Nuclear compaction index (NCI) for the following myocyte groups: (1) transduced with empty adenovirus; (2) and (3) transduced, respectively, with 50 and 75 m.o.i. Ad-hsp70; (4), (5) and (6) transduced with Ad-hi FGF2; (5) and (6), co-transduced with, respectively, 50 and 75 m.o.i. Ad-hsp70. Groups 5 and 6 were both significantly reduced compared to group 5; n=3 and $P<0.005$.

Figure 25

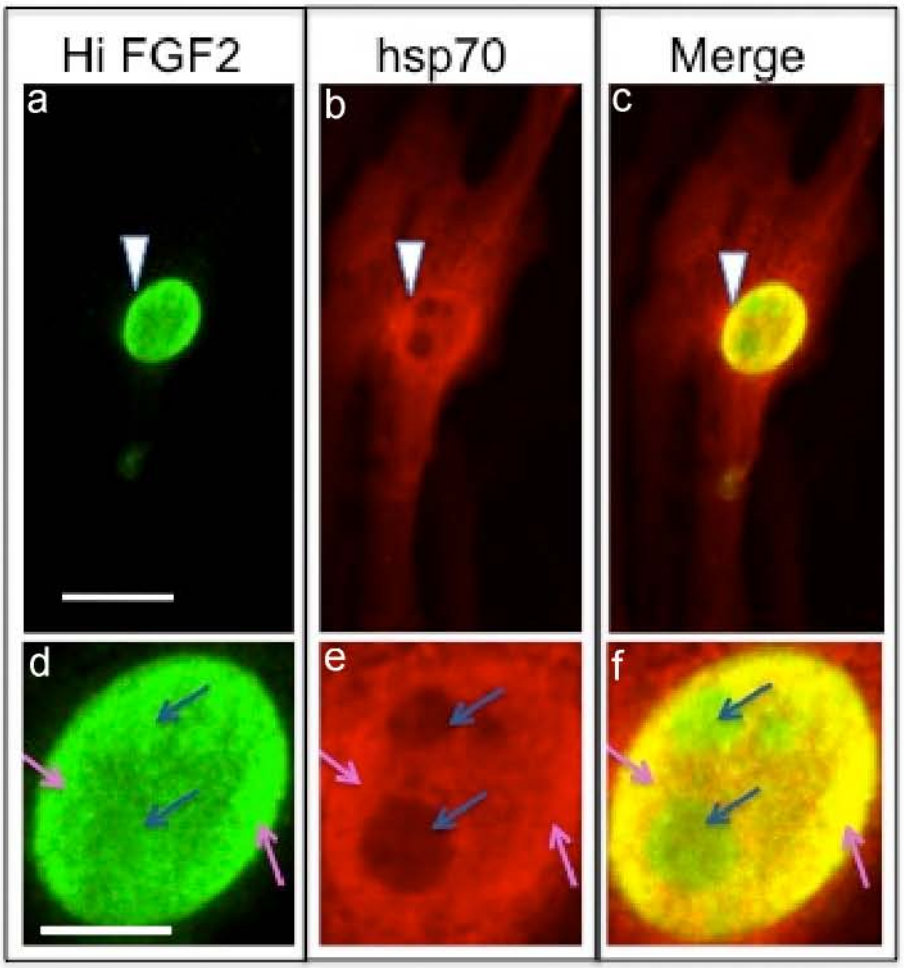

Figure 25. Close-up view of subcellular distribution of (overexpressed) hsp70 in the presence of overexpressed hi FGF2, in cardiomyocytes. Panels (a) and (b) show double-immunofluorescence staining for, respectively, hi FGF2 (anti-human hi FGF2 antibodies), green, and hsp70, red, while panel (c) shows the results of merging images (a) and (b). White arrowheads in the upper panels show the nuclear area, which is also shown in close-up in the corresponding lower panels (Panel d, e, f). Pink arrows point to nuclear sites of potential co-localization and interaction between hi FGF2 and hsp70. Blue arrows point to nucleolar areas which are devoid of anti-hsp70 staining but are still stained for hi FGF2. Size bar in panel (a) and panel (d) corresponds to 50 and 20 μM, respectively.

Figure 26

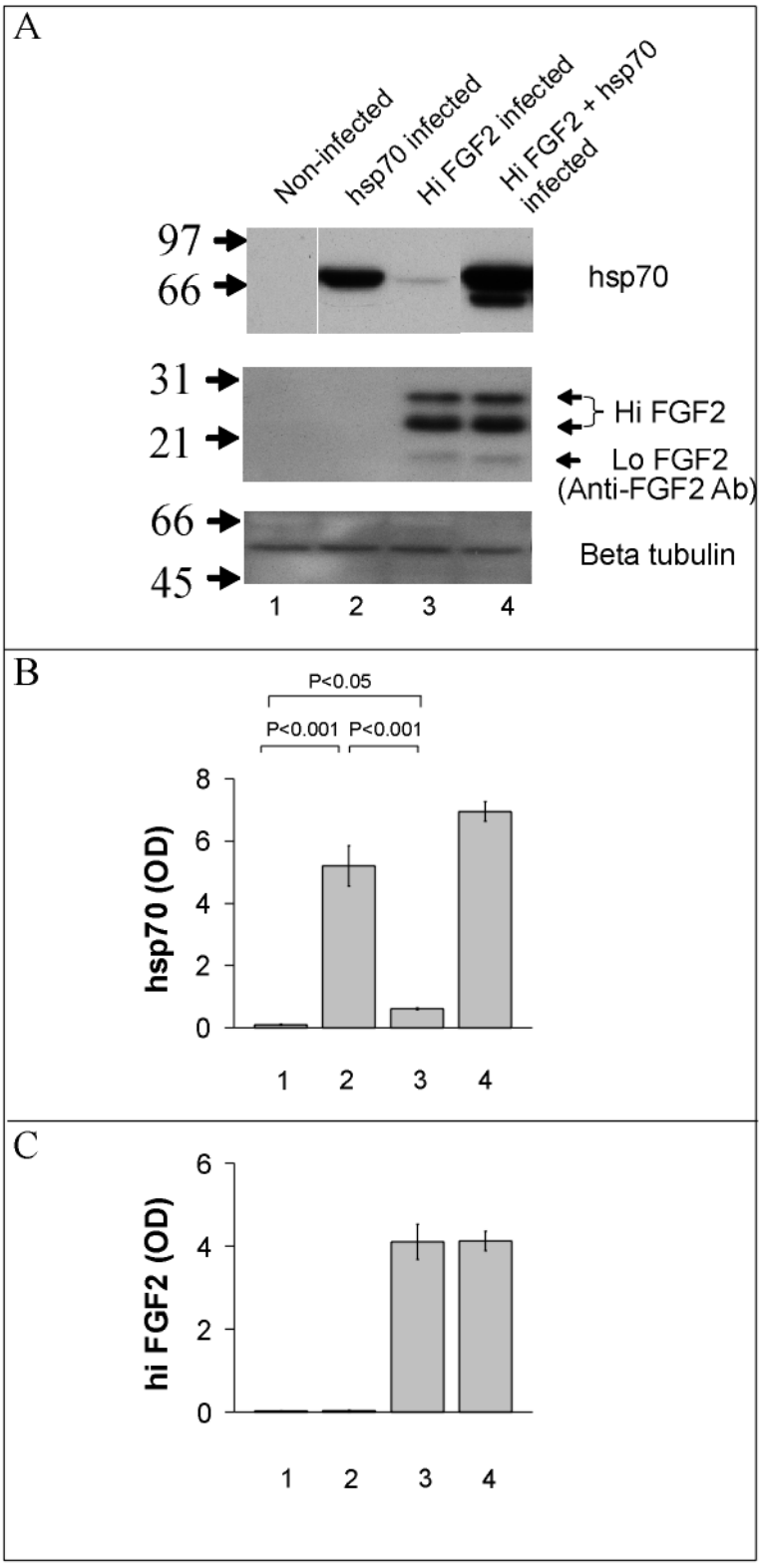
A
Non-infected
hsp70 infected
Hi FGF2 infected
Hi FGF2 + hsp70 infected
97
66
hsp70
31
21
Hi FGF2
Lo FGF2
(Anti-FGF2 Ab)
66
45
Beta tubulin
1
2
3
4
B
P<0.05
P<0.001
P<0.001
hsp70 (OD)
8
6
4
2
0
1
2
3
4
C
hi FGF2 (OD)
6
4
2
0
1
2
3
4

Figure 26. Detection of hsp70 and hi FGF2 overexpression. (A) Representative western blots, probed for hsp70, FGF2 (monoclonal anti-FGF2 antibodies) and β-tubulin, as indicated. Lanes 1, 2, 3 and 4 contain lysates from cardiac myocytes transduced with, respectively, control adenovirus, Ad-hsp70 (20 m.o.i.), Ad-hi FGF2 (200 m.o.i.), and, hi FGF2 (200 m.o.i.) and hsp70 (20 m.o.i.), at 72 hours post-transduction. Arrow points to an extra hsp70 band in lane 4. **Panels B and C** shows cumulative data of hsp70 and hi FGF2 levels (OD values; n=3 and $P < 0.05$ or 0.001, as indicated).

Figure 27 Rat neonatal cardiac fibroblasts

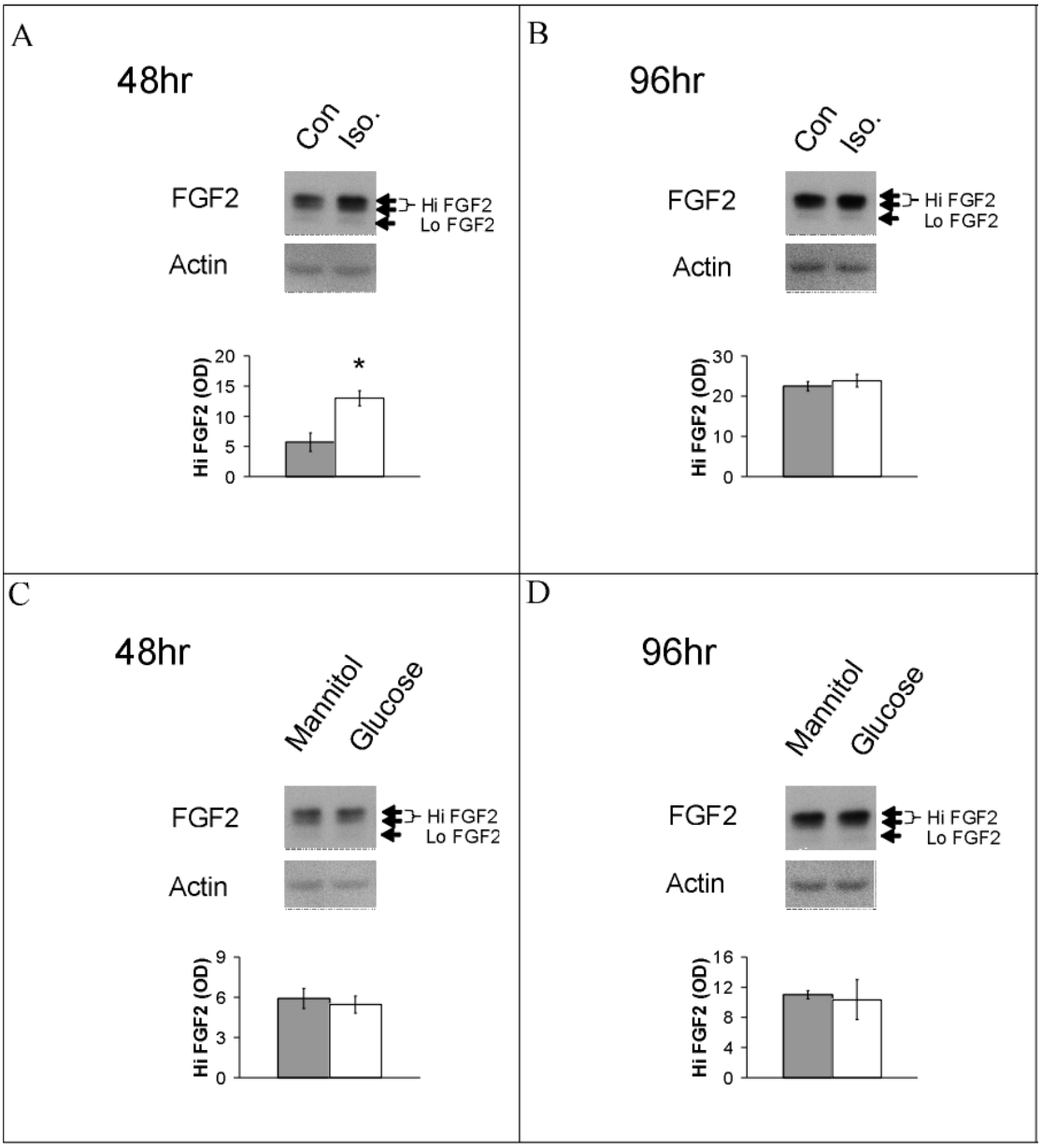

Figure 27. Rat neonatal cardiac fibroblasts; the effect of isoproterenol and glucose on hi FGF2 accumulation. Rat neonatal cardiac fibroblasts, subjected or not, to 'treatments' were analyzed, at 40μg protein/lane, by western blotting for hi FGF2. **(A) and (B).** Representative western blot images and corresponding cumulative data showing hi FGF2 signal (monoclonal anti-FGF2 antibodies)in isoproterenol-treated (iso; 10μM) cells compared to controls (con), at 48 and 96 hours, respectively. **(C) and (D).** Representative western blot images and corresponding cumulative data showing hi FGF2 signal (monoclonal anti-FGF2 antibodies) under high glucose (25 mM) or control (25 mM mannitol) conditions, at 48 and 96 hours, respectively. Staining for actin is used to indicate equivalent protein loading. Data are presented as mean ± SD, n=3. *P < 0.01.

Figure 28 Rat neonatal cardiac myocyte

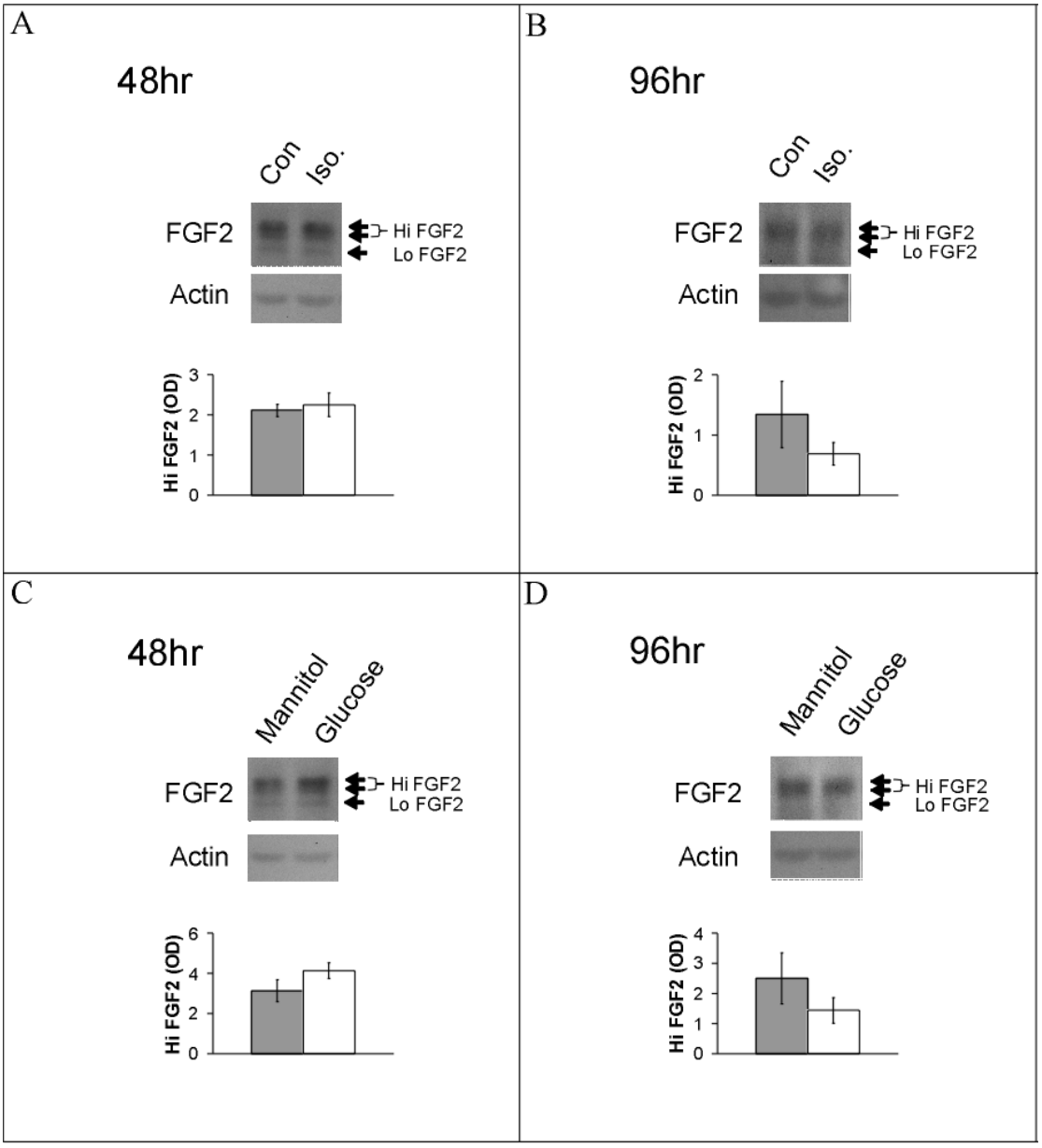

Figure 28. Rat neonatal cardiac myocytes; the effect of isoproterenol and glucose on intracellular hi FGF2 accumulation. Rat neonatal cardiac myocytes, subjected or not, to 'treatments' were analyzed, at 100 μg protein/lane, by western blotting for hi FGF2. **(A) and (B).** Representative western blot images and corresponding cumulative data showing hi FGF2 signal (monoclonal anti-FGF2 antibodies) in isoproterenol-treated (iso; 10μM) cells compared to controls (con), at 48 and 96 hours, respectively. **(C) and (D).** Representative western blot images and corresponding cumulative data showing hi FGF2 signal (monoclonal anti-FGF2 antibodies) under high glucose (25 mM) or control (25 mM mannitol) conditions, at 48 and 96 hours, respectively. Staining for actin is used to indicate equivalent protein loading. Data are presented as mean ± SD, n=3.

Figure 29 Rat adult cardiac myocytes

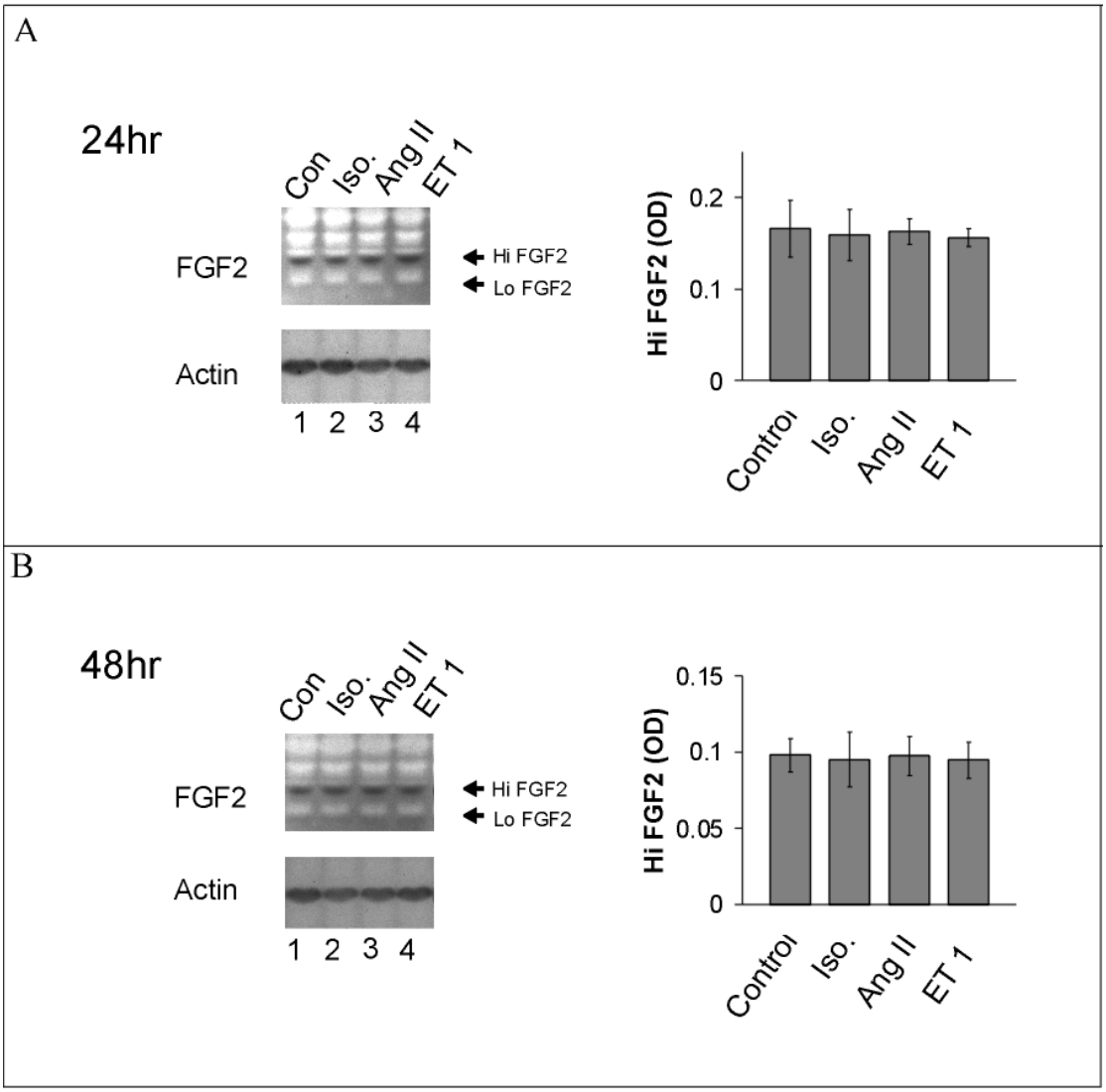

Figure 29. Rat adult cardiac myocytes; the effect of isoproterenol, angiotensin II, and endothelin I on hi FGF2 accumulation. Rat adult cardiac myocytes, subjected or not, to 'treatments' were analyzed, at 100 μg protein/lane, by western blotting for hi FGF2. **(A)**. Representative western blot images and corresponding cumulative data showing hi FGF2 signal (monoclonal anti-FGF2 antibodies) in untreated control myocytes (con), and in myocytes treated with isoproterenol (iso); angiotensin I (Ang II); endothelin I (ET-I), all at 10μM, as indicated, for 48 h. **(B).** As in (A) but after 96 h. Staining for actin is used to indicate equivalent protein loading. Data are presented as mean ± SD, n=3.

Figure 30 Human adult cardiac fibroblasts

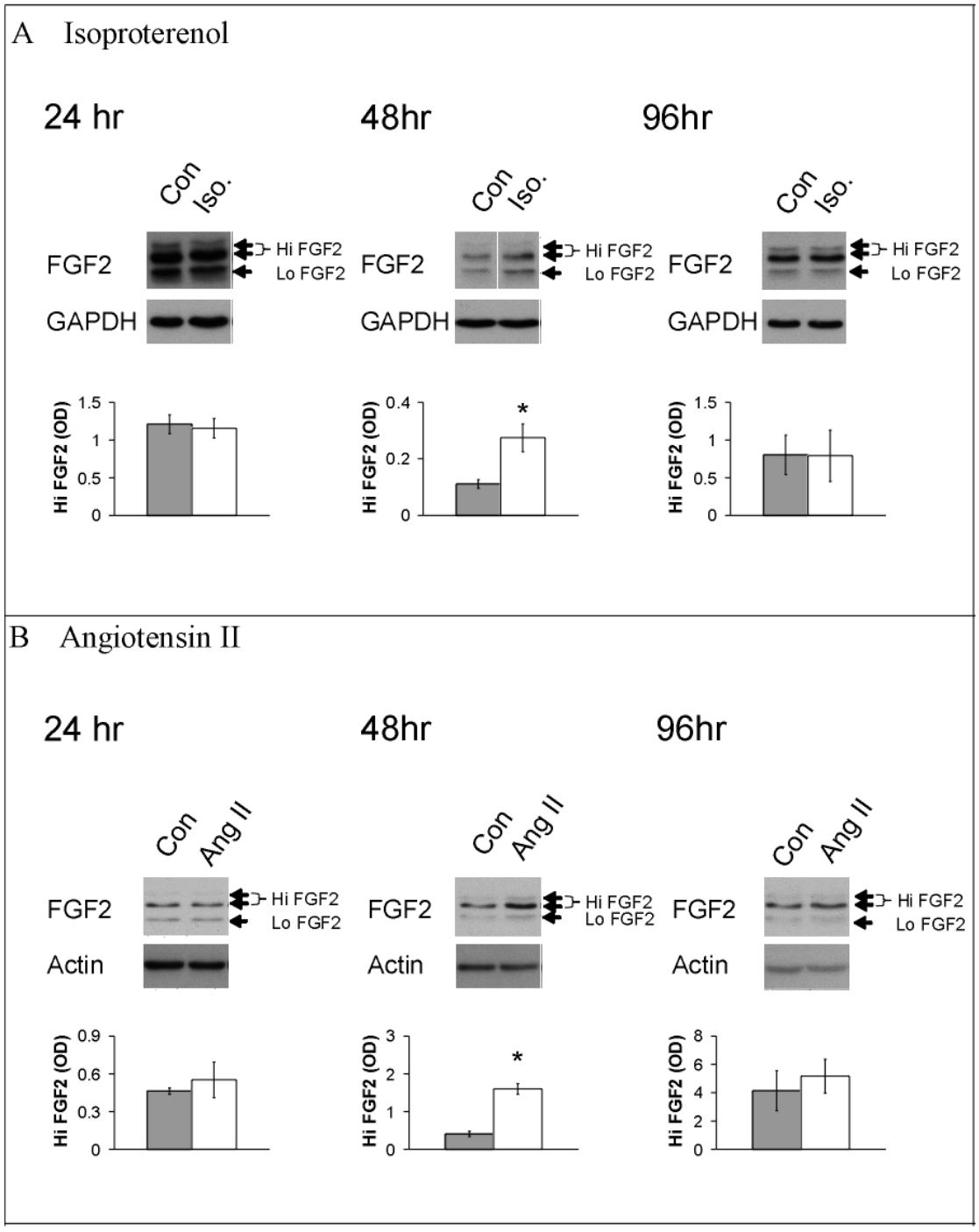

Figure 30 (continued) Human adult cardiac fibroblasts

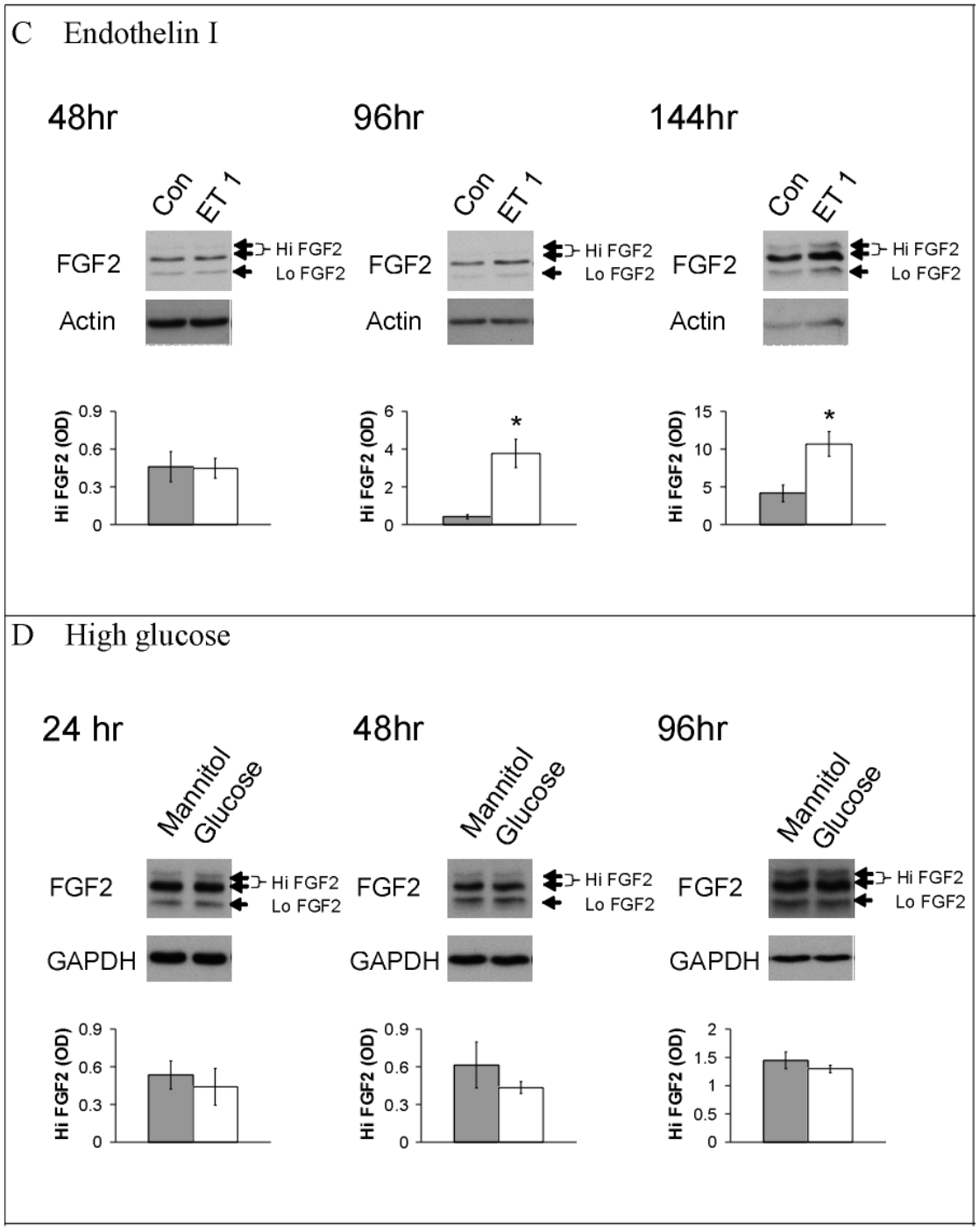

Figure 30. Human adult cardiac (atrial) fibroblasts; the effect of isoproterenol, angiotensin II, endothelin I and high glucose on hi FGF2 accumulation. Adult human cardiac (atrial) fibroblasts, subjected or not, to 'treatments' were analyzed by western blotting for hi FGF2. **(A).** Representative Western blots and corresponding cumulative data showing hi FGF2 signal (monoclonal anti-FGF2 antibodies) in untreated controls (con) and isoproterenol-treated (iso) cells at 24, 48 and 96 hours of treatment, as indicated. **(B).** Representative Western blots and corresponding cumulative data showing hi FGF2 signal (monoclonal anti-FGF2 antibodies) in untreated controls (con) and angiotensin II-treated (Ang II) cells at 24, 48 and 96 hours of treatment, as indicated. **(C).** Representative Western blots and corresponding cumulative data showing hi FGF2 signal (monoclonal anti-FGF2 antibodies) in untreated controls (con) and endothelin I (ET I) cells at 48, 96 and 144 hours of treatment, as indicated. **(D).** Representative Western blots and corresponding cumulative data showing hi FGF2 signal (monoclonal anti-FGF2 antibodies) in control, mannitol-treated (mannitol) and high glucose-treated (glucose) cells at 48, 96 and 144 hours of treatment, as indicated. Staining for actin or GAPDH is used to indicate equivalent protein loading. Data are presented as mean ± SD, n=3. *$P < 0.01$.

Figure 31

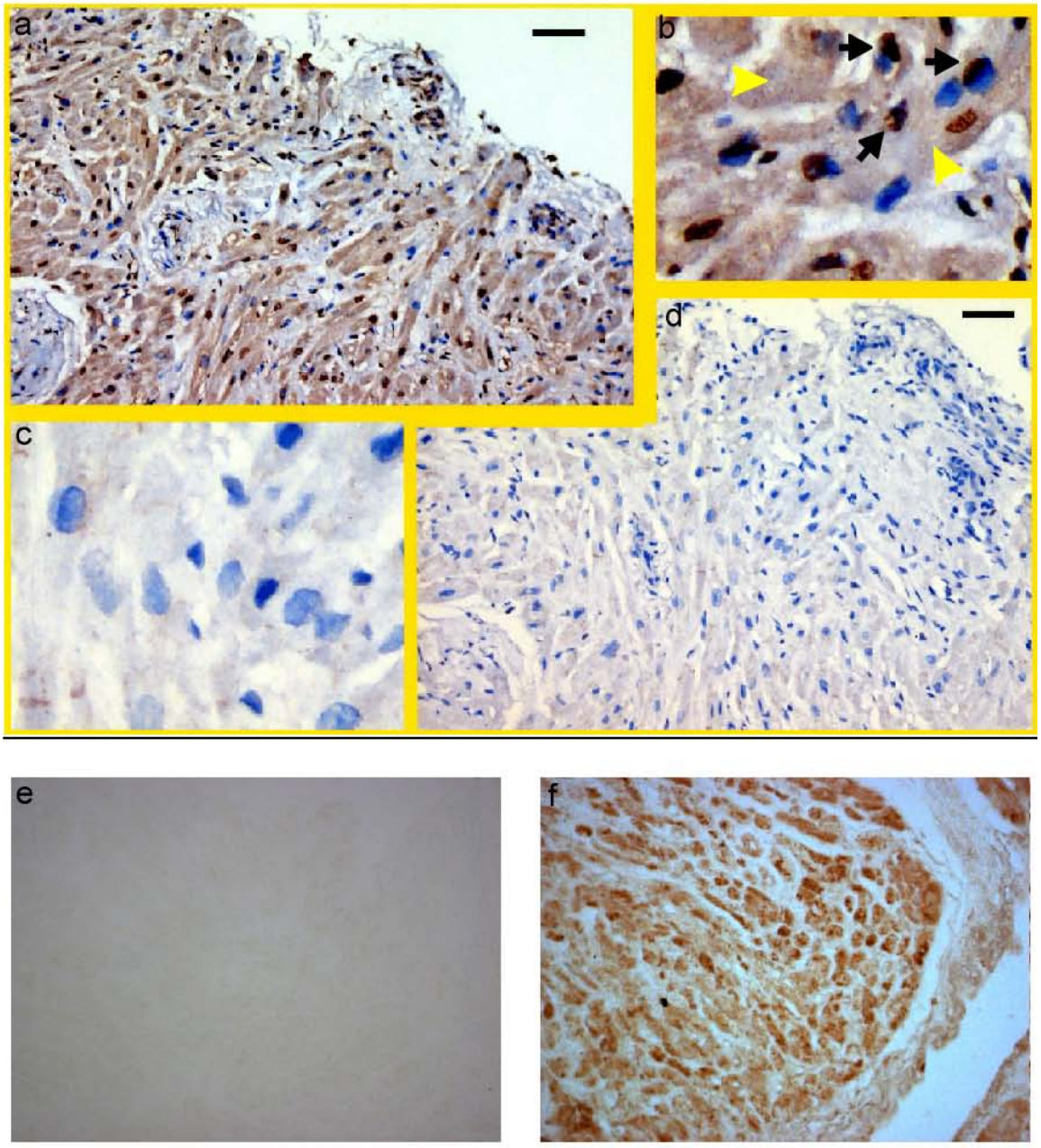

Figure 31. **Expression and localization of hi FGF2 in human cardiac (atrial) tissue assessed by immunocytochemistry and anti-hi FGF2 antibodies**. Paraffin sections from human atrial appendages were processed for immunocytochemical detection of hi FGF2 (brown color, due to horseradish peroxidase-conjugated secondary antibody and 3, 3-diaminobenzidine staining), using affinity purified rabbit polyclonal anti-human hi FGF2 antibodies; some sections were also counter-stained for nuclei (blue color) with hematoxylin. **Images (a) and (b)**. Double labeling for human hi FGF2 (brown) and nuclei (blue), in lower and higher magnification, respectively. Arrowheads point to cytosolic anti-human hi FGF2 staining of cardiomyocytes. Arrows point to nuclei staining densely for blue, as well as very darkly for hi FGF2. Sizing Bar =100μM. **Images (c) and (d)**. Staining for nuclei (blue), and HRP-DAB, in the absence of primary anti-human hi FGF2 antibody, at higher and lower magnification, respectively. Sizing Bar =100μM. **Images (e) and (f).** Staining for HRP-DAB only, in the absence and presence of primary (anti-hi FGF2) antibody.

Figure 32

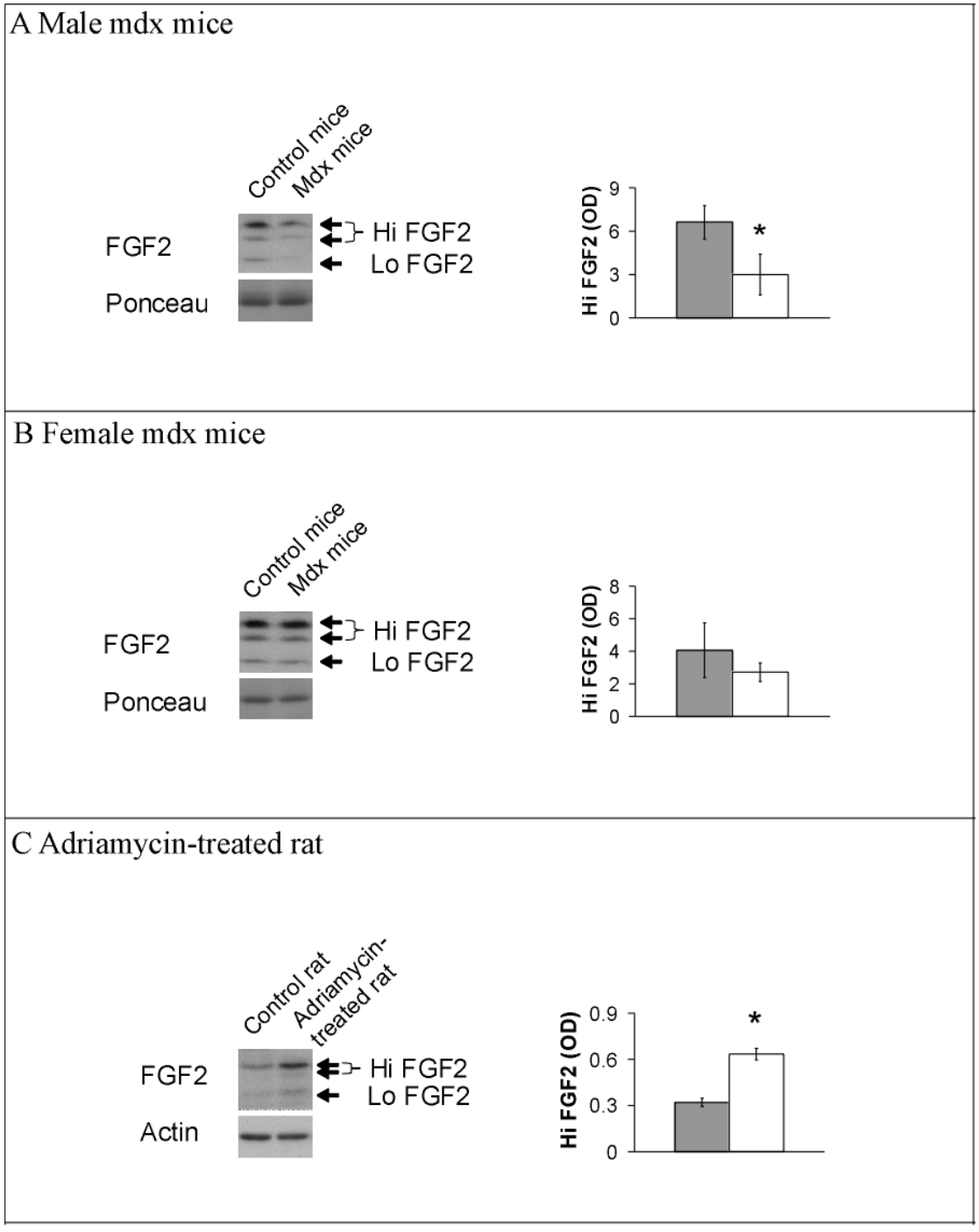
A Male mdx mice
Control mice
Mdx mice
FGF2
Ponceau
Hi FGF2
Lo FGF2
Hi FGF2 (OD)
9
6
3
0
*
B Female mdx mice
Control mice
Mdx mice
FGF2
Ponceau
Hi FGF2
Lo FGF2
Hi FGF2 (OD)
8
6
4
2
0
C Adriamycin-treated rat
Control rat
Adriamycin-treated rat
FGF2
Actin
Hi FGF2
Lo FGF2
Hi FGF2 (OD)
0.9
0.6
0.3
0
*

Figure 32. Cardiomyopathy models and cardiac Hi FGF2 accumulation. Cardiac tissues (ventricles) from normal or diseased animals were analyzed for hi FGF2 by western blotting. **(A) and (B). The mdx mouse**; representative western blot images and corresponding cumulative data showing hi FGF2 signal (monoclonal anti-FGF2 antibodies) in hearts of male and female mdx mice, respectively, compared to control hearts. Ponceau red staining is used to indicate equivalent loading. **(C). The adriamycin-treated rat**; representative western blot images and corresponding cumulative data showing hi FGF2 signal (monoclonal anti-FGF2 antibodies) in normal control hearts and hearts from rat subjected to adriamycin treatment, as indicated. Staining for actin is used to indicate equivalent protein loading. Data are presented as mean ± SD, n=4. *P < 0.01.

Figure 33

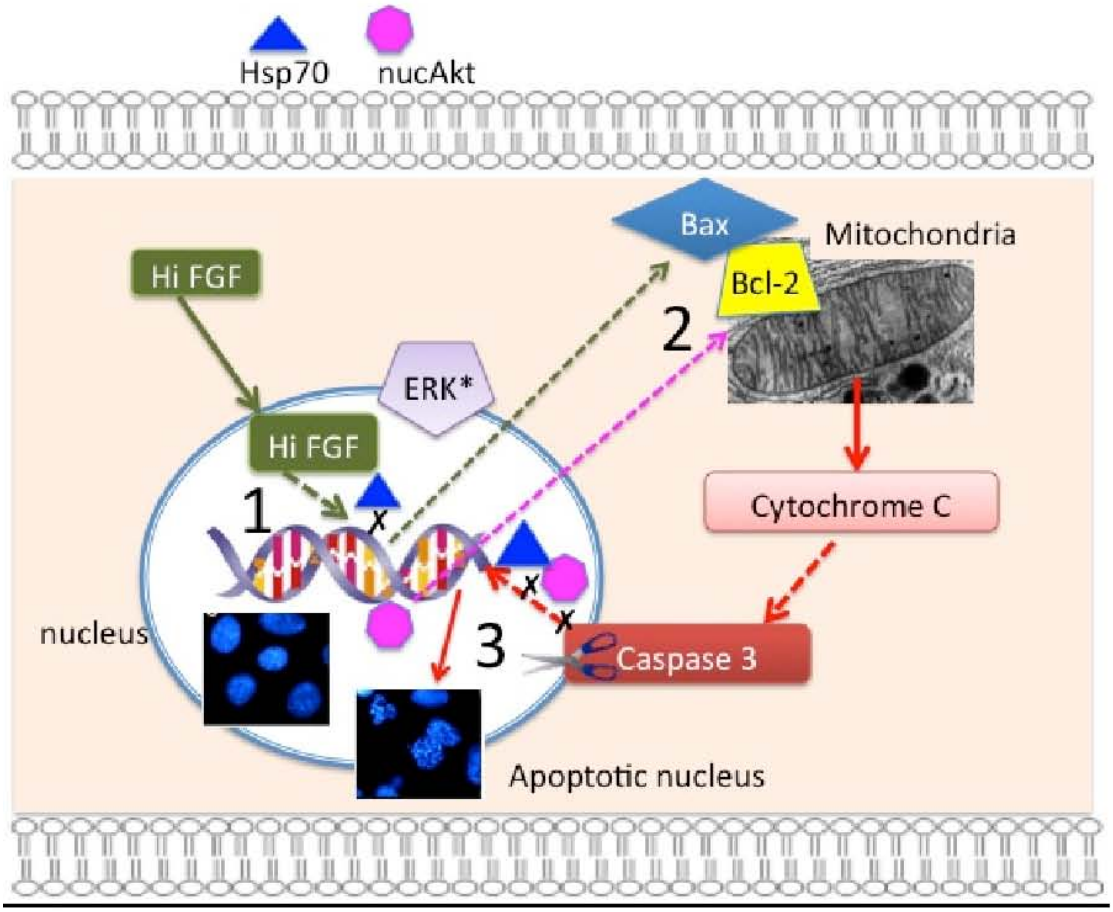
Hsp70
nucAkt
Bax
Mitochondria
Bcl-2
Hi FGF
2
ERK*
Hi FGF
1
Cytochrome C
nucleus
3
Caspase 3
Apoptotic nucleus

Figure 33. Hypothetical scheme of mechanisms mediating and antagonizing hi FGF2-induced apoptosis. We stipulate three steps in the pathway of hi FGF2 induced apoptosis. In step 1, hi FGF2 accumulates in the nucleus and triggers, likely by direct interaction with chromatin and altered gene expression, the production of signals (step 2) that promote translocation of Bax to mitochondria. Increased Bax will 'overtake' the anti-apoptotic Bcl-2 and promote release of cytochrome C to the cytosol, which will then activate series of events culminating in caspase 3 activation (step 3), and apoptotic nuclear fragmentation.

We have found that ERK activation that accompanies hi FGF2 overexpression is mediating hi FGF2-induced apoptosis and likely occurs before the Bax translocation (step 2). Overexpression of hsp70 may rescue the hi FGF2 phenotype: by preventing step 1 through its interaction with hi FGF2; preventing step 2 by promoting upregulation of prosurvival Bcl-2 proteins; or preventing step 3 by acting as a chaperone protein and protecting proteins from degradation by caspase 3-activated protease. Nuclear AKT likely rescues the hi FGF2 phenotype by upregulating PIM-1 which in turn upregulates Bcl-2 (step 2); it may also phosphorylate nuclear proteins altering their properties in a manner that prevents the effects of activated caspase 3 (step 3).

TABLE 1. POLYACRYLAMIDE GEL PREPARATION

Resolving gel	10 %	12 %	15 %
4x resolving gel buffer (181.5g/L Tris, 4g/L SDS, pH 8.8)	3 ml	3 ml	3 ml
30% Acrylamide/ Bis-acrylamide Stock	4 ml	4.8 ml	6 ml
Water	5 ml	4.2 ml	3 ml
TEMED	12 µl	12 µl	12 µl
Ammonium persulfate (APS)	90 µl	90 µl	90 µl

Stacking gel	4 %
4x Stacking gel buffer (60.6 g Tris, 4g SDS pH 6.8)	2.5ml
30%Acrylamide/ Bis-acrylamide Stock	1.5ml
Water	6ml
TEMED	12 µl
Ammonium persulfate (APS)	90µl

TABLE 2. ANTIBODIES AND APPLICATIONS

Antibodies	Source	Application		
		WB	IF	IP
Actin	Sigma (A2066), rabbit	1: 5000	N.A	N.A
Total AKT	Cell Signaling, (9272), rabbit	1:1000 Ab in 5% BSA	1:100	N.A
Phospho-Ser^{473}-AKT	Cell Signaling, (9271), rabbit	1:1000 Ab in 5% BSA	N.A	N.A
Phospho-Thr^{308}-AKT	Cell Signaling, (9275), rabbit	1:1000 Ab in 5% BSA	N.A	N.A
Anti-goat HRP	Jackson, (705-035-003), Donkey	10,000	N.A	N.A
Anti-mouse HRP	Jackson, (715-035-150), Donkey	1:10,000	N.A	N.A
Anti-rabbit HRP	Jackson, (711-035-152), Donkey	1:10,000	N.A	N.A
Bcl-2	BD transduction, (610539), Mouse	1:500	1: 100	N.A

FGF2*	Santa Cruz (sc-1390), goat	1: 400	N.A	N.A
FGF2*	Santa Cruz (Sc-79), goat	1:400	N.A	N.A
FGF2*	Upstate Biotechnology (05-118), mouse	1:1000	1:100	N.A
Anti-human hi FGF2 antibodies**	Synthetic peptide and antiserum were made by Sigma/Genosys, as per our specification	N.A.	1:50	4μg Ab for 900 μg total protein
GAPDH (0411)	Santa Cruz (sc-47724), mouse	1:1,000	N.A	N.A
hsp70 (K-20)	Santa Cruz (sc-1060), goat	N.A	N.A	N.A
hsp70 (W27)	Santa Cruz (sc-24), mouse	1: 800	1:50	1 μg Ab for 500 μg total protein
Lamin B	Santa Cruz, (sc-6217), goat	1:200	1:200	N.A

ERK1/2 (total)	Cell Signaling, (9102), rabbit	1:1000	N.A	N.A
Phospho-ERK1/2	Cell Signaling (9101), rabbit	1:1000	N.A	N.A
p68 RNA Helicase (2257C3a)	Santa Cruz (sc-81350), Mouse	1:800	1:200	1 µg Ab for 500 µg total protein
Beta Tubulin	Santa Cruz (sc-9104), rabbit	1:400	N.A	N.A

IF: Immunofluorescence

IP : Immunoprecipitation

WB : Western blotting (Antibodies were diluted in 1% skim milk powder in TBST, unless otherwise indicated)

* FGF2 antibodies recognize both lo and hi FGF2 isoforms

** FGF2 antibodies recognize only hi FGF2 isoforms

TABLE 3_1. HIGH PROBABILITY RESULTS FROM PEPTIDE SEQUENCING OF HPLC MASS SPECTROMETRY

Rank	log(e)	Mr	Accession	Description
1	-202.5	69.1	ENSP00000225792	ENSP00000225792 [5/2183] DDX5, Probable ATP-dependent RNA helicase DDX5 (EC 3.6.1.-)(DEAD box protein 5)(RNA helicase p68) [Source: UniProt P17844] Source: 3.6.1.-
2	-168.2	51.0	ENSP00000365458	ENSP00000365458 [79/2666] HNRNPK, Heterogeneous nuclear ribonucleoprotein K (hnRNP K)(Transformation up-regulated nuclear protein)(TUNP) [Source: UniProt P61978]
3	-166.7	70.0	ENSP00000406359	ENSP00000406359 [581/1066] Heat shock 70 kDa protein 1 (HSP70.1)(HSP70-1/HSP70-2) [Source: UniProt P08107]
4	-130.4	64.1	ENSP00000221419	ENSP00000221419 [27/1968] HNRNPL, Heterogeneous nuclear ribonucleoprotein L (hnRNP L) [Source: UniProt P14866]
5	-85.7	80.4	ENSP00000380033	(H) ENSP00000380033 [83/1059] DDX17, Probable ATP-dependent RNA helicase DDX17 (EC 3.6.1.-)(DEAD box protein 17)(RNAdependent helicase p72)(DEAD box protein p72) [Source: UniProt Q92841] Source: 3.6.1.-

Legend: analysis of a ~66kDa band from nuclear proteins (band 1) .

TABLE 3_2. HIGH PROBABILITY RESULTS FROM PEPTIDE SEQUENCING OF HPLC MASS SPECTROMETRY

Rank	log(e)	Mr	Accession	Description
1	-166.4	38.7	ENSP00000341826	ENSP00000341826 [30/2818] HNRPA1L3, Heterogeneous nuclear ribonucleoprotein A1 (hnRNP core protein A1)(Helixdestabilizing protein)(Single-strand RNA-binding protein) [Source: UniProt P09651] IPR000504 RRM RNP1
2	-114.3	31.3	ENSP00000225698	ENSP00000225698 [37/1403] C1QBP, Complement component 1 Q subcomponent-binding protein, mitochondrial precursor (Glycoprotein gC1qBP) (C1qBP) (GC1q-R protein) (Hyaluronan- binding protein 1) (Mitochondrial matrix protein p32) (p33). Source: Uniprot/SWISSPROT Q07021 Annotated domains: IPR003428 Mitochondrial glycoprotein
3	-96.0	27.7	ENSP00000258962	ENSP00000258962 [24/1377] SFRS1, Splicing factor, arginine/serine-rich 1 (pre-mRNA-splicing factor SF2, P33 subunit) (Alternative-splicing factor 1)(ASF-1) [Source: UniProt Q07955] IPR000504 RRM RNP1
4	-70. 9	21.9	ENSP00000307705	ENSP00000307705 [128/2978] HIST1H1E, Histone H1.4 (Histone H1b) [Source: UniProt P10412]
5	-56.8	27.4	NSP00000325905	ENSP00000325905 [3/1507] SFRS7, Splicing factor, arginine/serine-rich 7 (Splicing factor 9G8) [Source: UniProt Q16629]

Legend: analysis of a ~35kDa band from nuclear proteins (band 2) .

TABLE 3_3. HIGH PROBABILITY RESULTS FROM PEPTIDE SEQUENCING OF HPLC MASS SPECTROMETRY

Rank	log(e)	Mr	Accession	Description
1	-130.3	29.6	ENSP00000362744	ENSP00000362744 [21/1589] RPS4P13, 40S ribosomal protein S4, X isoform (Single copy abundant mRNA protein)(SCR10) [Source: UniProt P62701]
2	-126.0	28.4	ENSP00000254193	ENSP00000254193 [7/661] SNRPA1, U2 small nuclear ribonucleoprotein A' (U2 snRNP-A'). [Source: SWISSPROT (P09661)]
3	-122.3	28.6	ENSP00000417864	ENSP00000417864 [0/126]
4	-63.8	28.8	ENSP00000345848 (H)	ENSP00000345848 [75/1100] ANP32B, Acidic leucine-rich nuclear phosphoprotein 32 family member B (Acidic protein rich in leucines)(PHAPI2)(Silver-stainable protein SSP29) [Source: UniProt Q92688]
5	-61.4	32.8	ENSP00000360671	ENSP00000360671 [1248/2338] SLC25A5, solute carrier family 25 (mitochondrial carrier; adenine nucleotide translocator), member 5 [Source:HGNC Symbol;Acc:10991]

Legend: analysis of a ~28kDa band from cytosolic proteins (band 3) .

TABLE 3_4. HIGH PROBABILITY RESULTS FROM PEPTIDE SEQUENCING OF HPLC MASS SPECTROMETRY

Rank	log(e)	Mr	Accession	Description
1	-134.1	31.3	ENSP00000341885	ENSP00000341885 [17/2218] RPS2P12, 40S ribosomal protein S2 (S4)(LLRep3 protein) [Source: UniProt P15880]
2	-100.9	26.7	ENSP00000278572	ENSP00000278572 [126/2618] RPS3P3, 40S ribosomal protein S3 [Source: UniProt P23396]
3	-95.0	35.1	ENSP00000366013 E	NSP00000366013 [80/1472] GNB2L1, Guanine nucleotide-binding protein subunit beta-2-like 1 (Guanine nucleotide-binding protein subunit beta-like protein 12.3)(Receptor of activated protein kinase C 1)(RACK1) (Receptor for activated C kinase)(Cell proliferation-inducing gene 21 protein)(Human lung cancer oncogene 7 protein)(HLC-7) [Source: UniProt P63244]
4	-88.6	30.0	ENSP00000364721	ENSP00000364721 [39/1011] MAPRE1, microtubule-associated protein, RP/EB family, member 1 [Source:HGNC Symbol; Acc:6890]
5	-65.1	30.0	ENSP00000361076	ENSP00000361076 [213/1813] RPL7AP62, 60S ribosomal protein L7a (Surfeit locus protein 3)(PLA-X polypeptide) [Source: UniProt P62424]

Legend: analysis of a ~30 kDa band from cytosolic proteins (band 4) .

TABLE 3_5. HIGH PROBABILITY RESULTS FROM PEPTIDE SEQUENCING OF HPLC MASS SPECTROMETRY

Rank	log(e)	Mr	Accession	Description
1	-110.8	35.1	ENSP00000366013	ENSP00000366013 [44/1472] GNB2L1, Guanine nucleotide-binding protein subunit beta-2-like 1 (Guanine nucleotide-binding protein subunit beta-like protein 12.3)(Receptor of activated protein kinase C 1)(RACK1) (Receptor for activated C kinase)(Cell proliferation-inducing gene 21 protein)(Human lung cancer oncogene 7 protein)(HLC-7) [Source: UniProt P63244]
2	-110.8	31.3	ENSP00000225698	ENSP00000225698 [37/1403] C1QBP, Complement component 1 Q subcomponent-binding protein, mitochondrial precursor (Glycoprotein gC1qBP) (C1qBP) (GC1q-R protein) (Hyaluronan- binding protein 1) (Mitochondrial matrix protein p32) (p33). Source: Uniprot/SWISSPROT Q07021
3	-99.3	27.7	ENSP00000258962	ENSP00000258962 [24/1377] SFRS1, Splicing factor, arginine/serine-rich 1 (pre-mRNA-splicing factor SF2, P33 subunit) (Alternative-splicing factor 1)(ASF-1) [Source: UniProt Q07955]
4	-94.2	31.3	ENSP00000341885	ENSP00000341885 [36/2218] RPS2P12, 40S ribosomal protein S2 (S4)(LLRep3 protein) [Source: UniProt P15880]
5	-82.1	30.0	ENSP00000412809	ENSP00000412809 [8/508] no description available IPR001593 Ribosomal S3Ae IPR018281 Ribosomal S3Ae CS
6	-82.1	34.2	ENSP00000333504	ENSP00000333504 [328/2289] HNRPA1L3, No description Annotated domains: IPR000504 RNA-binding region RNP-1 (RNA recognition motif) IPR002086 Aldehyde dehydrogenase

Legend: analysis of a ~32kDa band from cytosolic proteins (band 5) .

TABLE 3_6. HIGH PROBABILITY RESULTS FROM PEPTIDE SEQUENCING OF HPLC MASS SPECTROMETRY

Rank	log(e)	Mr	Accession	Description
1	-161.2	37.4	ENSP00000346694	ENSP00000346694 [132/3098] HNRNPA2B1, Heterogeneous nuclear ribonucleoproteins A2/B1 (hnRNP A2 / hnRNP B1) [Source: UniProt P22626] IPR000504 RRM RNP1
2	-82.6	34.3	ENSP00000339027	ENSP00000339027 [241/2622] RPLP0P6, 60S acidic ribosomal protein P0 (L10E) [Source: UniProt P05388]
3	-80.1	32.6	ENSP00000296930	ENSP00000296930 [255/3065] NPM1P21, Nucleophosmin (NPM)(Nucleolar phosphoprotein B23)(Numatrin)(Nucleolar protein NO38) [Source: UniProt P06748] IPR004301 Nucleoplasmin
4	-77.5	34.2	ENSP00000333504 (H)	ENSP00000333504 [328/2289] HNRPA1L3, No description Annotated domains: IPR000504 RNA-binding region RNP-1 (RNA recognition motif) IPR002086 Aldehyde dehydrogenase
5	-76.8	35.6	ENSP00000384493	ENSP00000384493 [48/406] PPP2CB, Serine/threonine-protein phosphatase 2A catalytic subunit beta isoform (PP2A-beta)(EC 3.1.3.16) [Source: UniProt P62714] Source: 3.1.3.16 IPR004843 M-pesterase IPR006186 Ser/Thr-sp prot-phosphatase

Legend: analysis of a ~35kDa band from cytosolic proteins (band 6) .

TABLE 3_7. HIGH PROBABILITY RESULTS FROM PEPTIDE SEQUENCING OF HPLC MASS SPECTROMETRY

Rank	log(e)	Mr	Accession	Description
1	-127.8	36.5	ENSP00000362688	ENSP00000362688 [8/644] EIF3I, Eukaryotic translation initiation factor 3 subunit I (eIF3i)(Eukaryotic translation initiation factor 3 subunit 2)(eIF-3-beta)(eIF3 p36)(TGF-beta receptor-interacting protein 1)(TRIP-1) [Source: UniProt Q13347]
2	-117.0	32.6	ENSP00000296930	ENSP00000296930 [131/3065] NPM1P21, Nucleophosmin (NPM)(Nucleolar phosphoprotein B23)(Numatrin)(Nucleolar protein NO38) [Source: UniProt P06748] IPR004301 Nucleoplasmin
3	-94.1	41.2	ENSP00000262506	ENSP00000262506 [50/586] CSNK2A2, Casein kinase II subunit alpha' (CK II)(EC 2.7.11.1) [Source: UniProt P19784] Source: 2.7.11.1
4	-89.2	37.4	ENSP00000346694	ENSP00000346694 [275/3098] HNRNPA2B1, Heterogeneous nuclear ribonucleoproteins A2/B1 (hnRNP A2 / hnRNP B1) [Source: UniProt P22626] IPR000504 RRM RNP1
5	-69.2	37.2	ENSP00000351298	ENSP00000351298 [77/1370] PPP1CB, protein phosphatase 1, catalytic subunit, beta isoform 1; protein phosphatase 1, catalytic subunit, delta isoform; protein phosphatase 1-delta; protein phosphatase 1-beta; serine/threonine protein phosphatase PP1-beta catalytic subunit [Homo sapiens]. [Source: RefSeq (NM_002709)]

Legend: analysis of a ~38kDa band from cytosolic proteins (band 7) .

TABLE 3_8. HIGH PROBABILITY RESULTS FROM PEPTIDE SEQUENCING OF HPLC MASS SPECTROMETRY

Rank	log(e)	Mr	Accession	Description
1	-136.5	32.1	ENSP00000318012	ENSP00000318012 [18/1336] SET, SET PROTEIN (HLA-DR ASSOCIATED PROTEIN II) (PHAPII) (PHOSPHATASE 2A INHIBITOR I2PP2A). [Source: SWISSPROT (Q01105)] Annotated domains: IPR002164 Nucleosome assembly protein (NAP)
2	-127.3	39.9	ENSP00000276682	ENSP00000276682 [2/595] EIF3H, Eukaryotic translation initiation factor 3 subunit H (Eukaryotic translation initiation factor 3 subunit 3) (eIF-3 gamma) (eIF3 p40 subunit) (eIF3h). Source: Uniprot/SWISSPROT O15372 Annotated domains: IPR000555 Mov34/MPN/PAD-1
3	-104.2	45.5	ENSP00000357320	ENSP00000357320 [12/251] DAP3,
4	-101.8	42.5	ENSP00000319910	ENSP00000319910 [23/563] EIF3M, Eukaryotic translation initiation factor 3 subunit M (eIF3m)(PCI domain-containing protein 1)(Fetal lung protein B5)(hFL-B5) [Source: UniProt Q7L2H7]
5	-98.6	41.3	ENSP00000418008	ENSP00000418008 [0/6]

Legend: analysis of a ~40kDa band from cytosolic proteins (band 8) .

TABLE 3_9. HIGH PROBABILITY RESULTS FROM PEPTIDE SEQUENCING OF HPLC MASS SPECTROMETRY

Rank	log(e)	Mr	Accession	Description
1	-180.5	53.6	ENSP00000224237	ENSP00000224237 [2711/5013] VIM, vimentin [Source:HGNC Symbol;Acc:12692] IPR016044 F IPR006821 Intermed filament DNA bd IPR018039 Intermediate filament CS IPR009053 Prefoldin
2	-133.9	52.2	ENSP00000220849	ENSP00000220849 [13/642] EIF3E, Eukaryotic translation initiation factor 3 subunit E (eIF3e)(Eukaryotic translation initiation factor 3 subunit 6)(eIF-3 p48)(Viral integration site protein INT-6 homolog) [Source: UniProt P60228] IPR000717 PCI IPR016650 Transl init fac 3 su6 euk
3	-111.8	51.1	ENSP00000221413	ENSP00000221413 [56/863] RUVBL2, RuvB-like 2 (EC 3.6.1.-)(48 kDa TATA box-binding protein-interacting protein)(48 kDa TBP-interacting protein)(TIP49b)(Repressing pontin 52)(Reptin 52)(51 kDa erythrocyte cytosolic protein)(ECP-51)(TIP60-associated protein 54-beta)(TAP54-beta)(INO80 complex subunit J) [Source: UniProt Q9Y230] Source: 3.6.1.-
4	-106.7	46.8	ENSP00000260956	ENSP00000260956 [67/1029] SSB, Lupus La protein (Sjoegren syndrome type B antigen) (SS-B) (La ribonucleoprotein) (La autoantigen). Source: Uniprot/SWISSPROT P05455
5	-79.1	46.1	ENSP00000293831	ENSP00000293831 [258/2431] EIF4A1, Eukaryotic initiation factor 4A-I (eIF-4A-I)(eIF4A-I)(EC 3.6.1.-)(ATP-dependent RNA helicase eIF4A-1) [Source: UniProt P60842] Source: 3.6.1.-

Legend: analysis of a ~45kDa band from cytosolic proteins (band 9) .

TABLE 4. ShRNA SEQUENCES

Types of shRNA	**Open Biosystem Catalog No.**	**Mature antisense sequence**
P68 shRNA 1	V3LHS_636793	GAACCTCTGTCTTCGACCA
P68 shRNA 2	V2LHS_24065	CACTTTCTTTACACCTAAT
Scramble shRNA	RHS4346	ATCTCGCTTGGGCGAGAGTAAG

CHAPTER 4

DISCUSSION

Studies presented in the previous sections (Results chapter 3) addressed a number of questions aimed at extending our understanding of the intracrine action of hi FGF2 and its relationship to cardiac pathology. Our major findings will be discussed in detail below, and can be summarized as follows:

a. Hi FGF2 overexpression induces apoptotic cell death which can be prevented by increased expression of Bcl-2; nuclear Akt; the PIM-1 kinase; the heat shock protein hsp70.
b. The hi FGF2-induced phenotype, including TUNEL staining and nuclear compaction, is associated with sustained activation of ERK ½ and nuclear ERK ½, by an intracrine pathway.
c. Affinity chromatography followed by mass spectroscopy identified, for the first time, several proteins as potentially interacting with hi FGF2; of these, the p68 RNA helicase and hsp70 were further confirmed as interacting partners, as their corresponding antibodies co-precipitated hi FGF2, but not lo FGF2.
d. Decreasing endogenous p68 expression by shRNA had no effect on the hi FGF2 induced chromatin compaction and cell death.
e. Increased nuclear co-localization, and possibly interaction, between hi FGF2 and overexpressed hsp70 correlated with rescue from hi FGF2 induced cardiomyocyte cell death.

f. Several bioactive factors associated with cardiac pathology (isoproterenol, angiotensin II, endothelin I) upregulate endogenous hi FGF2 in cardiac non-myocytes.

g. Hi FGF2 is expressed in the human heart (atria) and localizes in both cytosol and nuclei, and in particular in nuclei with a pyknotic appearance.

The hi FGF2-induced chromatin compaction leads to apoptotic cell death. Hi FGF2 has long been known to exert distinct intracrine effects compared to lo FGF2, although there is no clear consensus as to the exact nature of these effects. A number of studies have reported a link between hi FGF2 over-expression in stable cell lines and cellular transformation [51, 54, 202]. On the other hand several studies, as listed in the introduction, have pointed to this isoform as a potential inhibitor of cell proliferation [57, 60] and inducer of cell death in certain cell types. We have shown that in HEK293 cells, increased hi FGF2 expression does indeed inhibit cell proliferation, as it decreases the appearance of 'markers' for proliferating cells such as Ki67 as well as BrdU incorporation (Fig.2). Our data are in agreement with a report by Quarto [60] who showed that hi FGF2 expression in NIH3T3 fibroblasts upregulates expression of genes promoting cell cycle arrest (such as *Nfl-x*, *Nupr*1), and tumor suppression (such as *St5*).

As expected from previous studies, we have found that nuclear hi FGF2 induces chromatin compaction (detectable by 24 h), followed by overtly apoptotic-looking nuclei by 72h in culture [58]. Additional criteria pointing to apoptotic cell death of

HEK293 cells in response to Hi FGF2 over-expression were: increased TUNEL staining (Fig.2); accumulation of active caspase 3[58]; evidence of cytochrome C release to the cytosol (Fig.3); and engagement of mitochondria-associated entities such as the Bcl-2 family of proteins.

Human or rat hi FGF2 exert similar effects on the nuclear morphology of HEK293 cells[58], indicating that the ability to cause chromatin compaction and cell death is not species-specific, as also observed in previous reports when rat or human hi FGF2 were expressed in rat or chicken cardiomyocytes [85-86, 197]. It should be noted that while the core 18 kDa lo FGF2 sequence is nearly identical between human and rat FGF2 (155 and 154 amino-acids, respectively), there are significant differences in the N-extension portion: it is composed of 41, 46, and 55 amino-acids in the 22–25 kDa human hi FGF2, compared to 26 and 34 amino-acids in its rat counterpart [203-204]. Despite these differences, both human and rat hi FGF2 had similar effects on chromatin, and cell death, indicating conservation of the hi FGF2-specific effect, and thus pointing to the possibility that these effects are exerted by, or at least require, 'common' sequence(s) within the N-extension. Overexpression of the N-terminal FGF2 extension by itself, however, does not induce cell death, suggesting that an intact hi FGF2 structure is required for the effect (Xin Ma, Master's thesis, University of Manitoba, 2003).

Another important point is that the effect of hi FGF2 on chromatin is not a secondary non-specific consequence of high levels of expression: similar levels of lo FGF2 or of mutated, non-nuclear hi FGF2 expression did not cause chromatin

compaction or cell death [58].

We examined whether the effects of hi FGF2 on chromatin were associated with and/or were dependent on a mitochondrial cell death pathway. Cytochrome C is a mitochondrial protein that is released to the cytosol by pro-apoptotic stimuli, thus the increased cytosolic cytochrome C in hi FGF2 expressing cultures shown here (Fig.3) is consistent with apoptotic cell death. We also asked if a mitochondrially mediated process linked to the induction of apoptosis was actually required to manifest the hi FGF2-triggered chromatin compaction. Release of cytochrome C to the cytosol can be the end result of effects exerted by combinations of Bcl-2-protein family members (such as the pro-apoptotic Bax, or the anti-apoptotic Bcl-2) on the mitochondria. We found that the effect of hi FGF2 could be attenuated in a background of Bcl-2 overexpression, which would be expected to counteract the pro-apoptotic effects of Bax (Fig.4). In a similar manner, inhibition of Bax with a specific inhibiting peptide also attenuated the effects of hi FGF2 on chromatin compaction [58]. As both interventions prevented the hi FGF2-induced chromatin compaction, we surmise that the effects of hi FGF2 on chromatin are dependent on mitochondrial engagement and activation of apoptosis involving members of the Bcl-2 family. We thus propose that nuclear hi FGF2 initiates a sequence of events, including changes in gene expression, resulting in sending as-yet-unidentified signals to the mitochondria, followed by mitochondrially mediated activation of a pro-apoptotic pathway that promotes chromatin compaction and cell death.

Hi FGF2 causes sustained activation of nuclear ERK½ by an intracrine

route. The ERK½ activating pathway is a major pathway stimulated by hi and lo FGF2 acting extracellularly [48]. We have previously shown, and confirmed here (Fig.5) that activation of the ERK½ pathway is required for the hi FGF2-induced effects on chromatin compaction and cell death [58]. Data presented here also support an intracrine effect to induce sustained activation of the ERK½ pathway by hi FGF2: its over-expression resulted in elevated ERK½ activity (both total and nuclear) at both 24 and 72 h post-transfection (Fig.8). This hi FGF2-associated ERK½ activity was not reduced by neutralizing anti-FGF2 antibodies, indicating that it was not caused by externalized FGF2 acting on cell surface receptors. It is theoretically possible that hi FGF2 stimulated the expression and/or release of ERK½ activating factors that in turn acted in a paracrine/autocrine mode. This is unlikely, since conditioned media from hi FGF2 over-expressing cultures did not exhibit increased potency for stimulating ERK (Fig.8). Taken together, our results point to an intracrine pathway of ERK½ activation that is promoted by hi FGF2 overexpression. Our results are in agreement with a previous report providing evidence that this pathway can be activated by intracrine-acting hi FGF2 in pancreatic cells [205]. Although ERK½ activation is required, activation of ERK½ is not by itself sufficient to induce chromatin compaction: lo FGF2 over-expression while causing similar levels of ERK½ activation (unpublished observations), does not have similar effects on chromatin.

Previous studies, also confirmed here (Fig.8), have demonstrated that the type of neutralizing antibodies used here, are recognizing all FGF2 isoforms and are effective in blocking the activity of extracellularly acting FGF2 [197, 205].

While numerous studies have implicated the ERK½ activating pathway in the promotion of cell survival and cytoprotection [206-208], several other studies, reviewed extensively in the Introduction, have shown that this pathway can also be used to promote cell death. Yang et al. [209] showed that hydrogen sulfide induced apoptosis in human aorta smooth muscle cells requires the activation of ERK½ and caspase 3. ERK½ has been implicated in chromatin remodeling or compaction [210], and MEK2 and ERK2 were shown to mediate an atypical form of programmed cell death in HEK293 cells [211]. Sustained stimulation of ERKs and/or nuclear ERKs were found to be pro-apoptotic in cells subjected to DNA damage causing agents [212], oxidative stress[213], or osteoclasts treated with 17β-estradiol [214]. Our findings therefore are in agreement with the second group of studies, and support the notion that sustained activation of the ERK½ pathway is required for the hi FGF2--triggered chromatin compaction and cell death in HEK293 cells. It is important to note that ERK activation may mediate an anti-apoptotic function when activated by extracellularly acting FGF2, since exogenous administration of lo FGF2 activates the ERK pathway [78] and protects the heart from ischemia-reperfusion induced myocardial damage. It is possible that different pathways (intracrine versus auto- or paracrine) can activate different pools of ERK½, affecting different downstream targets. At this point the molecular mechanism by which intracrine hi FGF2 caused sustained activation of ERK½ is unknown. It is possible that hi FGF2 stimulated a pattern of gene expression that culminates in the upregulation of the ERK½ activating pathway. There is some evidence from Gaubert et al. [205] that intracrine hi FGF2

upregulated the expression of protein kinase C δ which then went on to activate ERK½. A similar mechanism may operate in our system.

We also examined if the hi FGF2-induced ERK½ activation occurs upstream or downstream of the mitochondrial pathway. Having found that hi FGF2 remained capable of stimulating ERK½ in the presence of the Bip V5 peptide (i.e., in a background of Bax inhibition), we concluded that ERK½ activation is likely to occur upstream of the mitochondrial cell-death pathway. Our findings are in agreement with a study by Oh et al. [215] that provided evidence indicating that the ERK½ activating pathway acts upstream of mitochondrial dysfunction in ceramide-induced apoptosis of astrocytes. Our study is also consistent with a study by Park et al. [216] reporting H_2O_2-triggered ERK½ activation upstream of mitochondrial pathways leading to apoptosis in osteoblastic cells. It is intriguing that the lo FGF2 isoform, while capable of activating ERK½ and of translocating to the nucleus, is nevertheless incapable of causing chromatin compaction [57, 85-86, 197]. The only difference between hi and lo FGF2 is the N-terminal extension present in hi FGF2; pilot studies suggested that the N-extension is incapable of causing chromatin compaction or cell death by itself (unpublished observations). The N-extension is, however, important in conferring a distinct pattern of hi FGF2 localization in relation to chromatin [36]. Thus we speculate that the nuclear localization pattern and local interactions of hi FGF2 with chromatin (and possibly other proteins) exert direct effects on gene expression that result in decreased proliferative growth and mitochondrially mediated chromatin compaction and cell death, in a ERK½-dependent pathway.

Nuclear Akt, and its downstream kinase PIM-1, prevent the hi FGF2-induced chromatin compaction and cell death. Our previous studies demonstrated that nuclear localization of hi FGF2 was essential to its ability to promote chromatin compaction [58]. On the other hand, Sussman and colleagues have shown that nuclear localization of the Akt kinase was required for its anti-apoptotic effects [124]. We asked if the chromatin compaction effect of overexpressed nuclear hi FGF2 could also be prevented by the Akt-PIM-1 nuclear pathway. We were able to use primary cultured myocytes for these experiments, due to the availability of adenoviral vectors expressing total Akt, nuclear Akt, and PIM-1 (generously provided by Dr. M. Sussman). We demonstrated that overexpression of nuclear Akt, confirmed by immunolocalization, reversed the effects of hi FGF2 on chromatin compaction, and therefore the ensuing cell death (Fig.10). Our findings therefore confirmed the potent anti-apoptotic role of nuclear Akt [124, 131].

Previous reports [131] show that nuclear Akt increases expression of the PIM-1 kinase, and this increase plays an important downstream role in protecting from apoptosis. In agreement with this notion, overexpression of PIM-1 in cardiac myocytes (Fig.10) had similar effects as overexpression of nuclear Akt, by preventing hi FGF2-induced chromatin compaction. The nuclear Akt-PIM-1 pathway is reported to exert its anti-apoptotic effect by increasing expression of the anti-apoptotic members of the Bcl-2 family (Bcl-2_{XL}, Bcl-2), and to 'inactivate' the pro-apoptotic members (Bad, Bax) through phosphorylation [124]. It is very likely that a similar mechanism is operating in our system as we have shown that overexpression of Bcl-2,

or use of the Bax inhibiting peptide, block the effects of hi FGF2.

While both hi and lo FGF2 can promote Akt phosphorylation (and thus activation) when acting from the outside in, and exert a protective effect, at least in the short term [217], there is as yet no information as to how overexpressed intracrine hi or lo FGF2 may affect the Akt pathway. We found that only lo FGF2, not hi FGF2 overexpression was associated with increased p-Akt. The ability of overexpressed lo FGF2 to activate Akt may be part of the overall cytoprotective role of this FGF2 isoform. Lack of Akt activation by hi FGF2 overexpression on the other hand, may facilitate its apoptotic effects.

Affinity chromatography and HPLC-mass spectrometry identifies several proteins potentially interacting with hi FGF2 (not lo FGF2). Protein-protein interactions are an invaluable tool in understanding protein function. To further study hi FGF2 isoform-specific activities on chromatin and the cell in general, we decided to identify proteins that were interacting only with hi but not lo FGF2. The strategy we followed for isolating binding partners was affinity chromatography: we constructed hi FGF2 and lo FGF2 affinity columns (sepharose), as well as control columns (no conjugated protein). Analysis of nuclear and cytosolic HEK293 cell proteins that bound to these columns by gel chromatography and Coomassie blue staining pointed to the presence of several protein bands that appeared only in the hi FGF2 column eluate. Further analysis of these bands, by MS/MS Peptide Sequencing analysis gave rise to several candidate proteins for each gel band, presented in terms

of increased probability in Tables $3_{1\text{-}9}$.

Our approach has both advantages and limitations. Major advantages are that we are using highly purified proteins as 'bait'; the affinity columns furthermore can be used to isolate relatively large amounts of protein material which can then facilitate further analysis. Our method also avoids using antibody-recognition based approaches which can have problems with immunoglobulin contamination of samples. Limitations are also present. Since we used one-dimensional gel separation, fractionating based on size only, two or more proteins with similar molecular weight are likely to co-exist in one gel band and this could explain, in part, the multiple 'hits' per band. In addition, our method (affinity chromatography of cell fractions) does not necessarily reflect interactions within the cell. It is also important to note that the conjugated proteins were generated in *E. coli*, and are thus lacking post-translational modifications that might play a role in protein-protein interactions. Finally, our conjugated recombinant proteins are tagged with histidine residues at their N-termini, possibly interfering with protein-protein interactions. Thus our findings should be considered as 'suggestive' and not definitive, pointing to proteins that have the potential to bind (alone or as part of a complex) to hi FGF2 but not lo FGF2. For all these reasons it is essential to confirm the interaction between hi FGF2 and candidate proteins by additional methods.

For the purposes of this thesis, two proteins, the p68 RNA helicase and hsp70, were selected for further study. The following criteria were used for this selection: both proteins were singled out as 'high probability' (Table 3_1); molecular weight of

the proteins indicated by MS/MS corresponded to the size indicated by SDS/PAGE; and both proteins were in the nuclear fraction and thus may play a role in nuclear effects of hi FGF2 which is itself a predominantly nuclear protein. Finally, as reviewed in the Introduction, p68 helicase and hsp70 play important roles in the regulation of, respectively, gene silencing, and inhibition of apoptosis, events that relate (positively or negatively) to chromatin condensation. Thus either or both of these proteins may have a function in modulating the hi FGF2-induced chromatin condensation.

Although beyond the scope of the current work and thus not investigated further, several intriguing findings regarding hi FGF2-bound proteins were made. The most striking observation is that hi FGF2 seemed to interact with numerous proteins that bind RNA and are involved in many aspects of RNA biology, including translational regulation[218], indicating that this isoform may play a role in this context. Potential interaction with several subunits of eIF3 (translation initiation factor), such as eIF3e, i, h, m are of interest, in view of the fundamental role of eIF3 in protein translation. The mammalian eIF3 contains 13 distinct subunits (a-m), and they are all essential for translation initiation[219], both cap-dependent translation and cap-independent translation via IRES element recognition[220]. The potential interaction of hi FGF2 with hnRNPs is also of particular interest. The hnRNPs bind RNA, and although mainly nuclear, undergo nucleocytoplasmic shuffling[221], and thus participate in all aspects of nucleic acid metabolism, including packaging of nascent transcripts, alternative splicing, DNA repair, translation regulation, chromatin organization and

remodeling[218]. The hnRNP K has numerous interacting partners and is involved in many nuclear and cytoplasmic processes including transcription, mRNA silencing and chromatin remodeling; it acts as a 'docking' platform to integrate diverse cellular signals [218, 222]. In fact, some of the interacting partners of hnRNP K (in addition to other hnRNPs) include RNA helicases (such as DDX5), and C1QBP, all of which were also identified as potentially binding to hi FGF2 by our studies. Overall, an interaction of hnRNP K with hi FGF2 would be expected to 'recruit' signaling pathways to sites of hi FGF2 localization and so contribute to the hi FGF2 effects on chromatin.

Two additional potential binding partners for hi FGF2 attracted our attention and merit investigation in future studies. One of these, as already mentioned, is C1QBP. This protein has been reported to localize in many different subcellular sites, including the mitochondria. Recent evidence shows that C1QBP is indeed a mitochondrial protein that may play an important role in modulating opening of the permeability transition pore and thus in mitochondrially driven death [223-224]. Since we have shown that the hi FGF2-induced chromatin compaction and cell death require mitochondrial engagement, it is tempting to hypothesize that hi FGF2-C1QBP interaction could contribute to the apoptotic phenotype. The other protein of interest is B23/NPM (nucleophosmin) which is important for cell survival. B23 is a major nucleolar phosphoprotein that can interact with nuclear Akt; this interaction protects B23 from proteolytic degradation by caspase-3, and thus is important for preventing apoptotic cell death [225]. As discussed in the previous section, overexpression of

nuclear Akt prevented the effects of hi FGF2 on chromatin compaction and cell death. One can speculate that the interaction of hi FGF2 with B23 (if real) prevents the latter from exerting its pro-survival role and thus the cell proceeds to apoptosis. A surplus of nuclear Akt (which also binds B23) would be expected to compete for this interaction and thus rescue the cells from the effects of hi FGF2.

Hi FGF2 and p68 RNA helicase. Having confirmed that the p68 helicase is indeed expressed by various cell types in a manner detectable by commercially available antibodies, we proceeded to examine p68-hi FGF2 interaction by co-immunoprecipitation. While anti-p68, in addition to pulling down its cognate protein, did indeed co-precipitate endogenous hi FGF2 (from HEK293 cells), anti-hi FGF2 antibodies did not seem to co-precipitate p68. These apparently conflicting findings can be explained if we consider that the anti-hi FGF2 antibodies recognize epitopes present at the N-terminal extension of hi FGF2, the very same region responsible for differential binding of proteins (between hi and lo FGF2). It is possible that an interaction of p68 with hi FGF2 masks the epitopes recognized by anti-hi FGF2. Thus we suggest that p68 and human hi FGF2 do interact, but that hi FGF2 antibodies will only recognize 'free' hi FGF2.

DsRed labeled (rat) hi FGF2 promotes similar effects on chromatin compaction and cell death as its human counterpart [58]. Immunoprecipitation of endogenous p68, however, was unable to specifically co-precipitate rat DsRed hi FGF2, unlike its ability to co-precipitate endogenous human hi FGF2. One possible reason for this

discrepancy may be that there were relatively high levels of non-specific retention of DsRed hi FGF2 by the sepharose beads, and this may have masked any specific interaction. Another possibility is that the DsRed hi FGF2 did interact with p68, but that the interaction, and/or the DsRed tag, created a conformational change that prevented recognition of p68 by the immunoprecipitating antibody. Finally, we cannot exclude the possibility that the overexpressed DsRed hi FGF2 does not in fact interact with p68. If this possibility is correct, it would imply that a p68-hi FGF2 interaction is not required for the effects of (DsRed) hi FGF2 on chromatin. In broad agreement with the latter possibility, our shRNA p68 knockdown results suggested that p68 is not required for the (DsRed) hi FGF2-induced chromatin compaction. A substantial decrease in p68 levels (achieved by two different shRNAs) had no effect on nuclear compaction index. It should be noted, however, that some p68 did remain even after shRNA knockdown, thus we cannot exclude the possibility that even low p68 levels are sufficient to mediate the effects of hi FGF2 on chromatin.

Taken together, our experimental results suggested that although p68 may interact with endogenous hi FGF2, it may not be involved in the hi FGF2-induced effects on chromatin.

Recent reports have shown that p68 functions as a transcription co-activator for p53, a well known tumour suppressor gene which promotes cell death in response to DNA damage; p68 overexpression significantly up-regulated p53-responsive promoter activities, while p68 knockdown prevented p53-dependent apoptosis[169]. Decreased p68 therefore would be expected to oppose or decrease the hi FGF2

induced chromatin compaction and cell death, if both proteins were engaging the p53 pathway. Lack of an effect of p68 on the hi FGF 2-induced chromatin compaction implies that the latter is not likely to engage p53-mediated events.

Hi FGF2 and hsp70. As done for p68, we confirmed that hsp70 is indeed expressed by various cell types in a manner detectable by commercially available antibodies, and proceeded to examine hsp70-hi FGF2 interaction by co-immunoprecipitation. While anti-hsp70, in addition to pulling down its cognate protein, did indeed co-precipitate endogenous hi FGF2 (from HEK293 cells), anti-hi FGF2 antibodies did not seem to co-precipitate hsp70. These findings (similar to those for p68) can be explained if we assume that the hsp70-hi FGF2 interaction requires the N-terminal extension of hi FGF2 and results in masking of epitopes recognized by anti-hi FGF2 antibodies.

Our findings also suggested that hsp70 and p68 are binding to hi FGF2 in a mutually exclusive manner, likely on the same region of the N-terminal extension; immunoprecipitation with anti-p68 brought down endogenous hi FGF2 but not hsp70, and vice versa. The physiological significance of this finding is not clear at present, but it would suggest 'competing' functions between p68 and hsp70 in regards to hi FGF2. Conditions that upregulate hsp70 are linked to cell stress as well as cell survival and would also be expected to increase the proportion of hsp70 bound to hi FGF2, while correspondingly decrease the proportion of p68 (and/or other proteins) bound to hi FGF2. Overexpression of hsp70 was indeed effective in preventing the hi

FGF2-induced chromatin compaction in cardiomyocytes, in agreement with the pro-survival role of hsp70. In addition, this rescue effect correlated with increased nuclear localization of hsp70 (which was mostly cytosolic in the absence of hi FGF2 overexpression), increasing the probability of interaction with nuclear hi FGF2. It is reasonable to hypothesize that an increased interaction of hsp70 with hi FGF2 (an interaction dependent on its N-terminal domain) may prevent hi FGF2 from exerting its detrimental effects within the nucleus, since these effects are also dependent on the N-terminal extension of hi FGF2.

Total as well as nuclear hsp70 levels are known to increase during heat shock and other stresses. In the nucleus hsp70 is reported to stabilize the relative levels of nucleolin, an effect that is beneficial to cardiac myocytes and has been shown to be required for the ability of overexpressed hsp70 to protect these cells from H_2O_2-induced apoptosis[191]. Nucleolin, a relatively abundant protein that is present in the nucleolus as well as other cell sites, exerts its beneficial effects against apoptosis by stabilizing the mRNA for Bcl-2[226]. It is possible that such a mechanism may contribute to the ability of hsp70 overexpression to prevent the hi FGF2 induced chromatin compaction and cell death.

To summarize, we have identified novel interacting partners (p68 RNA helicase and hsp70) specific for hi FGF2, by affinity chromatography, followed by mass spectroscopy analysis, and confirmed their interactions by co-immunoprecipitation studies. At this point our data have not supported a role for p68 RNA helicase in mediating the effects of hi FGF2 on chromatin compaction and

cell death, but further studies are needed to fully explore this issue and the significance of p68-hi FGF2 interaction. On the other hand, hsp70 overexpression did prevent the effects of hi FGF2, in a manner linked to increased nuclear localization of hsp70 and possibly increased interaction with hi FGF2. At this point therefore we propose two possible scenarios by which hsp70 could prevent the effects of hi FGF2. Firstly, hsp70 likely protects and stabilizes nucleolin, which then stabilizes the anti-apoptotic Bcl2. Secondly, by directly binding to hi FGF2 (likely its N-terminal) hsp70 prevents it from exerting its effects on chromatin.

Endogenous hi FGF2 levels and cardiac stress. In previous studies, and also in work discussed in the preceding sections, increased levels of nuclear hi FGF2 were found to cause chromatin compaction and apoptotic cell death, based on *in vitro* models and hi FGF2 overexpression. For these studies to have biological relevance it was important to determine whether endogenous hi FGF2 can also become upregulated under a variety of conditions/stimuli that are known to promote apoptosis.

A variety of bioactive agents including those associated with adrenergic and neurohumoral stimulation are considered to play a causative role in pressure-overload induced cardiac hypertrophy and heart failure, conditions also characterized by enhanced incidence of cell death. In this context, angiotensin II, endothelin 1, as well as isoproterenol are all known to promote cardiac hypertrophy; they are also known to stimulate cardiac FGF2 gene expression in animal models [48] although their effects on FGF2 protein or hi FGF2 accumulation are only marginally studied. Our pilot data,

showing that angiotensin II, endothelin 1 and isoproterenol stimulated hi FGF2 upregulation in primary cardiac non-myocytes, suggest that adverse conditions are indeed linked to increased hi FGF2 and that the latter may play a role in the developing cardiac pathology. Whether endogenous hi FGF2 upregulation is however sufficient to cause cardiac cell death remains to be investigated.

Although cardiac fibroblasts, the major hi FGF2 expressors in cardiac ventricles[227], did show significant hi FGF2 upregulation, it is intriguing that neither angiotensin II, nor endothelin 1 had any effect on ventricular cardiac myocyte hi FGF2 levels, at least in culture. These findings would suggest that endogenous hi FGF2 does not play a role in the induction of cardiomyocyte cell death under adverse conditions. On the other hand, our laboratory has recently demonstrated that hi FGF2 can be secreted by cardiac fibroblasts in response to angiotensin II, and once secreted hi FGF2 can act on cardiac myocytes in a paracrine manner to promote hypertrophy[227]. Others have shown that extracellular hi FGF2 can become internalized by the cell and translocate to the nucleus where it directly affects gene expression [228]. It is therefore hypothetically possible that hi FGF2, externalized by cardiac non-myocytes, can then interact with myocytes, become internalized and accumulate in the nucleus. It would be very interesting to test if this internalized (not endogenous) hi FGF2 can promote cardiomyocyte chromatin compaction and cell death.

A strong relationship between cardiac hi FGF2 levels and exaggerated cardiac hypertrophy, fibrosis and overall pathology was recently reported: Ahmadi and

colleagues showed that transgenic mice defective in eNOS (nitric oxide synthase) expression developed a higher degree of cardiac hypertrophy and fibrosis compared to non-transgenic mice, when subjected to pressure overload hypertrophy; the maladaptive phenotype was further exaggerated in animals fed a high fat diet. Relative cardiac hi FGF2 levels closely correlated with the extent of cardiac morphological as well as functional deterioration [84]. Another example of increased hi FGF2 correlating with cardiac pathology was presented in this thesis: we found that hearts from adriamycin-treated rats (characterized by increased apoptosis, cardiomyocyte and mitochondrial deterioration[229]) had higher levels of hi FGF2 compared to controls.

We did not see a relationship between high glucose and hi FGF2 accumulation (*in vitro*), which would suggest that hyperglycemia, as encountered in diabetes, may not exert its pathological effects on the heart by hi FGF2 increases. In addition, our studies with the mdx mice did not show increased hi FGF2 associated with mdx cardiomyopathy. These are of course pilot studies, and have not taken into account an effect of age or cell type, so more thorough investigations would be required to address the issue of whether hi FGF2 is contributing to the *mdx* or diabetic cardiomyopathy. Taken together, our *in vitro* and animal model pilot studies, however, do support a role for hi FGF2 in some forms of cardiac pathology.

Finally, in collaboration with another PhD student in the lab (Jon-Jon Santiago) we documented, for the first time, the expression of hi FGF2 in human cardiac (atrial) tissue. While studies with isolated rat cardiomyocytes suggested relatively low levels

of endogenous hi FGF2 expression, immunostaining of human atrial tissue for hi FGF2 showed clear cardiomyocyte staining in both the cytosol and the nucleus. In fact, anti-hi FGF2 staining was particularly strong in nuclei that, based on their histological ('blue') staining could be considered as pyknotic. Thus our data from human atrial tissue are consistent with the possibility that endogenous hi FGF2 may play a role in human cardiac cell apoptosis, in diseased tissue. It is appreciated that these are pilot data; however the same pattern was seen in atrial tissue from several patient hearts. Our human ethics approval only allowed us to use atrial tissue discarded during standard cardiac surgery, without any information as to the patient condition or demographics. Future studies will need to determine the relationship between human atrial and ventricular cardiac pathology and apoptosis, to hi FGF2 expression and localization. Access to normal human tissue will also be required, to have some idea of the 'baseline' levels of endogenous hi FGF2 in the human heart. Nevertheless, our studies with human tissues have provided proof of principle that hi FGF2 is present in the human heart and may play a role in cardiac cell death, as was shown by the *in vitro* data.

In conclusion, we have shown that, at least *in vitro*, hi FGF2 overexpression leads to chromatin compaction and apoptosis that are linked to sustained ERK ½ activation, and release of cytochrome C from mitochondria. We have also shown that signals that can raise relative levels of the anti-apoptotic Bcl-2 protein, such as Bcl-2 overexpression, the nuclear Akt-PIM-1 pathway, or hsp70 action, can also prevent the

effects of hi FGF2. In my Master project, we provided evidence that the hi FGF2 induced nuclear compaction and cell death requires nuclear accumulation of hi FGF2, ERK activation and bax translocation and is linked to caspase 3 activation. Figure 33 illustrates a hypothetical scheme linking all identified signals.

There is very little information in the literature as to actual levels in sub-cellular / nuclear subcompartments and the role of endogenous hi FGF2 under pathological conditions. As cellular hi FGF2 is reported to be upregulated in response to various stress stimuli, and as prolonged tissue stress and dysfunction are accompanied by apoptotic cell death (as in heart failure, for example), endogenous hi FGF2 may play a role in this process. This notion is further strengthened by our studies, discussed in the preceding paragraph, showing that a number of stimuli linked to cardiac pathology can also upregulate endogenous hi FGF2, and that hi FGF2 is present within cardiomyocytes in the human heart, in apparent association with pyknotic nuclei. As the image for these pyknotic nuclei from tissue resemble the effects of overexpressed hi FGF2 in the nuclei of cells in culture, this work supports the notion that endogenous hi FGF2 may act in a manner similar to overexpressed hi FGF2 to promote chromatin compaction and cell death. It follows that processes related to hi FGF2 upregulation, hi FGF2-nuclear protein interactions, and the mechanism of hi FGF2-induced cell death represent potential therapeutic targets for preventing cell death.

CHAPTER 5

REFERENCES

1. Thomas, K.A., *Fibroblast growth factors.* FASEB J, 1987. **1**(6): p. 434-40.
2. Yu, P.J., et al., *Basic fibroblast growth factor (FGF-2): the high molecular weight forms come of age.* J Cell Biochem, 2007. **100**(5): p. 1100-8.
3. Chlebova, K., et al., *High molecular weight FGF2: the biology of a nuclear growth factor.* Cell Mol Life Sci, 2009. **66**(2): p. 225-35.
4. Kim, H.S., *Assignment1 of the human basic fibroblast growth factor gene FGF2 to chromosome 4 band q26 by radiation hybrid mapping.* Cytogenet Cell Genet, 1998. **83**(1-2): p. 73.
5. Shibata, F., A. Baird, and R.Z. Florkiewicz, *Functional characterization of the human basic fibroblast growth factor gene promoter.* Growth Factors, 1991. **4**(4): p. 277-87.
6. Pasumarthi, K.B., Y. Jin, and P.A. Cattini, *Cloning of the rat fibroblast growth factor-2 promoter region and its response to mitogenic stimuli in glioma C6 cells.* J Neurochem, 1997. **68**(3): p. 898-908.
7. Jin, Y., et al., *Role for early growth response-1 protein in alpha(1)-adrenergic stimulation of fibroblast growth factor-2 promoter activity in cardiac myocytes.* Mol Pharmacol, 2000. **57**(5): p. 984-90.
8. Tang, W., et al., *Involvement of Sp1 binding sequences in basal transcription of the rat fibroblast growth factor-2 gene in neonatal cardiomyocytes.* Life Sci, 2009. **84**(13-14): p. 421-7.
9. Urbich, C., et al., *HDAC5 is a repressor of angiogenesis and determines the angiogenic gene expression pattern of endothelial cells.* Blood, 2009. **113**(22): p. 5669-79.
10. Jimenez, S.K., et al., *Transcriptional regulation of FGF-2 gene expression in cardiac myocytes.* Cardiovascular Research, 2004. **62**(3): p. 548-57.
11. Zhang, S.C., et al., *Alternative splicing and differential subcellular localization of the rat FGF antisense gene product.* BMC Mol Biol, 2008. **9**: p. 10.
12. Zhang, S.C., et al., *Alternative splicing of the FGF antisense gene: differential subcellular localization in human tissues and esophageal adenocarcinoma.* J Mol Med, 2007. **85**(11): p. 1215-28.
13. MacFarlane, L.A., et al., *Regulation of fibroblast growth factor-2 by an endogenous antisense RNA and by argonaute-2.* Mol Endocrinol, 2010. **24**(4): p. 800-12.
14. Bost, L.M. and L.M. Hjelmeland, *Cell density regulates differential production of bFGF transcripts.* Growth Factors, 1993. **9**(3): p. 195-203.
15. Touriol, C., et al., *Expression of human fibroblast growth factor 2 mRNA is post-transcriptionally controlled by a unique destabilizing element present in the 3'-untranslated region between alternative polyadenylation sites.* J Biol Chem, 1999. **274**(30): p. 21402-8.

16. Touriol, C., et al., *Alternative translation initiation of human fibroblast growth factor 2 mRNA controlled by its 3'-untranslated region involves a Poly(A) switch and a translational enhancer.* J Biol Chem, 2000. **275**(25): p. 19361-7.
17. Arnaud, E., et al., *A new 34-kilodalton isoform of human fibroblast growth factor 2 is cap dependently synthesized by using a non-AUG start codon and behaves as a survival factor.* Mol Cell Biol, 1999. **19**(1): p. 505-14.
18. Vagner, S., et al., *Alternative translation of human fibroblast growth factor 2 mRNA occurs by internal entry of ribosomes.* Mol Cell Biol, 1995. **15**(1): p. 35-44.
19. Bonnal, S., et al., *A single internal ribosome entry site containing a G quartet RNA structure drives fibroblast growth factor 2 gene expression at four alternative translation initiation codons.* J Biol Chem, 2003. **278**(41): p. 39330-6.
20. Bonnal, S., et al., *Heterogeneous nuclear ribonucleoprotein A1 is a novel internal ribosome entry site trans-acting factor that modulates alternative initiation of translation of the fibroblast growth factor 2 mRNA.* J Biol Chem, 2005. **280**(6): p. 4144-53.
21. Pintucci, G., N. Quarto, and D.B. Rifkin, *Methylation of high molecular weight fibroblast growth factor-2 determines post-translational increases in molecular weight and affects its intracellular distribution.* Mol Biol Cell, 1996. **7**(8): p. 1249-58.
22. Bruns, A.F., C. Grothe, and P. Claus, *Fibroblast growth factor 2 (FGF-2) is a novel substrate for arginine methylation by PRMT5.* Biol Chem, 2009. **390**(1): p. 59-65.
23. Yu, P.J., et al., *Thrombin cleaves the high molecular weight forms of basic fibroblast growth factor (FGF-2): a novel mechanism for the control of FGF-2 and thrombin activity.* Oncogene, 2008. **27**(18): p. 2594-601.
24. Kardami, E., et al., *Fibroblast growth factor-2 and cardioprotection.* Heart Fail Rev, 2007. **12**(3-4): p. 267-77.
25. Feige, J.J. and A. Baird, *Basic fibroblast growth factor is a substrate for protein phosphorylation and is phosphorylated by capillary endothelial cells in culture.* Proc Natl Acad Sci U S A, 1989. **86**(9): p. 3174-8.
26. Vilgrain, I., A.M. Gonzalez, and A. Baird, *Phosphorylation of basic fibroblast growth factor (FGF-2) in the nuclei of SK-Hep-1 cells.* FEBS Lett, 1993. **331**(3): p. 228-32.
27. Vilgrain, I. and A. Baird, *Phosphorylation of basic fibroblast growth factor by a protein kinase associated with the outer surface of a target cell.* Mol Endocrinol, 1991. **5**(7): p. 1003-12.
28. Santiago, J.J., et al., *Cardiac fibroblast to myofibroblast differentiation in vivo and in vitro: expression of focal adhesion components in neonatal and adult rat ventricular myofibroblasts.* Dev Dyn, 2010. **239**(6): p. 1573-84.
29. Quarto, N., F.P. Finger, and D.B. Rifkin, *The NH2-terminal extension of high molecular weight bFGF is a nuclear targeting signal.* J Cell Physiol, 1991. **147**(2): p. 311-8.
30. Rifkin, D.B., et al., *Studies on FGF-2: nuclear localization and function of high molecular weight forms and receptor binding in the absence of heparin.* Mol Reprod Dev, 1994. **39**(1): p. 102-4; discussion 104-5.
31. Dono, R., D. James, and R. Zeller, *A GR-motif functions in nuclear accumulation of the large FGF-2 isoforms and interferes with mitogenic signalling.* Oncogene, 1998. **16**(16): p. 2151-8.
32. Tessler, S. and G. Neufeld, *Basic fibroblast growth factor accumulates in the nuclei of various bFGF-producing cell types.* J Cell Physiol, 1990. **145**(2): p. 310-7.
33. Foletti, A., F. Vuadens, and F. Beermann, *Nuclear localization of mouse fibroblast growth*

factor 2 requires N-terminal and C-terminal sequences. Cell Mol Life Sci, 2003. **60**(10): p. 2254-65.

34. Bugler, B., F. Amalric, and H. Prats, *Alternative initiation of translation determines cytoplasmic or nuclear localization of basic fibroblast growth factor.* Mol Cell Biol, 1991. **11**(1): p. 573-7.
35. Sheng, Z., J.A. Lewis, and W.J. Chirico, *Nuclear and nucleolar localization of 18-kDa fibroblast growth factor-2 is controlled by C-terminal signals.* J Biol Chem, 2004. **279**(38): p. 40153-60.
36. Claus, P., et al., *Differential intranuclear localization of fibroblast growth factor-2 isoforms and specific interaction with the survival of motoneuron protein.* J Biol Chem, 2003. **278**(1): p. 479-85.
37. Yoon, J.H. and R. Parker, *Coil-in-to snRNP assembly and Cajal bodies.* Nat Struct Mol Biol, 2010. **17**(4): p. 391-3.
38. Matera, A.G., *Cajal bodies.* Curr Biol, 2003. **13**(13): p. R503.
39. Hannan, R.D., et al., *Cardiac hypertrophy: a matter of translation.* Clin Exp Pharmacol Physiol, 2003. **30**(8): p. 517-27.
40. Kawamoto, A., et al., *Serum levels of VEGF and basic FGF in the subacute phase of myocardial infarction.* Int J Cardiol, 1998. **67**(1): p. 47-54.
41. Mignatti, P., T. Morimoto, and D.B. Rifkin, *Basic fibroblast growth factor, a protein devoid of secretory signal sequence, is released by cells via a pathway independent of the endoplasmic reticulum-Golgi complex.* J Cell Physiol, 1992. **151**(1): p. 81-93.
42. Florkiewicz, R.Z., J. Anchin, and A. Baird, *The inhibition of fibroblast growth factor-2 export by cardenolides implies a novel function for the catalytic subunit of Na+,K+-ATPase.* J Biol Chem, 1998. **273**(1): p. 544-51.
43. Szebenyi, G. and J.F. Fallon, *Fibroblast growth factors as multifunctional signaling factors.* Int Rev Cytol, 1999. **185**: p. 45-106.
44. Chu, C.L., J.A. Buczek-Thomas, and M.A. Nugent, *Heparan sulphate proteoglycans modulate fibroblast growth factor-2 binding through a lipid raft-mediated mechanism.* Biochem J, 2004. **379**(Pt 2): p. 331-41.
45. Detillieux, K.A., et al., *Biological activities of fibroblast growth factor-2 in the adult myocardium.* Cardiovascular Research, 2003. **57**(1): p. 8-19.
46. Maher, P.A., *Nuclear Translocation of fibroblast growth factor (FGF) receptors in response to FGF-2.* J Cell Biol, 1996. **134**(2): p. 529-36.
47. Reilly, J.F. and P.A. Maher, *Importin beta-mediated nuclear import of fibroblast growth factor receptor: role in cell proliferation.* J Cell Biol, 2001. **152**(6): p. 1307-12.
48. Kardami, E., et al., *Fibroblast growth factor 2 isoforms and cardiac hypertrophy.* Cardiovascular Research, 2004. **63**(3): p. 458-66.
49. Bossard, C., et al., *Translokin is an intracellular mediator of FGF-2 trafficking.* Nat Cell Biol, 2003. **5**(5): p. 433-9.
50. Brandenburger, Y., et al., *Increased expression of UBF is a critical determinant for rRNA synthesis and hypertrophic growth of cardiac myocytes.* FASEB J, 2001. **15**(11): p. 2051-3.
51. Delrieu, I., *The high molecular weight isoforms of basic fibroblast growth factor (FGF-2): an insight into an intracrine mechanism.* FEBS Lett, 2000. **468**(1): p. 6-10.
52. Bikfalvi, A., et al., *Differential modulation of cell phenotype by different molecular weight*

forms of basic fibroblast growth factor: possible intracellular signaling by the high molecular weight forms. J Cell Biol, 1995. **129**(1): p. 233-43.

53. Delrieu, I., et al., *Overexpression of the FGF-2 24-kDa isoform up-regulates IL-6 transcription in NIH-3T3 cells.* FEBS Lett, 1998. **436**(1): p. 17-22.
54. Dini, G., et al., *Overexpression of the 18 kDa and 22/24 kDa FGF-2 isoforms results in differential drug resistance and amplification potential.* J Cell Physiol, 2002. **193**(1): p. 64-72.
55. Cohen-Jonathan, E., et al., *Radioresistance induced by the high molecular forms of the basic fibroblast growth factor is associated with an increased G2 delay and a hyperphosphorylation of p34CDC2 in HeLa cells.* Cancer Res, 1997. **57**(7): p. 1364-70.
56. Lemiere, S., et al., *Overexpression of high molecular weight FGF-2 forms inhibits glioma growth by acting on cell-cycle progression and protein translation.* Exp Cell Res, 2008. **314**(20): p. 3701-11.
57. Hirst, C.J., et al., *High levels of CUG-initiated FGF-2 expression cause chromatin compaction, decreased cardiomyocyte mitosis, and cell death.* Mol Cell Biochem, 2003. **246**(1-2): p. 111-6.
58. Ma, X., et al., *Chromatin compaction and cell death by high molecular weight FGF-2 depend on its nuclear localization, intracrine ERK activation, and engagement of mitochondria.* J Cell Physiol, 2007. **213**(3): p. 690-8.
59. Grothe, C., et al., *Over-expression of the 18 kD and 21/23 kD fibroblast growth factor-2 isoforms in PC12 cells and Schwann cells results in altered cell morphology and growth.* Brain Res Mol Brain Res, 1998. **57**(1): p. 97-105.
60. Quarto, N., K.D. Fong, and M.T. Longaker, *Gene profiling of cells expressing different FGF-2 forms.* Gene, 2005. **356**: p. 49-68.
61. Piotrowicz, R.S., P.A. Maher, and E.G. Levin, *Dual activities of 22-24 kDA basic fibroblast growth factor: inhibition of migration and stimulation of proliferation.* J Cell Physiol, 1999. **178**(2): p. 144-53.
62. Piotrowicz, R.S., et al., *Inhibition of cell migration by 24-kDa fibroblast growth factor-2 is dependent upon the estrogen receptor.* J Biol Chem, 2001. **276**(6): p. 3963-70.
63. Ding, L., et al., *Inhibition of cell migration and angiogenesis by the amino-terminal fragment of 24kD basic fibroblast growth factor.* J Biol Chem, 2002. **277**(34): p. 31056-61.
64. Zhou, M., et al., *Fibroblast growth factor 2 control of vascular tone.* Nat Med, 1998. **4**(2): p. 201-7.
65. Chen, K., et al., *Decrease in excitatory neurons, astrocytes and proliferating progenitors in the cerebral cortex of mice lacking exon 3 from the Fgf2 gene.* BMC Neurosci, 2008. **9**: p. 94.
66. Azhar, M., et al., *Gene targeted ablation of high molecular weight fibroblast growth factor-2.* Dev Dyn, 2009. **238**(2): p. 351-7.
67. Garmy-Susini, B., et al., *Role of fibroblast growth factor-2 isoforms in the effect of estradiol on endothelial cell migration and proliferation.* Circ Res, 2004. **94**(10): p. 1301-9.
68. Liao, S., et al., *The cardioprotective effect of the low molecular weight isoform of fibroblast growth factor-2: the role of JNK signaling.* J Mol Cell Cardiol, 2007. **42**(1): p. 106-20.
69. Liao, S., et al., *The influence of FGF2 high molecular weight (HMW) isoforms in the development of cardiac ischemia-reperfusion injury.* J Mol Cell Cardiol, 2010. **48**(6): p. 1245-54.
70. Okada-Ban, M., et al., *Nuclear 24 kD fibroblast growth factor (FGF)-2 confers metastatic properties on rat bladder carcinoma cells.* Oncogene, 1999. **18**(48): p. 6719-24.

71. Haastert, K., et al., *Differentially promoted peripheral nerve regeneration by grafted Schwann cells over-expressing different FGF-2 isoforms.* Neurobiol Dis, 2006. **21**(1): p. 138-53.
72. Van den Berghe, L., et al., *FIF [fibroblast growth factor-2 (FGF-2)-interacting-factor], a nuclear putatively antiapoptotic factor, interacts specifically with FGF-2.* Mol Endocrinol, 2000. **14**(11): p. 1709-24.
73. Tewari, M., et al., *AAC-11, a novel cDNA that inhibits apoptosis after growth factor withdrawal.* Cancer Res, 1997. **57**(18): p. 4063-9.
74. Kim, J.W., et al., *AAC-11 overexpression induces invasion and protects cervical cancer cells from apoptosis.* Lab Invest, 2000. **80**(4): p. 587-94.
75. Burghes, A.H. and C.E. Beattie, *Spinal muscular atrophy: why do low levels of survival motor neuron protein make motor neurons sick?* Nat Rev Neurosci, 2009. **10**(8): p. 597-609.
76. Gringel, S., et al., *Nuclear fibroblast growth factor-2 interacts specifically with splicing factor SF3a66.* Biol Chem, 2004. **385**(12): p. 1203-8.
77. Padua, R.R., et al., *Basic fibroblast growth factor is cardioprotective in ischemia-reperfusion injury.* Mol Cell Biochem, 1995. **143**(2): p. 129-35.
78. Padua, R.R., et al., *FGF-2-induced negative inotropism and cardioprotection are inhibited by chelerythrine: involvement of sarcolemmal calcium-independent protein kinase C.* J Mol Cell Cardiol, 1998. **30**(12): p. 2695-709.
79. Jiang, Z.S., et al., *Non-angiogenic FGF-2 protects the ischemic heart from injury, in the presence or absence of reperfusion.* Cardiovascular Research, 2004. **62**(1): p. 154-66.
80. Jiang, Z.S., et al., *Acute protection of ischemic heart by FGF-2: involvement of FGF-2 receptors and protein kinase C.* Am J Physiol Heart Circ Physiol, 2002. **282**(3): p. H1071-80.
81. Jiang, Z.S., et al., *High molecular weight FGF-2 promotes postconditioning-like cardioprotection linked to activation of protein kinase C isoforms, as well as Akt and p70 S6 kinases. [corrected].* Can J Physiol Pharmacol, 2009. **87**(10): p. 798-804.
82. Jiang, Z.S., et al., *High- but not low-molecular weight FGF-2 causes cardiac hypertrophy in vivo; possible involvement of cardiotrophin-1.* J Mol Cell Cardiol, 2007. **42**(1): p. 222-33.
83. Padua, R.R. and E. Kardami, *Increased basic fibroblast growth factor (bFGF) accumulation and distinct patterns of localization in isoproterenol-induced cardiomyocyte injury.* Growth Factors, 1993. **8**(4): p. 291-306.
84. Ahmadie, R., et al., *A high-lipid diet potentiates left ventricular dysfunction in nitric oxide synthase 3-deficient mice after chronic pressure overload.* J Nutr, 2010. **140**(8): p. 1438-44.
85. Pasumarthi, K.B., et al., *Over-expression of CUG- or AUG-initiated forms of basic fibroblast growth factor in cardiac myocytes results in similar effects on mitosis and protein synthesis but distinct nuclear morphologies.* J Mol Cell Cardiol, 1994. **26**(8): p. 1045-60.
86. Sun, G., et al., *CUG-initiated FGF-2 induces chromatin compaction in cultured cardiac myocytes and in vitro.* J Cell Physiol, 2001. **186**(3): p. 457-67.
87. Berking, C., et al., *Basic fibroblast growth factor and ultraviolet B transform melanocytes in human skin.* Am J Pathol, 2001. **158**(3): p. 943-53.
88. Kerr, J.F., A.H. Wyllie, and A.R. Currie, *Apoptosis: a basic biological phenomenon with wide-ranging implications in tissue kinetics.* Br J Cancer, 1972. **26**(4): p. 239-57.
89. Elmore, S., *Apoptosis: a review of programmed cell death.* Toxicol Pathol, 2007. **35**(4): p. 495-516.
90. Horvitz, H.R., *Genetic control of programmed cell death in the nematode Caenorhabditis*

elegans. Cancer Res, 1999. **59**(7 Suppl): p. 1701s-1706s.
91. Formigli, L., et al., *Aponecrosis: morphological and biochemical exploration of a syncretic process of cell death sharing apoptosis and necrosis.* J Cell Physiol, 2000. **182**(1): p. 41-9.
92. Sperandio, S., I. de Belle, and D.E. Bredesen, *An alternative, nonapoptotic form of programmed cell death.* Proc Natl Acad Sci U S A, 2000. **97**(26): p. 14376-81.
93. Debnath, J., E.H. Baehrecke, and G. Kroemer, *Does autophagy contribute to cell death?* Autophagy, 2005. **1**(2): p. 66-74.
94. Mazarakis, N.D., A.D. Edwards, and H. Mehmet, *Apoptosis in neural development and disease.* Arch Dis Child Fetal Neonatal Ed, 1997. **77**(3): p. F165-70.
95. Hengartner, M.O., *The biochemistry of apoptosis.* Nature, 2000. **407**(6805): p. 770-6.
96. Bratton, D.L., et al., *Appearance of phosphatidylserine on apoptotic cells requires calcium-mediated nonspecific flip-flop and is enhanced by loss of the aminophospholipid translocase.* J Biol Chem, 1997. **272**(42): p. 26159-65.
97. Arur, S., et al., *Annexin I is an endogenous ligand that mediates apoptotic cell engulfment.* Dev Cell, 2003. **4**(4): p. 587-98.
98. Reutelingsperger, C.P. and W.L. van Heerde, *Annexin V, the regulator of phosphatidylserine-catalyzed inflammation and coagulation during apoptosis.* Cell Mol Life Sci, 1997. **53**(6): p. 527-32.
99. Gardai, S.J., et al., *Cell-surface calreticulin initiates clearance of viable or apoptotic cells through trans-activation of LRP on the phagocyte.* Cell, 2005. **123**(2): p. 321-34.
100. Papaliagkas, V., et al., *The proteins and the mechanisms of apoptosis: a mini-review of the fundamentals.* Hippokratia, 2007. **11**(3): p. 108-13.
101. Igney, F.H. and P.H. Krammer, *Death and anti-death: tumour resistance to apoptosis.* Nat Rev Cancer, 2002. **2**(4): p. 277-88.
102. Liu, X., et al., *Induction of apoptotic program in cell-free extracts: requirement for dATP and cytochrome c.* Cell, 1996. **86**(1): p. 147-57.
103. Wajant, H., *The Fas signaling pathway: more than a paradigm.* Science, 2002. **296**(5573): p. 1635-6.
104. Kischkel, F.C., et al., *Cytotoxicity-dependent APO-1 (Fas/CD95)-associated proteins form a death-inducing signaling complex (DISC) with the receptor.* EMBO J, 1995. **14**(22): p. 5579-88.
105. Wang, C. and R.J. Youle, *The role of mitochondria in apoptosis*.* Annu Rev Genet, 2009. **43**: p. 95-118.
106. Kluck, R.M., et al., *The release of cytochrome c from mitochondria: a primary site for Bcl-2 regulation of apoptosis.* Science, 1997. **275**(5303): p. 1132-6.
107. Saelens, X., et al., *Toxic proteins released from mitochondria in cell death.* Oncogene, 2004. **23**(16): p. 2861-74.
108. Slee, E.A., C. Adrain, and S.J. Martin, *Executioner caspase-3, -6, and -7 perform distinct, non-redundant roles during the demolition phase of apoptosis.* J Biol Chem, 2001. **276**(10): p. 7320-6.
109. Zhang, B., et al., *Partitioning apoptosis: a novel form of the execution phase of apoptosis.* Apoptosis, 2005. **10**(1): p. 219-31.
110. Sakahira, H., M. Enari, and S. Nagata, *Cleavage of CAD inhibitor in CAD activation and DNA degradation during apoptosis.* Nature, 1998. **391**(6662): p. 96-9.

111. Kothakota, S., et al., *Caspase-3-generated fragment of gelsolin: effector of morphological change in apoptosis.* Science, 1997. **278**(5336): p. 294-8.
112. Hao, Z., et al., *Specific ablation of the apoptotic functions of cytochrome C reveals a differential requirement for cytochrome C and Apaf-1 in apoptosis.* Cell, 2005. **121**(4): p. 579-91.
113. Hockenbery, D., et al., *Bcl-2 is an inner mitochondrial membrane protein that blocks programmed cell death.* Nature, 1990. **348**(6299): p. 334-6.
114. Patel, M.P., et al., *Targeting the Bcl-2.* Curr Opin Oncol, 2009. **21**(6): p. 516-23.
115. Cory, S. and J.M. Adams, *The Bcl2 family: regulators of the cellular life-or-death switch.* Nat Rev Cancer, 2002. **2**(9): p. 647-56.
116. Wei, M.C., et al., *Proapoptotic BAX and BAK: a requisite gateway to mitochondrial dysfunction and death.* Science, 2001. **292**(5517): p. 727-30.
117. Zong, W.X., et al., *BH3-only proteins that bind pro-survival Bcl-2 family members fail to induce apoptosis in the absence of Bax and Bak.* Genes Dev, 2001. **15**(12): p. 1481-6.
118. Willis, S.N., et al., *Apoptosis initiated when BH3 ligands engage multiple Bcl-2 homologs, not Bax or Bak.* Science, 2007. **315**(5813): p. 856-9.
119. Kim, H., et al., *Hierarchical regulation of mitochondrion-dependent apoptosis by BCL-2 subfamilies.* Nat Cell Biol, 2006. **8**(12): p. 1348-58.
120. Muchmore, S.W., et al., *X-ray and NMR structure of human Bcl-xL, an inhibitor of programmed cell death.* Nature, 1996. **381**(6580): p. 335-41.
121. Kuwana, T., et al., *Bid, Bax, and lipids cooperate to form supramolecular openings in the outer mitochondrial membrane.* Cell, 2002. **111**(3): p. 331-42.
122. Amaravadi, R. and C.B. Thompson, *The survival kinases Akt and Pim as potential pharmacological targets.* J Clin Invest, 2005. **115**(10): p. 2618-24.
123. Wendel, H.G., et al., *Survival signalling by Akt and eIF4E in oncogenesis and cancer therapy.* Nature, 2004. **428**(6980): p. 332-7.
124. Miyamoto, S., M. Rubio, and M.A. Sussman, *Nuclear and mitochondrial signalling Akts in cardiomyocytes.* Cardiovascular Research, 2009. **82**(2): p. 272-85.
125. Datta, S.R., et al., *Akt phosphorylation of BAD couples survival signals to the cell-intrinsic death machinery.* Cell, 1997. **91**(2): p. 231-41.
126. Brunet, A., et al., *Protein kinase SGK mediates survival signals by phosphorylating the forkhead transcription factor FKHRL1 (FOXO3a).* Mol Cell Biol, 2001. **21**(3): p. 952-65.
127. Kane, L.P., et al., *Akt-dependent phosphorylation specifically regulates Cot induction of NF-kappa B-dependent transcription.* Mol Cell Biol, 2002. **22**(16): p. 5962-74.
128. Mayo, L.D. and D.B. Donner, *A phosphatidylinositol 3-kinase/Akt pathway promotes translocation of Mdm2 from the cytoplasm to the nucleus.* Proc Natl Acad Sci U S A, 2001. **98**(20): p. 11598-603.
129. Cardone, M.H., et al., *Regulation of cell death protease caspase-9 by phosphorylation.* Science, 1998. **282**(5392): p. 1318-21.
130. Kops, G.J., et al., *Direct control of the Forkhead transcription factor AFX by protein kinase B.* Nature, 1999. **398**(6728): p. 630-4.
131. Muraski, J.A., et al., *Pim-1 regulates cardiomyocyte survival downstream of Akt.* Nat Med, 2007. **13**(12): p. 1467-75.
132. Fischer, K.M., et al., *Enhancement of myocardial regeneration through genetic engineering of*

cardiac progenitor cells expressing Pim-1 kinase. Circulation, 2009. **120**(21): p. 2077-87.
133. Krishnan, N., et al., *Prolactin-regulated pim-1 transcription: identification of critical promoter elements and Akt signaling.* Endocrine, 2003. **20**(1-2): p. 123-30.
134. Borillo, G.A., et al., *Pim-1 kinase protects mitochondrial integrity in cardiomyocytes.* Circ Res, 2010. **106**(7): p. 1265-74.
135. Fisher, S.A., B.L. Langille, and D. Srivastava, *Apoptosis during cardiovascular development.* Circ Res, 2000. **87**(10): p. 856-64.
136. Soonpaa, M.H. and L.J. Field, *Survey of studies examining mammalian cardiomyocyte DNA synthesis.* Circ Res, 1998. **83**(1): p. 15-26.
137. Dorn, G.W., 2nd, *Apoptotic and non-apoptotic programmed cardiomyocyte death in ventricular remodelling.* Cardiovascular Research, 2009. **81**(3): p. 465-73.
138. Olivetti, G., et al., *Apoptosis in the failing human heart.* N Engl J Med, 1997. **336**(16): p. 1131-41.
139. Narula, J., et al., *Mechanisms of disease: apoptosis in heart failure--seeing hope in death.* Nat Clin Pract Cardiovasc Med, 2006. **3**(12): p. 681-8.
140. Narula, J., et al., *Apoptosis and the systolic dysfunction in congestive heart failure. Story of apoptosis interruptus and zombie myocytes.* Cardiol Clin, 2001. **19**(1): p. 113-26.
141. Cagnol, S. and J.C. Chambard, *ERK and cell death: mechanisms of ERK-induced cell death--apoptosis, autophagy and senescence.* FEBS J, 2010. **277**(1): p. 2-21.
142. Chang, F., et al., *Signal transduction mediated by the Ras/Raf/MEK/ERK pathway from cytokine receptors to transcription factors: potential targeting for therapeutic intervention.* Leukemia, 2003. **17**(7): p. 1263-93.
143. Ramos, J.W., *The regulation of extracellular signal-regulated kinase (ERK) in mammalian cells.* Int J Biochem Cell Biol, 2008. **40**(12): p. 2707-19.
144. Murphy, L.O. and J. Blenis, *MAPK signal specificity: the right place at the right time.* Trends Biochem Sci, 2006. **31**(5): p. 268-75.
145. Blagosklonny, M.V., et al., *Taxol-induced apoptosis and phosphorylation of Bcl-2 protein involves c-Raf-1 and represents a novel c-Raf-1 signal transduction pathway.* Cancer Res, 1996. **56**(8): p. 1851-4.
146. Watabe, M., et al., *The cooperative interaction of two different signaling pathways in response to bufalin induces apoptosis in human leukemia U937 cells.* J Biol Chem, 1996. **271**(24): p. 14067-72.
147. Cagnol, S., E. Van Obberghen-Schilling, and J.C. Chambard, *Prolonged activation of ERK1,2 induces FADD-independent caspase 8 activation and cell death.* Apoptosis, 2006. **11**(3): p. 337-46.
148. Nowak, G., *Protein kinase C-alpha and ERK1/2 mediate mitochondrial dysfunction, decreases in active Na+ transport, and cisplatin-induced apoptosis in renal cells.* J Biol Chem, 2002. **277**(45): p. 43377-88.
149. Brown, L. and S. Benchimol, *The involvement of MAPK signaling pathways in determining the cellular response to p53 activation: cell cycle arrest or apoptosis.* J Biol Chem, 2006. **281**(7): p. 3832-40.
150. Zheng, A., A. Kallio, and P. Harkonen, *Tamoxifen-induced rapid death of MCF-7 breast cancer cells is mediated via extracellularly signal-regulated kinase signaling and can be abrogated by estrogen.* Endocrinology, 2007. **148**(6): p. 2764-77.

151. Matsunaga, Y., et al., *Involvement of activation of NADPH oxidase and extracellular signal-regulated kinase (ERK) in renal cell injury induced by zinc.* J Toxicol Sci, 2005. **30**(2): p. 135-44.
152. Kohda, Y., et al., *Involvement of Raf-1/MEK/ERK1/2 signaling pathway in zinc-induced injury in rat renal cortical slices.* J Toxicol Sci, 2006. **31**(3): p. 207-17.
153. She, Q.B., N. Chen, and Z. Dong, *ERKs and p38 kinase phosphorylate p53 protein at serine 15 in response to UV radiation.* J Biol Chem, 2000. **275**(27): p. 20444-9.
154. Yeh, P.Y., et al., *Phosphorylation of p53 on Thr55 by ERK2 is necessary for doxorubicin-induced p53 activation and cell death.* Oncogene, 2004. **23**(20): p. 3580-8.
155. Kohda, Y., J. Hiramatsu, and M. Gemba, *Involvement of MEK/ERK pathway in cephaloridine-induced injury in rat renal cortical slices.* Toxicol Lett, 2003. **143**(2): p. 185-94.
156. Ozben, B., et al., *Acute anterior myocardial infarction after chemotherapy for testicular seminoma in a young patient.* Clin Appl Thromb Hemost, 2007. **13**(4): p. 439-42.
157. Chen, X.L. and C. Kunsch, *Induction of cytoprotective genes through Nrf2/antioxidant response element pathway: a new therapeutic approach for the treatment of inflammatory diseases.* Curr Pharm Des, 2004. **10**(8): p. 879-91.
158. Arany, I., et al., *Cisplatin-induced cell death is EGFR/src/ERK signaling dependent in mouse proximal tubule cells.* Am J Physiol Renal Physiol, 2004. **287**(3): p. F543-9.
159. Hoyos, B., et al., *Activation of c-Raf kinase by ultraviolet light. Regulation by retinoids.* J Biol Chem, 2002. **277**(26): p. 23949-57.
160. Owens, D.M. and S.M. Keyse, *Differential regulation of MAP kinase signalling by dual-specificity protein phosphatases.* Oncogene, 2007. **26**(22): p. 3203-13.
161. Kondoh, K. and E. Nishida, *Regulation of MAP kinases by MAP kinase phosphatases.* Biochim Biophys Acta, 2007. **1773**(8): p. 1227-37.
162. Wu, W., et al., *Glucocorticoid receptor-induced MAPK phosphatase-1 (MPK-1) expression inhibits paclitaxel-associated MAPK activation and contributes to breast cancer cell survival.* J Biol Chem, 2005. **280**(6): p. 4117-24.
163. Ford, M.J., I.A. Anton, and D.P. Lane, *Nuclear protein with sequence homology to translation initiation factor eIF-4A.* Nature, 1988. **332**(6166): p. 736-8.
164. Hirling, H., et al., *RNA helicase activity associated with the human p68 protein.* Nature, 1989. **339**(6225): p. 562-4.
165. Fuller-Pace, F.V. and S. Ali, *The DEAD box RNA helicases p68 (Ddx5) and p72 (Ddx17): novel transcriptional co-regulators.* Biochem Soc Trans, 2008. **36**(Pt 4): p. 609-12.
166. Endoh, H., et al., *Purification and identification of p68 RNA helicase acting as a transcriptional coactivator specific for the activation function 1 of human estrogen receptor alpha.* Mol Cell Biol, 1999. **19**(8): p. 5363-72.
167. Fuller-Pace, F.V., *DExD/H box RNA helicases: multifunctional proteins with important roles in transcriptional regulation.* Nucleic Acids Res, 2006. **34**(15): p. 4206-15.
168. Watanabe, M., et al., *A subfamily of RNA-binding DEAD-box proteins acts as an estrogen receptor alpha coactivator through the N-terminal activation domain (AF-1) with an RNA coactivator, SRA.* EMBO J, 2001. **20**(6): p. 1341-52.
169. Bates, G.J., et al., *The DEAD box protein p68: a novel transcriptional coactivator of the p53 tumour suppressor.* EMBO J, 2005. **24**(3): p. 543-53.

170. Smith, N.D., et al., *The p53 tumor suppressor gene and nuclear protein: basic science review and relevance in the management of bladder cancer.* J Urol, 2003. **169**(4): p. 1219-28.
171. Suzuki, H.I., et al., *Modulation of microRNA processing by p53.* Nature, 2009. **460**(7254): p. 529-33.
172. Wilson, B.J., et al., *The p68 and p72 DEAD box RNA helicases interact with HDAC1 and repress transcription in a promoter-specific manner.* BMC Mol Biol, 2004. **5**: p. 11.
173. Ogilvie, V.C., et al., *The highly related DEAD box RNA helicases p68 and p72 exist as heterodimers in cells.* Nucleic Acids Res, 2003. **31**(5): p. 1470-80.
174. Evans, C.G., L. Chang, and J.E. Gestwicki, *Heat shock protein 70 (hsp70) as an emerging drug target.* J Med Chem, 2010. **53**(12): p. 4585-602.
175. Mayer, M.P. and B. Bukau, *Hsp70 chaperones: cellular functions and molecular mechanism.* Cell Mol Life Sci, 2005. **62**(6): p. 670-84.
176. Morano, K.A., *New tricks for an old dog: the evolving world of Hsp70.* Ann N Y Acad Sci, 2007. **1113**: p. 1-14.
177. Bork, P., C. Sander, and A. Valencia, *An ATPase domain common to prokaryotic cell cycle proteins, sugar kinases, actin, and hsp70 heat shock proteins.* Proc Natl Acad Sci U S A, 1992. **89**(16): p. 7290-4.
178. Zhu, X., et al., *Structural analysis of substrate binding by the molecular chaperone DnaK.* Science, 1996. **272**(5268): p. 1606-14.
179. Laufen, T., et al., *Mechanism of regulation of hsp70 chaperones by DnaJ cochaperones.* Proc Natl Acad Sci U S A, 1999. **96**(10): p. 5452-7.
180. Guzhova, I. and B. Margulis, *Hsp70 chaperone as a survival factor in cell pathology.* Int Rev Cytol, 2006. **254**: p. 101-49.
181. Teter, S.A., et al., *Polypeptide flux through bacterial Hsp70: DnaK cooperates with trigger factor in chaperoning nascent chains.* Cell, 1999. **97**(6): p. 755-65.
182. Thulasiraman, V., C.F. Yang, and J. Frydman, *In vivo newly translated polypeptides are sequestered in a protected folding environment.* EMBO J, 1999. **18**(1): p. 85-95.
183. Schmitt, E., et al., *Chemosensitization by a non-apoptogenic heat shock protein 70-binding apoptosis-inducing factor mutant.* Cancer Res, 2003. **63**(23): p. 8233-40.
184. Lanneau, D., et al., *Apoptosis versus cell differentiation: role of heat shock proteins HSP90, HSP70 and HSP27.* Prion, 2007. **1**(1): p. 53-60.
185. Gabai, V.L., et al., *Hsp72-mediated suppression of c-Jun N-terminal kinase is implicated in development of tolerance to caspase-independent cell death.* Mol Cell Biol, 2000. **20**(18): p. 6826-36.
186. Park, H.S., et al., *Hsp72 functions as a natural inhibitory protein of c-Jun N-terminal kinase.* EMBO J, 2001. **20**(3): p. 446-56.
187. Stankiewicz, A.R., et al., *Hsp70 inhibits heat-induced apoptosis upstream of mitochondria by preventing Bax translocation.* J Biol Chem, 2005. **280**(46): p. 38729-39.
188. Jaattela, M., et al., *Hsp70 exerts its anti-apoptotic function downstream of caspase-3-like proteases.* EMBO J, 1998. **17**(21): p. 6124-34.
189. Sakahira, H. and S. Nagata, *Co-translational folding of caspase-activated DNase with Hsp70, Hsp40, and inhibitor of caspase-activated DNase.* J Biol Chem, 2002. **277**(5): p. 3364-70.
190. Gao, T. and A.C. Newton, *The turn motif is a phosphorylation switch that regulates the binding of Hsp70 to protein kinase C.* J Biol Chem, 2002. **277**(35): p. 31585-92.

191. Jiang, B., et al., *Nucleolin/C23 mediates the antiapoptotic effect of heat shock protein 70 during oxidative stress.* FEBS J, 2010. **277**(3): p. 642-52.
192. Kee, H.J., et al., *Activation of histone deacetylase 2 by inducible heat shock protein 70 in cardiac hypertrophy.* Circ Res, 2008. **103**(11): p. 1259-69.
193. Nirde, P., et al., *Heat shock cognate 70 protein secretion as a new growth arrest signal for cancer cells.* Oncogene, 2010. **29**(1): p. 117-27.
194. Claus, P., A.F. Bruns, and C. Grothe, *Fibroblast growth factor-2(23) binds directly to the survival of motoneuron protein and is associated with small nuclear RNAs.* Biochem J, 2004. **384**(Pt 3): p. 559-65.
195. Nesbit, M., et al., *Basic fibroblast growth factor induces a transformed phenotype in normal human melanocytes.* Oncogene, 1999. **18**(47): p. 6469-76.
196. Doble, B.W., et al., *Protein kinase C-epsilon mediates phorbol ester-induced phosphorylation of connexin-43.* Cell Commun Adhes, 2001. **8**(4-6): p. 253-6.
197. Pasumarthi, K.B., E. Kardami, and P.A. Cattini, *High and low molecular weight fibroblast growth factor-2 increase proliferation of neonatal rat cardiac myocytes but have differential effects on binucleation and nuclear morphology. Evidence for both paracrine and intracrine actions of fibroblast growth factor-2.* Circ Res, 1996. **78**(1): p. 126-36.
198. McIntosh, L.M., R.E. Baker, and J.E. Anderson, *Magnetic resonance imaging of regenerating and dystrophic mouse muscle.* Biochem Cell Biol, 1998. **76**(2-3): p. 532-41.
199. Yue, Y., et al., *Microdystrophin gene therapy of cardiomyopathy restores dystrophin-glycoprotein complex and improves sarcolemma integrity in the mdx mouse heart.* Circulation, 2003. **108**(13): p. 1626-32.
200. Ludke, A.R., et al., *A concise description of cardioprotective strategies in doxorubicin-induced cardiotoxicity.* Can J Physiol Pharmacol, 2009. **87**(10): p. 756-63.
201. Kumar, D., et al., *Apoptosis in adriamycin cardiomyopathy and its modulation by probucol.* Antioxid Redox Signal, 2001. **3**(1): p. 135-45.
202. Arese, M., et al., *Nuclear activities of basic fibroblast growth factor: potentiation of low-serum growth mediated by natural or chimeric nuclear localization signals.* Mol Biol Cell, 1999. **10**(5): p. 1429-44.
203. Shimasaki, S., et al., *Complementary DNA cloning and sequencing of rat ovarian basic fibroblast growth factor and tissue distribution study of its mRNA.* Biochem Biophys Res Commun, 1988. **157**(1): p. 256-63.
204. Brigstock, D.R., et al., *Species-specific high molecular weight forms of basic fibroblast growth factor.* Growth Factors, 1990. **4**(1): p. 45-52.
205. Gaubert, F., et al., *Expression of the high molecular weight fibroblast growth factor-2 isoform of 210 amino acids is associated with modulation of protein kinases C delta and epsilon and ERK activation.* J Biol Chem, 2001. **276**(2): p. 1545-54.
206. Kanthou, C. and O. Benzakour, *Cellular effects and signalling pathways activated by the anti-coagulant factor, protein S, in vascular cells protein S cellular effects.* Adv Exp Med Biol, 2000. **476**: p. 155-66.
207. Jacobs, C.M., et al., *ERK2 prohibits apoptosis-induced subcellular translocation of orphan nuclear receptor NGFI-B/TR3.* J Biol Chem, 2004. **279**(48): p. 50097-101.
208. Baines, C.P. and J.D. Molkentin, *STRESS signaling pathways that modulate cardiac myocyte apoptosis.* J Mol Cell Cardiol, 2005. **38**(1): p. 47-62.

209. Yang, G., et al., *Cystathionine gamma-lyase overexpression inhibits cell proliferation via a H2S-dependent modulation of ERK1/2 phosphorylation and p21Cip/WAK-1.* J Biol Chem, 2004. **279**(47): p. 49199-205.
210. Zhou, X., et al., *Histone deacetylase 4 associates with extracellular signal-regulated kinases 1 and 2, and its cellular localization is regulated by oncogenic Ras.* Proc Natl Acad Sci U S A, 2000. **97**(26): p. 14329-33.
211. Castro-Obregon, S., et al., *Alternative, nonapoptotic programmed cell death: mediation by arrestin 2, ERK2, and Nur77.* J Biol Chem, 2004. **279**(17): p. 17543-53.
212. Tang, D., et al., *ERK activation mediates cell cycle arrest and apoptosis after DNA damage independently of p53.* J Biol Chem, 2002. **277**(15): p. 12710-7.
213. Stanciu, M. and D.B. DeFranco, *Prolonged nuclear retention of activated extracellular signal-regulated protein kinase promotes cell death generated by oxidative toxicity or proteasome inhibition in a neuronal cell line.* J Biol Chem, 2002. **277**(6): p. 4010-7.
214. Chen, J.R., et al., *Transient versus sustained phosphorylation and nuclear accumulation of ERKs underlie anti-versus pro-apoptotic effects of estrogens.* J Biol Chem, 2005. **280**(6): p. 4632-8.
215. Oh, H.L., et al., *Role of MAPK in ceramide-induced cell death in primary cultured astrocytes from mouse embryonic brain.* Neurotoxicology, 2006. **27**(1): p. 31-8.
216. Park, B.G., et al., *Role of mitogen-activated protein kinases in hydrogen peroxide-induced cell death in osteoblastic cells.* Toxicology, 2005. **215**(1-2): p. 115-25.
217. Jiang, Z.S., et al., *High molecular weight FGF-2 promotes postconditioning-like cardioprotection linked to activation of the protein kinase C isoforms Akt and p70 S6 kinase.* Can J Physiol Pharmacol, 2009. **87**(10): p. 798-804.
218. Han, S.P., Y.H. Tang, and R. Smith, *Functional diversity of the hnRNPs: past, present and perspectives.* Biochem J, 2010. **430**(3): p. 379-92.
219. Hinnebusch, A.G., *eIF3: a versatile scaffold for translation initiation complexes.* Trends Biochem Sci, 2006. **31**(10): p. 553-62.
220. Silvera, D., S.C. Formenti, and R.J. Schneider, *Translational control in cancer.* Nat Rev Cancer, 2010. **10**(4): p. 254-66.
221. Pinol-Roma, S. and G. Dreyfuss, *Shuttling of pre-mRNA binding proteins between nucleus and cytoplasm.* Nature, 1992. **355**(6362): p. 730-2.
222. Bomsztyk, K., O. Denisenko, and J. Ostrowski, *hnRNP K: one protein multiple processes.* Bioessays, 2004. **26**(6): p. 629-38.
223. Itahana, K. and Y. Zhang, *Mitochondrial p32 is a critical mediator of ARF-induced apoptosis.* Cancer Cell, 2008. **13**(6): p. 542-53.
224. McGee, A.M. and C.P. Baines, *Complement 1q binding protein inhibits the mitochondrial permeability transition pore and protects against oxidative stress-induced death.* Biochem J, 2010.
225. Lee, S.B., et al., *Nuclear Akt interacts with B23/NPM and protects it from proteolytic cleavage, enhancing cell survival.* Proc Natl Acad Sci U S A, 2008. **105**(43): p. 16584-9.
226. Otake, Y., et al., *Overexpression of nucleolin in chronic lymphocytic leukemia cells induces stabilization of bcl2 mRNA.* Blood, 2007. **109**(7): p. 3069-75.
227. Santiago, J.J., et al., *Preferential accumulation and export of high molecular weight FGF-2 by rat cardiac non-myocytes.* Cardiovascular Research, 2010.

228. Peng, H., et al., *Integrative nuclear FGFR1 signaling (INFS) pathway mediates activation of the tyrosine hydroxylase gene by angiotensin II, depolarization and protein kinase C.* J Neurochem, 2002. **81**(3): p. 506-24.
229. Li, T., I. Danelisen, and P.K. Singal, *Early changes in myocardial antioxidant enzymes in rats treated with adriamycin.* Mol Cell Biochem, 2002. **232**(1-2): p. 19-26.

APPENDIX

SPRINGER LICENSE
TERMS AND CONDITIONS

Dec 06, 2010

This is a License Agreement between Xin Ma ("You") and Springer ("Springer") provided by Copyright Clearance Center ("CCC"). The license consists of your order details, the terms and conditions provided by Springer, and the payment terms and conditions.

All payments must be made in full to CCC. For payment instructions, please see information listed at the bottom of this form.

License Number	2510360939799
License date	Sep 15, 2010
Licensed content publisher	Springer
Licensed content publication	Heart Failure Reviews
Licensed content title	Fibroblast growth factor-2 and cardioprotection
Licensed content author	Elissavet Kardami
Licensed content date	Jan 1, 2007
Volume number	12
Issue number	3
Type of Use	Thesis/Dissertation
Portion	Excerpts
Author of this Springer article	Yes and you are a contributor of the new work
Order reference number	
Title of your thesis / dissertation	Studies on signals mediating or preventing the intracrine induction of chromatin compaction and cell death by high molecular weight FGF2
Expected completion date	Dec 2010
Estimated size(pages)	250

Total 0.00 CAD

Terms and Conditions

Introduction

The publisher for this copyrighted material is Springer Science + Business Media. By clicking "accept" in connection with completing this licensing transaction, you agree that the following terms and conditions apply to this transaction (along with the Billing and Payment terms and conditions established by Copyright Clearance Center, Inc. ("CCC"), at the time that you opened your Rightslink account and that are available at any time at http://myaccount.copyright.com).

Limited License

With reference to your request to reprint in your thesis material on which Springer Science and Business Media control the copyright, permission is granted, free of charge, for the use indicated in your enquiry. Licenses are for one-time use only with a maximum distribution equal to the number that you identified in the licensing process.

This License includes use in an electronic form, provided it is password protected or on the university's intranet, destined to microfilming by UMI and University repository. For any other electronic use, please contact Springer at (permissions.dordrecht@springer.com or permissions.heidelberg@springer.com)

The material can only be used for the purpose of defending your thesis, and with a maximum of 100 extra copies in paper.

Although Springer holds copyright to the material and is entitled to negotiate on rights, this license is only valid, provided permission is also obtained from the (co) author (address is given with the article/chapter) and provided it concerns original material which does not carry references to other sources (if material in question appears with credit to another source, authorization from that source is required as well). Permission free of charge on this occasion does not prejudice any rights we might have to charge for reproduction of our copyrighted material in the future.

Altering/Modifying Material: Not Permitted

However figures and illustrations may be altered minimally to serve your work. Any other abbreviations, additions, deletions and/or any other alterations shall be made only with prior written authorization of the author(s) and/or Springer Science + Business Media. (Please contact Springer at permissions.dordrecht@springer.com or permissions.heidelberg@springer.com)

Reservation of Rights

Springer Science + Business Media reserves all rights not specifically granted in the combination of (i) the license details provided by you and accepted in the course of this licensing transaction, (ii) these terms and conditions and (iii) CCC's Billing and Payment terms and conditions.

Gratis licenses (referencing $0 in the Total field) are free. Please retain this printable license for your reference. No payment is required.

If you would like to pay for this license now, please remit this license along with your payment made payable to "COPYRIGHT CLEARANCE CENTER" otherwise you will be invoiced within 48 hours of the license date. Payment should be in the form of a check or money order referencing your account number and this invoice number RLNK10849383.
Once you receive your invoice for this order, you may pay your invoice by credit card. Please follow instructions provided at that time.

Make Payment To:
Copyright Clearance Center
Dept 001
P.O. Box 843006
Boston, MA 02284-3006

If you find copyrighted material related to this license will not be used and wish to cancel, please contact us referencing this license number 2510360939799 and noting the reason for cancellation.

Questions? customercare@copyright.com or +1-877-622-5543 (toll free in the US) or +1-978-646-2777.

JOHN WILEY AND SONS LICENSE TERMS AND CONDITIONS

Dec 06, 2010

This is a License Agreement between Xin Ma ("You") and John Wiley and Sons ("John Wiley and Sons") provided by Copyright Clearance Center ("CCC"). The license consists of your order details, the terms and conditions provided by John Wiley and Sons, and the payment terms and conditions.

All payments must be made in full to CCC. For payment instructions, please see information listed at the bottom of this form.

License Number	2510370524395
License date	Sep 15, 2010
Licensed content publisher	John Wiley and Sons
Licensed content publication	Journal of Cellular Physiology
Licensed content title	Chromatin compaction and cell death by high molecular weight FGF-2 depend on its nuclear localization, intracrine ERK activation, and engagement of mitochondria
Licensed content author	Xin Ma,Xitong Dang,Peter Claus,Cheryl Hirst,Robert R. Fandrich,Yan Jin,Claudia Grothe,Lorrie A. Kirshenbaum,Peter A. Cattini,Elissavet Kardami
Licensed content date	Dec 1, 2007
Start page	690
End page	698
Type of use	Dissertation/Thesis
Requestor type	Author of this Wiley article
Format	Print and electronic
Portion	Figure/table

Number of figures/tables	9
Original Wiley figure/table number(s)	Figure 2, Figure 4, Figure 6, Figure 7, Figure 8, Figure 9, Supplement Figure 2, Supplement Figure 3, Supplement Figure 4.
Will you be translating?	No
Order reference number	
Total	0.00 USD

Terms and Conditions

TERMS AND CONDITIONS

This copyrighted material is owned by or exclusively licensed to John Wiley & Sons, Inc. or one if its group companies (each a “Wiley Company”) or a society for whom a Wiley Company has exclusive publishing rights in relation to a particular journal (collectively “WILEY”). By clicking “accept” in connection with completing this licensing transaction, you agree that the following terms and conditions apply to this transaction (along with the billing and payment terms and conditions established by the Copyright Clearance Center Inc., (“CCC’s Billing and Payment terms and conditions”), at the time that you opened your Rightslink account (these are available at any time at http://myaccount.copyright.com).

Terms and Conditions

1. The materials you have requested permission to reproduce (the "Materials") are protected by copyright.

2. You are hereby granted a personal, non-exclusive, non-sublicensable, non-transferable, worldwide, limited license to reproduce the Materials for the purpose specified in the licensing process. This license is for a one-time use only with a maximum distribution equal to the number that you identified in the licensing process. Any form of republication granted by this licence must be completed within two years of the date of the grant of this licence (although copies prepared before may be distributed thereafter). Any electronic posting of the Materials is limited to one year from the date permission is granted and is on the condition that a link is placed to the journal homepage on Wiley’s online journals publication platform at www.interscience.wiley.com. The Materials shall not be used in any other manner or for any other purpose. Permission is granted subject to an appropriate acknowledgement given to the author, title of the material/book/journal and the publisher and on the understanding that nowhere in the text is a previously published source acknowledged for all or part of this Material. Any third party material is expressly excluded from this permission.

3. With respect to the Materials, all rights are reserved. No part of the Materials may be copied, modified, adapted, translated, reproduced, transferred or distributed, in any form or

by any means, and no derivative works may be made based on the Materials without the prior permission of the respective copyright owner. You may not alter, remove or suppress in any manner any copyright, trademark or other notices displayed by the Materials. You may not license, rent, sell, loan, lease, pledge, offer as security, transfer or assign the Materials, or any of the rights granted to you hereunder to any other person.

4. The Materials and all of the intellectual property rights therein shall at all times remain the exclusive property of John Wiley & Sons Inc or one of its related companies (WILEY) or their respective licensors, and your interest therein is only that of having possession of and the right to reproduce the Materials pursuant to Section 2 herein during the continuance of this Agreement. You agree that you own no right, title or interest in or to the Materials or any of the intellectual property rights therein. You shall have no rights hereunder other than the license as provided for above in Section 2. No right, license or interest to any trademark, trade name, service mark or other branding ("Marks") of WILEY or its licensors is granted hereunder, and you agree that you shall not assert any such right, license or interest with respect thereto.

5. WILEY DOES NOT MAKE ANY WARRANTY OR REPRESENTATION OF ANY KIND TO YOU OR ANY THIRD PARTY, EXPRESS, IMPLIED OR STATUTORY, WITH RESPECT TO THE MATERIALS OR THE ACCURACY OF ANY INFORMATION CONTAINED IN THE MATERIALS, INCLUDING, WITHOUT LIMITATION, ANY IMPLIED WARRANTY OF MERCHANTABILITY, ACCURACY, SATISFACTORY QUALITY, FITNESS FOR A PARTICULAR PURPOSE, USABILITY, INTEGRATION OR NON-INFRINGEMENT AND ALL SUCH WARRANTIES ARE HEREBY EXCLUDED BY WILEY AND WAIVED BY YOU.

6. WILEY shall have the right to terminate this Agreement immediately upon breach of this Agreement by you.

7. You shall indemnify, defend and hold harmless WILEY, its directors, officers, agents and employees, from and against any actual or threatened claims, demands, causes of action or proceedings arising from any breach of this Agreement by you.

8. IN NO EVENT SHALL WILEY BE LIABLE TO YOU OR ANY OTHER PARTY OR ANY OTHER PERSON OR ENTITY FOR ANY SPECIAL, CONSEQUENTIAL, INCIDENTAL, INDIRECT, EXEMPLARY OR PUNITIVE DAMAGES, HOWEVER CAUSED, ARISING OUT OF OR IN CONNECTION WITH THE DOWNLOADING, PROVISIONING, VIEWING OR USE OF THE MATERIALS REGARDLESS OF THE FORM OF ACTION, WHETHER FOR BREACH OF CONTRACT, BREACH OF WARRANTY, TORT, NEGLIGENCE, INFRINGEMENT OR OTHERWISE (INCLUDING, WITHOUT LIMITATION, DAMAGES BASED ON LOSS OF PROFITS, DATA, FILES, USE, BUSINESS OPPORTUNITY OR CLAIMS OF THIRD PARTIES), AND WHETHER OR NOT THE PARTY HAS BEEN ADVISED OF THE POSSIBILITY OF SUCH DAMAGES. THIS LIMITATION SHALL APPLY NOTWITHSTANDING

ANY FAILURE OF ESSENTIAL PURPOSE OF ANY LIMITED REMEDY PROVIDED HEREIN.

9. Should any provision of this Agreement be held by a court of competent jurisdiction to be illegal, invalid, or unenforceable, that provision shall be deemed amended to achieve as nearly as possible the same economic effect as the original provision, and the legality, validity and enforceability of the remaining provisions of this Agreement shall not be affected or impaired thereby.

10. The failure of either party to enforce any term or condition of this Agreement shall not constitute a waiver of either party's right to enforce each and every term and condition of this Agreement. No breach under this agreement shall be deemed waived or excused by either party unless such waiver or consent is in writing signed by the party granting such waiver or consent. The waiver by or consent of a party to a breach of any provision of this Agreement shall not operate or be construed as a waiver of or consent to any other or subsequent breach by such other party.

11. This Agreement may not be assigned (including by operation of law or otherwise) by you without WILEY's prior written consent.

12. These terms and conditions together with CCC’s Billing and Payment terms and conditions (which are incorporated herein) form the entire agreement between you and WILEY concerning this licensing transaction and (in the absence of fraud) supersedes all prior agreements and representations of the parties, oral or written. This Agreement may not be amended except in a writing signed by both parties. This Agreement shall be binding upon and inure to the benefit of the parties' successors, legal representatives, and authorized assigns.

13. In the event of any conflict between your obligations established by these terms and conditions and those established by CCC’s Billing and Payment terms and conditions, these terms and conditions shall prevail.

14. WILEY expressly reserves all rights not specifically granted in the combination of (i) the license details provided by you and accepted in the course of this licensing transaction, (ii) these terms and conditions and (iii) CCC’s Billing and Payment terms and conditions.

15. This Agreement shall be governed by and construed in accordance with the laws of England and you agree to submit to the exclusive jurisdiction of the English courts.

16. Other Terms and Conditions:

BY CLICKING ON THE "I ACCEPT" BUTTON, YOU ACKNOWLEDGE THAT YOU HAVE READ AND FULLY UNDERSTAND EACH OF THE SECTIONS OF AND PROVISIONS SET FORTH IN THIS AGREEMENT AND THAT YOU ARE IN

AGREEMENT WITH AND ARE WILLING TO ACCEPT ALL OF YOUR OBLIGATIONS AS SET FORTH IN THIS AGREEMENT.

V1.2

Gratis licenses (referencing $0 in the Total field) are free. Please retain this printable license for your reference. No payment is required.

If you would like to pay for this license now, please remit this license along with your payment made payable to "COPYRIGHT CLEARANCE CENTER" otherwise you will be invoiced within 48 hours of the license date. Payment should be in the form of a check or money order referencing your account number and this invoice number RLNK10849393.
Once you receive your invoice for this order, you may pay your invoice by credit card. Please follow instructions provided at that time.

Make Payment To:
Copyright Clearance Center
Dept 001
P.O. Box 843006
Boston, MA 02284-3006

If you find copyrighted material related to this license will not be used and wish to cancel, please contact us referencing this license number 2510370524395 and noting the reason for cancellation.

Questions? customercare@copyright.com or +1-877-622-5543 (toll free in the US) or +1-978-646-2777.

OXFORD UNIVERSITY PRESS LICENSE TERMS AND CONDITIONS

Dec 06, 2010

This is a License Agreement between Xin Ma ("You") and Oxford University Press ("Oxford University Press") provided by Copyright Clearance Center ("CCC"). The license consists of your order details, the terms and conditions provided by Oxford University Press, and the payment terms and conditions.

All payments must be made in full to CCC. For payment instructions, please see information listed at the bottom of this form.

License Number	2563230805978
License date	Dec 06, 2010
Licensed content publisher	Oxford University Press
Licensed content publication	Cardiovascular Research
Licensed content title	Preferential accumulation and export of high molecular weight FGF-2 by rat cardiac non-myocytes:
Licensed content author	Jon-Jon Santiago, Xin Ma, Leslie J. McNaughton, Barbara E. Nickel, Brian P. Bestvater, Liping Yu, Robert R. Fandrich, Thomas Netticadan, Elissavet Kardami
Licensed content date	08/09/2010
Type of Use	Thesis/Dissertation
Institution name	
Title of your work	Studies on signals mediating or preventing the intracrine induction of chromatin compaction and cell death by high molecular weight FGF2
Publisher of your work	n/a
Expected publication date	Dec 2010
Permissions cost	0.00 USD
Value added tax	0.00 USD

Total 0.00 USD

Total 0.00 USD

Terms and Conditions

STANDARD TERMS AND CONDITIONS FOR REPRODUCTION OF MATERIAL FROM AN OXFORD UNIVERSITY PRESS JOURNAL

1. Use of the material is restricted to the type of use specified in your order details.

2. This permission covers the use of the material in the English language in the following territory: world. If you have requested additional permission to translate this material, the terms and conditions of this reuse will be set out in clause 12.

3. This permission is limited to the particular use authorized in (1) above and does not allow you to sanction its use elsewhere in any other format other than specified above, nor does it apply to quotations, images, artistic works etc that have been reproduced from other sources which may be part of the material to be used.

4. No alteration, omission or addition is made to the material without our written consent. Permission must be re-cleared with Oxford University Press if/when you decide to reprint.

5. The following credit line appears wherever the material is used: author, title, journal, year, volume, issue number, pagination, by permission of Oxford University Press or the sponsoring society if the journal is a society journal. Where a journal is being published on behalf of a learned society, the details of that society must be included in the credit line.

6. For the reproduction of a full article from an Oxford University Press journal for whatever purpose, the corresponding author of the material concerned should be informed of the proposed use. Contact details for the corresponding authors of all Oxford University Press journal contact can be found alongside either the abstract or full text of the article concerned, accessible from www.oxfordjournals.org Should there be a problem clearing these rights, please contact journals.permissions@oxfordjournals.org

7. If the credit line or acknowledgement in our publication indicates that any of the figures, images or photos was reproduced, drawn or modified from an earlier source it will be necessary for you to clear this permission with the original publisher as well. If this permission has not been obtained, please note that this material cannot be included in your publication/photocopies.

8. While you may exercise the rights licensed immediately upon issuance of the license at the end of the licensing process for the transaction, provided that you have disclosed complete and accurate details of your proposed use, no license is finally effective unless and until full payment is received from you (either by Oxford University Press or by Copyright Clearance Center (CCC)) as provided in CCC's Billing and Payment terms and conditions. If full payment is not received on a timely basis, then any license preliminarily granted shall be

deemed automatically revoked and shall be void as if never granted. Further, in the event that you breach any of these terms and conditions or any of CCC's Billing and Payment terms and conditions, the license is automatically revoked and shall be void as if never granted. Use of materials as described in a revoked license, as well as any use of the materials beyond the scope of an unrevoked license, may constitute copyright infringement and Oxford University Press reserves the right to take any and all action to protect its copyright in the materials.

9. This license is personal to you and may not be sublicensed, assigned or transferred by you to any other person without Oxford University Press's written permission.

10. Oxford University Press reserves all rights not specifically granted in the combination of (i) the license details provided by you and accepted in the course of this licensing transaction, (ii) these terms and conditions and (iii) CCC's Billing and Payment terms and conditions.

11. You hereby indemnify and agree to hold harmless Oxford University Press and CCC, and their respective officers, directors, employs and agents, from and against any and all claims arising out of your use of the licensed material other than as specifically authorized pursuant to this license.

12. Other Terms and Conditions:

v1.4

Gratis licenses (referencing $0 in the Total field) are free. Please retain this printable license for your reference. No payment is required.

If you would like to pay for this license now, please remit this license along with your payment made payable to "COPYRIGHT CLEARANCE CENTER" otherwise you will be invoiced within 48 hours of the license date. Payment should be in the form of a check or money order referencing your account number and this invoice number RLNK10895278.
Once you receive your invoice for this order, you may pay your invoice by credit card. Please follow instructions provided at that time.

Make Payment To:
Copyright Clearance Center
Dept 001
P.O. Box 843006
Boston, MA 02284-3006

If you find copyrighted material related to this license will not be used and wish to cancel, please contact us referencing this license number 2563230805978 and noting the reason for cancellation.